ENDOTHELIAL CELL FUNCTION USING A TISSUE ENGINEERED BLOOD VESSEL MODEL: A CASE STUDY OF CELL-CELL COMMUNICATION

A Dissertation
Presented to
The Academic Faculty

by

Tiffany Lynn Johnson

In Partial Fulfillment
of the Requirements for the Degree
Doctor of Philosophy in the
Department of Biomedical Engineering

Georgia Institute of Technology
Emory University
May 2006

ENDOTHELIAL CELL FUNCTION USING A TISSUE ENGINEERED BLOOD VESSEL MODEL: A CASE STUDY OF CELL-CELL COMMUNICATION

Approved by:

Dr. Robert M. Nerem, Advisor
School of Mechanical Engineering
Georgia Institute of Technology

Dr. Matthew Pollman
Director of New Ventures
Guidant Corporation

Dr. Larry V. McIntire
Department of Biomedical Engineering
Georgia Institute of Technology &
Emory University

Dr. W. Robert Taylor
Department of Biomedical Engineering
Georgia Institute of Technology &
Emory University

Dr. Zorina Galis
Professor of Surgery
Indiana University
Research Fellow,
Lilly Research Laboratories

Dr. Hanjoong Jo
Department of Biomedical Engineering
Georgia Institute of Technology &
Emory University

Date Approved: March 30, 2006

To my family

ACKNOWLEDGEMENTS

I would like to express my heartfelt gratitude to the significant number of people who supported me in the development of this dissertation. To my advisor, Dr. Robert Nerem, who always supported my ideas and interests in both research and in life, thank you for your generosity, patience and educating spirit. I would like to acknowledge by committee members, Dr. Zorina Galis, Dr. Hanjoong Jo, Dr. Larry McIntire, Dr. Matthew Pollman and Dr. Robert Taylor, for their assistance and guidance in steering this research. Thank you to the Morehouse School of Medicine Genomics Core Lab and especially Cindy Hu and Guoshen Wang for their technical assistance and friendship. I would also like to thank the Georgia Tech/Emory Center for the Engineering of Living Tissues and the American Heart Association for funding which made this work possible.

Graduate school is certainly not an individual effort and I would like to thank the many members of the Nerem lab for their help over the years. Thank you to Lisa Cox and Steve Woodard for their constant presence and willingness to help whenever a situation arose. For all the lab experiences and memories, I would like to thank JoSette Broiles, Jonathan Butcher, Adele Doyle, Matthew Prohaska and Stacey Schutte. I extend a special thank you to Taby Ahsan for sharing her knowledge and insight with great patience. In particular, I would like to thank Ann Ensley for her guidance, willingness to brainstorm and for sharing the challenges of the final years of graduate school. For their friendship from the first day through the entire experience of graduate school, my sincere appreciation goes to Kyla Ross, Jamie Chilton, Mutsumi Conrad and Ciara Tate.

Finally, I would like to thank my family, without whom I would not be here today. To Alex, Keith and Suzanne, for bringing joy to my life and reminding me what really matters. To Michael, for endless love and patience through every day of this journey and unwavering support of my dreams.

To my parents, who always believe in me.

TABLE OF CONTENTS

LIST OF TABLES

LIST OF FIGURES

LIST OF SYMBOLS AND ABBREVIATIONS

-/-	homozygous negative
+/-	heterozygous positive and negative
Ang2	angiopoeitin 2
ANOVA	analysis of variance
ATP	adenosine triphosphate
BCA	bicinchoninic acid
BrdU	5-bromo-2'-deoxyuridine
cdc	cell division cycle
cdca	cell division cycle associated
cdk	cyclin dependent kinase
cDNA	complementary DNA
cox	cyclooxygenase
CT	threshold cycle
Cx	connexin
Cx26	connexin 26
Cx37	connexin 37
Cx40	connexin 40
Cx43	connexin 43
Cx45	connexin 45
Cy3	cyanine 3
Cy5	cyanine 5
CYP1A1	cytochrome p450 1A1

CYP1B1	cytochrome p450 1B1
Da	dalton
DMSO	dimethyl sulphoxide
DNA	deoxyribonucleic acid
DNase	DNA nuclease
E12.5	embryonic day 12.5
EC	endothelial cell
EGF	epidermal growth factor
eNOS	endothelial nitric oxide synthase
EPCR	endothelial protein C receptor
FBS	fetal bovine serum
FGF	fibroblast growth factor
FGL-2	fibrinogen-like 2
FITC	fluorescein
GJ	gap junction
GPX	glutathione peroxidase
HAEC	human aortic endothelial cell
HASMC	human aortic smooth muscle cell
HCL	hydrochloric acid
HeM/HeT	Heteromeric/Heterotypic
HoM/HeT	Homomeric/Heterotypic
HoM/HoT	Homomeric/Homotypic
HUVEC	human umbilical vein endothelial cell

IGF	insulin growth factor
IPA	Ingenuity Pathways Analysis
IPKB	Ingenuity Pathways Knowledge Base
IRES	internal ribosome entry sequence
JNK	janus kinase
LDL	low density lipoprotein
LSM	laser scanning microscope
MAPK	mitogen activated protein kinase
MCM	minichromosome maintenance deficient
MEGJ	myoendothelial gap junction
MESF	molecules of equivalent soluble fluorescence
mL	milliliter
MMP	matrix metalloprotease
mRNA	message RNA
MTC	multiple testing correction
MW	molecular weight
NC	negative control
nM	nanomolar
NRP	neuropilin
PAR-4	proteinase activated receptor 4
PBS	phosphate buffered saline
PCNA	proliferating cell nuclear antigen
PCR	polymerase chain reaction

PE	phycoerythrin
PECAM	platelet endothelial cell adhesion molecule
PGF	placental growth factor
PVDF	polyvinylidene fluoride
redox	reduction-oxidation
RIPA	radioimmunoprecipitation
RNA	ribonucleic acid
RNAi	RNA interference
Rnase	RNA nuclease
rRNA	ribosomal RNA
-RT	minus reverse transcriptase
RT-PCR	reverse transcription polymerase chain reaction
SDS	sodium dodecyl sulfate
siRNA	short interfering RNA
SMC	smooth muscle cell
SOD-1	superoxide dismutase 1
SSRE	shear stress response element
TEWM	tissue engineered wall model
TGF-β1	transforming growth factor beta 1
TNF-α	tumor necrosis factor alpha
tRNA	transfer RNA
T-TBS	tween tris buffered saline
uORF	upstream open reading frame

UTR	untranslated region
UV	ultraviolet
VEC	vascular endothelial cell
VEGF	vascular endothelial growth factor
vWF	von Willibrand factor
μg/mL	micrograms per milliliter
μL	microliter
μM	micromolar

SUMMARY

Atherosclerosis is an inflammatory disease which develops focally in regions of the vasculature where there is dysfunction of endothelial cells modulated in part by shear stress from flowing blood. To address the clinical crisis of atherosclerosis, tissue engineering has focused on development of a living blood vessel substitute for use as a vascular graft in bypass surgery. Despite substantial progress in understanding the biological basis and developing clinical treatments for cardiovascular disease, critical challenges remain. As a novel strategy to improve understanding of basic human vascular biology and develop superior tissue engineered grafts, this dissertation combines the scientific and clinical approaches by using a tissue engineered blood vessel as a more physiologic in vitro model to study endothelial cell biology. Through the use of transcriptional profiling, results demonstrate significant changes in endothelial cell gene expression using the tissue engineered blood vessel model. Furthermore, the presence of a more physiologic substrate alters the cellular response to shear stress which is a critical mediator of vascular pathology. A case study of endothelial cell function in this system focuses on cell-cell communication through gap junctions. Endothelial cell connexins which form gap junctions are shown to be differentially regulated by substrate and shear stress. Moreover, gap junction communication between endothelial cells is modulated by the mechanical environment. Studies using RNA interference to knockdown expression of individual connexin isotypes demonstrate integrated regulation of connexins yet unique roles in endothelial cell function. Collectively, results exemplify the sensitivity of endothelial cell phenotype to substrate and shear stress and underline the importance of using more physiologic models in the study of basic cell biology.

CHAPTER ONE: Introduction

One-third of American adults suffer from at least one form of cardiovascular disease thus generating a patient population of over 71 million. Widespread prevalence of cardiovascular disease results in one death every 35 seconds and is responsible for shortening the American life expectancy by seven years. (1) Atherosclerosis is one major type of cardiovascular disease and involves the development of plaque in the innermost lining of blood vessels which can lead to stroke or myocardial infarction. To address the crisis of atherosclerosis, development of clinical treatments and understanding through research have been aggressively pursued.

Endothelial cells which line the inner surface of blood vessels have been the focus of research into both physiologic and pathologic mechanisms. The endothelium serves multiple purposes including barrier formation between blood and tissue, control of blood coagulation and regulation of vascular tone. (2) One critical discovery is the link between mechanical forces and endothelial cell behavior, especially the influence of shear forces from flowing blood which can render the vessel resistant or susceptible to atherosclerosis. (3) Multifaceted dysfunction of endothelial cells from increased permeability to altered cell adhesion is involved in progression of atherosclerosis, however despite decades of investigation; a comprehensive understanding of mechanisms underlying this disease is still elusive. (4, 5)

While research into endothelial cells and atherosclerosis continues, clinical treatment to prevent plaque rupture and possible stroke or myocardial infarction often requires bypass surgery. This procedure uses a graft to provide an alternate route for

blood flow thus avoiding passage through the diseased vessel. Although grafts of synthetic material remain patent in large arteries, small diameter vessels can occlude thus requiring harvest of vessel segments from another region of the patient's body for use as a conduit. Due to the pain of two procedures and the lack of healthy vessel available in many patients, alternative graft sources are being investigated.

The goal of tissue engineering is the development of living substitutes to repair, replace or enhance tissue function. Tissue engineered substitutes are an attractive solution to many diseases because of the opportunity to use healthy, normal tissue as a therapy. (6) Strategies to generate engineered cardiovascular tissues have incorporated synthetic and biological matrices, multiple cell types and bioreactors for application of chemical, electrical and mechanical stimuli. While development of tissue engineered blood vessels as a source of small diameter vascular grafts has made significant advances, numerous challenges remain prior to their widespread use in a clinical setting. (7, 8)

Despite years of significant effort in biology of endothelial cells to understand their roles in maintenance of healthy vessels and progression of disease, a myriad of questions remain. While studies conducted using both *in vitro* and *in vivo* experimental settings have provided valuable scientific insight and aided in the advancement of clinical therapies, results from these two environments have not always been predictive of each other or the human body. Understanding the disconnect between *in vitro* experiments, *in vivo* animal studies and human patients will lead to a further scientific understanding of endothelial cell biology and impact treatment of vascular disease. This opportunity is provided by the field of tissue engineering where technology is used to recreate the native cellular environment in a controlled and reproducible manner resulting in more

physiologic models for the study of basic biology. Use of engineered human tissue will lead to an improved understanding of basic biology as well as an emergence of superior tissue engineered substitutes. Therefore this dissertation uses a tissue engineered blood vessel to model the vascular wall microenvironment for study of basic human endothelial cell biology.

Within the context of endothelial cell biology, numerous areas are under investigation for their roles in vascular development and disease. Studies presented here focus on endothelial cell communication through gap junctions. Communication between cells is critical to normal function and disease progression because cells do not function in isolation, but coordinate to generate a tissue-level response to stimuli. (9, 10) Endothelial gap junctions, which provide direct communication between cells, have been implicated in multiple vascular diseases including atherosclerosis and hypertension. (11, 12) While evidence is building regarding endothelial gap junction sensitivity to mechanical forces, growth factors and cytokines, substantial questions remain regarding their roles in physiologic and pathologic processes. (13, 14) Furthermore, preliminary data gathered in this study using the tissue engineered blood vessel model indicated differential expression of endothelial connexins which are the building blocks of gap junctions. Therefore this dissertation evaluates the response of endothelial gap junctions to substrate and shear stress and investigates the unique functions of the three endothelial connexin isotypes.

The central hypothesis of this dissertation is that endothelial cell behavior is altered by the presence of smooth muscle cells, extracellular matrix and fluid flow.

Investigation of the central hypothesis is achieved through the following specific aims and corresponding hypotheses.

Specific Aim 1

Hypothesis: Exposure of endothelial cells to a tissue engineered blood vessel substrate alters gene expression in response to static and shear mechanical environments.

Specific Aim: Compare transcriptional profiles of endothelial cells on a collagen coated slide to cells on a tissue engineered blood vessel under laminar shear stress and static conditions.

Specific Aim 2

Hypothesis: Endothelial cell gap junction expression and function will be influenced by substrate and mechanical environment.

Specific Aim: Compare endothelial cell connexin expression and gap junction communication on a collagen coated slide and tissue engineered blood vessel under laminar shear stress and static conditions.

Specific Aim 3

Hypothesis: Three connexin isotypes (Cx37, Cx40, Cx43) have unique functions in endothelial cell biology and response to shear stress.

Specific Aim: Knockdown expression of individual connexins to determine their specific roles in endothelial gap junction communication, cell proliferation and cell morphology.

CHAPTER TWO: Background

Introduction

To address the clinical crisis of atherosclerosis, both the study of basic vascular biology and the development of novel therapies will be required. While substantial progress has been made in understanding the physiology and pathology of endothelial cell, new strategies are needed for advancement. Furthermore, great strides have been made in the development of tissue engineered vascular grafts but clinical application of this therapy has not yet been realized. This dissertation combines the efforts to understand and treat cardiovascular disease by using a tissue engineered blood vessel as a more physiologic in vitro model for the study of basic human endothelial cell biology.

Atherosclerosis is a disease of the blood vessel wall that was originally identified by hard lesions which appeared to have composition similar to gruel. It is now recognized to be a progressive, inflammatory disease of the vasculature which results from a combination of genetic predisposition and lifestyle risk factors. (15) While high cholesterol and inflammatory cytokines are systemic in nature, atherosclerotic plaque develops focally in regions of the vascular tree where the endothelium is dysfunctional. (16) Endothelial dysfunction is clinically characterized by a loss of nitric oxide production and therefore reduced endothelium-dependent vasodilation. (17) The shift in phenotype to a state of dysfunction is also characterized by increases in endothelial adhesiveness, permeability, proliferation and thrombogenesis. (18) Atherosclerosis begins as a fatty streak with the accumulation of lipid-laden macrophages known as foam cells in the vascular wall beneath the endothelium. Dysfunction of endothelial cells and

inflammation lead to increased uptake of lipids which are then scavenged by recruited monocytes in the subendothelial space. Fatty streaks progress to form intermediate then advanced lesions which are accelerated by other conditions such as hypertension, diabetes, high cholesterol and various inflammatory triggers. The major steps involved in atherosclerotic plaque development and progression to advanced stages include endothelial injury, monocyte recruitment, macrophage development, foam cell formation, lipid deposition, platelet activation, smooth muscle cell migration and proliferation, and synthesis and deposition of extracellular matrix. (19) Much is known about factors contributing to development of atherosclerosis, however a comprehensive understanding of underlying mechanisms has not yet been achieved.

The dangers of atherosclerosis are in the downstream consequences of plaque expansion or rupture and the currently unpredictable nature of these events. While plaques can grow to block the lumen thus preventing blood flow, the vessel most often compensates through positively remodeling to maintain the lumenal opening. In the event of plaque rupture, release of the contents leads to thrombosis which blocks the lumen and prevents blood from flowing. Loss of blood flow to the heart results in myocardial infarction, loss of blood flow to the brain results in stroke, and loss of blood flow in the peripheral vasculature can lead to limb amputation due to tissue death. Efforts are currently underway to understand what causes plaque rupture and how to predict this clinical event prior to major complications. Vulnerability of plaque appears to be dependent not only on external factors such as mechanical forces and circulating inflammatory stimuli, but also on the composition of the plaque itself. (20)

As the pathology of atherosclerosis continues to be studied and methods for reliably predicting clinical events are being developed, treatment of patients is ongoing. Management of risk factors through diet, exercise and treatment of high blood pressure and high cholesterol aims to slow the progression of atherosclerosis. For patients whose vascular disease is deemed a current threat or those who have experienced a major cardiac event, treatment is by stent or bypass surgery. (21) Treatment by balloon angioplasty and stenting serves to reopen a vessel where plaque is encroaching into the lumen and hold it open with structural support. Treatment with bypass surgery involves placing an alternative conduit, either a synthetic graft, vein graft or arterial graft, around the diseased vessel to divert blood flow and ensure perfusion to downstream tissue.

With the increasing number of patients requiring bypass surgery due to atherosclerotic lesions and the failure of synthetic grafts to replace small diameter arteries, clinicians and researchers began investigating methods for improving synthetic grafts. Failure of small diameter synthetic vascular grafts was most often due to thrombosis which is not seen in replacement of larger diameter vessels. Initial approaches included coating the graft lumen with proteins such as albumin, collagen or heparin in attempts to reduce the thrombogenicity. (22, 23) The next step in improving synthetic graft success was to line the lumen with endothelial cells prior to implantation to provide a natural non-thrombogenic surface. (24, 25) While limited success was achieved, expansion of endothelial cells in culture is required and mixed results have prevented widespread adoption of this technique. Since synthetic small diameter grafts result in thrombosis, vein grafting is often used to bypass diseased arterial conduits. Although vein grafts provide a living tissue replacement, their properties differ from

arteries and therefore failure and re-operation can be a consequence. (26) Modification of vein grafts through genetic engineering has been extensively investigated however a viable therapeutic strategy has not been developed. (27) When failure of synthetic grafts and vein grafts presented numerous challenges, clinicians turned to arterial grafting and the development of new options promised by the field of tissue engineering. (28)

Cellular and tissue engineering are multi-disciplinary fields which apply the principles of engineering to the problems of biology and medicine to create new scientific understanding and clinical therapies. (29, 30) The goal of tissue engineering is to develop living tissue substitutes which can repair, replace or enhance native tissue function. Tissue engineering offers the clinical world the option of treating patients with normal, healthy tissue to restore health due to any number of diseases. While great progress has been made, numerous challenges have arisen which have increased our appreciation for the complexity of tissue development and function. Current work in the field of tissue engineering is focused on almost every tissue imaginable; however we will focus this discussion on development of the blood vessel. Recent progress and new challenges in the area of cardiovascular tissue engineering have been recently reviewed by several groups. (6-8)

An early strategy in tissue engineering of blood vessels was to remove all cellular material from existing vessels and implant the acellular tissue since it possesses adequate strength as well as biological properties. (31, 32) The next step was to seed this acellular matrix with cells which could interact with the biological matrix and develop a living tissue. (33) As development of engineered substitutes progressed, it became apparent that presence of cells and extracellular matrix was not sufficient to develop tissue but that

additional stimuli such as mechanical forces and specific nutrients were required. (34) With the increasing appreciation of biological complexity in the development of tissue engineered substitutes, native development of the vasculature was closely examined for clues. (35)

Although numerous approaches have been taken, early development of tissue engineered vascular grafts focused on mimicking the structure and function of native vessels. One early strategy used smooth muscle cells dispersed in a tubular collagen gel to mimic the medial layer and then lined this tube with endothelial cells to create an intimal layer. While biological in nature, this early blood vessel construct required an exterior synthetic graft to provide adequate strength for *in vivo* implantation. (36) A second *in vitro* biological approach involves long term culture of smooth muscle cells with numerous growth factors to induce generation of extensive extracellular matrix. Smooth muscle cell-matrix sheets are then rolled into a tubular shape, the lumen is seeded with endothelial cells and the exterior is wrapped with a fibroblast-matrix sheet for additional strength. (37) Several biomaterials-based approaches have been pursued where living cells are seeded onto a synthetic material which provides structural integrity while cells develop their own extracellular matrix environment. One example of this strategy involved seeding smooth muscle cells onto tubular polymeric scaffolds and culturing them in bioreactors applying mechanical force prior to seeding the lumen with endothelial cells. (38, 39) Finally, a novel *in vivo* approach was taken to generate a small diameter vascular graft which would provide an autologous tissue source and therefore avoid complications due to immune rejection. Silastic tubing was inserted into the peritoneal cavity of multiple animal models and following several weeks of implantation,

the tubing/tissue structure was harvested and the artificial material removed leaving a biological conduit with a medial-like layer and a nonthrombogenic inner lining. (40)

The primary focus of tissue engineering has been the development of living tissues to repair, replace or enhance tissue function in a clinical setting. However, a potentially untapped result of advances in tissue engineering is the use of engineered substitutes as more physiologic *in vitro* models. This approach combines the control of *in vitro* systems with the complexity of *in vivo* systems to generate new insight into cell biology. Furthermore, a unique advantage of tissue engineering is the ability to use human cells to generate human tissue for experimentation without a danger to patients. Our laboratory recently combined the development of tissue engineered vascular grafts with the study of endothelial mechanotransduction by using the tissue engineered blood vessel as a model substrate during endothelial cell exposure to fluid flow. Early studies examined porcine endothelial cell morphology and proliferation under the combined influences of extracellular matrix, smooth muscle cells and shear stress.(41) More recent work has incorporated human endothelial and smooth muscle cells in studying morphology, proliferation and migration of endothelial cells in this more physiologic model.(42, 43)

Endothelial Cell Biology

Endothelial cells line all the blood vessels of the body and have numerous critical functions due to their presence at the interface of blood and tissue. Their primary functions include barrier formation, regulation of blood coagulation and control of vascular tone. (2) As mediators between blood and tissue, endothelial cells are involved

in numerous systemic and cardiovascular diseases. (4, 5) For the purpose of this dissertation, the review of endothelial cell function will be restricted to interactions with shear stress, extracellular matrix and smooth muscle cells.

Endothelial cell behavior in response to shear stress has been extensively studied since the observation that regions of the arterial tree where flow is unidirectional and axially aligned have no intimal thickening whereas regions of low shear stress and flow separation exhibit intimal thickening and correspond with the presence of atherosclerosis.(44) Early *in vivo* studies of endothelial function in these regions demonstrated altered cell morphology as well as proliferation rates.(45-47) More recent *in vivo* investigations have demonstrated distinct and highly complex transcriptional profiles of cells in disturbed and undisturbed flow regions.(48)

To better understand the relationship between endothelial cells and fluid shear stress, extensive investigations have been conducted *in vitro* due to development of the cone-plate viscometer and parallel plate flow chamber.(49, 50) These early systems applied a steady, laminar shear stress to a monolayer of endothelial cells to mimic athero-protective regions of the vasculature and later oscillatory, pulsatile and re-created human vascular waveforms were added to the repertoire.(51-53) Early *in vitro* studies confirmed *in vivo* observations regarding the influence of shear stress on endothelial morphology and proliferation.(54-56) The apparent complexity of endothelial behavior began to build as studies investigated endothelial cell functions which are altered by shear stress and the mechanisms underlying this mechanical influence.

Potassium ion channels and calcium signaling are sensitive not only to presence of flow but also type of shear stress. (57-59) With respect to the specific pathogenesis of

atherosclerosis, shear stress affects endothelial uptake of LDL as well as chemotactic molecules involved in recruitment of monocytes into the vascular wall. (60-62) In addition to chemotactic signals to cells in flowing blood, endothelial cells modulate expression of surface adhesion molecules in response to shear stress. (63, 64) With respect to endothelial-blood interactions, numerous coagulation molecules including thrombomodulin and the plasminogen activators (tissue and urokinase) are affected by fluid flow. (65-67) Multiple mediators of inflammation and the reduction-oxidation balance in endothelial cells are also affected by the nature of the mechanical environment imparted by flowing blood. (68-70)

With so many cell functions affected by shear stress, it became clear that the major signal transduction pathways must also be affected. Studies identified shear-induced changes in the mitogen-activated protein kinases, protein kinase C and NF-kappa B. (71-74) The question of mechanisms behind endothelial cell response to shear stress and the "mechanosensors" involved in transducing these signal became hotly debated. Discovery of a shear stress response element in the promoter region of several genes confirmed a direct influence of fluid flow on transcription. (75, 76) Additional mechanosensors including ion channels, caveolae, G proteins and integrins were quickly added to the list. (77, 78)

Widespread belief in broad endothelial gene expression changes induced by mechanical environment was confirmed in multiple studies. (79) More recently, transcriptional profiling has demonstrated the extent of changes in endothelial gene expression and the cell's ability to distinguish between different types of shear stress. Microarray analysis of cells exposed to steady laminar shear and arterial waveforms from

athero-susceptible and athero-resistant regions of the vasculature have provided valuable insight. (80-83) The endothelial cell sensitivity to shear stress and relationship to atherosclerosis presented here is merely the tip of the iceberg. Recent reviews provide an excellent picture of the links between disease, cell biology and mechanical forces. (3, 84, 85)

While not as heavily investigated as the role of shear stress in modulating endothelial phenotype, research has also been conducted into the effects of other environmental components such as extracellular matrix and smooth muscle cells on endothelial function. Investigations were launched into the role of extracellular matrix and endothelial function with specific focus on angiogenesis, vascular migration and vascular patterning as motivated by the field of cancer biology. Different basement membrane proteins appear in a spatially and temporally regulated manner during angiogenesis *in vivo* and also control cell proliferation *in vitro*.(86) Further sensitivity of endothelial cells to extracellular matrix was demonstrated in studies showing differential regulation between assembled, solid forms and degraded, soluble forms with influence being determined by composition, structural integrity as well as exposure of various degradation sites.(87) Over the course of angiogenesis, extracellular matrix proteins were shown to both stabilize the vessel as well as promote migration and proliferation.(88) The mechanisms by which extracellular matrix controls vessel patterning including the binding and display of growth factors, chemo-attractant and chemo-repellant molecules.(89)

Beyond studies of the microvasculature, endothelial cells in culture are both affected by extracellular matrix substrates provided and are involved in secreting their

own basement membrane. (90, 91) Not only do endothelial cells generate extracellular matrix but they also degrade it as needed thus implying a highly interactive relationship. (92) With regard to specific endothelial functions, matrix is also known to control growth and differentiation as well as production of molecules including glycosaminoglycans and prostaglandin.(93, 94) A naturally-derived complex extracellular matrix often used in studies of endothelial cell biology is a reconstituted basement membrane secreted by the EHS mouse sarcoma. Commercially known as Matrigel, the presence of numerous basement membrane proteins in defined proportions has significantly contributed to the understanding of vascular network formation.(95)

Investigations of shear stress and extracellular matrix influence on endothelial cell behavior converged with the study of integrin signaling. Endothelial adhesion to specific extracellular matrix proteins through members of the integrin family alters cellular response via specific signal transduction pathways.(96, 97) These same integrin signaling pathways are critical in transmitting signals induced by shear stress.(98) Thus we are reminded that endothelial cells *in vivo* are exposed not only to shear stress or only extracellular matrix but both stimuli concurrently.

The *in vivo* endothelial cell environment also includes a number of other cell types in both the blood and the vascular wall. Smooth muscle cells underlying the endothelium in large conduits and pericytes wrapping the microvasculature have been studied extensively in their own right as well as in conjuction with endothelial cells.(99, 100) With a focus on atherosclerosis, this discussion will be limited to endothelial-smooth muscle interactions of the arteries.

To study the relationship between endothelial and smooth muscle cells *in vitro*, a number of co-culture systems were developed. Soluble, unidirectional communication has been investigated using conditioned medium or cell homogenate applied from one cell type to the other.(101) Soluble, bidirectional communication thus including feedback mechanisms is examined using co-cultures of the two cell types separated by a porous membrane.(102-104) Finally, contact-mediated communication has been studied using bilayer or spheroid culture methods.(105, 106) Initial studies focused on endothelial control of smooth muscle cell function including growth factor production, migration and proliferation.(101, 103, 107) Later studies recognized the corresponding influence of smooth muscle cells on endothelial cell function. Smooth muscle cells were shown to influence endothelial proliferation, cytokine secretion and growth factor production as well as endothelial quiescence and response to external growth factors.(106, 108)

With the development of models demonstrating endothelial response to shear stress and resulting smooth muscle vasoactivity, the concurrent presence of shear stress and smooth muscle cells in the *in vivo* endothelial environment was underlined. One elegant system to evaluate simultaneous presence of smooth muscle cells and shear stress on endothelial cells involved co-culture of the two cell types of opposite sides of polypropylene capillary tubes which were then bundled together and fluid flowed through the lumens thus shearing the endothelial cells.(109) The dual influence of smooth muscle cells and shear stress was then shown to influence endothelial nitric oxide synthase (eNOS) and cyclooxygenase (Cox) expression, both of which have an established role in vascular disease.(110) Another approach uses endothelial and smooth muscle cells co-

cultured on opposite sides of a permeable membrane and a modified parallel plate flow chamber to shear the endothelial surface. Results demonstrated that smooth muscle cell contact induced endothelial cell adhesion molecule expression under static conditions however the presence of shear stress would counteract this effect.(111) Thus we conclude not only are shear stress and smooth muscle cells both regulators of endothelial behavior; they have influence over similar pathways.

Cell Communication: Connexins & Gap Junctions

In studying endothelial cell function in physiologic and pathologic processes, it is clear that each does not act independently but instead there is a coordinated response. Communication between endothelial cells is critical to numerous functions and occurs through soluble factors, binding of cell surface receptors and even transmission of physical forces. (10) One method of cell-cell communication in the endothelium is by the most direct pathway: an open pore between two cells for the instant sharing of information. This pore is created by gap junctions which are the focus of several studies in this dissertation and will thus be reviewed in detail.

A gap junction forms when a hemichannel from one cell docks with a hemichannel from a neighboring cell to create a pore connecting the two cells together. Hemichannels, also called connexons, are an array of six connexin proteins which bond to form a single unit which is inserted into the plasma membrane. The gap junction channel opens and closes to allow the flow of electrical and chemical information in the form of ions, second messengers and metabolites smaller than 1000Da. Figure 2.1 depicts a schematic of the hierarchy of gap junction assembly.

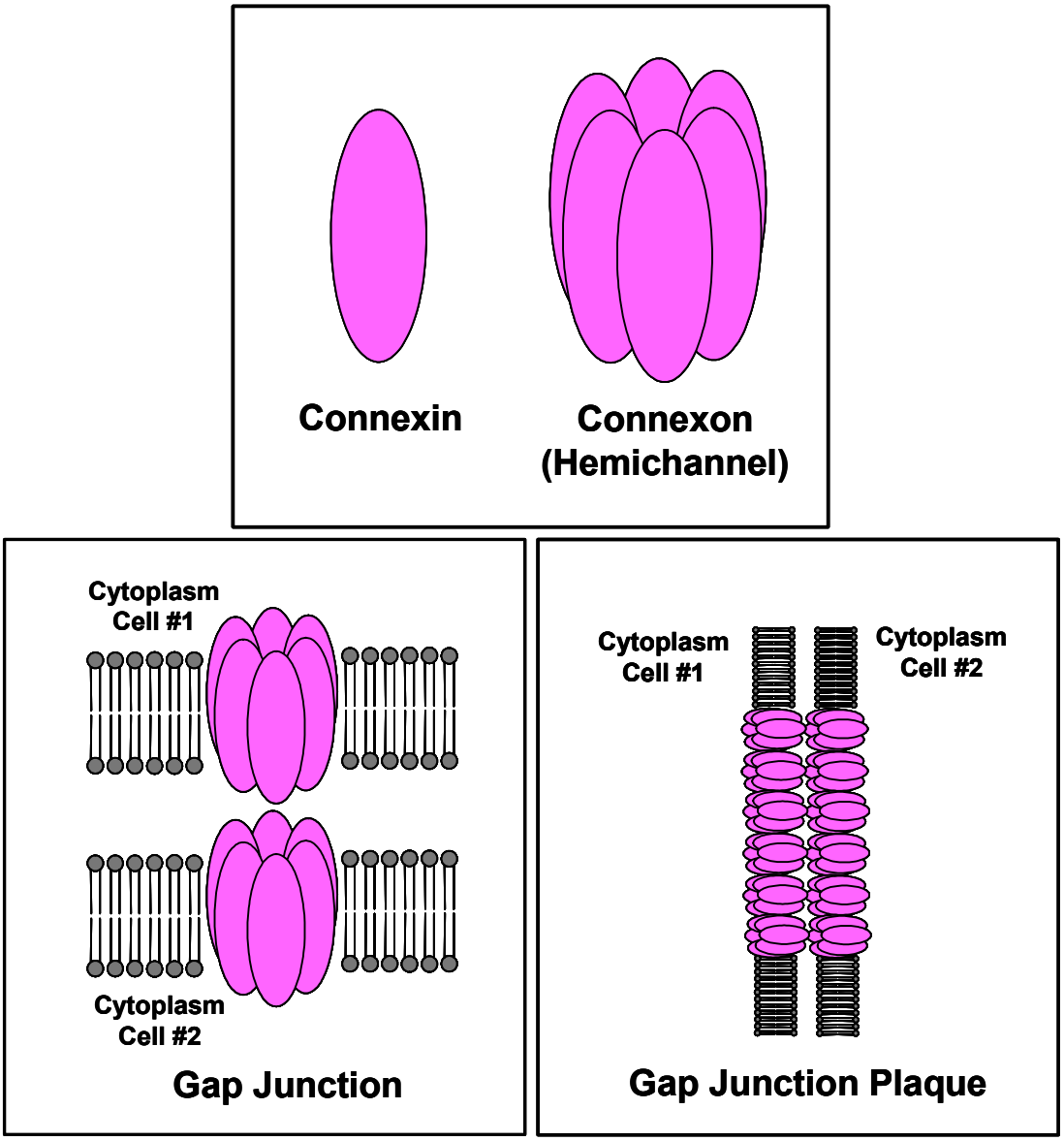

Figure 2.1 Connexin, Hemichannel, Gap Junction and Gap Junction Plaque Hierarchy

A single connexin protein (of which there are over 20 isotypes) clusters with five other connexins in a hexameric array to form a connexon (hemichannel). One hemichannel from each of two neighboring cells docks together to form a gap junction and then multiple gap junctions cluster together in the membrane to form a gap junction plaque.

Currently over twenty isotypes of connexin have been identified and are named by their molecular weight. Figure 2.2 shows the structure of a connexin protein in the cell membrane. The protein contains four transmembrane regions along with two extracellular domains and one cytoplasmic loop. The N-terminus and C-terminus are both located within the cytoplasm. While the majority of the connexin protein structure is conserved amongst the different isotypes, unique characteristics are usually found in the C-terminus which is thought to potentially be involved in gating and giving the channel particular charge and size characteristics. (112)

Gap junctions cluster in the membrane at regions of cell-cell contact to form a gap junction plaque and regulate flow of chemical and electrical information through their pores. While classically connexins and hemichannels were thought to only function when assembled into gap junctions, new evidence demonstrates otherwise. Hemichannels are routinely identified in the cell membrane but it has been assumed that their pores were closed and they were simply moving towards a gap junction plaque. (113) Data now shows that hemichannels do open with functions including release of ATP and propagation of calcium waves. Furthermore, their open/closed state is highly regulated by membrane voltage and pH. (114-116) There is also new evidence supporting functions for connexins which are independent of hemichannels or gap junctions. Connexins are often seen in the nucleus or cytoplasm and studies have shown they play roles in controlling cell growth and tumorigenicity as well as cell differentiation. (117) While knowledge regarding connexin and hemichannel functions is building, understanding of specific regulatory mechanisms remains limited.

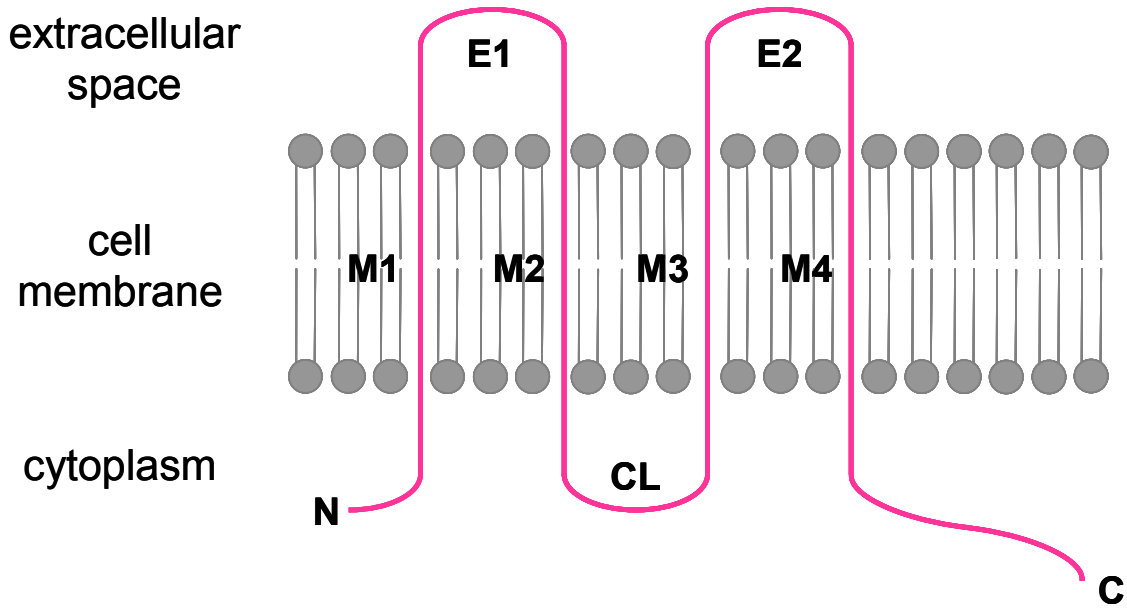

Figure 2.2 General Connexin Protein Structure

Connexin protein structure is conserved across multiple isotypes and contains four transmembrane regions, two extracellular domains, one cytoplasmic loop. The N-terminus and C-terminus are located within the cytoplasm and are thought to be involved in gating of the gap junction pore.

Connexins and gap junctions in the cardiovascular system were first studied in the heart for their roles in connecting cells of the myocardium and propagating electrical signals regulating heart beat. Changes in levels of connexin expression or alterations in pattern of connexin expression are known to lead to numerous cardiac rhythm abnormalities. (118) Recently interest in the role of connexins in the vascular wall has begun to build with evidence that they play critical and poorly understood roles in vascular development and disease. Endothelial cells are known to express Connexin 37, Connexin 40 and Connexin 43 while smooth muscle cells express Connexin 40, Connexin 43 and Connexin 45. (13, 119) Distribution of these connexins varies amongst vascular beds and in different species as well as between *in vivo* and *in vitro* experimental settings. (120, 121) It is thought that the heterogeneity in cellular and vascular bed distribution is linked to specialized functions of the connexin isotypes and needs for cellular communication that are not yet understood. (122) Gap junctions coordinate cellular responses within the endothelium and also within the layers of smooth muscle cells in the vascular media. In addition to homocellular connections, heterocellular connections also exist. Most notably, there are myoendothelial gap junctions (MEGJ) which link endothelial cells and smooth muscle cells together. (120, 123) While their existence was only recently confirmed, it is believed that signals passed through myoendothelial gap junctions function to control vascular tone. (124).

Properties and Regulation of Gap Junctions

The life cycle of a gap junction is usually rapid with half-lives documented starting at 1 hour and regulation occuring at numerous points. Connexins are transcribed

from the DNA into mRNA and then translated into protein in the rough endoplasmic reticulum (ER). Connexin proteins oligomerize into hemichannels in the rough ER or in the trans Golgi network. They are trafficked to the cell surface in vesicles and inserted into the plasma membrane where they travel to the periphery of a gap junction plaque to dock with hemichannels from a neighboring cell. (113, 125) Connexins which are misfolded do not get incorporated into the membrane but are degraded in the proteosome. Gap junctions are removed from the center of the plaque in annular gap junctions, which contains hemichannels and membrane from both cells, and are trafficked to lysosomes where they are degraded. Degradation is not an all or none phenomenon as there are documented cases of partial truncation and diversion to the proteosome rather than the lysosome. (126, 127)

While much regulation of gap junction function is related to the open/closed state of the pore and trafficking of channels to and from the membrane, it is increasingly clear that connexins are highly regulated. A widespread trend of mismatched levels of mRNA and protein for connexins in the literature is noted in multiple recent reviews. (128-130) Explanations for this phenomenon may lie in the complex processes used by cells to control connexin expression, gap junction formation and cell communication; however the mechanisms underlying these processes are largely unknown. Initial investigations of gene structure and mRNA translation provide some insight into potential mechanisms however studies in these areas are ongoing.

At the transcriptional level, mouse genes for Cx37, Cx40 and Cx43 have been analyzed to evaluate structure and potential regulatory mechanisms. All three genes contain a TATA box and numerous putative transcription factor sites. Cx37 is known to

also contain a GC box and a CCAAT box which may be involved in its regulation. (130) Cx40 and Cx43 both contain transcription factor binding sites for SP-1, AP-1 and AP-2 as well as several other sites unique to each gene. (131, 132) Human connexin sequences are similar to the mouse although some differences have been noted and future studies based on the sequencing of the human genome are sure to provide additional information. (133-135)

At the post-transcriptional level, multiple mechanisms are thought to be involved in connexin regulation including mRNA stability, mRNA localization, rate of translation, efficiency of translation, and translation in the absence of normal machinery. Specific mechanisms of control for connexins which are currently being investigated include sequences in the 5'UTR (untranslated region) and uORF (upstream open reading frame) as well as the presence of an IRES (internal ribosome entry sequence).

Cx37 is the least investigated of the vascular connexins due to its relatively recent identification and restricted expression in the body. Post-transcriptional control has not been specifically investigated for Cx37 although differing levels of mRNA and protein have been commonly seen. (130) Additionally, all connexin genes have a 5'UTR longer than the normal length for cellular mRNAs (>50 nucleotides) which has been suggested to include a mechanism of regulation which requires a longer sequence. (136) Mouse Cx40 was shown to contain a number of alternative promoters which result in multiple mRNA transcripts which contain identical coding regions but varied 5'UTR. (128) It is currently unknown if this influences the translatability of the Cx40 message but similar structures in Cx32 and Cx43 have just such an effect. Additionally, some Cx40 mRNA transcripts contain an extra noncoding exon whose function is currently unknown but has

been hypothesized to be involved in translataional control, mRNA localization or mRNA stability.

Due to the early identification and widespread importance of Cx43, it is the most heavily investigated of the vascular connexins. Analysis of Cx43 structure has identified mechanisms of post-transcriptional control involving an IRES and additional exons for alternative 5'UTRs. (129, 137) An internal ribosome entry sequence (IRES) as detected in Cx43 is relatively uncommon in cellular mRNA because it allows the ribosome to translate the mRNA into protein from a point inside the sequence rather than at the 5' cap which is normally required to start translation machinery. The advantage of this system is that translation can occur under cellular conditions where the 5' cap may be unavailable thus allowing the cell to maintain production of critical proteins. (136) Furthermore, it has been shown that IRES activity in cellular mRNAs can be modulated by mitotic stimuli, hypoxia and other stresses which adds an additional level of control. (138) Finally, analysis of mouse Cx43 structure has shown the presence of four additional exons encoding for different 5'untranslated regions (UTR). (129) Using different promoters and alternative splicing there are nine different mouse Cx43 mRNA transcripts which vary only in non-coding regions and have been demonstrated to exhibit a range of translational efficiencies. It is unknown at this time if the human Cx43 sequence also contains multiple additional 5'UTRs and if so, whether they play a role in mRNA stability and translation.

Along with regulation of mRNA and protein expression, connexin function is also modulated through phosphorylation sites. All connexins except Cx26 are phosphoproteins although the precise interacting partners and downstream functions for

each connexin isotype are not fully known. Phosphorylation has been implicated in connexin biosynthesis, trafficking, assembly, membrane insertion, channel gating, internalization and degradation. (113, 114, 126, 139) Connexin 43 is most extensively studied for its phosphorylation properties with several known consensus sites identified in the carboxy terminus which is located in the cytoplasm during membrane insertion. Several of these phosphorylation sites are known targets of protein kinases including protein kinase C and MAPK. (140) Both mouse and human Connexin 37 are thought to be phosphorylated mainly on their serine residues, however interacting proteins have not be definitively determined. (141, 142)

Six individual connexin proteins assemble together to form one hemichannel and two hemichannels form one gap junction, thus twelve connexin proteins are involved in creation of one gap junction. It was originally believed that only connexins of one isotype could interact to form a hemichannel or gap junction, however the ability of certain connexins to mix and match has now been demonstrated. (112, 143) Three types of gap junction channels are possible: i) homomeric/homotypic ii) homomeric/heterotypic iii) heteromeric/heterotypic. Homomeric or heteromeric refers to the connexins which make up a hemichannel and homotypic or heterotypic refers to the hemichannels which make up a gap junction. Homomeric/Homotypic (HoM/HoT) gap junctions are assembled from one type of connexin making up the hemichannel in one cell binding to a hemichannel from another cell made of the same connexins. Homomeric/Heterotypic (HoM/HeT) gap junctions are assembled from two hemichannels where the connexins in each hemichannel are the same but the hemichannels from the two cells are of different connexins. Heteromeric/Heterotypic

(HeM/HeT) gap junctions are assembled from hemichannels with more than one type of connexin. If two connexins are expressed in a given cell population, then 14 hemichannel combinations are possible resulting in 196 possible gap junction combinations. If three connexins are expressed in a given cell population, then 21 hemichannel combinations are possible resulting in 441 possible gap junction combinations.

To further complicate matters, mixed gap junctions have properties of voltage-dependent gating, chemical gating, permeability and selectivity which are different from their single-connexin counterparts. (144-146) Gating of gap junction channels is often regulated by membrane voltage and different connexin isotypes are sensitive to different voltage ranges. Compared to HoM/HoT junctions, HoM/HeT junctions exhibit a variable degree of asymmetry in voltage gating rather than an average of the two connexins involved. This may be explained by multiple voltage-sensitive gates or modification of gating behavior in docking of the two different hemichannels. In HeM/HeT junctions, one might assume that the overall channel gating behavior would arise from the relative contributions of each connexin involved. While this is sometimes the case, studies have demonstrated behaviors not predicted solely by composition. This may be explained by some connexins dominating over others, interactions amongst connexins within the hemichannel and interactions between the two hemichannels.

Gap junction gating is also influenced by chemical environment and most notably the pH. Data suggest that connexin-connexin and hemichannel-hemichannel interactions combine to influence the sensitivity and kinetics of the pH-sensitive gating response. A similar phenomenon is seen in channel permeability and selectivity. While these

characteristics are predominantly determined by the size of the channel pore, there are also electrostatic charges lining the pore and charges lining the vestibule region which contribute to specificity. It appears that some connexins dominate over each other, similar to a "limiting reagent" phenomenon, however the numerous combinations of HeM/HeT channels in addition to the multiple dyes with various characteristics make a thorough characterization of these properties very difficult.

Of the vascular connexins, Cx37 and Cx40 are known to form HoM/HeT junction with conductance properties different from homotypic Cx37 or Cx40 junctions. (147) Heteromeric mixing of Cx37 and Cx40 is certainly possible but has not been investigated to date. Cx37 and Cx43 form both HoM/HeT and HeM/HeT junctions. Heterotypic cell pairs display asymmetric voltage dependence and the HeM/HeT cell pairs have characteristics distinct from HoM/HoT and HoM/HeT combinations indicating interactions between the connexin isotypes. (142, 148) Connexins 40 and 43 have also been demonstrated to form HoM/HeT and HeM/HeT gap junctions. Each combination has properties which are distinct from other permutations indicating both connexin-connexin and hemichannel-hemichannel interactions. (149-151)

Vascular Connexins

With a focus on endothelial cell biology, it is most intriguing to note that while gap junctions form between endothelial cells, they also form between endothelial cells and smooth muscle cells, pericytes and neutrophils. Investigating these heterocellular gap junctions is important in understanding the roles they play in normal vascular function and disease. It is widely believed that the direct communication between

endothelial cells and smooth muscle cells, in addition to the connections which exist among each cell type, allow the vascular wall to act as a unit in response to a stimulus. (122) Early studies of conductivity in arterioles first suggested that endothelial and smooth muscle cells are electrically coupled in both a homocellular and heterocellular manner. (152) Subsequently, multiple dyes were used to trace the patterns of the potential endothelial-smooth muscle cell coupling units. (153) Anatomical evidence for myoendothelial gap junctions was then uncovered along with studies identifying movement of calcium and endothelial-derived hyperpolarizing factor directly between the two cell types. (154-156) The first *in vitro* study of myoendothelial gap junctions was recently reported where an endothelial-smooth muscle cell co-culture system was developed to better understand the role of specific connexin isotypes in their formation. (157)

Similar to smooth muscle cells, gap junctions between pericytes and endothelial cells have been detected *in vivo*. (158) *In vitro* investigations have shown gap junctions between microvascular endothelial cells, between pericytes and in co-culture models, transfer of dye and nucleotides between the two cell types. (159) More recently it was discovered that endothelial cells communicate directly with cells present in blood. Neutrophils couple to endothelial cells through gap junctions during transmigration into the vascular wall. (160)

Gap junctions in the vascular system are responsible for communication between cells and coordinating signals for a tissue-level response. However, as with most biological systems critical to normal function, alterations in the system can lead to disease and disease in turn can impact the system. While roles for connexins have been

identified in both cardiac dysfunction and angiogenesis, we will focus on the evidence linking gap junctions to hypertension and atherosclerosis. (11, 118, 161, 162) In a recent study, the Cx43 gene was knocked out only in vascular endothelial cells therefore providing a model in which the role of connexins in the vascular wall can be studied without the confounding influence of perinatal death or impaired fertility of mice. Of particular interest is the finding that the VEC Cx43-/- mice exhibit hypotension and bradycardia compare to heterozygous littermates indicating a role for endothelial cell Cx43 in maintaining normal vascular function.(163) Further demonstrating the link between connexins and hypertension are results from spontaneously hypertensive rats which show reduced connexin expression compared to normal controls. (164) Rats induced for hypertension also show reduced Cx37 and Cx43 expression but no change in Cx40 expression in endothelial cells compared to normotensive animals. This reduction can be partially recovered by one drug treatment and completely restored by another drug treatment. (165)

Connexins in the vascular wall have also been linked to the prevalence of atherosclerosis and have been shown to vary in expression with the progression of plaques. Heterozygous Cx43+/- mice exhibit a 50% decrease in atherosclerotic plaques *in vivo* and *in vitro* experiments have shown that statins reduce the Cx43 expression in endothelial and smooth muscle cell cultures. (166) Cx37 and Cx40 expression is reduced in endothelial cells of hyperlipidemic mice and only Cx37 levels recover with lipid-lowering drug treatment. (167) An altered pattern of connexin expression in endothelial and smooth muscle cells is seen in non-diseased arteries, early atheromas and advanced

atheromas. (168) Finally, naturally occurring Cx37 variants have also been implicated in the prevalence of atherosclerosis in human populations. (169)

With their primary function being to promote communication between cells, gap junctions are critical in development of many tissues. There are four connexins expressed in the developing mouse heart: Cx37, Cx40, Cx43 and Cx45. Cx37 is expressed in endothelial cells of blood vessels and in the endocardium, Cx40 is expressed in myocytes and appears to be regionally controlled while Cx43 often has either overlapping or complementary expression to Cx40 depending on the tissue region. (170) Knockout connexin models elucidate functions in development but attempts to study connexin influence on vascular wall biology have been hampered by the widespread expression of these molecules in other tissues and the drastic influence of knocking out the gene in all tissues. Cx37-/- mice are viable but females are infertile because of abnormal development of both oocytes and ovarian follicles. (171) Cx40-/- mice are viable but have prolonged atrioventricular conduction, right bundle branch block and a predisposition for arrhythmias. Furthermore, Cx40-/- mice have diminished conduction of arteriolar dilatation in response to acetylcholine and bradykinin and are hypertensive but have no other obvious blood vessel abnormalities. (172) Cx43-/- mice die perinatally due to abnormal development of the pulmonary outflow tract from atypical migration of cardiac neural crest cells. (173) Single knockout connexin mice have characterized phenotypes which are largely non-blood vessel related because of the widespread expression of these molecules and their presumed functional overlap within the vessel wall. When *in vivo* expression of connexins is reduced further using a multiple knockout strategy, there are severe blood vessel abnormalities indicating an important interplay

between the functions of connexins. Cx37-/- Cx40-/- mice die perinatally with hemorrhages and severe blood vessel dilatation. (174) Cx40-/- Cx43-/- have also been reported to die at E12.5 with malformed hearts including abnormally rotated ventricles.(175)

While knockout models provide valuable information regarding the missing gene, several reports have identified effects on non-ablated connexins. Evaluation of Cx40-/- mice found expression of Cx37 protein upregulated three-fold and redistributed in a more homogeneous manner. (176) In a separate study of Cx37-/- and Cx40-/- mice, data showed a drop in endothelial Cx40 protein in Cx37-/- animals and a drop in endothelial Cx37 protein in Cx40-/- animals however no changes in mRNA levels were detected. (177, 178) An additional evaluation of Cx40-/- animals showed reduced staining of endothelial Cx43 at the cell membrane and reduced expression of smooth muscle cell Cx43. (179) Evidence of reduced Cx43 expression in smooth muscle cells of animals where Cx43 was knocked out only in endothelial cells (VEC Cx43-/-) supports the hypothesis that effects on non-ablated connexins are not restricted to one cell type. (163) Following a complementary approach, a study which transfected endothelial cells with an adenovirus for Cx37 demonstrated no change in Cx43 mRNA but a substantial drop in Cx43 protein. (180)

While effects on non-targeted connexins in knockout models suggest overlapping functions of connexin isotypes, differential responses to chemical and pathologic stimuli have been demonstrated. In endothelial cells, Cx43 is highly expressed in subconfluent cultures and levels decrease at confluence while Cx37 levels are minimal at subconfluence and rise when cells contact. Furthering this polarity in behavior of

connexin isotypes is response to TGF-β1 where Cx43 levels increase and Cx37 levels decrease. (181) Nitric oxide has also been shown to differentially affect endothelial connexin isotypes by decreasing coupling of gap junctions which contain Cx37 and increasing new formation of gap junctions which contain Cx40. (182, 183) In response to injury *in vivo*, rat endothelial connexin expression drops initially and then over time Cx40 expression returns to normal while Cx37 and Cx43 are expressed at higher levels than uninjured artery. (162) In response to injury *in vitro*, wounding of an endothelial monolayer results in upregulation of Cx43 at the wounded edge, decrease in Cx37 at the injury site and no change in Cx40. (184) Exposure of human endothelial cells to TNF-α resulted in a downregulation of Cx37 and Cx40 mRNA while Cx43 mRNA was unaffected. (185) Finally, sepsis induced in a rat model increased Cx40 mRNA but did not alter expression of endothelial Cx37 or Cx43. (186)

Of particular interest in the cardiovascular system where mechanical forces are known regulators of cell function, is the response of connexins and gap junctions to physical stimuli. The first insight into the potential regulation of gap junctions by mechanical forces grew out of a study focused on mapping the regional distribution of Cx37, Cx40 and Cx43 in rat endothelium. (187) While the distribution of Cx37 and Cx40 appeared in similar widespread patterns, it was noted that Cx43 expression was found mainly in regions near aortic branches where blood flow is disturbed. Introduction of a flow disturbance into this model resulted in a strong upregulation of Cx43 in areas not previously showing high levels of expression. An *in vitro* study of vascular cells and mechanical forces found a sustained upregulation of Cx43 protein in rat aortic smooth

muscle cells exposed to 20% stretch for 24 hours and a transient upregulation in Cx43 mRNA in endothelial cells exposed to laminar shear stress. (188)

Further investigation of endothelial cell Cx43 regulation by shear stress was conducted using an *in vitro* parallel plate flow chamber system which exposed cells to four types of fluid shear from recirculating to fully developed laminar flow. (189) It was found that Cx43 mRNA was transiently upregulated by all flow patterns however upregulation was only sustained after 30 hours in areas of disturbed, recirculating flow. Furthermore, Cx43 protein appeared disorganized in regions of disturbed flow and cells showed little coupling as assessed by dye transfer indicating limited gap junction communication. More recently, other endothelial cell connexins (Cx37 and Cx40) were also investigated in this *in vitro* flow system. (190) Patterns of protein expression and roles of different connexin isotypes in endothelial gap junction communication were investigated using dye transfer techniques in conjuction with peptide channel blockers. In addition to studies focusing on vascular connexin response to mechanical forces, differential expression by shear stress has been reported in numerous microarray studies. (48, 81, 83)

Although this dissertation focuses on gap junctions in the blood vessel wall, it is also interesting to note recent evidence of mechanical regulation in heart valves. A microarray study evaluating gene expression of normal porcine valve leaflets identified a downregulation of Cx43 in endothelial cells from the aortic side of the leaflet compared to the ventricular side. (191) Additionally, a separate immunohistological study evaluated the presence of connexin proteins on the upstream and downstream surfaces of rat heart valves. Assessment of valve endothelial cells concluded equal expression of

Cx37 on both sides of the valve, no detectable expression of Cx40 protein and a differential expression of Cx43 with higher expression on the upstream surface compared to the downstream surface. (192)

CHAPTER THREE: Experimental Methods

Experimental Procedures

Human Cell Culture

Human aortic endothelial cells (HAEC) (Cambrex) were cultured to passage 6 in MCDB 131 supplemented with 5% FBS, 1% penicillin-streptomycin, 1% l-glutamine, 10ng/ml EGF, 2ng/ml FGF-basic, 1ng/ml VEGF, 2ng/ml IGF-1, 50µg/ml ascorbic acid and 1µg/ml hydrocortisone. Human aortic smooth muscle cells (HASMC) (Cambrex) were cultured to passage 8 in MCDB 131 supplemented with 5% FBS, 1% penicillin-streptomycin, 1% l-glutamine, 0.5ng/ml EGF, 2ng/ml FGF-basic, 5µg/ml insulin. All experiments were conducted in a co-culture media of MCDB 131 supplemented with 5% FBS, 1% penicillin-streptomycin, 1% l-glutamine, 0.5ng/ml EGF and 2ng/ml FGF-basic which were common to both cell culture mediums.

Substrate Fabrication

Adsorbed Collagen Slide

The Adsorbed Collagen Slide substrate was created by coating a glass slide with 50 µg/ml collagen type I (BD Biosciences) and allowing protein to adsorb to the surface for one hour prior to removal of the solution. Endothelial cells were seeded at a density of 40,000 cells/cm^2 to produce a confluent monolayer and cultured for 48 hours prior to exposure to static or shear conditions.

For RNA interference studies, a silicone gasket was adhered to the perimeter of the glass slide. The gasket then provided a means to contain higher fluid volumes needed

for transfection but could be removed prior to static or shear stress experiments. Following adhesion of the gasket, slides were autoclaved and coated with 50 μg/ml collagen type I for one hour. Endothelial cells were then seeded at 35,000 cells/cm^2 and cultured for 24 hours prior to transfection.

Tissue Engineered Blood Vessel Wall Model (TEWM)

The Tissue Engineered Wall Model substrate was created by suspending 1 million HASMC per ml in 5x concentrated MCDB-131, 10% FBS and 2 mg/ml rat tail type I collagen (BD Biosciences). Sodium hydroxide was added to neutralize the acidic collagen solution and promote polymerization. Tubular HASMC-collagen gels were created using a central mandrel during gelation and were cultured for six days to allow for cell-mediated compaction of the collagen fibers. The tubular gels were then cut longitudinally and embedded in agar to expose a flat lumen for seeding of HAEC and fluid shear experiments. (43) Figure 3.1 shows a tubular HASMC-collagen gel following static culture in panel A and then embedded in agar supported by a polycarbonate mold in panel B. Endothelial cells were seeded at a density of 40,000 cells/cm^2 to produce a confluent monolayer and cultured for 48 hours prior to exposure to static or shear conditions.

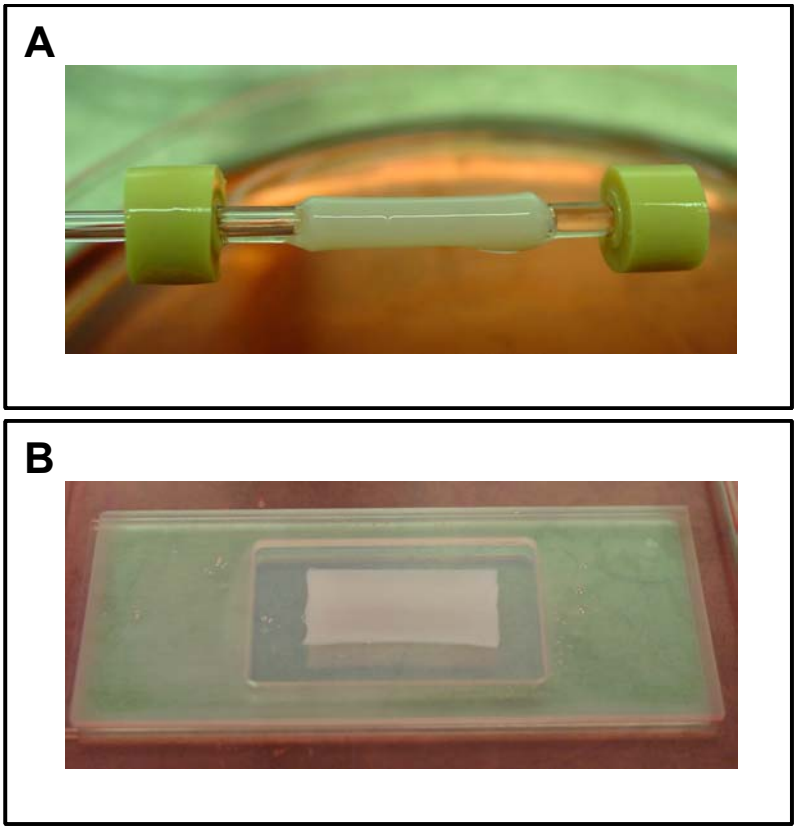

Figure 3.1 Tissue Engineered Blood Vessel Wall Model
Panel A shows a tubular HASMC-collagen gel following six days of static culture. Panel B shows the TEWM which results from cutting open the tubular gel and immobilizing the substrate using agar and a polycarbonate mold.

Exposure to Shear Stress

The parallel plate flow chamber used to expose endothelial cells to laminar shear stress has been previously established in our laboratory. (42, 49) In this closed loop, a peristaltic pump moves medium from a container into a pulse dampener and then through parallel plates where endothelial cells are exposed to a steady laminar shear stress. Shear stress is controlled by fluid flow rate and dimensions of the chamber according to the equation: $\tau = 6Q\mu/bh^2$. Exposure of endothelial cells on the tissue engineered wall model was accomplished by placing the entire mold/agar apparatus into the flow chamber as depicted in Figure 3.2. To expose endothelial cells on the slide to shear stress, the identical system was used except instead of the mold immobilized TEWM in the flow chamber, the collagen coated slide was inserted. Endothelial cells on all substrates were exposed to a shear stress of 15 dynes/cm^2 for 24 hours.

Endothelial Isolation from TEWM

To evaluate endothelial cell gene and protein expression following culture on the TEWM, pure endothelial cells must be removed without contamination of neighboring smooth muscle cells. To achieve a pure population of endothelial cells with adequate quantity for further analysis, a positive selection technique was developed. Following cell exposure to static or shear stress conditions, the TEWM lumen was briefly treated with 600U/ml collagenase and scraped gently to release cells near the surface. The cell mixture was incubated with a primary PE-conjugated antibody to PECAM-1 (Santa Cruz) to label only endothelial cells and not smooth muscle cells.

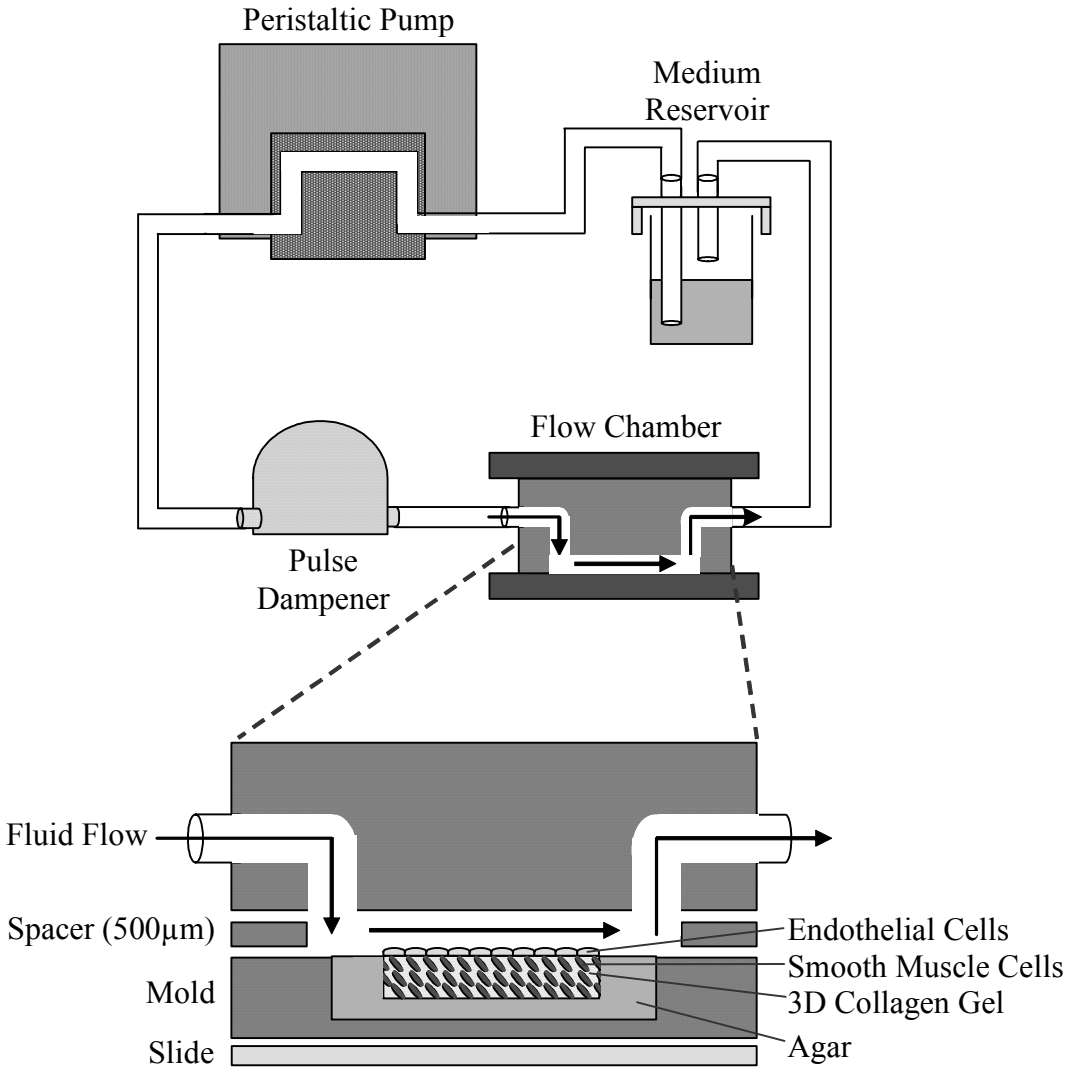

Figure 3.2 Parallel Plate Flow Circuit Exposes Endothelial Cells to Shear Stress
Endothelial cells can be exposed to shear stress in the flow chamber on a TEWM substrate (as depicted) or on an Adsorbed Collagen Slide substrate.

Following a brief wash, the cell mixture was then incubated with a magnetic bead-conjugated secondary antibody to PE which binds the primary antibody. The cell mixture with labeled endothelial cells was passed through a separation column placed in a magnetic field. Due to the magnetic bead secondary antibody, endothelial cells were trapped in the column and smooth muscle cells passed through into the negative effluent. Following multiple washes, the separation column is removed from the magnetic field and trapped endothelial cells are flushed out into the positive effluent. With the entire process lasting 45 minutes and conducted almost entirely on ice or at 4°C, endothelial cells can be fixed or lysed for mRNA or protein analysis.

Effectiveness of the magnetic separation procedure was validated using pre-labeled endothelial cells mixed with smooth muscle cells and flow cytometry analysis post-separation. Endothelial cells in culture were incubated with 5μM cell tracker orange (Molecular Probes) in DMSO and serum-free media for 45 minutes to label the cytoplasm which would allow them to be distinguished from unlabeled smooth muscle cells in downstream analysis. Orange endothelial cells were then seeded onto the TEWM which contained unlabeled smooth muscle cells. Following the magnetic separation technique, samples of cell mixture (column feed), negative effluent and positive effluent were analyszed using flow cytometry.

Figure 3.3 details composition of the cell mixture before and after magnetic separation. Panel A shows the column feed which contains both endothelial cells (fluorescent orange) and smooth muscle cells (autofluorescence only). Panel B shows the composition of the positive effluent which contains cells which were trapped in the separation column by the magnetic field.

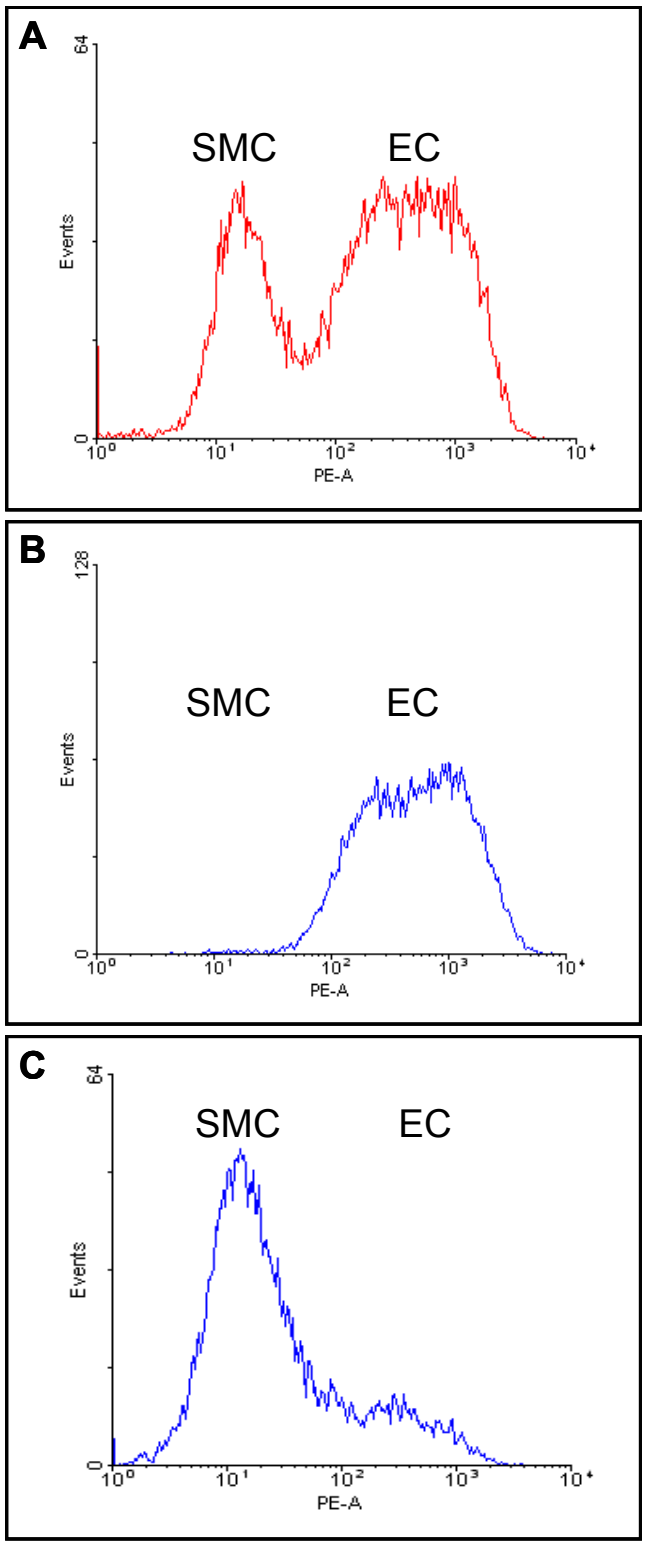

Figure 3.3 Validation of Endothelial Cell – Smooth Muscle Cell Separation
Panel A shows the mixture of endothelial and smooth muscle cells removed from the TEWM which is fed into the magnetic separation column. Panel B shows the positive effluent which is retrieved from the column following separation containing pure endothelial cells. Panel C shows the negative effluent which passes through the magnetic separation column and contains mostly smooth muscle cells.

Pure endothelial cells are selected by the column as shown by the presence of the fluorescent orange peak and absence of the smooth muscle cell peak. Panel C shows the composition of the negative effluent which contains cells which passed through the separation column and magnetic field. This cell mixture contains mostly smooth muscle cells with some endothelial cells which were not trapped in the column. Thus by positive selection using PECAM-1 based magnetic separation, a pure population of endothelial cells can be obtained in a rapid and reliable manner.

To explore any effects of the magnetic cell separation on endothelial cell gene expression, microarrays were used to compare transcriptional profiles. Endothelial cells were either i) lysed and RNA collected immediately or ii) followed the entire labeling and magnetic separation procedure prior to lysis and RNA isolation. Microarray comparisons (n=2) detected changes in 34 genes (fold change > 1.5 and p-value < 0.01) out of a total possible 12,814 genes. With changes in only 0.2% of genes and fold changes not exceeding 3-fold, the procedure does not significantly alter endothelial cell gene expression and can thus be used for subsequent analysis.

RNA Interference

RNA interference was conducted using short interfering RNA (siRNA) designed by and purchased commercially from Ambion. Multiple sequences were tested for ability to knockdown target connexin mRNA at least 70% without other adverse effects (eg. cell death). In addition to sequences targeting connexins, a negative control siRNA labeled with Cy3 (Negative Control #1 – Ambion 4621) which does not target any known human sequence was used to develop transfection protocols and to evaluate the effect of the

transfection procedure on endpoints. The following siRNA sequences designed for the human sequence were successfully used to knockdown connexin mRNA.

Cx37: Ambion siRNA ID#7185, annealed, standard purity

Cx37 Sense (5' to 3'): GGACUUGAUCACAAAAAAAtt

Cx37 Antisense (5' to 3'): UUUUUUUGUGAUCAAGUCCtg

Cx40: Ambion siRNA ID#145161, annealed, standard purity

Cx40 Sense (5' to 3'): GGUAAACGAUGCUUGGAAUtt

Cx40 Antisense (5' to 3'): AUUCCAAGCAUCGUUUACCtt

Cx43: Ambion siRNA ID# 144485, annealed, standard purity

Cx43 Sense (5' to 3'): GCCUUAUUCAUGAGGCUUAtt

Cx43 Antisense (5' to 3'): UAAGCCUCAUGAAUAAGGCtg

Endothelial cells were transfected under serum-free conditions using OptiMEM medium (Invitrogen) with the chemical transfection reagent Oligofectamine (Invitrogen). Development of transfection protocols using Cy3-labeled negative control siRNA allowed for confirmation of siRNA entry into endothelial cells and residence over time. Dosage studies showed knockdown of each connexin mRNA by >80% with siRNA concentrations ranging from 10nM to 80nM. Figure 3.4 shows a dosage study of the siRNA sequence identified which successfully knocks down Cx37. Comparison to the OptiMEM control shows a significant reduction in Cx37 mRNA with treatment doses ranging from 10nM to 80nM. Figure 3.5 shows a dosage study of the siRNA sequence identified which successfully knocks down Cx40. Comparison to the OptiMEM control shows a significant reduction in Cx40 mRNA with treatment doses ranging from 10nM to 80nM.

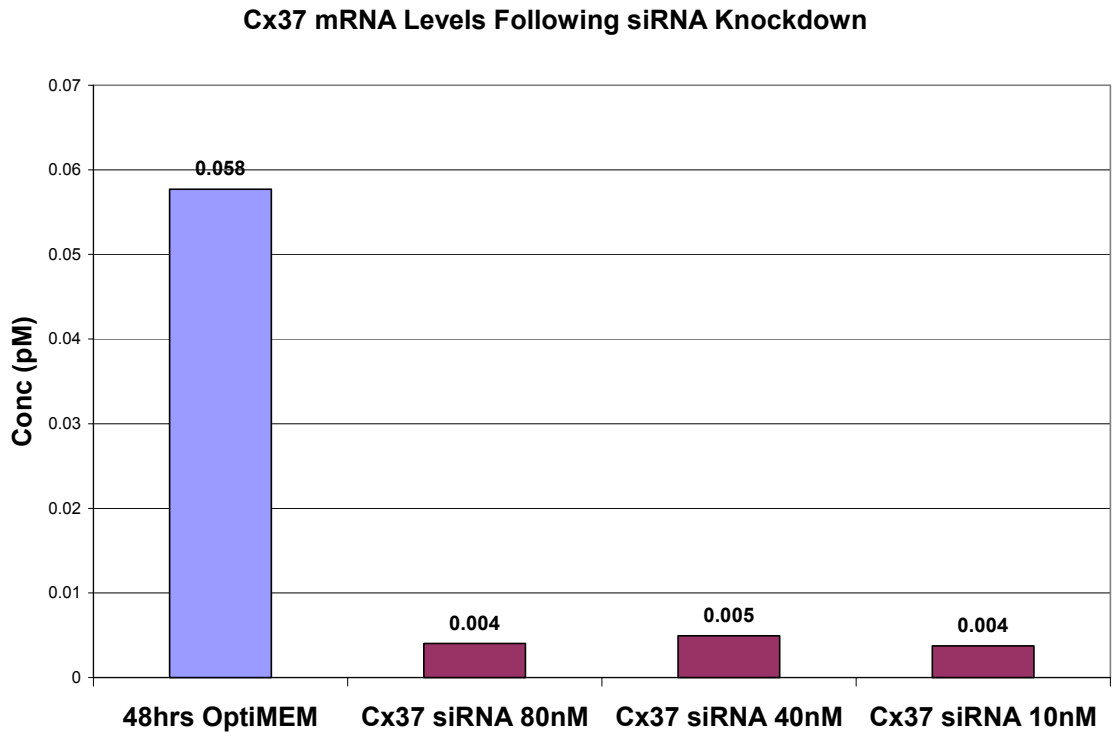

Figure 3.4 Dosage Study of Cx37 siRNA Knockdown of Cx37 mRNA

Endothelial cells treated with Cx37 siRNA at multiple treatment dosages show reduced expression of Cx37 mRNA compared to a control sample.

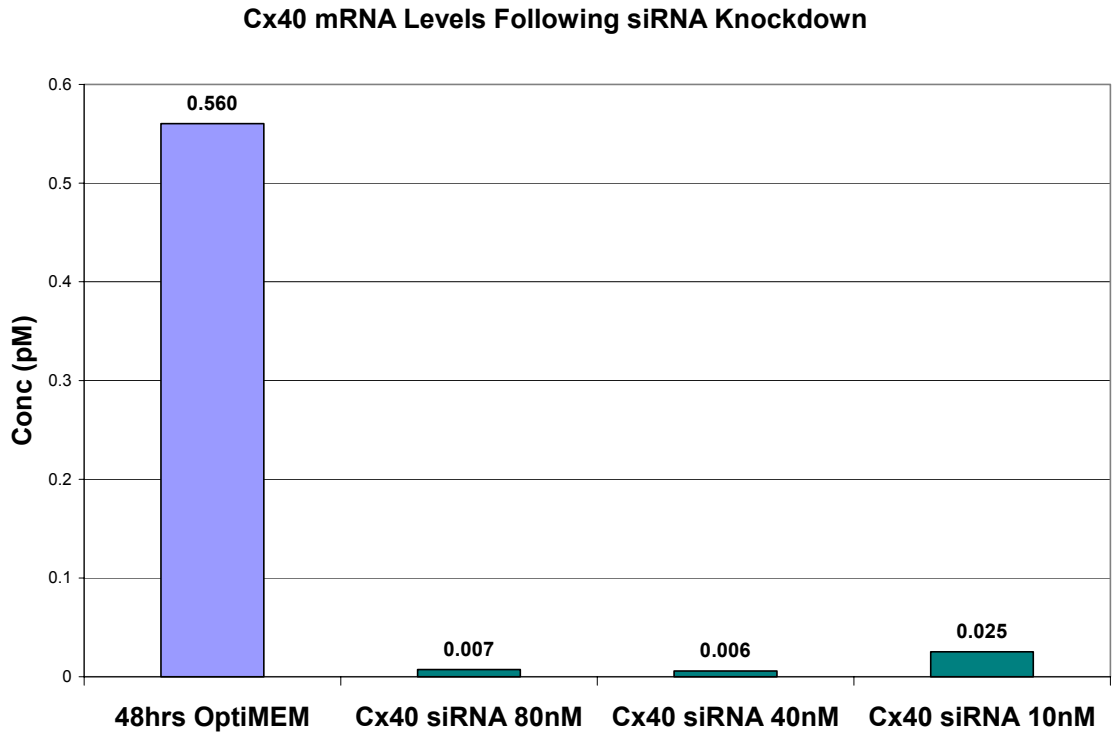

Figure 3.5 Dosage Study of Cx40 siRNA Knockdown of Cx40 mRNA
Endothelial cells treated with Cx40 siRNA at multiple treatment dosages show reduced expression of Cx40 mRNA compared to a control sample.

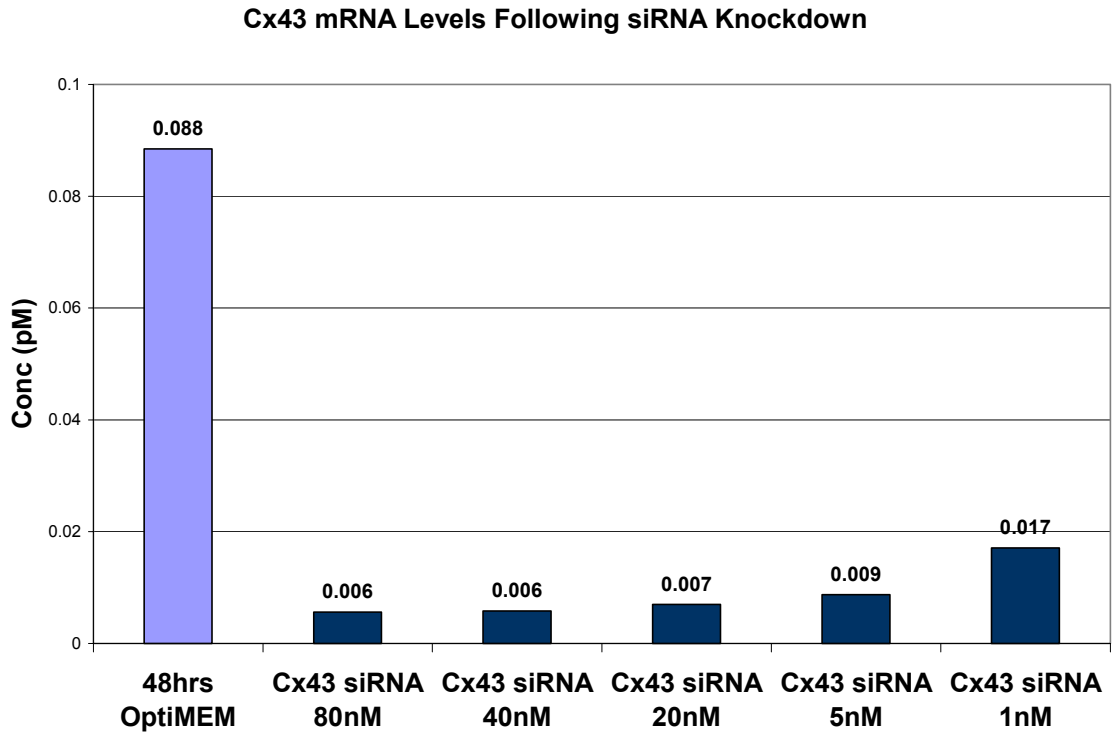

Figure 3.6 Dosage Study of Cx43 siRNA Knockdown of Cx43 mRNA
Endothelial cells treated with Cx43 siRNA at multiple treatment dosages show reduced expression of Cx43 mRNA compared to a control sample.

Figure 3.6 shows a dosage study of the siRNA sequence identified which successfully knocks down Cx43. Comparison to the OptiMEM control shows a significant reduction in Cx43 mRNA with treatment doses ranging from 5nM to 80nM. A broader range of siRNA dose using in this study shows a reduced capability to knock down Cx43 mRNA at the 1nM level.

A time course study using 10nM siRNA demonstrated knockdown of target mRNA for 96 hours following transfection. Cells were transfected starting at time zero for six hours, at which point serum was added to promote cell survival. At 48 hours, transfection reagents were removed and cells were exposed to experimental medium. This time course of RNAi steps was identical to the timeline of later experiments. Figure 3.7 shows time course data for knockdown of connexin mRNA in siRNA treated samples compared to controls. Panel A shows knockdown of Cx37 mRNA by Cx37 siRNA and panel B shows knockdown of Cx43 mRNA by Cx43 siRNA. Connexin levels are higher in OptiMEM controls compared to siRNA treated cells at 24 hours and 48 hours while cells are still exposed to transfection reagents. Removal of transfection reagents and addition of experimental medium results in an increase of connexin mRNA in control samples but the knockdown remains in effect in siRNA treated samples. Time course data shows a knockdown in connexin mRNA using RNA interference as early as 24 hours after transfection and lasting to at least 96 hours post-transfection.

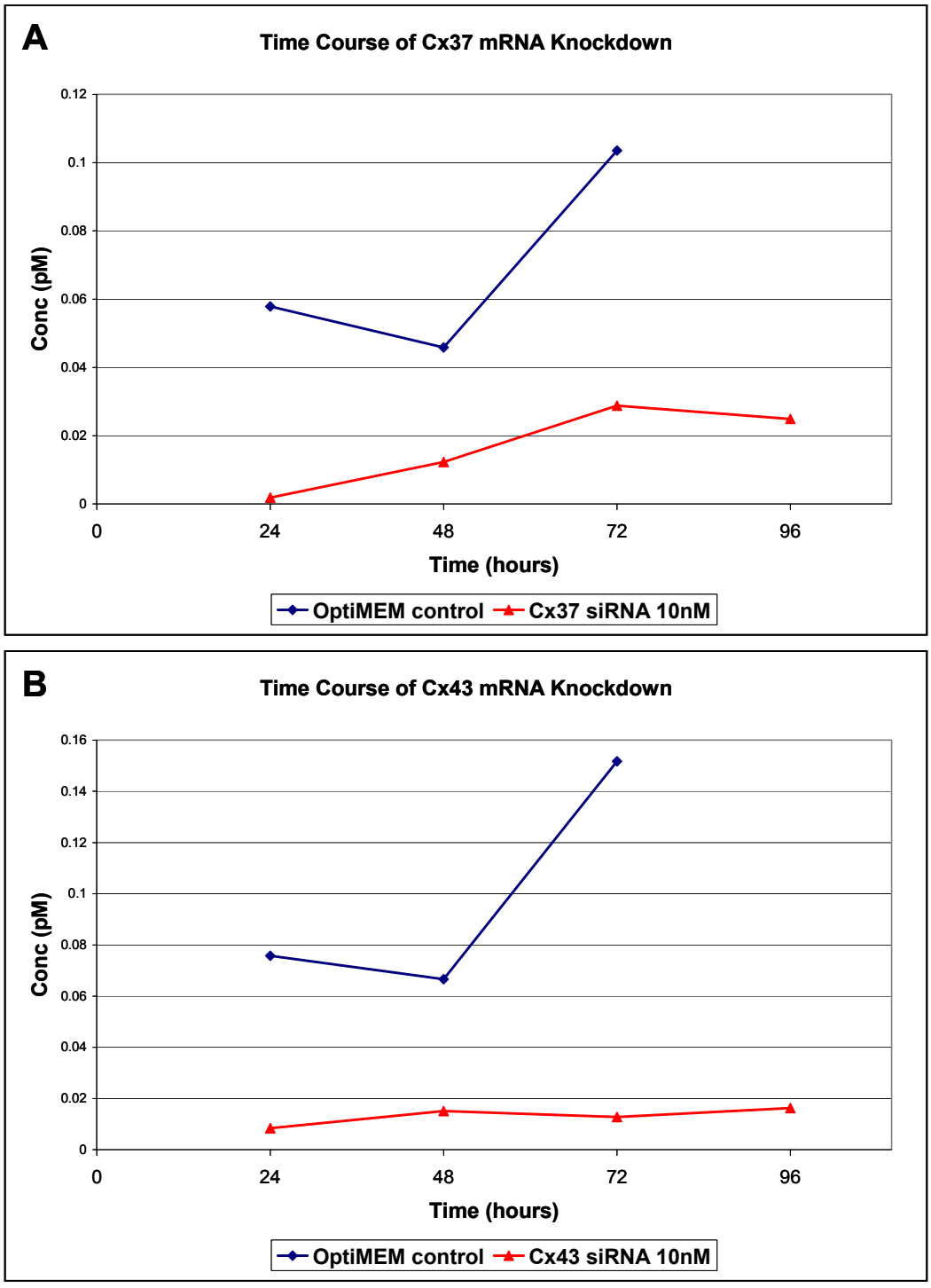

Figure 3.7 Time Course of Connexin mRNA Knockdown by siRNA

Endothelial cells treated with a low dose (10nM) of siRNA show reduced expression of target mRNA up to 96 hours following transfection. Panel A shows time course of Cx37 mRNA following Cx37 siRNA transfection compared to control. Panel B shows time course of Cx43 mRNA following Cx43 siRNA transfection compared to control.

To avoid any potential side effects of abundant siRNA in the cells but ensure a cushion of adequate knockdown, a concentration of 40nM was chosen for all studies. Thus the siRNA transfection and experimental timeline is as follows.

Endothelial cells were seeded onto collagen coated glass slides and cultured for 24 hours prior to transfection at which point they are 90% confluent. Stock siRNA in sterile, RNase-free water is diluted in OptiMEM medium and oligofectamine transfection reagent is also diluted in OptiMEM medium. The two mixtures are combined to create a transfection cocktail which sits at room temperature for 20 minutes to allow complexing of siRNA by oligofectamine. Endothelial monolayers are rinsed twice in OptiMEM to remove any remaining culture medium and thus all serum and antibiotics. OptiMEM is added to endothelial slides and the transfection cocktail is added dropwise to each sample. Cells are transferred to the incubator at 37°C and transfection proceeds for 6 hours. During the transfection process, the final concentration of siRNA is 40nM and the final concentration of oligofectamine is 0.4% (10μL in 2.5mL). After six hours, a volume of experimental media with 22% FBS is added to the OptiMEM/oligofectamine/siRNA mixture to restore the total FBS concentration to 5%. Slides are incubated for an additional 42 hours (total of 48 hours since transfection) prior to removal of the mixture of OptiMEM/oligofectamine/siRNA/FBS/experimental media and beginning of the 24 hour experimental period where cells are exposed to static or laminar shear stress. All manipulations of siRNA are conducted under sterile, RNase-free, DNase-free conditions to preserve integrity of sequences and samples.

Experimental Assays

RNA Isolation

Total RNA was extracted from endothelial cells using an RNeasy kit (Qiagen) with an added DNase digestion step. To evaluate quality of RNA prior to microarray or RT-PCR analysis, samples were assessed using the RNA 6000 Nano LabChip (Agilent) on an Agilent Bioanalyzer 2100. Profiles of ribosomal peaks were evaluated for degradation as a measure of overall RNA degradation and preliminary measurements of RNA quantity were determined. Bioanalyzer analysis can evaluate integrity of RNA samples using very low quantities due to its quantitative range of 25-500ng/μl. Of total RNA samples, approximately 90% is ribosomal RNA while only 1-3% is mRNA. Ribosomes have two subunits of differing size which allows for gel separation and evaluation. By examining the degradation of ribosomal RNA subunits, the degree of possible mRNA degradation can be determined since degradation is not specific to type of RNA. Figure 3.8 depicts electopherogram analysis of two RNA samples. Panel A shows an intact endothelial RNA sample with two clearly defined ribosomal peaks. Panel B shows a partially degraded endothelial RNA sample which is apparent from the double peak and bumpy baseline. Following screening by Bioanalyzer, quantity of high quality RNA was assessed by absorbance at 260nm prior to use in microarray or reverse transcription to cDNA for RT-PCR analysis.

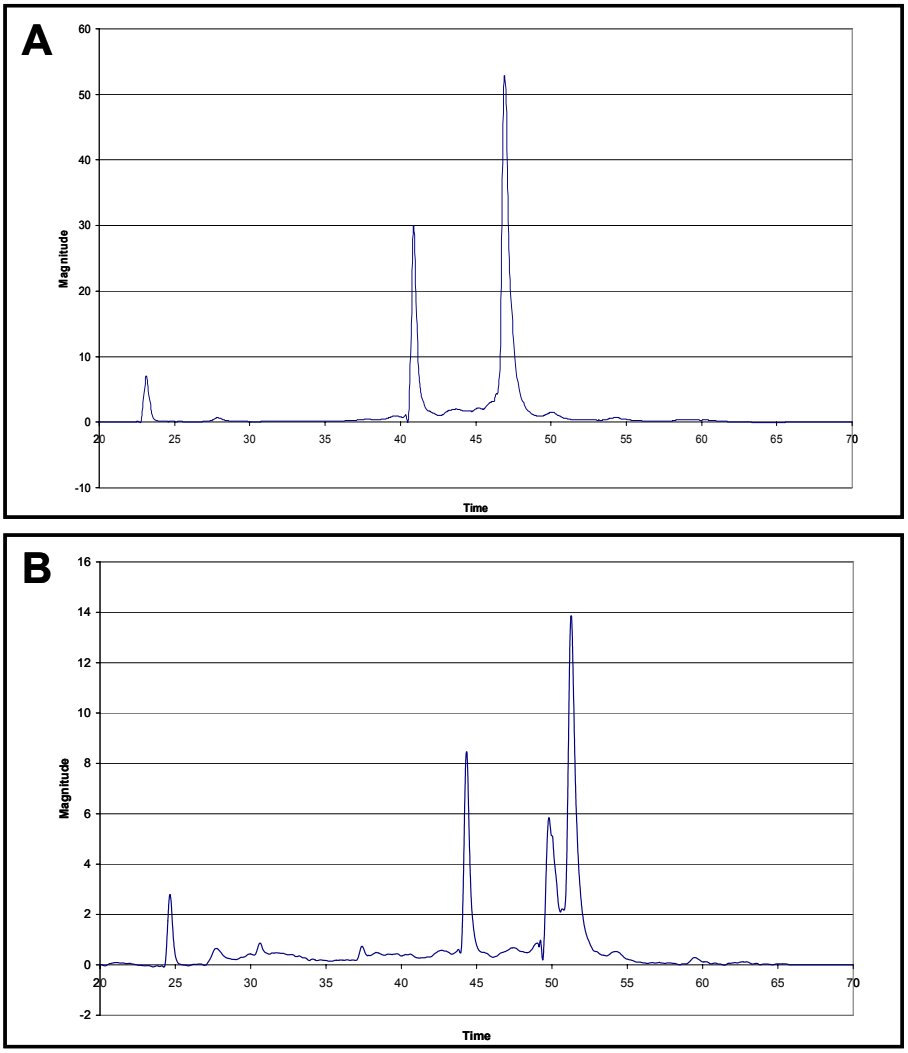

Figure 3.8 Bioanalyzer Analysis of Endothelial RNA Integrity

Bioanalyzer analysis evaluates quality of RNA samples prior to use in RT-PCR or microarray analysis. Panel A shows intact RNA with two clearly defined ribosomal subunit peaks. Panel B shows degraded RNA with a double peak in one subunit and bumpy baseline.

Microarray Hybridization

Following quality analysis by Bioanalyzer 2100 and quantity assessment by UV absorbance, 500ng of total RNA from experimental samples and from Reference RNA were prepared for competitive microarray hybridization. Samples were amplified using the Agilent Low RNA Input Fluorescent Linear Amplification Kit and labeled with Cy-3 and Cy-5 CTP (Perkin-Elmer). Hybridization was performed using the Agilent In Situ Hybridization Plus kit to 44,000 60-mer Human Whole Genome Oligo Microarrays (Agilent). Arrays were scanned using the Agilent dual laser DNA microarray scanner with SureScan technology and image extraction was conducted using Agilent Feature Extraction software 7.5.1.

Microarray Data Analysis

GeneSpring® software was used to normalize data, interpret triplicates, filter spots and generate experiment files for gene expression analysis. It was also used to calculate significance and fold change values for all genes. Ingenuity Pathways Analysis® was used to interpret genes identified as significant in the context of known biological functions and disease states.

Following hybridization, scanning and image extraction, raw data was analyzed using GeneSpring® software. First, the entire data set was examined to determine the number of spots on the array from which a signal could be read. Each spot on each array was given an evaluation and the total number of spots with flags present or marginal was determined. The second criteria was that flags for each spot be present or marginal in all twelve arrays analyzed. Following identification of spots which can be analyzed, an

ANOVA was run on the entire data set using the multiple testing correction (MTC) method: Benjamini and Hochberg False Discovery Rate. Each gene was assigned a p-value based on this ANOVA with MTC and the cutoff criteria was p-value < 1. A multiple testing correction is necessary to adjust p-values in analysis of large sets of microarray data since the number of false positives is proportional to the number of tests performed. For further analysis, the data set was split into pairwise comparisons and a student's t-test was conducted on each pair of samples to determine significance for the comparison in question. With the cutoff criteria of t-test p-value < 1, the number of genes was further reduced and the number of candidate genes for each comparison was identified. Following the number of candidate genes being identified for each comparison, the next step was to identify the genes which were significantly different. To limit false positives, the most stringent set of criteria was used to identify significantly regulated genes: ANOVA with MTC p-value < 0.05 and t-test p-value < 0.05 and fold change > 1.5.

Data were analyzed through the use of Ingenuity Pathways Analysis (Ingenuity® Systems, www.ingenuity.com). The purpose of Ingenuity Pathways Analysis (IPA) was to evaluate gene microarray data in a systematic fashion to gain insight regarding affected biological pathways and disease mechanisms. For this software analysis, the user inputs genes designated as significant based upon user-defined criteria. Genes which are entered into the program are overlaid into the Ingenuity Pathways Knowledge Base (IPKB) which is a constantly evolving database of molecular interactions developed based on published, peer-reviewed literature. Genes that are deemed significant by the user and are found to interact with at least one other gene in the IPKB are designated

"focus genes". IPA then uses computational algorithms to identify networks of molecular interactions which are enriched for the focus genes. Networks are ranked based on number of focus genes and overall size and are also assigned biological functions based on known diseases and cellular events. IPA also conducts a Functional Analysis to identify the biological functions and/or diseases that are most significant in each data set. Fischer's exact test is used to calculate a p-value determining the probability that each biological function and/or disease assigned to that data set is due to chance alone. Thus, analysis by IPA aids in biological interpretation of microarray data sets.

Quantitative RT-PCR

Quantitative RT-PCR was used to assess mRNA expression in endothelial cells exposed to multiple experimental treatments. One microgram of high quality endothelial RNA was reverse transcribed using the First Strand cDNA Synthesis Kit (Invitrogen) for each experimental sample. Additionally, a –RT control sample was generated for each experimental sample following the cDNA synthesis procedure except for exclusion of the reverse transcription enzyme. By conducting PCR on the –RT control as well as cDNA for each sample, any contamination of genomic DNA could be detected.

Primers were designed using Primer Express (Applied Biosystems) and oligos were created by Integrated DNA Systems.

Primer sequences are listed below for the four genes used in microarray data validation.

Ang2 Forward: TCCTCCTGCCAGAGATGGAC

Ang2 Reverse: TGCACAGCATTGGACACGTA

CYP1B1 Forward: TTTCGGCTGCCGCTACAG

CYP1B1 Reverse: ACTCTTCGTTGTGGCTGAGCA

E-selectin Forward: TTGGTAGCTGGACTTTCTGCTG

E-selectin Reverse: CATTTCCGAAGCCAGAGGAG

Pentaxin 3 Forward: TGGACAACGAAATAGACAATGGA

Pentaxin 3 Reverse: CTGACCGCAGTCGCACG

Primer sequences are listed below for the three connexins expressed in endothelial cells.

Cx37 Forward: CATGGAGCCCGTGTTTGTG

Cx37 Reverse: GAGACAAAGCAGTCCACGAGG

Cx40 Forward: GGGCACTCTGCTCAACACCT

Cx40 Reverse: TGAAGCCCACCTCCATGGT

Cx43 Forward: TTAAGGGAAAGAGCGACCCTT

Cx43 Reverse: GACCCACAGTCTTTGGCAGG

Standards for each gene of interest were generated using PCR amplification and agarose gel separation. Amplicons were extracted from agarose gel (Omega Bio-Tek) and pure cDNA was eluted. Following quantification using UV absorbance, standards of known concentration were generated for each gene of interest. Quantitative RT-PCR was conducted using cDNA from samples (in triplicate) and standards (in triplicate) with SYBR® Green PCR Master Mix (Applied Biosystems) on an ABI 7700 (Applied Biosystems) real time PCR machine. Data was quantified using the absolute standard method where serial dilutions of the standard were plotted against C_T values to generate a correlation used to convert sample C_T values into concentrations.

Flow Cytometry

Single cell suspensions of endothelial cells were fixed in 4% formaldehyde for 5 minutes, permeabilized in 0.1% Triton X-100 for 5 minutes and then incubated for 1 hour in 4% donkey serum to block non-specific binding of antibodies. Cells were labeled with one of the following primary antibodies at 1:100 dilution: Rabbit Anti-Mouse Cx37 (Alpha Diagnostic), Goat Anti-Human Cx40 (Santa Cruz Biotechnology), Goat Anti-Human Cx43 (Santa Cruz Biotechnology) for 1 hour at 37°C. Following two washes in T-TBS solution, cells were incubated with one of the following secondary antibodies: FITC-conjugated Donkey Anti-Rabbit (Jackson ImmunoResearch) or FITC-conjugated Donkey Anti-Goat (Jackson ImmunoResearch). Control samples were fixed, permeabilized and blocked with experimental samples, then labeled with secondary antibody alone to account for autoflourescence and non-specific binding of secondary antibody. Cell suspensions were analyzed using a BD LSR digital flow cytometer to determine mean fluorescence intensity of control and experimental samples. During each sample run, standard beads (Bangs Labs) were analyzed to create a standard curve for conversion of fluorescence intensity measurements to units of MESF (molecules of equivalent soluble fluorescence).

Western Blotting

Endothelial cells were lysed in RIPA buffer (Sigma) with added protease inhibitor cocktail (Sigma) and centrifuged at 10,000rpm for 10 minutes to pellet DNA. Supernatant was collected and protein content was quantified using the BCA protein assay (Pierce) in comparison to albumin standards. Samples were mixed with Laemmeli

buffer and heated at 95°C for 5 minutes prior to loading onto 12% Tris-Glycine gels (Invitrogen). Following electrophoresis using Tris/Glycine/SDS running buffer (BioRad) of samples alongside a See Blue Plus 2 (Invitrogen) lane marker and a Magic Mark XP (Invitrogen) western protein standard of known molecular weights, proteins were transferred using Tris/Glycine transfer buffer (BioRad) to a PVDF membrane (BioRad). Blots were incubated overnight at 4°C in 5% milk in T-TBS to block non-specific binding before incubation with the primary antibody for 1 hour at room temperature. Blots were labeled with one of the following antibodies: Rabbit Anti-Mouse Cx37 (Alpha Diagnostic) at 1:500, Rabbit Anti-Mouse Cx40 (Alpha Diagnostic) at 1:500, Rabbit Anti-Mouse Cx43 (Chemicon) at 1:1000 in 5% milk in T-TBS. Following three washes in T-TBS, blots were labeled the following secondary antibody: Horseradish Peroxidase Donkey Anti-Rabbit (Jackson ImmunoResearch) at 1:5000. To measure signal, blots were covered with ECL Plus (Amersham Biosciences) for 5 minutes and then exposed to film. Following staining of blots for the connexin protein of interest, membranes were stripped and reprobed for actin to ensure equal loading. Antibodies used for this step were Mouse Anti-Actin (Calbiochem) and Horseradish Peroxidase Goat Anti-Mouse (Calbiochem).

Immunocytochemistry

To visualize connexin proteins, immunocytochemistry was conducted on endothelial cells following exposure to static or shear conditions. Samples were fixed using 4% formaldehyde for 5 minutes for Slide samples and 1 hour for TEWM samples, permeabilized in 0.1% Triton X-100 for 5 minutes and then incubated for 1 hour in 4%

donkey serum to block non-specific binding of antibodies. Cells were labeled with one of the following primary antibodies at 1:100 dilution: Rabbit Anti-Mouse Cx37 (Alpha Diagnostic), Goat Anti-Human Cx40 (Santa Cruz Biotechnology), Goat Anti-Human Cx43 (Santa Cruz Biotechnology) for 1 hour at 37°C. Following two washes with PBS, cells were incubated with one of the following secondary antibodies: FITC-conjugated Donkey Anti-Rabbit (Jackson ImmunoResearch) or FITC-conjugated Donkey Anti-Goat (Jackson ImmunoResearch). Samples were imaged using a laser-scanning confocal microscope with a 40x oil objective.

Dye Transfer Assay

Following exposure of endothelial monolayers to static or shear stress conditions, assessment of dye transfer between cells was conducted as a measure of gap junction communication. In this assay of gap junction function, cells are loaded with two membrane-impermeant dyes: i) a small dye which can pass through gap junctions and ii) a large dye which cannot pass through gap junctions and is used to mark cells originally loaded with dye. Following a defined period of time, cells are fixed and imaged to evaluate the extent of dye transferred from cells originally loaded with dye to neighboring cells as a measure of cell coupling by gap junctions. In this study the dye used to pass through gap junctions is Biocytin (ε-biotinoyl-L-lysine) with a molecular weight of 372Da and neutral charge (Molecular Probes) and the dye used to mark cells originally loaded with dye is Tetramethylrhodamine Dextran (flouro-ruby) with a molecular weight of 10,000Da (Molecular Probes).

Immediately upon removal from the static dish or flow chamber, monolayers are rinsed in Dulbecco's PBS and excess fluid is blotted off. A mixture of 4mg/ml Biocytin and 5mg/ml Rhodamine-Dextran in PBS is dripped onto the monolayer surface which is then scratched with a diamond-tipped pen (tip diameter 0.25mm). Samples are immediately placed in the incubator at 37°C for 2 minutes to allow passage of dye. Excess dye is quickly removed, samples are rinsed in PBS and fixed in 4% formaldehyde for 20 minutes. While the dextran is fluorescent, biocytin requires a secondary antibody for detection. Monolayers are permeabilized with 0.1% Triton X-100 for 5 minutes and incubated with 4% donkey serum for 30 minutes to block non-specific binding prior to labeling with a secondary antibody Oregon Green 488 NeutrAvidin (Molecular Probes). Samples were imaged using a Nikon E600 fluorescent microscope using filters to separately detect red and green signals.

Proliferation Analysis

Endothelial cell proliferation was assessed using BrdU which is incorporated into DNA being synthesized during S-phase of the cell cycle. BrdU is then detected using primary and secondary antibodies thus proliferating nuclei can be compared to non-proliferating nuclei. BrdU (5-bromo-2'-deoxyuridine) (MP Biomedicals) is added to experimental medium of slides being exposed to static or shear stress at a final concentration of 20μg/mL for the final 6 hours of the 24 hour experimental time period. At the end of the 6 hour exposure to BrdU, slides are fixed in 4% formaldehyde for 20 minutes. Cells are permeabilized by exposure to ice cold acetone for 10 minutes and then DNA is denatured by exposure to 2N HCL for 15 minutes at 37°C. Following

neutralization and restoration of pH, slides are incubated with 5% donkey serum for 1 hour at room temperature to block non-specific binding. Slides are then incubated for 2 hours at 37°C with 1:50 dilution of Mouse anti-BrdU (Sigma), rinsed with PBS and incubated with 1:200 Cy3-conjugated Donkey Anti-Mouse (Jackson ImmunoResearch) and 20μg/mL Hoechst 33258 (Molecular Probes) to detect both proliferating and non-proliferation nuclei. Slides are imaged using a laser scanning confocal microscope and images are analyzed using ImagePro software.

Morphological Analysis

To evaluate cell morphology, endothelial monolayers are stained for actin filaments and measured for elongation and angle of orientation. Endothelial cell slides are fixed in 4% formaldehyde for 5 minutes, permeabilized in 0.1% Triton X-100 for 5 minutes and incubated in 4% donkey serum for 30 minutes at room temperature. Monolayers are stained using Rhodamine-conjugated phalloidin (Invitrogen) which is a mushroom toxin that binds tightly to actin filaments. Staining is conducted using 1:200 phalloidin and Hoechst 33258 to identify nuclei. Samples are imaged using a Nikon E600 fluorescent microscope using a triple filter to detect both red and blue signals. Images are analyzed using LSM 5 Image Browser (Zeiss) and an overlay writing tool is used to manually determine perimeter, area and angle of orientation. Angle of orientation is measured from horizontal which is the axis of fluid shear stress. Using perimeter and area data, a shape index of each cell is calculated according to the formula: $SI = (4*\Pi*Area)/(Perimeter^2)$. The shape index ranges from 0 (indicating a straight line) to 1 (indicated a circle) and quantifies elongation of endothelial cells.

CHAPTER FOUR: Transcriptional Profiling of Endothelial Cells Using a Tissue Engineered Blood Vessel Model

Introduction

Over the past several decades, there has been an explosion in research targeting the endothelium; the single-cell thick inner lining of blood vessels. Endothelial cells are involved in numerous pathologic conditions which currently threaten global health in addition to playing a critical role in growth and development of the vasculature. All of these studies investigating the role of endothelial cells in atherosclerosis or in angiogenesis or research evaluating their potential use as a therapy for myocardial infarction must choose a setting in which to ask questions: *in vitro* or *in vivo*.

In vitro systems are simplified and controlled which allows reproducible probing of fundamental cellular mechanisms. *In vitro* studies are particularly useful in isolating cellular pathways and in investigating response to an individual stimulus such as a growth factor or mechanical force. *In vivo* systems more accurately represent the complexity in which the pathologic condition or developmental state resides. In this physiologic environment, stimuli such as blood vessel structure and systemic circulation are included resulting in more variable, yet potentially more applicable data. *In vivo* studies are extremely valuable when evaluating multifaceted processes such as atherosclerotic plaque development, growth of new blood vessels and control of hemostasis. While the information gained through the use of *in vitro* and *in vivo* studies has been exceptionally valuable in building our understanding of the endothelium, there

is often a disconnect in relating *in vitro* and *in vivo* observations. So we must ask if there is a way to bridge the gap between these two classical experimental settings.

The primary focus of tissue engineering has been to develop living tissue substitutes which have a therapeutic value by repairing, replacing or enhancing function of native tissue. However, there is an intermediate goal of tissue engineering whereby the living substitutes being generated can be used as more physiologic *in vitro* models. Tissue engineered constructs provide the link between traditional *in vitro* and *in vivo* systems as they are more complex than a single cell type on tissue culture plastic and yet are more controlled than an *in vivo* setting which includes all the physiologic variables. Tissue engineering provides the opportunity to evaluate cellular response to multiple stimuli as would be found *in vivo*, and yet these stimuli are controlled in a fashion which is the hallmark of *in vitro* studies. A unique advantage of tissue engineering is the potential to develop human tissue models from human cells. The opportunity to investigate human biological mechanisms and disease processes or test potential therapies without risk of endangering patients will promote tissue engineering to the forefront of research strategies.

Endothelial cell behavior in response to shear stress has been extensively studied since the observation that regions of the arterial tree where flow is unidirectional and axially aligned have no intimal thickening whereas regions of low shear stress and flow separation exhibit intimal thickening and correspond with the presence of atherosclerosis. (44) Early *in vivo* studies noted altered endothelial cell morphology and proliferation rates in these regions and subsequent *in vitro* studies on influence of shear stress confirmed these observations. (45, 46, 54-56) Ensuing studies investigating endothelial

cell response to different types of shear stress found broad influence on cell behavior including altered LDL uptake, adhesion molecule expression and oxidation-reduction state. (60, 63, 68) With extensive influence of shear stress on endothelial function being demonstrated, numerous mechanisms of control were investigated including the discovery of a shear stress response element (SSRE) in the promoter region of several genes confirming control over transcription. (75, 76) More recent investigations using transcriptional profiling techniques have demonstrated the extent of shear stress influence on gene expression both *in vivo* and *in vitro*. (48, 80, 81, 83)

Motivated by the fields of developmental and cancer biology, studies into extracellular matrix influence on endothelial cell function have shown distinct roles in angiogenesis, vascular migration and vascular patterning. Various basement membrane proteins have been shown to appear in a spatially and temporally regulated manner during angiogenesis *in vivo* and these same molecules have been shown to control cell proliferation *in vitro*. (86) Furthermore, endothelial cells are sensitive to the state of the extracellular matrix including whether it is assembled or in soluble form and which degradation sites may be exposed. (87) The complexity of extracellular matrix influence on endothelial cells is further expanded to include binding and display of growth factors which then serve as chemo-repellent or chemo-attractive signals in vessel patterning. (89) Interest in endothelial cells and extracellular matrix also extends into studies of extracellular matrix degradation especially in the context of atherosclerosis and understanding plaque integrity. (193)

In addition to shear stress and extracellular matrix, the *in vivo* endothelial cell environment also includes interactions with a number of other cell types in the blood and

vascular wall. Pericytes wrapping the microvasculature and smooth muscle cells underlying the endothelium in large conduits have an interactive relationship with endothelial cells in which each cell type contributes to the phenotype of the other. (100) To better understand atherosclerosis, hypertension and restenosis, several studies have investigated the relationship between endothelial cells and smooth muscle cells using co-culture systems. Through both soluble and contact-mediated mechanisms, studies have shown reciprocal influence on cell proliferation, migration and growth factor production. (103, 107) Smooth muscle cells have also been shown to influence endothelial cytokine secretion, response to external growth factors and tube formation. (106, 108)

While research examining endothelial response to an individual stimulus has greatly expanded our understanding of their function, *in vitro* investigations including two stimuli have confirmed the complexity of cell behavior and the importance of the whole of the cellular microenvironment. Influence of extracellular matrix and shear stress on endothelial function converged with the study of integrin signaling. Endothelial adhesion to extracellular matrix proteins by specific members of the integrin family alters the cellular response via specific signal transduction pathways. (96) However, it is these same integrin signaling pathways which are critical in transmitting signals induced by shear stress. (98) The simultaneous presence of smooth muscle cells and shear stress has been examined through the development of *in vitro* co-culture models which allow heterocellular contact yet expose only the endothelial surface to fluid flow. (109, 111) Studies using these systems have shown altered endothelial nitric oxide synthase (eNOS) and cyclooxygenase (cox) expression as well as altered adhesion molecule expression. (110, 111)

Development of tissue engineered blood vessels has been motivated by the clinical need for small diameter vascular grafts which will remain patent over time and reduce the need to harvest vessels from other areas of the body. Numerous approaches using synthetic or naturally-derived materials and animal or human cells have been developed in a quest to produce a strong and biologically-active graft. (37, 38) One particular biological approach involves dispersing smooth muscle cells within a tubular collagen type I gel to mimic the media and then seeding the lumen with endothelial cells to mimic the intima. (36) This strategy is advantageous as it reconstructs the basic structure of a native vessel and by including multiple components of the endothelial microenvironment, is more complex than a traditional *in vitro* model. However, it is much simplified compared to a native artery thus allowing reproducibility and control. Use of this tissue engineered wall model (TEWM) generated from human cells in previous studies conducted in our lab has shown a distinct influence on endothelial cell morphology, proliferation and migration. (42, 43) To further understand the scope of microenvironment influence on endothelial cell behavior, the goal of this study is to examine the effect of substrate and shear stress on endothelial cell gene expression.

Experimental Design and Methods

Experimental Design

The approach taken to investigate influence of substrate and shear stress on endothelial cell gene expression is to examine transcriptional profiles of cells on traditional and tissue engineered substrates under different mechanical environments. Transcriptional profiling using microarray technology provides the opportunity to

examine cellular gene expression without pre-selecting genes which are hypothesized to be affected. Furthermore, to gain insight most applicable to human development and disease, this study takes advantage of the tissue engineering approach by using human cells to create a human blood vessel model. To examine the effect of shear stress, endothelial cells are exposed to either static or laminar shear stress (15 dynes/cm^2) conditions. To examine the effect of substrate, endothelial cells are exposed to two environments. As a point of reference, a traditional *in vitro* model of monomer type I collagen adsorbed to glass is used. As a more physiologic *in vitro* model, a biologically-based blood vessel substitute is used. This tissue engineered model is a three-dimensional type I collagen gel containing dispersed human aortic smooth muscle cells to mimic the components and structure of the medial layer. Confluent endothelial monolayers are cultured on each substrate for 48 hours prior to exposure to static or shear conditions for 24 hours. Endothelial cell RNA is then isolated to conduct microarray analysis for transcriptional profiling and to conduct RT-PCR analysis for confirmation of microarray gene expression findings. Similarities and differences in endothelial gene expression from the four experimental conditions provides insight into the influence of substrate and shear stress on multiple aspects of endothelial cell function.

Experimental Methods

Cell Culture

Human aortic endothelial cells (HAEC) (Cambrex) were cultured to passage 6 in MCDB 131 supplemented with 5% FBS, antibiotics and growth factors while human aortic smooth muscle cells (HASMC) (Cambrex) were cultured to passage 8 in MCDB

131 supplemented with 5% FBS, antibiotics and growth factors. All experiments were conducted in a co-culture media of MCDB 131 supplemented with 5% FBS, antibiotics and growth factors common to both cell culture mediums.

Substrate Fabrication

Two types of substrate were used in this study: Adsorbed Collagen Slide and Tissue Engineered Wall Model (TEWM). The Adsorbed Collagen Slide was created by coating glass slides with 50 μg/ml collagen type I (BD Biosciences) and allowing protein to adsorb to the surface for one hour prior to removal of the solution. The Tissue Engineered Wall Model was created by suspending 1 million HASMC per ml in 5x concentrated MCDB-131, 10% FBS and 2 mg/ml rat tail type I collagen (BD Biosciences). Sodium hydroxide was added to neutralize the acidic collagen solution and promote polymerization. Tubular HASMC-collagen gels were created using a central mandrel during gelation and were cultured for six days to allow for cell-mediated compaction of the collagen fibers. The tubular gels were then cut longitudinally and embedded in agar to expose a flat lumen for seeding of HAEC and fluid shear experiments. (43) Endothelial cells were seeded on both models at a density of 40,000 cells/cm^2 to produce a confluent monolayer and cultured for 48 hours prior to exposure to static or shear conditions.

Exposure to Shear Stress

The parallel plate flow chamber used to expose endothelial cells to laminar shear stress has been previously established in our laboratory. (42, 49) In this closed loop, a

peristaltic pump moves medium from a container into a pulse dampener and then through parallel plates where endothelial cells are exposed to a steady laminar shear stress. Shear stress is controlled by fluid flow rate and dimensions of the chamber according to the equation: $\tau = 6Q\mu/bh^2$. Exposure of endothelial cells on the tissue engineered wall model was accomplished by embedding the depth of the collagen gel in agar supported by a polycarbonate mold. The entire mold/agar apparatus was then placed into the flow chamber as depicted in Figure 4.1. Endothelial cells on the Slide or TEWM were exposed to a shear stress of 15 dynes/cm^2 for 24 hours.

Endothelial Isolation from Tissue Engineered Wall Model

To evaluate endothelial cell gene expression following culture on the TEWM, pure endothelial cells must be removed without contamination of neighboring smooth muscle cells. Following cell exposure to static or shear stress conditions, the TEWM lumen was briefly exposed to collagenase to release cells near the surface. Endothelial cells were isolated from the cell mixture using a magnetic separation technique whereby a primary PE-conjugated antibody to PECAM-1 (Santa Cruz) followed by a magnetic bead-conjugated secondary antibody to PE positively selects for endothelial cells. Following passage through a separation column placed in a magnetic field, endothelial cells were collected and lysed for further analysis. Effectiveness of the magnetic sorting procedure was validated using pre-labeled endothelial cells mixed with smooth muscle cells and flow cytometry analysis post-separation.

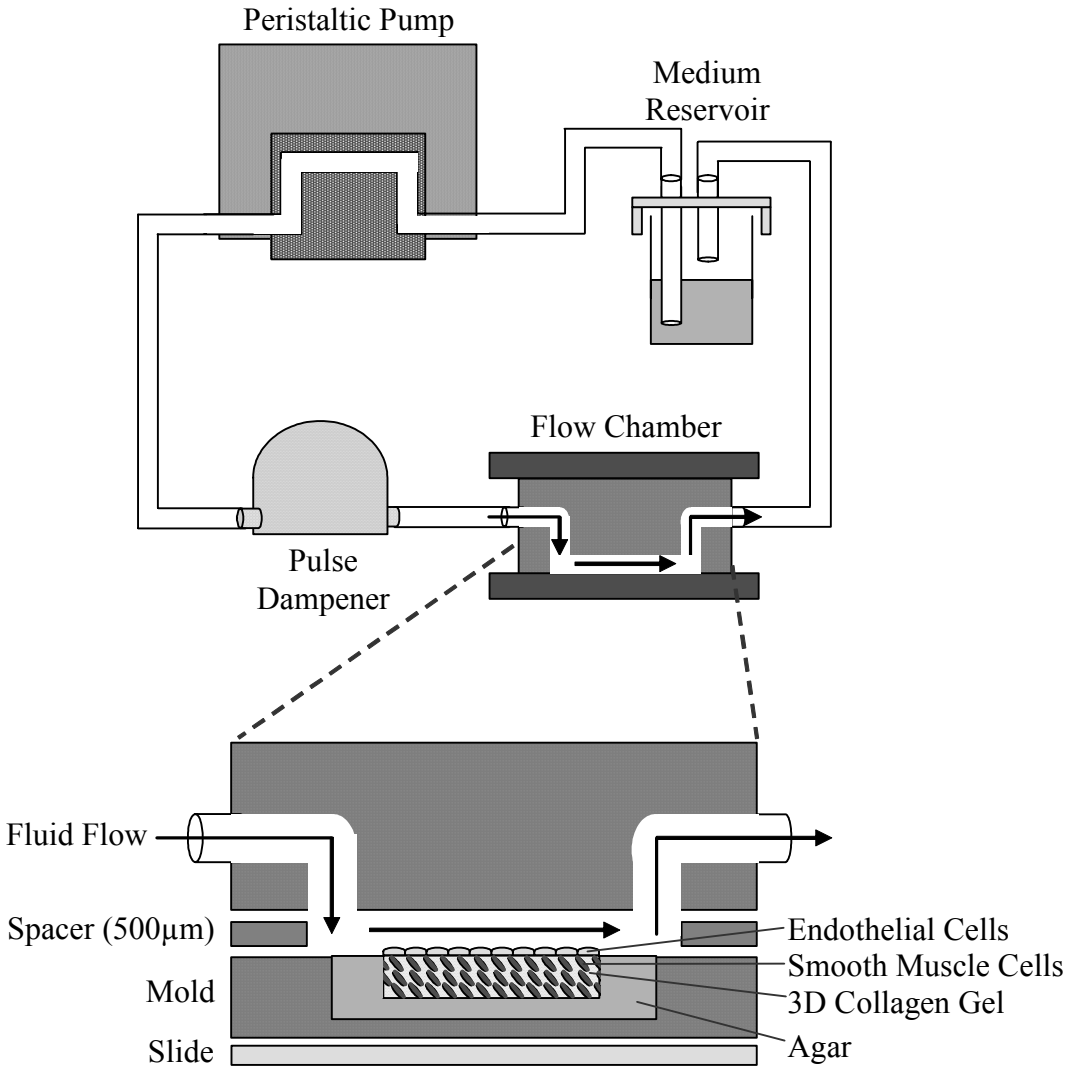

Figure 4.1 Parallel Plate Flow Circuit Exposes Endothelial Cells to Shear Stress

RNA Isolation and Analysis

Total RNA was extracted from endothelial cells using an RNeasy kit (Qiagen) with an added DNAse digestion step. To evaluate quality of RNA prior to microarray or RT-PCR analysis, samples were assessed using the RNA 6000 Nano LabChip (Agilent) on an Agilent Bioanalyzer 2100. Profiles of ribosomal peaks were evaluated for degradation as a measure of overall RNA degradation and preliminary measurements of RNA quantity were determined. Quantity of high quality RNA was assessed by absorbance at 260nm prior to use in microarray or reverse transcription to cDNA for RT-PCR.

Quantitative RT-PCR

One microgram of high quality endothelial RNA was reverse transcribed using the First Strand cDNA Synthesis Kit (Invitrogen) for each experimental sample. Primers were designed using Primer Express (Applied Biosystems) and oligos were created by Integrated DNA Systems. Primer sequences are listed below for four genes used in microarray data validation.

Ang2 Forward: TCCTCCTGCCAGAGATGGAC

Ang2 Reverse: TGCACAGCATTGGACACGTA

CYP1B1 Forward: TTTCGGCTGCCGCTACAG

CYP1B1 Reverse: ACTCTTCGTTGTGGCTGAGCA

E-selectin Forward: TTGGTAGCTGGACTTTCTGCTG

E-selectin Reverse: CATTTCCGAAGCCAGAGGAG

Pentaxin 3 Forward: TGGACAACGAAATAGACAATGGA

Pentaxin 3 Reverse: CTGACCGCAGTCGCACG

Standards of known concentration were generated using PCR amplification and agarose gel extraction for each gene of interest. Quantitative RT-PCR was conducted using cDNA from samples (in triplicate) and standards (in triplicate) with SYBR® Green PCR Master Mix (Applied Biosystems) on an ABI 7700 (Applied Biosystems) real time PCR machine. Data was quantified using the absolute standard method where serial dilutions of the standard were plotted against C_T values to generate a correlation used to convert sample C_T values into concentrations.

Microarray Experimental Design

Experimental Samples

Endothelial cell RNA samples from four experimental conditions were used: Slide Static, Slide Shear, TEWM Static, TEWM Shear. For each experimental condition, there were three independent samples resulting in a total number of twelve microarrays. Each experimental sample was competitively hybridized against Universal Human Reference RNA (Stratagene) to allow for multiple comparisons within the data set and comparison to public data depositories. The microarray experimental design is detailed below.

A. Slide Static vs. Reference RNA (n=3)
B. Slide Shear vs. Reference RNA (n=3)
C. TEWM Static vs. Reference RNA (n=3)
D. TEWM Shear vs. Reference RNA (n=3)

To examine the influence of shear stress on endothelial cell gene expression, arrays A and B can be compared using a Slide substrate and arrays C and D can be compared

using a TEWM substrate. To examine the influence of substrate on endothelial cell gene expression, arrays A and C can be compared under Static conditions and arrays B and D can be compared under Shear conditions.

Microarray Analysis

Following quality analysis by Bioanalyzer 2100 and quantity assessment by UV absorbance, 500ng of total RNA from experimental samples and from Reference RNA were prepared for competitive microarray hybridization. Samples were amplified using the Agilent Low RNA Input Fluorescent Linear Amplification Kit and labeled with Cy-3 and Cy-5 CTP (Perkin-Elmer). Hybridization was performed using the Agilent In Situ Hybridization Plus kit to 44,000 60-mer Human Whole Genome Oligo Microarrays (Agilent). Arrays were scanned using the Agilent dual laser DNA microarray scanner with SureScan technology and image extraction was conducted using Agilent Feature Extraction software 7.5.1. GeneSpring® software was used to normalize data, interpret triplicates, filter spots and generate experiment files for gene expression analysis. It was also used to calculate significance and fold change values for all genes. Ingenuity Pathways Analysis® was used to interpret genes identified as significant in the context of known biological functions and disease states.

Results

Microarray Data Analysis Criteria

Microarray analysis was conducted on twelve samples of endothelial cell mRNA to evaluate transcription under four different experimental conditions. The four

conditions were the following: Slide Shear, Slide Static, TEWM Shear, TEWM Static and each condition had experimental samples in triplicate. Following hybridization, scanning and image extraction, raw data was analyzed using GeneSpring® software. Figure 4.2 shows the steps taken in processing the raw data into a defined number of candidate genes. First, the entire data set was examined to determine the number of spots on the array from which a signal could be read. Each spot on each array was given an evaluation and the total number of spots with flags present or marginal was 40987. The second criteria was that flags for each spot be present or marginal in all twelve arrays analyzed which reduced the number of genes to 40821. Following identification of spots which can be analyzed, an ANOVA was run on the entire data set using the multiple testing correction (MTC) method: Benjamini and Hochberg False Discovery Rate. Each gene was assigned a p-value based on this ANOVA with MTC and the cutoff criteria of p-value < 1 reduced the number of genes to 40754. A multiple testing correction is necessary to adjust p-values in analysis of large sets of microarray data since the number of false positives is proportional to the number of tests performed. For further analysis, the data set was split into the following four pairwise comparisons:

1) Slide Shear vs. Slide Static
2) TEWM Shear vs. TEWM Static
3) Slide Static vs. TEWM Static
4) Slide Shear vs. TEWM Shear

While the ANOVA with MTC p-value remained affiliated with each gene, a student's t-test was conducted on each pair of samples to determine significance for the comparison in question. With the cutoff criteria of t-test p-value < 1, the number of genes was further

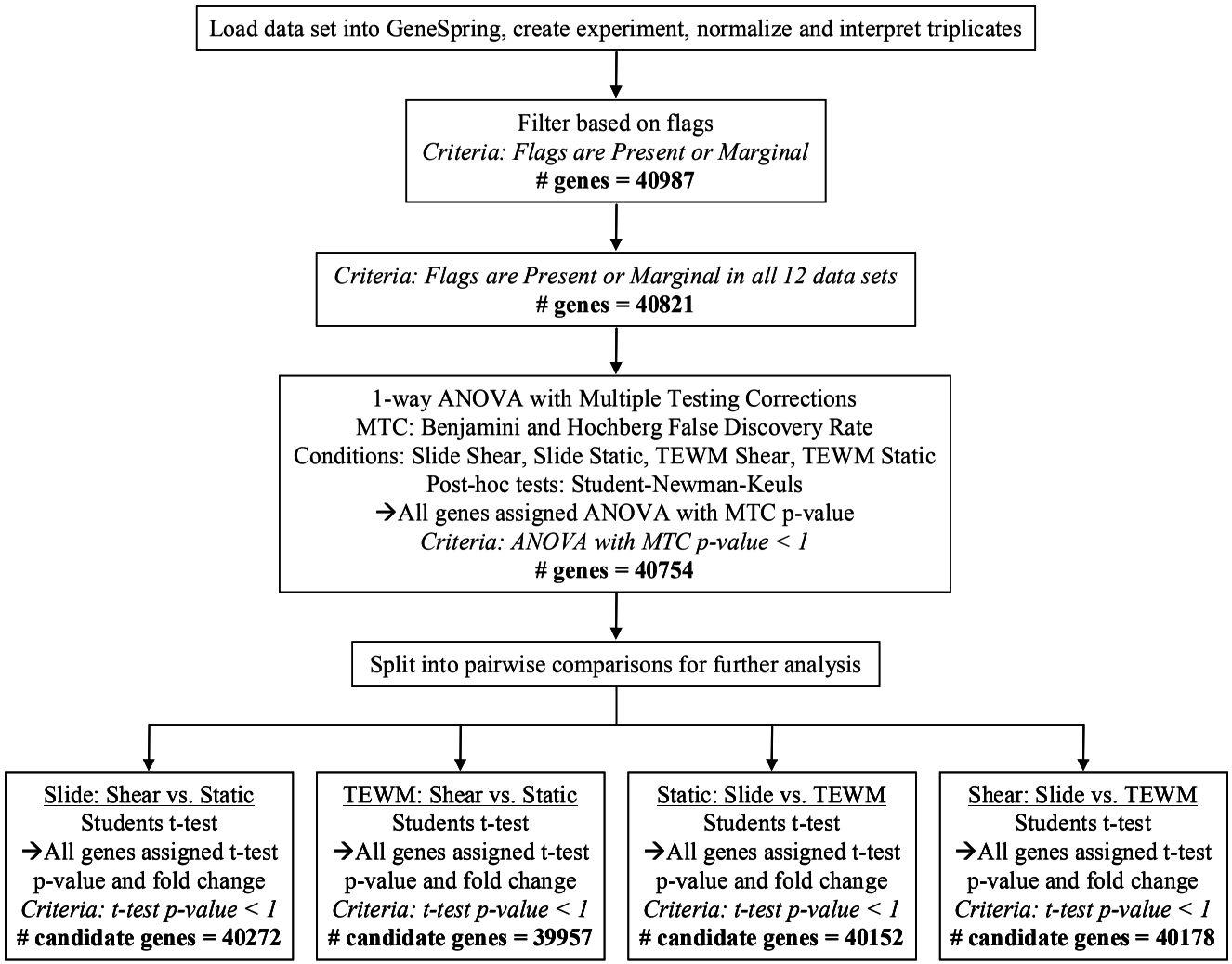

Figure 4.2 Microarray Data Analysis Flow Chart to Determine Candidate Genes

reduced and the number of candidate genes for each comparison was identified (see Figure 4.2 for values).

Following the number of candidate genes being identified for each comparison, the next step was to identify the genes which were significantly different. The candidate genes already meet the following criteria:

1) Flags are Present or Marginal in all 12 arrays
2) ANOVA with MTC p-value < 1
3) t-test p-value < 1

To evaluate the most appropriate method for selecting significantly different genes, the following five significance criteria were applied to the candidate gene list one at a time.

1) t-test p-value < 0.05
2) ANOVA with MTC p-value < 0.05
3) t-test p-value < 0.05 AND fold change > 1.5
4) ANOVA with MTC p-value < 0.05 AND fold change > 1.5
5) ANOVA with MTC p-value < 0.05 AND t-test p-value < 0.05 AND fold change > 1.5

Table 4.1 shows the number of genes meeting analysis cutoffs following application of the different significance criteria. To limit false positives, the most stringent set of criteria was used to identify significantly regulated genes: ANOVA with MTC p-value < 0.05 AND t-test p-value < 0.05 AND fold change > 1.5. Arguments can be made for more stringent or more relaxed criteria; however the author felt this combination provided the best balance to identify mathematically and biologically significant genes for further investigation.

Table 4.1 Number of Genes Meeting Analysis Significance Criteria

Cutoff Criteria	Slide: Shear vs. Static	TEWM: Shear vs. Static	Static: Slide vs. TEWM	Shear: Slide vs. TEWM
Number of Candidate Genes	**40272**	**39957**	**40152**	**40178**
t-test p-value < 0.05	6156	7263	8674	5213
ANOVA with MTC p-value < 0.05	5634	5624	5628	5631
t-test p-value < 0.05 AND fold change > 1.5	2397	2429	2783	2006
ANOVA with MTC p-value < 0.05 AND fold change > 1.5	1735	1775	1940	1419
ANOVA with MTC p-value < 0.05 AND t-test p-value < 0.05 AND fold change > 1.5	**1668**	**1685**	**1900**	**1278**

Validation of Microarray Data

To validate significance of genes identified using microarray analysis, a separate technique examining levels of mRNA expression was used. Quantitative RT-PCR was conducted on four genes identified as significantly expressed in microarray analysis: angiopoeitin 2, cytochrome p450 1B1, E-selectin, and pentaxin 3. Samples were created, mRNA isolated and cDNA generated from three experiments for TEWM samples (Static and Shear) and four experiments for Slide samples (Static and Shear). Using significance criteria of t-test p-value < 0.05 and fold change > 1.5 for RT-PCR data, a comparison of gene expression is listed in Table 4.2. Of fourteen incidences of significant regulation identified by microarray analysis, twelve were confirmed significant by RT-PCR. The two not determined significant by RT-PCR which were identified by microarray analysis met fold change criteria but did not meet t-test p-value criteria. Of these validation genes, there were no cases of genes identified as significant by RT-PCR which were not identified as significant by microarray analysis. From this comparison we conclude that although the microarray data may contain false positives or false negatives, the data set as a whole can be considered valid.

Comparison of Microarray Data Sets

The microarray analysis consisted of four types of samples which represented two substrates and two mechanical environments (Slide Static, Slide Shear, TEWM Static, TEWM Shear). To draw conclusions on the effect of substrate and shear stress, the

Table 4.2 Comparison of Endothelial Cell Gene Expression by Microarray and RT-PCR

Bold and Underlined denoted meets significance criteria (t-test p<0.05 and fold change>1.5)
Red text denotes gene downregulation and blue text denotes gene upregulation

Gene Name	Genbank ID	Slide: Shear vs. Static				TEWM: Shear vs. Static				Static: Slide vs. TEWM				Shear: Slide vs. TEWM				All Array Data
		PCR Shear/Static		Array Shear/Static		PCR Shear/Static		Array Shear/Static		PCR Slide/TEWM		Array Slide/TEWM		PCR Slide/TEWM		Array Slide/TEWM		
		fold change	ttest p-value	fold change	ttest p-value	fold change	ttest p-value	fold change	ttest p-value	fold change	ttest p-value	fold change	ttest p-value	fold change	ttest p-value	fold change	ttest p-value	ANOVA MTC p-value
Ang2	NM_001147	**0.41**	**0.001**	**0.19**	**0.001**	0.23	0.095	**0.23**	**0.006**	**0.22**	**0.045**	**0.29**	**0.002**	**0.39**	**0.028**	**0.24**	**0.008**	**0.001**
CYP1B1	NM_000104	**918.37**	**0.006**	**23.55**	**1.5E-06**	**390.71**	**0.000**	**73.47**	**3.8E-07**	0.14	0.228	1.36	0.007	**0.33**	**0.001**	**0.44**	**5.0E-04**	**4.4E-07**
Eselectin	NM_000450	4.41	0.403	0.74	0.403	**13.55**	**0.002**	**5.31**	**0.043**	**0.23**	**0.013**	**0.20**	**0.002**	**0.08**	**0.001**	**0.03**	**0.003**	**0.005**
Pentaxin 3	NM_002852	**0.27**	**0.001**	**0.15**	**9.4E-05**	0.34	0.345	**0.24**	**0.015**	**30.19**	**0.001**	**13.00**	**0.002**	**24.48**	**0.003**	**8.05**	**1.2E-04**	**3.4E-04**

samples were split into the following pairwise comparisons with a corresponding number of significantly regulated genes as described previously.

1) Slide: Shear vs. Static – 1668 significant genes
2) TEWM: Shear vs. Static – 1685 significant genes
3) Static: Slide vs. TEWM – 1900 significant genes
4) Shear: Slide vs. TEWM – 1278 significant genes

The comparison Slide: Shear vs. Static examines the influence of mechanical environment while the cells are on a Slide substrate. The comparison TEWM: Shear vs. Static examines the influence of mechanical environment while the cells are on a TEWM substrate. The comparison Static: Slide vs. TEWM examines the influence of substrate while the cells are under static conditions. The comparison Shear: Slide vs. TEWM examines the influence of substrate while the cells are under shear stress conditions. These four comparisons individually provide great insight into the influence of substrate and shear stress; however, further insight can be gained by cross-comparing these four data sets.

Figure 4.3 shows the number of genes which are common or unique in the Shear vs. Static comparisons on either the Slide or TEWM substrate. In other words, there are 681 genes expressed differently under shear stress compared to static on both substrates. However there are 987 genes expressed differently under shear which appear uniquely on the Slide substrate while there are 1004 genes expressed differently under shear which appear uniquely on the TEWM substrate. Figure 4.4 shows the number of genes which are common or unique in the Slide vs. TEWM comparisons under either Static or Shear conditions. In this cross-comparison, there are 661 genes expressed differently on the

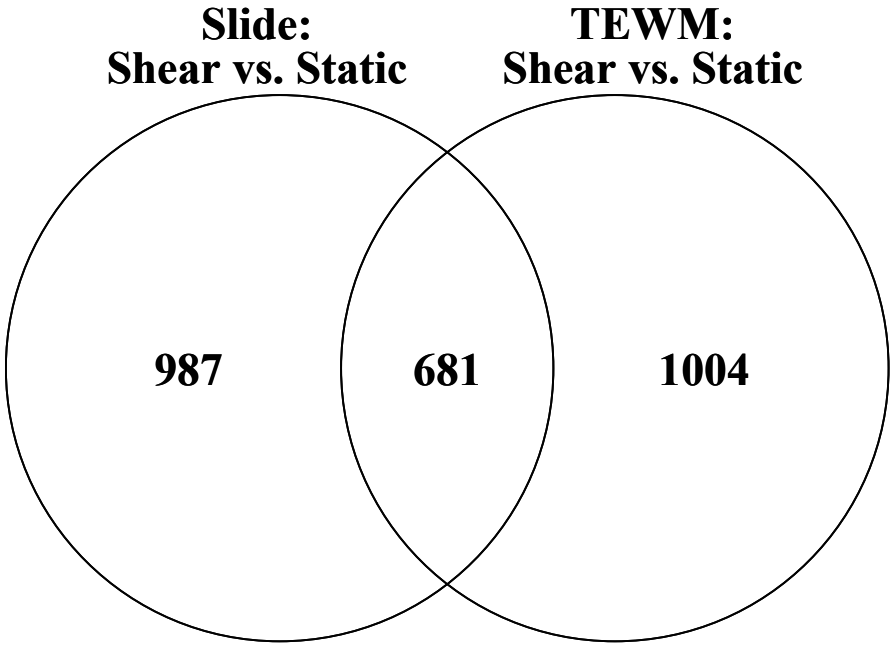

Figure 4.3 Number of Genes Common or Unique to Shear vs. Static Array Data

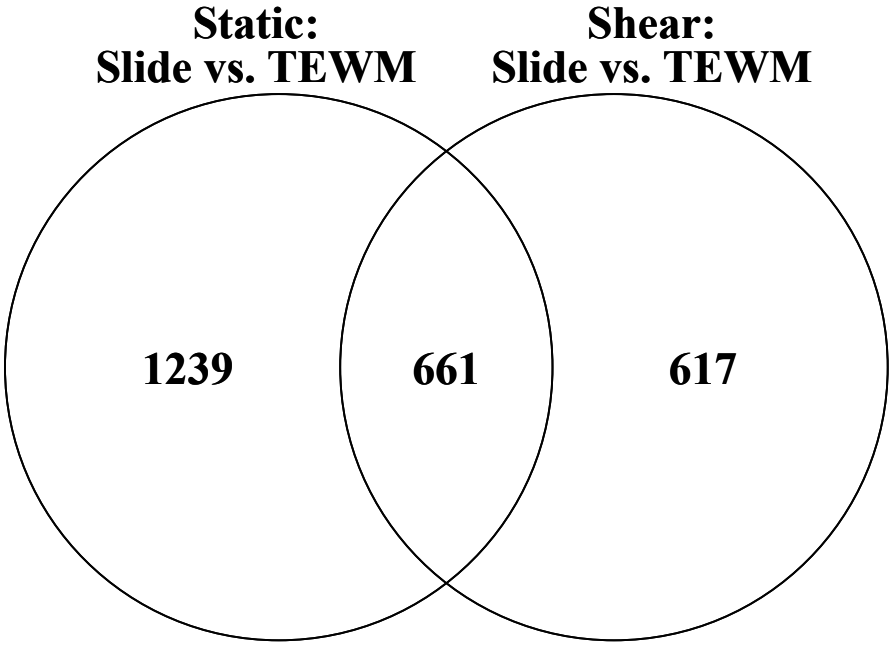

Figure 4.4 Number of Genes Common or Unique to Slide vs. TEWM Array Data

two substrates under both mechanical environments. However there are 1239 genes expressed differently on the two substrates which appear only under static conditions and 617 genes expressed differently on the two substrates which appear only under shear stress conditions. A final comparison is overlapping all four of the pairwise comparisons to identify genes which are significantly regulated by substrate and shear stress at each combination. Such an analysis results in 122 genes identified. Results of these cross-comparisons confirm that some genes are regulated by a particular stimulus regardless of other stimuli applied, however most often the effect of one stimulus is dependent on the presence or absence of another stimulus. Thus we conclude that the whole of the cellular microenvironment is important in determining the overall cell phenotype.

Ingenuity Pathways Analysis

Data were analyzed through the use of Ingenuity Pathways Analysis (Ingenuity® Systems, www.ingenuity.com). The purpose of Ingenuity Pathways Analysis (IPA) was to evaluate gene microarray data in a systematic fashion to gain insight regarding affected biological pathways and disease mechanisms. For this software analysis, the user inputs genes designated as significant based upon user-defined criteria. Genes which are entered into the program are overlaid into the Ingenuity Pathways Knowledge Base (IPKB) which is a constantly evolving database of molecular interactions developed based on published, peer-reviewed literature. Genes that are deemed significant by the user and are found to interact with at least one other gene in the IPKB are designated "focus genes". IPA then uses computational algorithms to identify networks of molecular interactions which are enriched for the focus genes. Networks are ranked

based on number of focus genes and overall size and are also assigned biological functions based on known diseases and cellular events. IPA also conducts a Functional Analysis to identify the biological functions and/or diseases that are most significant in each data set. Fischer's exact test is used to calculate a p-value determining the probability that each biological function and/or disease assigned to that data set is due to chance alone.

For IPA application to the Slide_TEWM_Static_Shear data set, genes previously designated as significant (ANOVA with MTC p-value < 0.05 AND t-test p-value < 0.05 AND fold change > 1.5) were used. For each pairwise comparison, the input data set included the Genbank ID, fold change, and ANOVA with MTC p-value. Table 4.3 shows the number of genes entered and the number of focus genes identified following comparison of input data with the IPKB. Based on these focus genes, networks were generated for each pairwise comparison and biological functions were assigned. Functional Analysis was conducted on each data set and significant biological functions and diseases were identified. For further insight into gene regulation by substrate and shear stress, charts were generated which compared functions identified for the Shear vs. Static data and also for the Slide vs. TEWM data. Figure 4.5 shows a Functional Analysis chart for the TEWM: Shear vs. Static and Slide: Shear vs. Static data sets which compare the probability that genes in the stated categories are significantly affected by the experimental conditions. In a similar fashion, Figure 4.6 shows a Functional Analysis chart for the Static: Slide vs. TEWM and Shear: Slide vs. TEWM data sets which compare the probability that genes in the stated categories are significantly affected by the experimental conditions. Functional Analysis identified approximately 60 biological

Table 4.3 Number of Focus Genes in Ingenuity Pathways Analysis

Identification Criteria	Slide: Shear vs. Static	TEWM: Shear vs. Static	Static: Slide vs. TEWM	Shear: Slide vs. TEWM
Number of Significant Genes	1668	1685	1900	1278
Number of Focus Genes	690	659	817	535

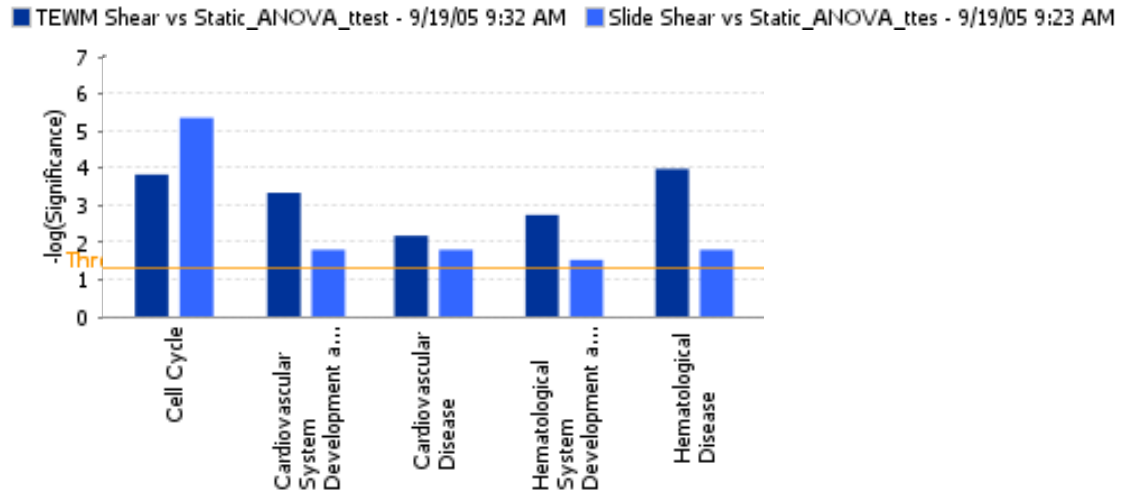

Figure 4.5 IPA Functional Analysis for Shear vs. Static Array Data – Selected Categories

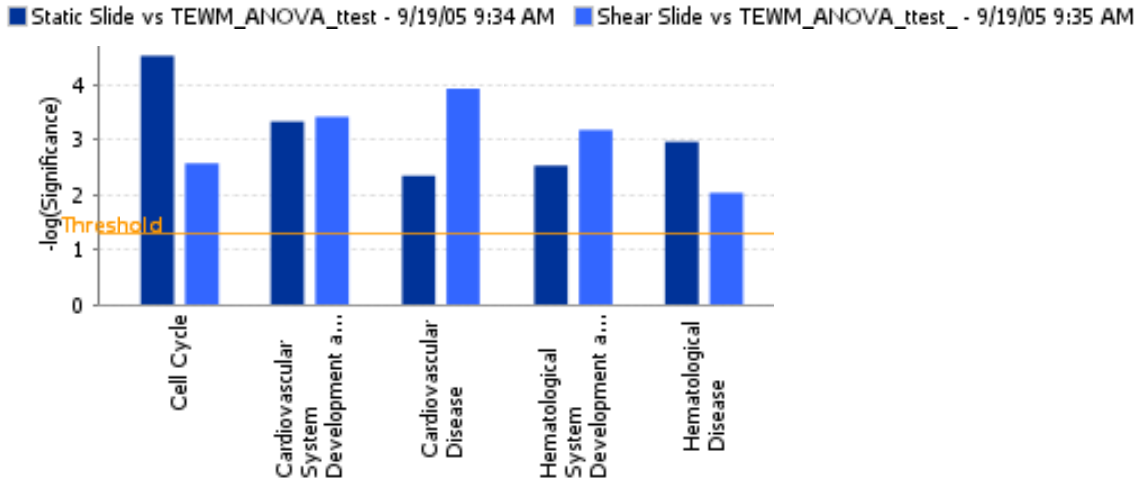

Figure 4.6 IPA Functional Analysis for Slide vs. TEWM Array Data – Selected Categories

functions and/or diseases significantly regulated in each of the four data sets. The following five functional categories are shown in the figures and will be discussed in further detail:

1) Cell Cycle
2) Cardiovascular System Development and Function
3) Cardiovascular Disease
4) Hematological System Development and Function
5) Hematological Disease

Discussion

As the motivation of this study was to evaluate endothelial cell gene expression in the context of developing more physiologic *in vitro* models to study vascular biology, we will focus on genes identified by IPA Functional Analysis as involved in Cardiovascular System Development & Function, Cardiovascular Disease, Hematological System Development & Function and Hematological Disease. Genes identified are known to be involved in the cardiovascular and hematological systems and many have been studied for their particular roles in development or disease progression. Many have uniquely cardiovascular functions and have been identified previously as shear or substrate responsive while others are newly identified as such in this study. As an example of cell function not limited to the cardiovascular and hematological systems, we will first examine changes in gene expression of genes associated with cell cycle.

Biological Function: Cell Cycle

Control of cell cycle is a complex series of feedback loops and checkpoints which are critical in biological development and many disease states. For endothelial cells, there is reduced cell proliferation in mature, healthy arteries while regions susceptible to atherosclerotic plaque have increased cell proliferation. Additionally, levels of endothelial cell proliferation seen *in vitro* are often much higher than those seen *in vivo* which makes the cell cycle an ideal candidate for investigation of substrate and shear stress influence using a more physiologic *in vitro* model. IPA analysis showed significant changes in genes involved in the cell cycle for all four pairwise comparisons suggesting a dramatic influence of shear stress and substrate on this important biological function. Table 4.4 shows fold change (calculated as Shear/Static) and t-test p-value data for genes identified by IPA Functional Analysis in the Slide: Shear vs. Static and TEWM: Shear vs. Static microarray comparisons which are involved in cell cycle.

Initial impressions of the data set note the large number of cell cycle genes which change expression and the extreme changes in magnitude for many of the genes. In first examining the Slide: Shear vs. Static data set, there are 42 genes which are changing expression and 38 of these are downregulated under shear compared to static conditions whereas four are upregulated under shear. Of the families of genes involved in cell cycle progression, there is a reduction in five of the cyclin genes (cyclin A2, cyclin B1, cyclin B2, cyclin D2 and cyclin H), in six of the cell division cycle (cdc) and cdc-associated genes (cdc6, cdc7, cdc20, cdc45L, cdca5, cdca7) and changes in the cyclin-dependent kinase (cdk) 4 and cdk-inhibitors. Changes in gene expression were also detected for other machinery involved in cell cycle progression including centromere proteins,

Table 4.4 Cell Cycle Genes in Shear vs. Static Comparisons

Red text denotes gene downregulation and blue text denotes gene upregulation
'x' denotes failure to meet significance criteria (t-test p<0.05 and ANOVA p<0.05 and fold change>1.5)

Gene ID	Gene Name	Genbank ID	Slide: Shear vs. Static		TEWM: Shear vs. Static	
			fold change	t-test p-value	fold change	t-test p-value
CCNA2	cyclin A2	NM_001237	0.3000	0.0006	x	x
CCNB1	cyclin B1	NM_031966	0.1600	0.0014	0.3830	0.0052
CCNB1IP1	cyclin B1 interacting protein 1	NM_021178	x	x	0.6110	0.0020
CCNB2	cyclin B2	NM_004701	0.1310	0.0000	0.4130	0.0137
CCND1	cyclin D1	BC014078	x	x	0.6120	0.0283
CCND2	cyclin D2	M90813	0.5460	0.0019	0.6210	0.0115
CCNDBP1	cyclin D-type binding-protein 1	NM_012142	x	x	1.6040	0.0048
CCNH	cyclin H	NM_001239	0.4090	0.0091	0.6540	0.0139
CDC6	CDC6 cell division cycle 6	NM_001254	0.1620	0.0000	0.5230	0.0007
CDC7	CDC7 cell division cycle 7	NM_003503	0.5410	0.0052	x	x
CDC20	CDC20 cell division cycle 20	NM_001255	0.4300	0.0003	x	x
CDC25B	cell division cycle 25B	NM_021874	x	x	1.5910	0.0001
CDC45L	CDC45 cell division cycle 45-like	NM_003504	0.2790	0.0005	0.6490	0.0033
CDCA5	cell division cycle associated 5	NM_080668	0.1140	0.0001	0.3930	0.0071
CDCA7	cell division cycle associated 7	NM_031942	0.1630	0.0002	0.4290	0.0001
CDK4	cyclin-dependent kinase 4	NM_000075	0.4880	0.0006	x	x
CDKN1A	cyclin-dependent kinase inhibitor 1A	NM_000389	x	x	1.5600	0.0156
CDKN1B	cyclin-dependent kinase inhibitor 1B	NM_004064	1.7440	0.0238	1.8630	0.0017
CDKN1C	cyclin-dependent kinase inhibitor 1C	NM_000076	x	x	0.4580	0.0039
CDKN3	cyclin-dependent kinase inhibitor 3	NM_005192	0.2290	0.0005	0.5740	0.0140
CDT1	DNA replication factor	NM_030928	0.6270	0.0008	x	x
CENPA	centromere protein A	NM_001809	0.0733	0.0000	0.4120	0.0141
CENPE	centromere protein E	NM_001813	0.4160	0.0003	x	x
CENPF	centromere protein F	NM_016343	0.0980	0.0000	0.4160	0.0125
CHAF1A	chromatin assembly factor 1, subunit A	NM_005483	0.3640	0.0008	x	x
CHAF1B	chromatin assembly factor 1, subunit B	NM_005441	0.4620	0.0035	x	x
CHEK1	CHK1 checkpoint	NM_001274	0.4780	0.0100	0.6640	0.0055
CHEK2	CHK2 checkpoint	NM_007194	0.5550	0.0009	x	x
FOXM1	forkhead box M1	NM_021953	0.5620	0.0024	x	x
GTSE1	G-2 and S-phase expressed 1	NM_016426	0.3670	0.0012	0.6590	0.0360
H2AFX	H2A histone family, member X	NM_002105	0.4350	0.0027	x	x
H3F3B	H3 histone, family 3B	BC020466	x	x	2.0300	0.0022
HCAP-G	chromosome condensation protein G	NM_022346	0.0721	0.0001	0.1960	0.0027
HDAC1	histone deacetylase 1	NM_004964	x	x	1.5280	0.0016
HIST1H1B	histone 1, H1b	NM_005322	0.2750	0.0061	x	x
HIST1H2AC	histone 1, H2ac	U90551	x	x	2.3950	0.0001
HIST1H4C	histone 1, H4c	NM_003542	0.3130	0.0002	x	x
HIST2H2AA	histone 2, H2aa	AY131971	2.0930	0.0004	3.1850	0.0009
KNTC1	kinetochore associated 1	NM_014708	0.5150	0.0199	x	x
KNTC2	kinetochore associated 2	NM_006101	0.0713	0.0000	0.2320	0.0044
MCM2	minichromosome maintenance deficient 2	NM_004526	0.5280	0.0020	x	x
MCM3	minichromosome maintenance deficient 3	NM_002388	0.3790	0.0008	x	x
MCM4	minichromosome maintenance deficient 4	NM_005914	0.3330	0.0025	x	x
MCM5	minichromosome maintenance deficient 5	NM_006739	0.4640	0.0001	x	x
MCM6	minichromosome maintenance deficient 6	NM_005915	0.2770	0.0017	0.6330	0.0023
MCM7	minichromosome maintenance deficient 7	NM_005916	0.3960	0.0004	x	x
MCM8	minichromosome maintenance deficient 8	NM_032485	0.4390	0.0014	x	x
MCM10	minichromosome maintenance deficient 10	AB042719	0.6440	0.0306	x	x
PCNA	proliferating cell nuclear antigen	NM_002592	0.3990	0.0014	x	x
PLCD1	phospholipase C, delta 1	NM_006225	1.5320	0.0004	x	x
RHOA	ras homolog gene family, member A	NM_001664	1.6190	0.0054	2.3220	0.0001

chromatin assembly factors, histone and histone family members, kinetochore associated proteins and minichromosome maintenance (MCM) genes. As a measure of overall level of proliferation, the gene for proliferating cell nuclear antigen (PCNA) is downregulated under shear stress compared to static conditions.

In examining the TEWM: Shear vs. Static data set, there are 28 genes changing expression and 19 of these are downregulated under shear compared to static whereas nine are upregulated under shear compared to static. Of the families of genes involved in cell cycle progression, there is a reduction in four of the cyclin genes (cyclin B1, cyclin B2, cyclin D2 and cyclin H), in six of the cdc and cdc-associated genes (cdc6, cdc45L, cdca5 and cdca7) and changes in the cyclin-dependent kinase inhibitors. There are also changes in gene expression for other cell cycle machinery however these changes are not as numerous as seen on the Slide substrate.

The Shear vs. Static data sets provide information on genes which change expression under shear stress compared to static conditions and by comparing the two data sets, one can gain insight into how a change in substrate affects the response to the mechanical environment. Of the 51 genes identified between these two data sets to be involved in cell cycle, 19 of them are responsive to mechanical environment on both substrates. However, a comparison of the magnitude of fold changes for these genes shows an interesting trend. For 16 of the 19 genes, there is a greater change in gene expression between shear and static on the Slide than on the TEWM. Additionally, the three genes which do not have a greater change in expression on the Slide are the only three which have an upregulation in expression under shear compared to static.

From the Shear vs. Static microarray comparisons, we can conclude that cell cycle gene expression decreases dramatically in endothelial cells on the Slide when exposed to shear compared to static. Cell cycle gene expression also decreases in endothelial cells on the TEWM when exposed to shear compared to static, however this decrease is not as large as that seen on the Slide. The greater drop in cell cycle on the Slide is reflected in the total number of genes changing in response to shear as well as in the fold change magnitude of genes which decrease on both substrates. One potential explanation for this observation is that the Slide Static proliferates more than the TEWM Static and therefore shear induces a greater drop in activity to reduce Slide proliferation levels. An additional potential explanation is that endothelial cells on the TEWM are less responsive to shear stress than cells on the Slide. In the case of either explanation, the data demonstrates that the presence of a substrate affects endothelial cell response to shear stress. However, to evaluate the possible explanations, data from the Slide vs. TEWM can be used to examine the effect of substrate on cell cycle.

Table 4.5 shows fold change (calculated as Slide/TEWM) and t-test p-value data for genes identified by IPA Functional Analysis in the Static: Slide vs. TEWM and Shear: Slide vs. TEWM microarray comparisons to be involved in cell cycle. Initial impressions of the data set include extensive cell cycle gene expression differences between the two substrates under static conditions and very few differences between the two substrates under shear conditions.

Looking at the Static: Slide vs. TEWM data, there are 26 genes differentially expressed between the two substrates under static conditions and 23 of those are upregulated on the Slide compared to the TEWM while three are downregulated. Of the

Table 4.5 Cell Cycle Genes in Slide vs. TEWM Comparisons

Red text denotes gene downregulation and blue text denotes gene upregulation
'x' denotes failure to meet significance criteria (t-test $p<0.05$ and ANOVA $p<0.05$ and fold change>1.5)

Gene ID	Gene Name	Genbank ID	Static: Slide vs. TEWM		Shear: Slide vs. TEWM	
			fold change	t-test p-value	fold change	t-test p-value
BRCA1	breast cancer 1, early onset	NM_007294	2.4970	0.0008	x	x
CCNA2	cyclin A2	NM_001237	2.5760	0.0026	x	x
CCNB1	cyclin B1	NM_031966	4.0190	0.0006	x	x
CCNB2	cyclin B2	NM_004701	4.3180	0.0022	x	x
CCNH	cyclin H	BF368083	1.8280	0.0001	x	x
CDC6	CDC6 cell division cycle 6 homolog	NM_001254	3.6760	0.0000	x	x
CDC20	CDC20 cell division cycle 20 homolog	NM_001255	2.1450	0.0000	x	x
CDC25C	cell division cycle 25C	NM_001790	1.6180	0.0036	x	x
CDC45L	CDC45 cell division cycle 45-like	NM_003504	3.0040	0.0002	x	x
CDCA7	cell division cycle associated 7	NM_031942	3.0410	0.0001	x	x
CDGAP	Cdc42 GTPase-activating protein	AB033030	0.5380	0.0030	0.6230	0.0094
CDKN1C	cyclin-dependent kinase inhibitor 1C	NM_000076	0.4500	0.0003	x	x
CDKN3	cyclin-dependent kinase inhibitor 3	NM_005192	3.1260	0.0003	x	x
CDT1	DNA replication factor	NM_030928	1.5010	0.0004	x	x
CENPA	centromere protein A	NM_001809	5.4280	0.0012	x	x
CENPE	centromere protein E	NM_001813	2.2030	0.0005	x	x
CENPF	centromere protein F	NM_016343	4.2700	0.0009	x	x
CENPH	centromere protein H	NM_022909	1.5400	0.0017	x	x
CHEK1	CHK1 checkpoint	NM_001274	2.1420	0.0000	x	x
FOXM1	forkhead box M1	NM_021953	1.8240	0.0030	x	x
H1F0	H1 histone family, member 0	NM_005318	0.5270	0.0008	0.5410	0.0026
H2AFX	H2A histone family, member X	NM_002105	1.7750	0.0005	x	x
H2AFZ	H2A histone family, member Z	NM_002106	1.5520	0.0159	x	x
H3F3B	H3 histone, family 3B	BC020466	x	x	0.5360	0.0076
HIST1H1B	histone 1, H1b	NM_005322	2.3580	0.0095	x	x
HIST1H3D	histone 1, H3d	NM_003530	1.5390	0.0406	x	x
HIST2H2AA	histone 2, H2aa	AY131971	x	x	0.4980	0.0080
PCNA	proliferating cell nuclear antigen	NM_002592	2.0280	0.0002	x	x

various genes involved in cell cycle progression, endothelial cells on the Slide express higher levels of cyclins, cdc and cdc-associated genes, centromere proteins and histone family members. As a measure of overall cell proliferation, PCNA gene expression on the Slide is twice as high as expression on the TEWM. From this data, we conclude that baseline cell cycle activity under static conditions is higher on the Slide than on the TEWM. The pattern of gene expression seen in the Shear: Slide vs. TEWM data is drastically different from the data set under static conditions. When comparing cell cycle gene expression in endothelial cells on the Slide and TEWM under shear stress, there are only four genes which are differentially regulated and all four have reduced expression on the Slide compared to the TEWM. Two of which are also downregulated on the Slide under static conditions and the other two were not differentially regulated by the substrate under static but only appear in the context of shear stress. Furthermore, we see no significant difference in levels of PCNA in the Slide Shear compared to the TEWM Shear. Thus we conclude that cell cycle activity is relatively comparable on the two substrates under shear stress conditions.

Compiling these data sets to paint a picture of cell cycle activity in response to substrate and shear stress, we conclude that the presence of shear stress greatly reduces differences in cell cycle gene expression between the Slide and TEWM. The extreme reduction in cell cycle on the Slide and lesser reduction on the TEWM in response to shear stress are explained by higher cell cycle activity on the Static Slide. From the Shear vs. Static comparisons, we conclude that shear stress reduces cell cycle activity on each substrate; however the nature of the substrate alters the extent of the shear effect. Shear stress and substrate both affect cell cycle gene expression and the presence or

absence of one stimulus alters the conclusions drawn regarding the effect of the other stimulus. The cell cycle gene expression data exemplifies the need for more physiologic *in vitro* models as it is very apparent how components of the endothelial microenvironment combine to affect the overall cell phenotype.

Biological Function: Cardiovascular and Hematological Systems

Table 4.6 shows genes identified by IPA Functional Analysis in the Slide: Shear vs. Static and TEWM: Shear vs. Static microarray comparisons which are involved in the cardiovascular and hematological systems. This table gives fold change (calculated as Shear/Static) and t-test p-value data as well as categories of cell function for each gene identified. Data from these comparisons can identify genes which are differentially expressed under shear or static mechanical environments. Moreover, genes which are regulated by shear on both substrates or on only one substrate can be further evaluated. The total number of cardiovascular and hematological system genes identified using Ingenuity Pathways Analysis in the Shear vs. Static data set is 40. Of these, 26 are differentially expressed on the Slide substrate with 17 upregulated under shear and 9 downregulated under shear. On the TEWM substrate, 33 are differentially expressed under shear with 25 upregulated and eight downregulated.

Table 4.7 shows genes identified by IPA Functional Analysis in the Static: Slide vs. TEWM and Shear: Slide vs. TEWM microarray comparisons which are involved in the cardiovascular and hematological systems. This table gives fold change (calculated as Shear/Static) and t-test p-value data as well as categories of cell function for each gene identified. Data from these comparisons can identify genes which are differentially

Table 4.6 Cardiovascular and Hematological System Genes in Shear vs. Static Comparisons

Red text denotes gene downregulation and blue text denotes gene upregulation
'x' denotes failure to meet significance criteria (t-test p<0.05 and ANOVA p<0.05 and fold change>1.5)

Category	Gene ID	Gene Name	Genbank ID	Slide: Shear vs. Static		TEWM: Shear vs. Static	
				fold change	t-test p-value	fold change	t-test p-value
cell adhesion	SELE	selectin E (endothelial adhesion molecule 1)	NM_000450	x	x	5.3100	0.0433
cell adhesion	VCAM1	vascular cell adhesion molecule 1	NM_001078	0.6650	0.0230	x	x
cell adhesion	ITGA1	integrin, alpha 1	X68742	x	x	1.8420	0.0084
cell adhesion	ITGA6	integrin, alpha 6	NM_000210	1.7470	0.0055	x	x
cell adhesion	ITGAV	integrin, alpha V	NM_002210	x	x	3.1790	0.0223
cell adhesion	ITGB3	integrin, beta 3	M35999	0.3300	0.0015	0.3870	0.0006
cell adhesion	ITGB4	integrin, beta 4	NM_000213	1.8090	0.0097	1.5410	0.0031
cell surface receptor	NRP1	neuropilin 1	AF086016	x	x	0.6660	0.0053
cell surface receptor	NRP2	neuropilin 2	AK024680	2.7720	0.0001	x	x
cell surface receptor	PDGFRA	platelet-derived growth factor receptor, alpha	NM_006206	x	x	2.4150	0.0004
coagulation	F2RL3	factor II (thrombin) receptor-like 3 (PAR-4)	AF080214	1.9550	0.0254	1.9460	0.0269
coagulation	PLAT	plasminogen activator, tissue	NM_000930	0.4320	0.0057	x	x
coagulation	PLAU	plasminogen activator, urokinase	NM_002658	0.6650	0.0059	x	x
coagulation	THBD	thrombomodulin	NM_000361	2.2420	0.0001	x	x
enzyme	ANG	angiogenin, ribonuclease, RNase A family, 5	NM_001145	x	x	1.6480	0.0022
enzyme	LIPG	lipase, endothelial	NM_006033	2.7630	0.0000	1.8740	0.0239
growth factor	ANGPT2	angiopoietin 2	NM_001147	0.1850	0.0012	0.2250	0.0055
growth factor	ANGPTL2	angiopoietin-like 2	BC012368	x	x	0.5980	0.0033
growth factor	BMP4	bone morphogenetic protein 4	NM_001202	0.4270	0.0003	0.5350	0.0191
growth factor	PDGFB	platelet-derived growth factor, beta	NM_002608	x	x	0.6160	0.0171
growth factor	PDGFC	platelet derived growth factor C	NM_016205	0.4730	0.0007	x	x
growth factor	VEGF	vascular endothelial growth factor	AK098750	x	x	1.6550	0.0009
growth factor	VEGFC	vascular endothelial growth factor C	NM_005429	0.4430	0.0001	1.6290	0.0074
matrix molecule	COL12A1	collagen, type XII, alpha 1	NM_004370	x	x	0.4490	0.0014
matrix molecule	COL17A1	collagen, type XVII, alpha 1	NM_130778	2.7070	0.0205	3.9960	0.0079
matrix molecule	COL5A1	collagen, type V, alpha 1	NM_000093	x	x	1.5950	0.0118
matrix molecule	COL9A3	collagen, type IX, alpha 3	NM_001853	1.6130	0.0008	1.5160	0.0012
matrix molecule	FN1	fibronectin 1	NM_002026	x	x	2.3800	0.0073
matrix turnover	MMP1	matrix metalloproteinase 1	NM_002421	7.4440	0.0000	3.7450	0.0214
matrix turnover	MMP10	matrix metalloproteinase 10	NM_002425	4.1380	0.0000	2.8170	0.0218
peptidase	CTSC	cathepsin C	NM_148170	0.5670	0.0031	0.5170	0.0038
redox balance	CYP1A1	cytochrome P450, 1A1	NM_000499	3.8770	0.0006	3.8210	0.0003
redox balance	CYP1B1	cytochrome P450, 1B1	NM_000104	23.5500	0.0000	73.4700	0.0000
redox balance	HMOX1	heme oxygenase (decycling) 1	NM_002133	5.3610	0.0002	6.4300	0.0001
redox balance	PTGS2	prostaglandin-endoperoxide synthase 2 (cox-2)	BC013734	3.9300	0.0000	5.7060	0.0024
redox balance	SOD1	superoxide dismutase 1, soluble	NM_000454	x	x	2.2480	0.0003
transcription factor	EPAS1	endothelial PAS domain protein 1	BC015869	2.0010	0.0010	2.6070	0.0002
transcription factor	KLF2	Kruppel-like factor 2 (lung)	NM_016270	3.1770	0.0001	7.2140	0.0006
transport	GJA5	gap junction protein, alpha 5 (connexin 40)	NM_005266	x	x	2.3070	0.0019
transport	LDLR	low density lipoprotein receptor	NM_000527	1.8470	0.0087	3.2550	0.0004

Table 4.7 Cardiovascular and Hematological System Genes in Slide vs. TEWM Comparisons

Red text denotes gene downregulation and blue text denotes gene upregulation
'x' denotes failure to meet significance criteria (t-test p<0.05 and ANOVA p<0.05 and fold change>1.5)

Category	Gene ID	Gene Name	Genbank ID	Static: Slide vs. TEWM		Shear: Slide vs. TEWM	
				fold change	t-test p-value	fold change	t-test p-value
cell adhesion	ICAM1	intercellular adhesion molecule 1	NM_000201	0.4280	0.0028	0.6600	0.0282
cell adhesion	ICAM2	intercellular adhesion molecule 2	NM_000873	x	x	1.5890	0.0257
cell adhesion	SELE	selectin E (endothelial adhesion molecule 1)	NM_000450	0.1960	0.0023	0.0274	0.0030
cell adhesion	ITGA1	integrin, alpha 1	X68742	0.4450	0.0015	0.1940	0.0003
cell adhesion	ITGA3	integrin, alpha 3	NM_005501	1.6260	0.0200	1.9380	0.0169
cell adhesion	ITGB4BP	integrin beta 4 binding protein	NM_181468	1.5160	0.0003	x	x
cell surface receptor	KDR	kinase insert domain receptor	NM_002253	0.5060	0.0003	x	x
cell surface receptor	LDLR	low density lipoprotein receptor	BC014514	2.9200	0.0083	1.9340	0.0055
cell surface receptor	ROBO1	roundabout 1	NM_133631	0.5840	0.0018	0.1810	0.0048
coagulation	A2M	alpha-2-macroglobulin	M36501	0.0662	0.0002	0.1470	0.0052
coagulation	FGL2	fibrinogen-like 2	NM_006682	0.3150	0.0001	x	x
coagulation	PLAU	plasminogen activator, urokinase	NM_002658	1.7780	0.0091	x	x
coagulation	PROCR	protein C receptor, endothelial (EPCR)	NM_006404	1.9310	0.0011	1.5240	0.0168
coagulation	TFPI2	tissue factor pathway inhibitor 2	NM_006528	0.0869	0.0001	0.1090	0.0034
coagulation	THBD	thrombomodulin	NM_000361	0.4500	0.0027	x	x
coagulation	VWF	von Willebrand factor	NM_000552	0.6600	0.0001	x	x
enzyme	LOX	lysyl oxidase	NM_002317	2.9920	0.0001	1.9970	0.0110
growth factor	ANGPT2	angiopoietin 2	AJ289780	0.1880	0.0003	x	x
growth factor	ESM1	endothelial cell-specific molecule 1	NM_007036	x	x	0.5650	0.0030
growth factor	VEGF	vascular endothelial growth factor	AK098750	x	x	0.6590	0.0158
matrix molecule	COL12A1	collagen, type XII, alpha 1	NM_004370	0.2130	0.0001	0.3680	0.0005
matrix molecule	COL17A1	collagen, type XVII, alpha 1	NM_130778	3.8100	0.0120	2.5810	0.0193
matrix molecule	COL4A1	collagen, type IV, alpha 1	NM_001845	0.2730	0.0000	0.4440	0.0019
matrix molecule	COL4A2	collagen, type IV, alpha 2	NM_001846	0.3200	0.0000	0.4060	0.0013
matrix molecule	COL6A1	collagen, type VI, alpha 1	NM_001848	x	x	0.5500	0.0156
matrix molecule	COL8A1	collagen, type VIII, alpha 1	NM_001850	2.1020	0.0098	1.8410	0.0015
matrix molecule	COL9A3	collagen, type IX, alpha 3	NM_001853	0.5230	0.0007	0.5570	0.0000
matrix molecule	FN1	fibronectin 1	NM_002026	1.6660	0.0441	x	x
matrix molecule	LAMA5	laminin, alpha 5	NM_005560	1.5710	0.0057	x	x
matrix molecule	LAMB3	laminin, beta 3	NM_000228	3.0610	0.0000	x	x
matrix turnover	MMP1	matrix metalloproteinase 1	NM_002421	0.3620	0.0014	x	x
matrix turnover	MMP11	matrix metalloproteinase 11	NM_005940	0.3910	0.0000	0.5550	0.0057
matrix turnover	MMP14	matrix metalloproteinase 14	NM_004995	0.5270	0.0014	x	x
membrane protein	CAV1	caveolin 1	BC006432	1.9890	0.0086	2.9670	0.0008
membrane protein	EFNA1	ephrin-A1	NM_004428	0.2420	0.0001	0.1850	0.0006
membrane protein	EFNB2	ephrin-B2	NM_004093	0.4370	0.0000	0.2540	0.0009
peptidase	ADAM10	a disintegrin and metalloproteinase domain 10	NM_001110	x	x	0.6510	0.0319
peptidase	ADAM19	a disintegrin and metalloproteinase domain 19	NM_033274	0.5810	0.0007	x	x
peptidase	ADAMTS4	adam with thrombospondin type 1 motif, 4	NM_005099	0.5290	0.0000	0.5250	0.0010
peptidase	CTSF	cathepsin F	NM_003793	0.5870	0.0004	x	x
peptidase	ECEL1	endothelin converting enzyme-like 1	NM_004826	x	x	1.5790	0.0001
redox balance	CYP1B1	cytochrome P450, 1B1	NM_000104	x	x	0.4370	0.0005
redox balance	GPX1	glutathione peroxidase 1	NM_000581	0.6020	0.0009	0.5050	0.0080
redox balance	PTGS1	prostaglandin-endoperoxide synthase 1 (cox-1)	M59979	2.8670	0.0001	x	x
transcription factor	EPAS1	endothelial PAS domain protein 1	BC015869	0.6180	0.0005	0.4740	0.0016

expressed by the experimental substrates: Slide or TEWM. Moreover, we can evaluate how the mechanical environment to which these cells are exposed influences the substrate effect. The total number of cardiovascular and hematological system genes identified using Ingenuity Pathways Analysis in the Slide vs. TEWM data set is 45. Of these, 38 are differentially expressed under Static conditions with 13 upregulated on the Slide and 25 downregulated on the Slide. Under Shear conditions, there are 30 genes differentially expressed by the two substrates with nine genes upregulated on the Slide and 21 downregulated on the Slide.

To further investigate the effect of substrate and shear stress on the identified genes of the cardiovascular and hematological systems, we will discuss them in the context of the following areas of endothelial cell function:

a) Cell adhesion through integrins
b) Coagulation balance
c) Extracellular matrix deposition
d) Extracellular matrix turnover
e) Reduction-oxidation balance
f) Vascular patterning and angiogenesis

Gene expression data has been taken from Table 4.6 and Table 4.7 and re-stated in a table for each area to simplify analysis and discussion.

Cell Adhesion through Integrins

Endothelial cell adhesion through integrin family members is an active area of research due to their established involvement in angiogenesis and well as response to

shear stress. Migration of endothelial cells and sensing of extracellular matrix molecules using outside-in signal transduction pathways are an important part of vessel growth. (194) Integrins are also well established in the endothelial cell response to fluid shear stress as the cells must be attached to the matrix in order to sense and transduce mechanical signals. (72) In addition, integrins have been shown to play an intermediary role in major signaling cascades involving Shc and JNKs as well as Rho activation. (195) With their prominent roles in extracellular matrix recognition and mechanical signal transduction, differential regulation by substrate and shear stress seen here is not unexpected.

Table 4.8 shows data for integrin genes significantly expressed in all four pairwise microarray comparisons. In first evaluating response in Shear vs. Static data sets, there is a mixed expression pattern. On the Slide substrate, shear upregulates α_6 and β_4 expression while downregulating β_3 expression. On the TEWM substrate, shear upregulates α_1, α_V, and β_4 expression while downregulating β_3 expression. Furthermore, downregulation of β_3 and upregulation of β_4 are present on both substrates while regulation of α_1, α_6, and α_V are specific to the substrate provided. Thus we conclude that expression of integrin family members are influenced by mechanical environment, however the identity of integrins changing can depend on the substrate and the direction of change in response to shear stress is specific to the identity of the integrin family member. In then evaluating the Slide vs. TEWM data sets, there is also a mixed expression pattern. Integrin α_1 is downregulated on the Slide compared to the TEWM whereas α_3 and integrin β_4 binding protein are upregulated on the Slide. Integrin α_1 is the only gene which directly shows significant regulation by both shear stress and substrate,

Table 4.8 Integrin Gene Expression in Microarray Data Comparisons

Red text denotes gene downregulation and blue text denotes gene upregulation
'x' denotes failure to meet significance criteria (t-test $p<0.05$ and ANOVA $p<0.05$ and fold change>1.5)

Gene ID	Gene Name	Slide: Shear vs. Static		TEWM: Shear vs. Static		Static: Slide vs. TEWM		Shear: Slide vs. TEWM	
		fold change	t-test p-value	fold change	t-test p-value	fold change	t-test p-value	fold change	t-test p-value
ITGA1	integrin, alpha 1	x	x	1.8420	0.0084	0.4450	0.0015	0.1940	0.0003
ITGA6	integrin, alpha 6	1.7470	0.0055	x	x	x	x	x	x
ITGAV	integrin, alpha V	x	x	3.1790	0.0223	x	x	x	x
ITGB3	integrin, beta 3	0.3300	0.0015	0.3870	0.0006	x	x	x	x
ITGB4	integrin, beta 4	1.8090	0.0097	1.5410	0.0031	x	x	x	x
ITGA3	integrin, alpha 3	x	x	x	x	1.6260	0.0200	1.9380	0.0169
ITGB4BP	integrin beta 4 binding protein	x	x	x	x	1.5160	0.0003	x	x

however other integrin genes show shifts in fold change magnitude depending on the combination of substrate and shear stress which is present.

Coagulation Balance

Providing a non-thrombogenic surface for blood flow and participation in the coagulation cascade when necessary are critical functions of the endothelium. Shear stress regulation of proteins involved in the coagulation cascade has been established for many of the important regulatory molecules. (65-67) Both pro-coagulant and anti-coagulant molecules are differentially regulated by shear stress and substrate as shown in Table 4.9. In examining the Shear vs. Static data sets, we see upregulation of the pro-coagulant molecule PAR-4 on both the Slide and TEWM substrates. There is also change in anti-coagulant molecules with a downregulation of tissue plasminogen activator and urokinase plasminogen activator and upregulation of thrombomodulin under Shear compared to Static on the Slide but no significant difference on the TEWM. In examining the Slide vs. TEWM data sets, we see regulation by substrate of several genes which are also regulated by shear stress: urokinase plasminogen activator and thrombomodulin. Under Static conditions, there is upregulation on the Slide of the procoagulant molecules vWF and FGL-2 and the anti-coagulant molecules thrombomodulin and tissue factor pathway inhibitor 2. In the presence of shear stress, the differences in coagulation gene expression between the two substrates are reduced so that only the upregulation of endothelial protein C receptor (EPCR) and downregulation of alpha-2-macroglobulin and tissue factor pathway inhibitor 2 are similar to what is seen under static conditions. The expression levels of genes involved in the coagulation

Table 4.9 Coagulation Gene Expression in Microarray Data Comparisons

Red text denotes gene downregulation and blue text denotes gene upregulation
'x' denotes failure to meet significance criteria (t-test $p<0.05$ and ANOVA $p<0.05$ and fold change>1.5)

Gene ID	Gene Name	Slide: Shear vs. Static		TEWM: Shear vs. Static		Static: Slide vs. TEWM		Shear: Slide vs. TEWM	
		fold change	t-test p-value	fold change	t-test p-value	fold change	t-test p-value	fold change	t-test p-value
F2RL3	factor II (thrombin) receptor-like 3 (PAR-4)	1.9550	0.0254	1.9460	0.0269	x	x	x	x
PLAT	plasminogen activator, tissue	0.4320	0.0057	x	x	x	x	x	x
PLAU	plasminogen activator, urokinase	0.6650	0.0059	x	x	1.7780	0.0091	x	x
THBD	thrombomodulin	2.2420	0.0001	x	x	0.4500	0.0027	x	x
A2M	alpha-2-macroglobulin	x	x	x	x	0.0662	0.0002	0.1470	0.0052
FGL2	fibrinogen-like 2	x	x	x	x	0.3150	0.0001	x	x
PROCR	protein C receptor, endothelial (EPCR)	x	x	x	x	1.9310	0.0011	1.5240	0.0168
TFPI2	tissue factor pathway inhibitor 2	x	x	x	x	0.0869	0.0001	0.1090	0.0034
VWF	von Willebrand factor	x	x	x	x	0.6600	0.0001	x	x

cascade are influenced by substrate and shear stress, however based on the genes identified here, there is no clear trend in tipping the overall balance towards a pro-coagulant or anti-coagulant phenotype. As with previous gene examples, we see that regulation is dependent not only on substrate or shear stress but the combined presence or absence of multiple stimuli.

Extracellular Matrix Deposition

Extracellular matrix proteins have wide-ranging effects on cell phenotype with established roles in adhesion, migration, proliferation and differentiation while also often contributing to the mechanical properties of the tissue of which they are a part. Blood vessel extracellular matrix molecules have been extensively studied for their roles in numerous diseases such as atherosclerosis, hypertension and restenosis, thus it is interesting to evaluate endothelial production of extracellular matrix molecules in response to the microenvironment components: shear stress and substrate. Table 4.10 shows data for multiple matrix molecules which are significantly differentially regulated in at least one of the four microarray comparisons. In examining the Shear vs. Static data sets, there is an overall trend where shear appears to increase gene expression of matrix molecules suggesting an active deposition of new extracellular matrix. Shear stress increases expression of collagen XVII and collagen IX on both substrates, although the magnitude of fold change is dependent on the substrate. Shear stress also regulates the expression of collagen XII, collagen V and fibronectin but only in endothelial cells on the TEWM substrate. Overall there is an increase in extracellular matrix gene expression in

Table 4.10 Extracellular Matrix Gene Expression in Microarray Data Comparisons

Red text denotes gene downregulation and blue text denotes gene upregulation
'x' denotes failure to meet significance criteria (t-test $p<0.05$ and ANOVA $p<0.05$ and fold change>1.5)

Gene ID	Gene Name	Slide: Shear vs. Static		TEWM: Shear vs. Static		Static: Slide vs. TEWM		Shear: Slide vs. TEWM	
		fold change	t-test p-value	fold change	t-test p-value	fold change	t-test p-value	fold change	t-test p-value
COL12A1	collagen, type XII, alpha 1	x	x	0.4490	0.0014	0.2130	0.0001	0.3680	0.0005
COL17A1	collagen, type XVII, alpha 1	2.7070	0.0205	3.9960	0.0079	3.8100	0.0120	2.5810	0.0193
COL5A1	collagen, type V, alpha 1	x	x	1.5950	0.0118	x	x	x	x
COL9A3	collagen, type IX, alpha 3	1.6130	0.0008	1.5160	0.0012	0.5230	0.0007	0.5570	0.0000
FN1	fibronectin 1	x	x	2.3800	0.0073	1.6660	0.0441	x	x
COL4A1	collagen, type IV, alpha 1	x	x	x	x	0.2730	0.0000	0.4440	0.0019
COL4A2	collagen, type IV, alpha 2	x	x	x	x	0.3200	0.0000	0.4060	0.0013
COL6A1	collagen, type VI, alpha 1	x	x	x	x	x	x	0.5500	0.0156
COL8A1	collagen, type VIII, alpha 1	x	x	x	x	2.1020	0.0098	1.8410	0.0015
LAMA5	laminin, alpha 5	x	x	x	x	1.5710	0.0057	x	x
LAMB3	laminin, beta 3	x	x	x	x	3.0610	0.0000	x	x

response to shear stress but the breadth of this response and behavior of individual genes often depends on the substrate present.

To further evaluate the influence of substrate on extracellular matrix gene expression, Table 4.10 contains data on the Slide vs. TEWM comparisons. There is a mixture of upregulation and downregulation of endothelial matrix genes in response to substrate. Genes which are expressed at lower levels on the Slide than the TEWM include collagen XII, collagen IV (α_1), collagen IV (α_2), collagen VI and collagen IX. Genes which are expressed at higher levels on the Slide than the TEWM include collagen XVII, collagen VIII, fibronectin, laminin α_5 and laminin β_3. For the majority of genes, the differences due to substrate are consistent regardless of mechanical environment, however the presence of shear stress does eliminate the difference due to substrate for fibronectin and both laminins. Numerous basement membrane genes (collagen IV, fibronectin and laminin) are differentially regulated between the Slide and TEWM suggesting that the substrate provided to the endothelial cells alters their production of basement membrane. With matrix molecules having extensive effects on cell function, altered production due to substrate and shear stress provides another mechanism through which cell phenotype can be modulated.

Extracellular Matrix Turnover

Along with deposition of extracellular matrix is the equally important degradation and turnover of matrix molecules which has also been implicated in vascular development and disease.(196, 197) Table 4.11 contains data from Shear vs. Static and Slide vs. TEWM microarray comparisons for several matrix metalloproteinase genes

Table 4.11 Matrix Turnover Gene Expression in Microarray Data Comparisons

Red text denotes gene downregulation and blue text denotes gene upregulation
'x' denotes failure to meet significance criteria (t-test $p<0.05$ and ANOVA $p<0.05$ and fold change>1.5)

Gene ID	Gene Name	Slide: Shear vs. Static		TEWM: Shear vs. Static		Static: Slide vs. TEWM		Shear: Slide vs. TEWM	
		fold change	t-test p-value	fold change	t-test p-value	fold change	t-test p-value	fold change	t-test p-value
MMP1	matrix metalloproteinase 1	7.4440	0.0000	3.7450	0.0214	0.3620	0.0014	x	x
MMP10	matrix metalloproteinase 10	4.1380	0.0000	2.8170	0.0218	x	x	x	x
MMP11	matrix metalloproteinase 11	x	x	x	x	0.3910	0.0000	0.5550	0.0057
MMP14	matrix metalloproteinase 14	x	x	x	x	0.5270	0.0014	x	x

which are a family of proteinases responsible for extracellular matrix protein degradation. In comparing mechanical environments by examining Shear vs. Static data sets, shear stress upregulates expression on both substrates of MMP-1 which is known to cleave collagen of types I, II, III, VII and X. Also on both substrates, shear stress upregulates expression of MMP-10 which degrades fibronectin and gelatin of types I, III, IV and V as well as weakly degrades several types of collagen. In evaluating the Slide vs. TEWM data sets, there is a general trend of reduced MMP expression on the Slide compared to the TEWM. With this general observation, one could hypothesize that the presence of a more complex substrate stimulates endothelial cells to increase remodeling. The interplay of stimuli is again apparent as MMP-1 and MMP-14 are not differentially regulated by substrate in the presence of shear stress.

Reduction-Oxidation Balance

Oxidative stress is considered a leading cause of atherosclerosis progression and vascular dysfunction. Production and catabolism of free radicals and activated oxygen species by endothelial cells has been heavily investigated in order to understand mechanisms by which atherosclerotic plaque develops. (198) With the reduction-oxidation balance an important mediator of vascular disease, response of genes involved in the balance to substrate and shear stress is of great interest. Table 4.12 shows data from Shear vs. Static and Slide vs. TEWM microarray comparisons. Looking first at the Shear vs. Static data, there is a clear trend of upregulation of identified redox genes under shear stress compared to static conditions on both substrates. There is a significant upregulation in CYP1A1 and CYP1B1 family members in response to shear on both

Table 4.12 Reduction-Oxidation Gene Expression in Microarray Data Comparisons

Red text denotes gene downregulation and blue text denotes gene upregulation
'x' denotes failure to meet significance criteria (t-test $p<0.05$ and ANOVA $p<0.05$ and fold change>1.5)

Gene ID	Gene Name	Slide: Shear vs. Static		TEWM: Shear vs. Static		Static: Slide vs. TEWM		Shear: Slide vs. TEWM	
		fold change	t-test p-value	fold change	t-test p-value	fold change	t-test p-value	fold change	t-test p-value
CYP1A1	cytochrome P450, 1A1	3.8770	0.0006	3.8210	0.0003	x	x	x	x
CYP1B1	cytochrome P450, 1B1	23.5500	0.0000	73.4700	0.0000	x	x	0.4370	0.0005
HMOX1	heme oxygenase (decycling) 1	5.3610	0.0002	6.4300	0.0001	x	x	x	x
PTGS2	prostaglandin-endoperoxide synthase 2 (cox-2)	3.9300	0.0000	5.7060	0.0024	x	x	x	x
SOD1	superoxide dismutase 1, soluble	x	x	2.2480	0.0003	x	x	x	x
GPX1	glutathione peroxidase 1	x	x	x	x	0.6020	0.0009	0.5050	0.0080
PTGS1	prostaglandin-endoperoxide synthase 1 (cox-1)	x	x	x	x	2.8670	0.0001	x	x

Slide and TEWM substrates which confirm recent reports of their shear regulation. (199) There is also upregulation of heme oxygenase-1, superoxide dismutase-1 and cox-2 which have all also been reported to respond to shear stress environments. (68, 69) Identity of the substrate does not seem to greatly affect the shear response of these genes; however there is detection of SOD-1 only on the TEWM substrate and greater fold change of cox-2 and CYP1B1 on the TEWM compared to the Slide.

In evaluating the Slide vs. TEWM data sets, there is little difference between the two substrates under static or shear conditions for the redox genes identified. Gene expression of glutathione peroxidase-1 (GPX1), which is involved in catabolism of activated oxygen species and free radical detoxification, is downregulated on the Slide compared to the TEWM under Static and Shear conditions. There is also a reduction in CYP1B1 expression on the Slide compared to the TEWM under Shear conditions which correlates to the fold changes seen in the Shear vs. Static data for this gene. Finally, there is upregulation of cox-1 on the Slide compared to the TEWM but only when the cells are under static conditions. Overall, we conclude that there is an upregulation of redox genes under shear stress compared to static conditions on both substrates. The slightly greater response to shear stress by the redox genes in endothelial cells on the TEWM also suggests that substrate has an effect on oxidative stress. This microarray data underlines the importance of shear stress in regulating the reduction-oxidation balance and provides new insight on the potential role of substrate.

Vascular Patterning and Angiogenesis

Development of new blood vessels, whether prompted by normal development or pathologic conditions, is a complex series of processes involving many players and carefully orchestrated cues. While multiple genes are involved in the steps of vascular patterning and angiogenesis, there are several genes known to have specific functions in blood vessel development. Table 4.13 contains data from the microarray comparisons for several genes involved in vascular patterning and angiogenesis which were significantly regulated in response to substrate and shear stress.

In examining the Shear vs. Static data sets, three genes are identified which were not previously recognized as being sensitive to mechanical environment. Two related molecules, neuropilin 1 and neuropilin 2, are cell surface glycoproteins with established roles in axon guidance and more recently have been associated with angiogenesis. (200) Neuropilins bind semaphorins and specific isoforms of PGF and VEGF to mediate chemorepulsive and chemoattractive signals and they are among the many neural patterning genes which are now recognized to have similar functions in blood vessel patterning. (201) Although the two neuropilins are identified here as responsive to shear stress, their shear response depends on the substrate present as NRP1 is downregulated under shear only on the TEWM and NRP2 is upregulated under shear only on the Slide. A third gene identified as differentially regulated under shear stress compared to static conditions is the ribonuclease angiogenin. Angiogenin is a protein which moves into the nucleus where it is thought to control tRNAs as well as rRNA transcription and therefore may be a control point for multiple angiogenic factors. (202) In this study, angiogenin is upregulated under shear stress but only in endothelial cells on the TEWM substrate. It

Table 4.13 Vascular Patterning and Angiogenesis Gene Expression in Microarray Data Comparisons

Red text denotes gene downregulation and blue text denotes gene upregulation
'x' denotes failure to meet significance criteria (t-test $p<0.05$ and ANOVA $p<0.05$ and fold change>1.5)

Gene ID	Gene Name	Slide: Shear vs. Static		TEWM: Shear vs. Static		Static: Slide vs. TEWM		Shear: Slide vs. TEWM	
		fold change	t-test p-value	fold change	t-test p-value	fold change	t-test p-value	fold change	t-test p-value
NRP1	neuropilin 1	x	x	0.6660	0.0053	x	x	x	x
NRP2	neuropilin 2	2.7720	0.0001	x	x	x	x	x	x
ANG	angiogenin, RNase A family, 5	x	x	1.6480	0.0022	x	x	x	x
ROBO1	roundabout 1	x	x	x	x	0.5840	0.0018	0.1810	0.0048
EFNA1	ephrin-A1	x	x	x	x	0.2420	0.0001	0.1850	0.0006
EFNB2	ephrin-B2	x	x	x	x	0.4370	0.0000	0.2540	0.0009

has not previously been recognized as shear-responsive in endothelial cells; however it was recently reported to be upregulated in mouse embryonic stem cells which were exposed to laminar shear stress in efforts to promote a cardiovascular lineage. (203) Identification of these endothelial genes as shear-responsive, with the response being dependent on substrate, underlines the importance of cues from the cell microenvironment in vascular patterning and angiogenesis.

Examination of the Slide vs. TEWM data in Table 4.13 identifies three additional genes which are differentially regulated by substrate under static and shear stress conditions. Gene expression of robo-1, ephrin A1 and ephrin B2 is downregulated in endothelial cells on the Slide compared to the TEWM under both Static and Shear conditions. These three genes are membrane proteins and all have established roles in axon guidance and neural migration and are now recognized to play similar roles in vascular patterning. (201, 204) Additionally, members of the ephrin family interact at the arterial-venous interface and ephrin B2, which is significantly regulated here, is present only on arterial endothelium. While expression of these three genes is higher on the TEWM than the Slide under static conditions, the presence of shear stress only increases the disparity between the two substrates as reflected in the greater fold change magnitudes. Identification of numerous genes important in vascular patterning and angiogenesis as differentially regulated by shear stress and substrate is important in understanding their many functions in development of the vasculature. Furthermore, the more physiologic nature of the tissue engineered blood vessel provides an improved *in vitro* model for studying processes in blood vessel development.

Conclusions

The expansive nature of microarray data is useful for mining of any number of particular genes but interpretation of the data as a whole can often be difficult. Data presented here is a small fraction of the information generated from this study however the discussion of select areas of biological function serves to demonstrate the widespread influence of shear stress and substrate. By examining expression of genes involved in the cell cycle, we can conclude that the type of mechanical environment and nature of the substrate have broad impact on endothelial behavior. Specifically, shear stress reduces cell cycle activity on both substrates but the type of substrate present alters the extent of shear effect. Comparisons of the two substrates show higher cell cycle activity on the Slide under static conditions but there is little difference in cell cycle gene expression between the substrates under shear conditions.

In focusing on multiple areas of biological function within the cardiovascular and hematological systems, we see extensive regulation of gene expression by substrate and shear stress but the exact influence of these stimuli depends on the function in question and the identity of each gene. Integrin family gene expression shows significant regulation by both shear stress and substrate. However the specific integrin determines whether the expression varies with mechanical environment or with substrate and the type of response, whether upregulation or downregulation. Genes involved in the coagulation balance show a similar mixed pattern of influence with pro-coagulant and anti-coagulant molecules differentially upregulated or downregulated by both shear stress and substrate. In the presence of shear stress, the differences in coagulation gene

expression between the two substrates is reduced, however there is no general trend in tipping the coagulation balance in one direction or the other.

Genes encoding for extracellular matrix tend to increase in response to shear stress but the breadth of the response and behavior of individual genes often depends on the substrate concurrently present. However, for the majority of genes the substrate is a greater influence and differences due to substrate are consistent regardless of mechanical environment. The counterparts to genes for matrix deposition are those for matrix turnover which also show responsiveness to shear stress and substrate. Shear stress upregulates MMP expression on both substrates but there is a general trend of reduced expression on the Slide compared to the TEWM regardless of mechanical environment.

In examining genes involved in oxidation and reduction, there is a clear trend of upregulation under shear stress compared to static conditions on both substrates. Contrary to the general trend seen in extracellular matrix genes, substrate does not seem to greatly affect expression of redox genes with few significant differences identified and substrate effect seen only in fold change magnitudes in response to shear stress. The pattern of expression for genes involved specifically in vascular patterning and angiogenesis is more mixed with significant influence of both shear stress and substrate. Genes of this biological function identified here were not previously recognized to be shear and substrate responsive which underlines the importance of cues from the cell microenvironment and the novel insight which can be gained from using more physiologic *in vitro* models.

Data in each of the areas of biological function which were discussed contain genes which are sensitive to shear stress, genes which are sensitive to substrate and genes

which are sensitive to both stimuli. Overall some areas are more influenced by shear stress, such as genes in the redox balance, whereas other areas are more influenced by substrate, such as genes for extracellular matrix proteins. Other cell functions, most notably the cell cycle, are dramatically influenced by both mechanical environment and substrate. For all areas of biological function examined, the profile of gene expression is different for each combination of stimuli thus emphasizing the sensitivity of endothelial cells to cues from the microenvironment.

While this study provides new insight into endothelial cell behavior and explores the use of tissue engineered blood vessels in vascular biology, it has numerous limitations which are a basis for future work. In particular, the stimuli being provided are still simplistic approximations of the physiologic environment. The tissue engineered wall model (TEWM) is a more physiologic substrate than traditional *in vitro* models such as tissue culture plastic or the Slide substrate used in these studies, but it is a basic reconstruction of the vessel wall. The TEWM is missing important matrix components present *in vivo* such as elastin and other types of collagen. Furthermore, it does not achieve a native configuration with the current components such as collagen fiber structure and density of smooth muscle cells. The steady laminar shear stress is a more physiologic mechanical force than static culture however it is a crude approximation of the complexity of fluid flow experienced by the endothelium. A more physiologic system would use waveforms from different regions of the arterial tree and potentially compare these with steady flow or with each other. Another next step would be the addition of environmental cues other than substrate and shear stress. Other biological components such as plasma and blood cells as well as mechanical forces such as pressure

and cyclic strain have previously been shown to influence endothelial function. Additional of these physiologic cues to a system of multiple stimuli would increase the understanding of their effects by placing them in context with other components of the microenvironment.

As the more physiologic stimuli presented here are only a first step, the information provided by transcriptional profiling is only the beginning of insight into endothelial cell function. Additional information regarding protein expression and how the mRNA profile translates into the protein profile is required for biological understanding. Moreover, the way in which an array of proteins in a cell translates into a unified function in response to a challenge of the system must be investigated. As systems biology and technology for profiling advance along with development of more sophisticated analysis tools, researchers will be able to compile expansive data sets from different levels of cell control to paint a picture of overall function.

In conclusion, this study is intended as a first step towards a better understanding of endothelial cell biology and the use of more physiologic *in vitro* models provided by tissue engineering. Using the data presented in this study, pursuit of mechanisms of influence and identification of pathways sensitive to substrate and shear stress could provide novel insight into physiologic and pathologic conditions. Furthermore, the improved understanding of biological response to environmental cues will aid in the development of improved physiologic *in vitro* models. The iterative cycle of enhanced models and superior information will drive research to its ultimate goal of addressing physiologic and pathologic needs.

CHAPTER FIVE: Influence of Substrate and Shear Stress on Endothelial Gap Junctions

Introduction

Gap junctions and their building blocks, connexins, have long been identified as critical to cell communication and tissue function. They are found in almost every cell in the body and currently over 20 types of connexins, usually named by their molecular weight, have been identified in humans. Within a cell, a single connexin protein assembles with five other connexins to form a hexameric array called a connexon or hemichannel. Each hemichannel is trafficked to the cell membrane where it docks and covalently seals with a hemichannel from a neighboring cell to form a gap junction. Gap junctions then cluster in the membrane at regions of cell-cell contact to form a gap junction plaque and regulate flow of chemical and electrical information through their pores. While these fundamental processes of gap junctions have been established in model cell systems, little is understood about their synthesis, assembly, gating and function in native tissues.

Connexins in the cardiovascular system were first studied in the heart for their roles in conduction of electrical signals in the myocardium. Changes in connexin expression level or changes in ratio of connexin isotypes have been linked to cardiac abnormalities. (205) Recent interest in the role of connexins in the vascular wall has begun to build with evidence that they play critical and poorly understood roles in vascular development and disease. Endothelial cells are known to expression Connexin 37, Connexin 40 and Connexin 43 while smooth muscle cells express Connexin 40,

Connexin 43 and Connexin 45. (13, 119) Distribution of these connexins varies amongst vascular beds and in different species as well as between *in vivo* and *in vitro* experimental settings. (120, 121) It is thought that the heterogeneity in cellular and vascular bed distribution is linked to specialized functions of the connexin isotypes and needs for cellular communication which are not yet understood. (122) Gap junctions coordinate cellular responses within the endothelium and also within the layers of smooth muscle cells in the vascular media. However in addition to homocellular connections, heterocellular connections also exist. Most notably, there are myoendothelial gap junctions (MEGJ) which link endothelial cells and smooth muscle cells together. (120, 123) While their existence was only recently confirmed, it is believed that signals passed through myoendothelial gap junctions function to control vascular tone. (124).

With their primary function being to promote communication between cells, gap junctions are critical in development of many tissues. There are four connexins expressed in the developing mouse heart: Cx37, Cx40, Cx43 and Cx45. Cx37 is expressed in endothelial cells of blood vessels and in the endocardium, Cx40 is expressed in myocytes and appears to be regionally controlled while Cx43 often has either overlapping or complementary expression to Cx40 depending on the tissue region. (170) Knockout connexin models elucidate functions in development but attempts to study connexin influence on vascular wall biology have been hampered by the widespread expression of these molecules in other tissues and the drastic influence of knocking out the gene in all tissues. Cx37-/- mice are viable but females are infertile because of abnormal development of both oocytes and ovarian follicles. (171) Cx40-/- mice are viable but have prolonged atrioventricular conduction, right bundle branch block and a

predisposition for arrhythmias. Furthermore, Cx40-/- mice have diminished conduction of arteriolar dilatation in response to acetylcholine and bradykinin and are hypertensive but have no other obvious blood vessel abnormalities. (172) Cx43-/- mice die perinatally due to abnormal development of the pulmonary outflow tract from atypical migration of cardiac neural crest cells. (173) Single knockout connexin mice have characterized phenotypes which are largely non-blood vessel related because of the widespread expression of these molecules and their presumed functional overlap within the vessel wall. When *in vivo* expression of connexins is reduced further using a multiple knockout strategy, there are severe blood vessel abnormalities indicating an important interplay between the functions of connexins. Cx37-/- Cx40-/- mice die perinatally with hemorrhages and severe blood vessel dilatation. (174) Cx40-/- Cx43-/- have also been reported to die at E12.5 with malformed hearts including abnormally rotated ventricles.(175)

While roles for connexins have been identified in both cardiac dysfunction and angiogenesis, we will focus on the recent evidence linking gap junctions to hypertension and atherosclerosis. (118, 161, 162) In a recent study, the Cx43 gene was knocked out only in vascular endothelial cells therefore providing a model in which the role of connexins in the vascular wall can be studied without the confounding influence of perinatal death or impaired fertility of mice. Of particular interest is the finding that the VEC Cx43-/- mice exhibit hypotension and bradycardia compare to heterozygous littermates indicating a role for endothelial cell Cx43 in maintaining normal vascular function.(163) Further demonstrating the link between connexins and hypertension are results from spontaneously hypertensive rats which show reduced connexin expression

compared to normal controls. (164) Rats induced for hypertension also show reduced Cx37 and Cx43 expression but no change in Cx40 expression in endothelial cells compared to normotensive animals. This reduction can be partially recovered by one drug treatment and completely restored by another drug treatment. (165)

Connexins in the vascular wall have also been linked to the prevalence of atherosclerosis and have been shown to vary in expression with the progression of plaques. Heterozygous Cx43+/- mice exhibit a 50% decrease in atherosclerotic plaques *in vivo* and *in vitro* experiments have shown that statins reduce the Cx43 expression in endothelial and smooth muscle cell cultures. (166) Cx37 and Cx40 expression is reduced in endothelial cells of hyperlipidemic mice and only Cx37 levels recover with lipid-lowering drug treatment. (167) An altered pattern of connexin expression in endothelial and smooth muscle cells is seen in non-diseased arteries, early atheromas and advanced atheromas. (168) Finally, naturally occurring Cx37 variants have also been implicated in the prevalence of atherosclerosis in human populations. (169)

With links between gap junctions and atherosclerosis being established, there have been several studies investigating the response of vascular connexins to mechanical stimuli. The first insight into the potential regulation of gap junctions by physical forces grew out of a study focused on mapping the regional distribution of Cx37, Cx40 and Cx43 in rat endothelium. (187) While the distribution of Cx37 and Cx40 appeared in similar widespread patterns, it was noted that Cx43 expression was found mainly in regions near aortic branches where blood flow is disturbed. Introduction of a flow disturbance into this model resulted in a strong upregulation of Cx43 in areas not previously showing high levels of expression. An *in vitro* study of vascular cells and

mechanical forces found a sustained upregulation of Cx43 protein in rat aortic smooth muscle cells exposed to 20% stretch for 24 hours and a transient upregulation in Cx43 mRNA in endothelial cells exposed to laminar shear stress. (188) Further investigation of endothelial cell Cx43 regulation by shear stress was conducted using an *in vitro* parallel plate flow chamber system which exposed cells to four types of fluid shear from recirculating to fully developed laminar flow. (189) It was found that Cx43 mRNA was transiently upregulated by all flow patterns however upregulation was only sustained after 30 hours in areas of disturbed, recirculating flow. Furthermore, Cx43 protein appeared disorganized in regions of disturbed flow and cells showed little coupling as assessed by dye transfer indicating limited gap junction communication. More recently, other endothelial cell connexins (Cx37 and Cx40) were also investigated in this *in vitro* flow system. (190) Patterns of protein expression and roles of different connexin isotypes in endothelial gap junction communication were investigated using dye transfer techniques in conjuction with peptide channel blockers. In addition to studies focusing on vascular connexin response to mechanical forces, differential expression by shear stress has been reported in numerous microarray studies. (48, 81, 83, 191)

The link between endothelial cells and smooth muscle cells in the vascular wall is most intriguing when investigating the role gap junctions play in normal vascular function as well as disease. It is widely believed that the direct communication between these two cell types, in addition to the connections which exist among each cell type, allow the vascular wall to act as a unit in response to a stimulus. (122) Early studies of conductivity in arterioles first suggested that endothelial and smooth muscle cells are electrically coupled in both a homocellular and heterocellular manner. (152)

Subsequently, multiple dyes were used to trace the patterns of the potential endothelial-smooth muscle cell coupling units. (153) Anatomical evidence for myoendothelial gap junctions was then uncovered along with studies identifying movement of calcium and endothelial-derived hyperpolarizing factor directly between the two cell types. (154-156) The first *in vitro* study of myoendothelial gap junctions was recently reported where an endothelial-smooth muscle cell co-culture system was developed to better understand the role of specific connexin isotypes in their formation. (157)

Due to their emerging importance in vascular development and disease, this study focuses on connexins and gap junctions in human endothelial cells. As these structures serve to communicate information within the cellular microenvironment, we hypothesize that they are also regulated by stimuli present in the microenvironment. Therefore the goal of this study is to investigate the influence of substrate and shear stress on endothelial cell connexin expression and gap junction communication.

Experimental Design and Methods

Experimental Design

The approach taken to investigate influence of substrate and shear stress on endothelial cell gap junctions is to examine connexin mRNA expression, protein expression and cell-cell communication in cells on traditional and tissue engineered substrates under different mechanical environments. To profile the influence of substrate and shear stress, techniques will examine the three connexin isotypes present in endothelial cells (Cx37, Cx40 and Cx43) at the gene and protein levels while function will be evaluated by protein location and movement of dye through gap junctions.

Furthermore, to gain insight most applicable to human development and disease, this study takes advantage of the tissue engineering approach by using human cells to create a human blood vessel model. To examine the effect of shear stress, endothelial cells are exposed to either static or laminar shear stress (15 dynes/cm^2) conditions. To examine the effect of substrate, endothelial cells are exposed to two environments. As a point of reference, a traditional *in vitro* model of monomer type I collagen adsorbed to glass is used. As a more physiologic *in vitro* model, a biologically-based blood vessel substitute is used. This tissue engineered model is a three-dimensional type I collagen gel containing dispersed human aortic smooth muscle cells to mimic the components and structure of the medial layer. Confluent endothelial monolayers are cultured on each substrate for 48 hours prior to exposure to static or shear conditions for 24 hours. Similarities and differences in endothelial cells from the four experimental conditions provide insight into the influence of substrate and shear stress on multiple aspects of endothelial cell connexin expression and gap junction communication.

Experimental Methods

Cell Culture

Human aortic endothelial cells (HAEC) (Cambrex) were cultured to passage 6 in MCDB 131 supplemented with 5% FBS, antibiotics and growth factors while human aortic smooth muscle cells (HASMC) (Cambrex) were cultured to passage 8 in MCDB 131 supplemented with 5% FBS, antibiotics and growth factors. All experiments were conducted in a co-culture media of MCDB 131 supplemented with 5% FBS, antibiotics and growth factors common to both cell culture mediums.

Substrate Fabrication

Two types of substrate were used in this study: Adsorbed Collagen Slide and Tissue Engineered Wall Model (TEWM). The Adsorbed Collagen Slide was created by coating glass slides with 50 μg/ml collagen type I (BD Biosciences) and allowing protein to adsorb to the surface for one hour prior to removal of the solution. The Tissue Engineered Wall Model was created by suspending 1 million HASMC per ml in 5x concentrated MCDB-131, 10% FBS and 2 mg/ml rat tail type I collagen (BD Biosciences). Sodium hydroxide was added to neutralize the acidic collagen solution and promote polymerization. Tubular HASMC-collagen gels were created using a central mandrel during gelation and were cultured for six days to allow for cell-mediated compaction of the collagen fibers. The tubular gels were then cut longitudinally and embedded in agar to expose a flat lumen for seeding of HAEC and fluid shear experiments. (43) Endothelial cells were seeded on both models at a density of 40,000 cells/cm^2 to produce a confluent monolayer and cultured for 48 hours prior to exposure to static or shear conditions.

Exposure to Shear Stress

The parallel plate flow chamber used to expose endothelial cells to laminar shear stress has been previously established in our laboratory. (42, 49) In this closed loop, a peristaltic pump moves medium from a container into a pulse dampener and then through parallel plates where endothelial cells are exposed to a steady laminar shear stress. Shear stress is controlled by fluid flow rate and dimensions of the chamber according to the

equation: $\tau = 6Q\mu/bh^2$. Exposure of endothelial cells on the tissue engineered wall model was accomplished by embedding the depth of the collagen gel in agar supported by a polycarbonate mold. The entire mold/agar apparatus was then placed into the flow chamber. Endothelial cells on the Slide or TEWM were exposed to a shear stress of 15 dynes/cm^2 for 24 hours.

Endothelial Isolation from Tissue Engineered Wall Model

To evaluate endothelial cell gene and protein expression following culture on the TEWM, pure endothelial cells must be removed without contamination of neighboring smooth muscle cells. Following cell exposure to static or shear stress conditions, the TEWM lumen was briefly exposed to collagenase to release cells near the surface. Endothelial cells were isolated from the cell mixture using a magnetic separation technique whereby a primary PE-conjugated antibody to PECAM-1 (Santa Cruz) followed by a magnetic bead-conjugated secondary antibody to PE positively selects for endothelial cells. Following passage through a separation column placed in a magnetic field, endothelial cells were collected and lysed or fixed for further analysis. Effectiveness of the magnetic sorting procedure was validated using pre-labeled endothelial cells mixed with smooth muscle cells and flow cytometry analysis post-separation.

RNA Isolation and Analysis

Total RNA was extracted from endothelial cells using an RNeasy kit (Qiagen) with an added DNAse digestion step. To evaluate quality of RNA prior to RT-PCR

analysis, samples were assessed using the RNA 6000 Nano LabChip (Agilent) on an Agilent Bioanalyzer 2100. Profiles of ribosomal peaks were evaluated for degradation as a measure of overall RNA degradation and preliminary measurements of RNA quantity were determined. Quantity of high quality RNA was assessed by absorbance at 260nm prior to reverse transcription to cDNA for RT-PCR.

Quantitative RT-PCR

One microgram of high quality endothelial RNA was reverse transcribed using the First Strand cDNA Synthesis Kit (Invitrogen) for each experimental sample. Primers were designed using Primer Express (Applied Biosystems) and oligos were created by Integrated DNA Systems. Primer sequences are listed below for the three connexins expressed in endothelial cells.

Cx37 Forward: CATGGAGCCCGTGTTTGTG

Cx37 Reverse: GAGACAAAGCAGTCCACGAGG

Cx40 Forward: GGGCACTCTGCTCAACACCT

Cx40 Reverse: TGAAGCCCACCTCCATGGT

Cx43 Forward: TTAAGGGAAAGAGCGACCCTT

Cx43 Reverse: GACCCACAGTCTTTGGCAGG

Standards of known concentration were generated using PCR amplification and agarose gel extraction for each gene of interest. Quantitative RT-PCR was conducted using cDNA from samples (in triplicate) and standards (in triplicate) with SYBR® Green PCR Master Mix (Applied Biosystems) on an ABI 7700 (Applied Biosystems) real time PCR machine. Data was quantified using the absolute standard method where serial

dilutions of the standard were plotted against C_T values to generate a correlation used to convert sample C_T values into concentrations.

Flow Cytometry

Single cell suspensions of endothelial cells were fixed in 4% formaldehyde for 5 minutes, permeabilized in 0.1% Triton X-100 for 5 minutes and then incubated for 1 hour in 4% donkey serum to block non-specific binding of antibodies. Cells were labeled with one of the following primary antibodies at 1:100 dilution: Rabbit Anti-Mouse Cx37 (Alpha Diagnostic), Goat Anti-Human Cx40 (Santa Cruz Biotechnology), Goat Anti-Human Cx43 (Santa Cruz Biotechnology) for 1 hour at 37°C. Following two washes in T-TBS solution, cells were incubated with one of the following secondary antibodies: FITC-conjugated Donkey Anti-Rabbit (Jackson ImmunoResearch) or FITC-conjugated Donkey Anti-Goat (Jackson ImmunoResearch). Control samples were fixed, permeabilized and blocked with experimental samples, then labeled with secondary antibody alone to account for autoflourescence and non-specific binding of secondary antibody. Cell suspensions were analyzed using a BD LSR digital flow cytometer to determine mean fluorescence intensity of control and experimental samples. During each sample run, standard beads were analyzed to create a standard curve for conversion of fluorescence intensity measurements to units of MESF (molecules of equivalent soluble fluorescence).

Immunocytochemistry

Immunocytochemistry was conducted on endothelial cells on the Slide or TEWM substrate following exposure to static or shear conditions. Samples were fixed using 4% formaldehyde for 5 minutes for Slide samples and 1 hour for TEWM samples. Staining procedures were identical to flow cytometry analysis with steps for permeabilization, blocking, primary antibody incubation and secondary antibody incubation. Samples were imaged using a laser-scanning confocal microscope with a 40x oil objective.

Dye Transfer Assay

Following exposure of endothelial monolayers to static or shear stress conditions, assessment of dye transfer between cells was conducted as a measure of gap junction communication. In this assay of gap junction function, cells are loaded with two membrane-impermeant dyes: i) a small dye which can pass through gap junctions and ii) a large dye which cannot pass through gap junctions and is used to mark cells originally loaded with dye. Following a defined period of time, cells are fixed and imaged to evaluate the extent of dye transferred from cells originally loaded with dye to neighboring cells as a measure of cell coupling by gap junctions. In this study the dye used to pass through gap junctions is Biocytin (ε-biotinoyl-L-lysine) with a molecular weight of 372Da and neutral charge (Molecular Probes) and the dye used to mark cells originally loaded with dye is Tetramethylrhodamine Dextran (flouro-ruby) with a molecular weight of 10,000Da (Molecular Probes).

Immediately upon removal from the static dish or flow chamber, monolayers are rinsed in Dulbecco's PBS and excess fluid is blotted off. A mixture of 4mg/ml Biocytin

and 5mg/ml Rhodamine-Dextran in PBS is dripped onto the monolayer surface which is then scratched with a diamond-tipped pen (tip diameter 0.25mm). Samples are immediately placed in the incubator at 37°C for 2 minutes to allow passage of dye. Excess dye is quickly removed, samples are rinsed in PBS and fixed in 4% formaldehyde for 20 minutes. While the dextran is fluorescent, biocytin requires a secondary antibody for detection. Monolayers are permeabilized with 0.1% Triton X-100 for 5 minutes and incubated with 4% donkey serum for 30 minutes to block non-specific binding prior to labeling with a secondary antibody Oregon Green 488 NeutrAvidin (molecular probes). Samples were imaged using a Nikon E600 fluorescent microscope using filters to separately detect red and green signals.

Results

Connexin Gene Expression

The influence of substrate and shear stress on endothelial cell connexin gene expression was first identified using microarray analysis. Comparison of endothelial cells on the Slide or TEWM substrate under Static or Shear conditions resulted in the differential expression of connexins as shown in Table 5.1. ANOVA with multiple testing corrections showed significantly different regulation of Cx37 and Cx40 but not Cx43. Pairwise comparisons of the two flow environments on both substrates and comparisons of the two substrates under both flow environments showed a significant upregulation of Cx37 and Cx40 gene expression under shear stress compared to static on the TEWM substrate. Furthermore, there was also a significant downregulation of Cx37 on the TEWM compared to the Slide under static conditions. The significant regulation

of connexins by substrate and shear stress warranted further investigation, especially in light of the differential responses of the three endothelial connexin isotypes.

To further evaluate gene expression, RT-PCR was used to quantify levels of connexin mRNA in endothelial cells on the two experimental substrates under static and shear stress conditions. The three connexin isotypes known to be expressed by endothelial cells: Cx37, Cx40 and Cx43, were detected under all experimental conditions. Figure 5.1 shows mRNA expression for the four experimental conditions as quantified using standards of known concentration. Analysis by 2-way ANOVA identifies a significant effect of shear stress on Cx37 mRNA. However, while there is not a significant effect of substrate, the substrate alters the influence of shear stress as indicated by the significant interaction p-value. Figure 5.2 displays Cx40 mRNA expression in endothelial cells of the four experimental conditions and it is interesting to note that Cx40 is expressed at higher levels that Cx37 or Cx43. Shear stress significantly upregulates Cx40 mRNA to similar levels on both substrates while substrate does not have a significant effect nor does it significantly alter the influence of flow environment. Figure 5.3 displays levels of Cx43 mRNA in endothelial cells of the four experimental conditions which are similar to expression levels of Cx37 mRNA. For Cx43, there is a significant influence of substrate on mRNA with reduced levels in endothelial cells on the TEWM compared to the Slide. There is no significant effect of shear stress or interaction of flow and substrate.

Table 5.1 Connexin Gene Expression in Microarray Data

Bold and Underlined denotes meets significance criteria (t-test p<0.05 and fold change>1.5)
Red text denotes gene downregulation and blue text denotes gene upregulation

Array Spot ID	Genbank ID	Gene Name	Slide: Shear vs. Static		TEWM: Shear vs. Static		Static: TEWM vs. Slide		Shear: TEWM vs. Slide		ANOVA MTC p-value
			Array Shear/Static		Array Shear/Static		Array TEWM/Slide		Array TEWM/Slide		
			fold change	ttest p-value	fold change	ttest p-value	fold change	ttest p-value	fold change	ttest p-value	
A_23_P1083	NM_002060	Cx37	1.02	0.891	**4.43**	**0.001**	**0.51**	**0.003**	2.22	0.054	**0.014**
A_23_P371729	NM_005266	Cx40	1.10	0.550	**2.31**	**0.002**	0.72	0.048	1.51	0.099	**0.034**
A_24_P55295	NM_000165	Cx43	0.96	0.947	1.65	0.102	0.71	0.077	1.22	0.575	0.535

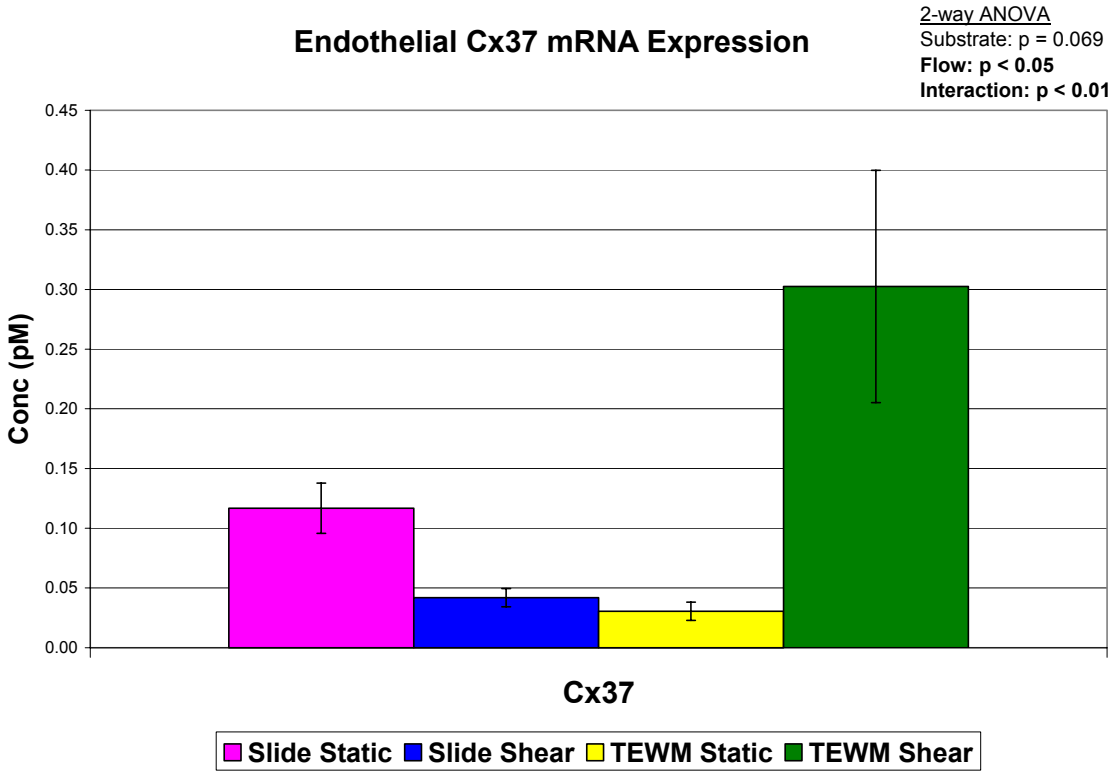

Figure 5.1 Endothelial Cx37 mRNA Expression Assessed by RT-PCR
Error bars represent SEM and statistical analysis by 2-way ANOVA is detailed.

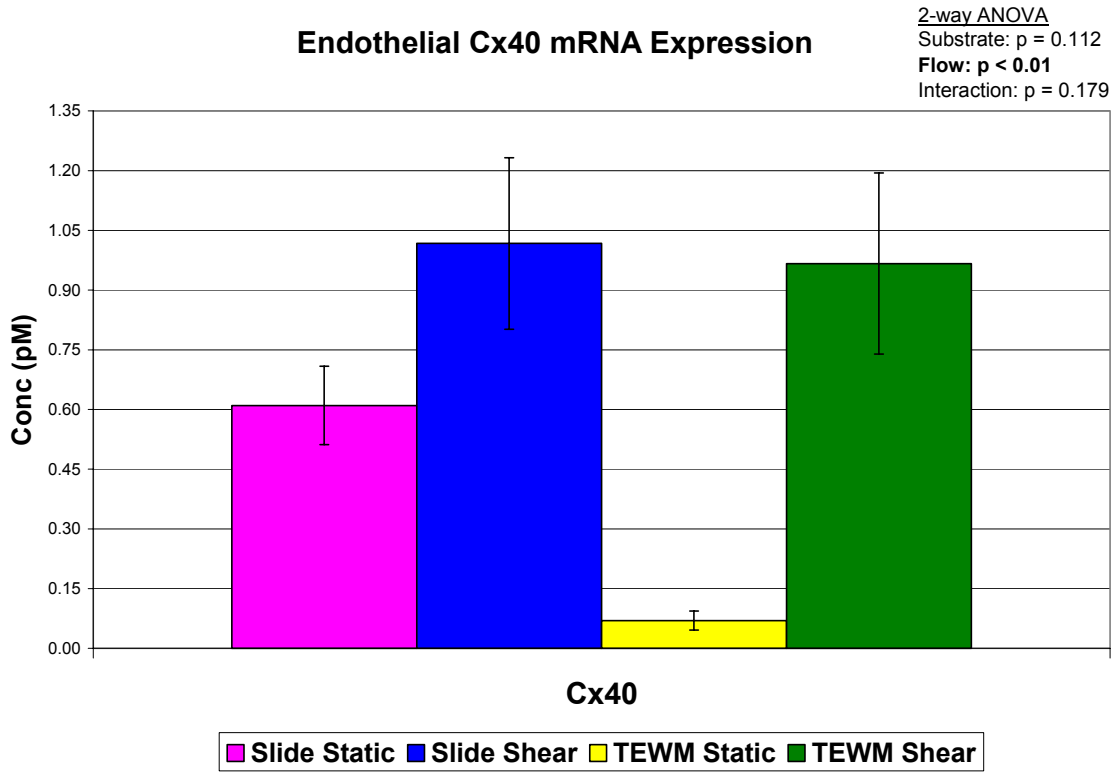

Figure 5.2 Endothelial Cx40 mRNA Expression Assessed by RT-PCR
Error bars represent SEM and statistical analysis by 2-way ANOVA is detailed.

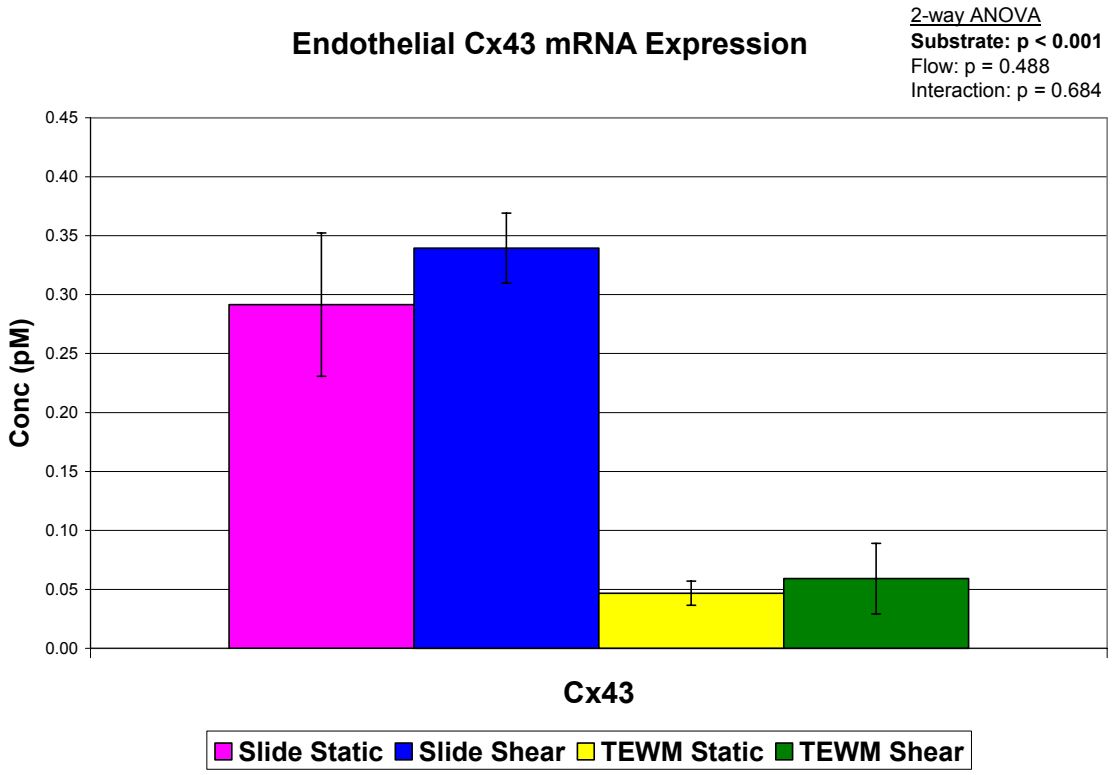

Figure 5.3 Endothelial Cx43 mRNA Expression Assessed by RT-PCR
Error bars represent SEM and statistical analysis by 2-way ANOVA is detailed.

Connexin Protein Expression

Flow cytometry was used to examine the total levels of connexin protein expression in endothelial cells as influenced by substrate and shear stress. Figure 5.4 shows expression of Cx37 protein which was quantified using standards of known fluorescence intensity in MESF (molecules of equivalent soluble fluorescence). Analysis by 2-way ANOVA shows no significant effect of shear stress but there is a significant effect of substrate on Cx37 protein levels. Under both mechanical environments, there is an increased expression in endothelial cells on the TEWM compared to the Slide. There is also no significant effect of flow on Cx40 protein levels, but Cx40 is significantly influenced by substrate as shown in Figure 5.5. Cx40 protein is increased in endothelial cells on the TEWM compared to the Slide and no significant effect of flow is detected. Figure 5.6 displays levels of Cx43 protein in endothelial cells of the four experimental conditions. Shear stress does not significantly affect Cx43 protein levels, however substrate significantly alters Cx43 with a dramatic increase in endothelial cells on the TEWM.

To further evaluate endothelial connexin protein expression and gain insight into the location of these proteins, immunocytochemistry was used to stain endothelial monolayers on both substrates under static and shear stress conditions. Figure 5.7 shows staining of the three connexin isotypes following exposure of endothelial cells on the slide substrate to static or shear stress conditions. Panels on the left (A, B and C) are of monolayers under static conditions and panels on the right (D, E and F) are of monolayers following exposure to laminar shear stress. Cx37 protein is shown in panels A and D, Cx40 protein is shown in panels B and E, and Cx43 protein is shown in panels

C and F. Connexins appear in punctate patterns at the cell membrane or in the cytoplasm. Bright white dots are clusters of connexins in gap junction plaques at the cell membrane or as annular gap junctions in the cytoplasm (denoted in Figure 5.7 with red arrowheads). More diffuse white dots are connexins or hemichannels which are more spread out and have not congregated with others (denoted in Figure 5.7 with green arrowheads). Under static conditions, all three connexins are visible at the membrane and in the cytoplasm. Under shear stress, fewer connexins are present at the membrane but gap junction plaques still exist and connexins are still present in the cytoplasm.

Figure 5.8 shows staining of the three connexin isotypes following exposure of endothelial cells on the TEWM substrate to static or shear stress conditions. Panels on the left (A, B and C) are of monolayers under static conditions and panels on the right (D, E and F) are of monolayers following exposure to laminar shear stress. Cx37 protein is shown in panels A and D, Cx40 protein is shown in panels B and E, and Cx43 protein is shown in panels C and F. As on the slide substrate, connexins appear in a punctate pattern either at the cell membrane or in the cytoplasm. Imaging of endothelial cells on the TEWM substrate is more difficult than the Slide due to the subtle topography of the TEWM surface and auto-fluorescence of the collagen gel. However, diffuse membrane staining of connexins is still visible in several images, most clearly in panel A. More intense staining of Cx40 and Cx43 is visible in endothelial cells on the TEWM substrate; however it does not appear to be concentrated at the endothelial cell-endothelial cell borders.

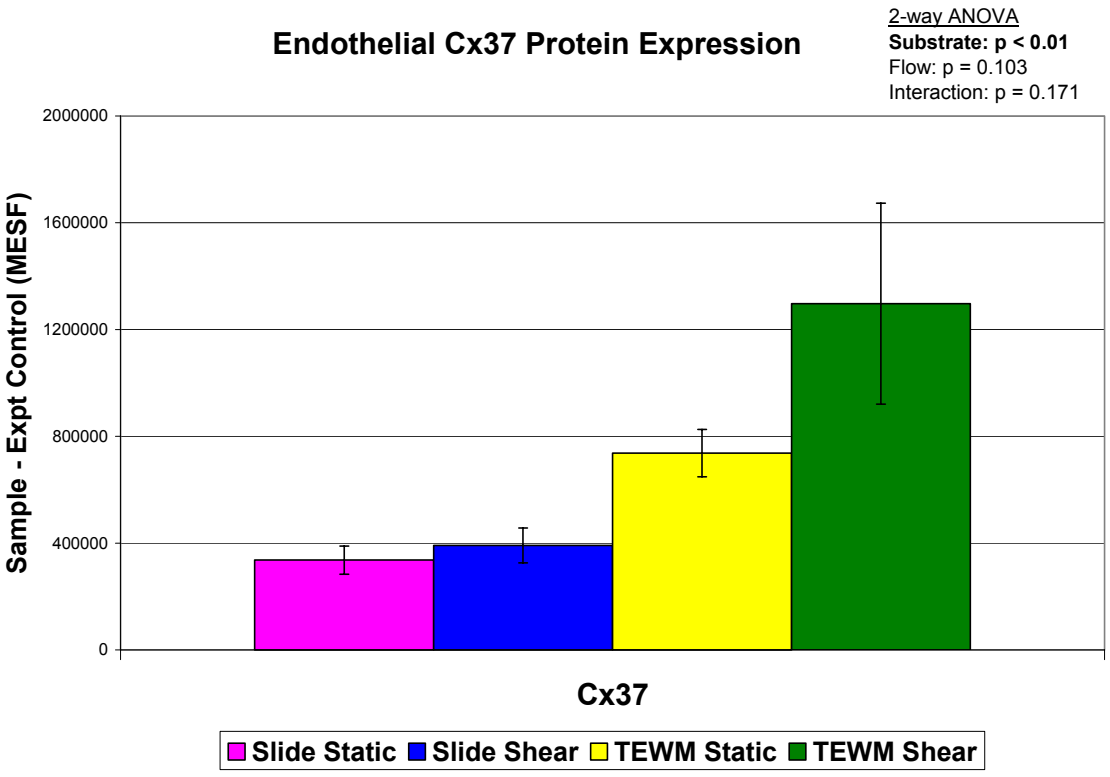

Figure 5.4 Endothelial Cx37 Protein Expression Assessed by Flow Cytometry
Error bars represent SEM and statistical analysis by 2-way ANOVA is detailed.

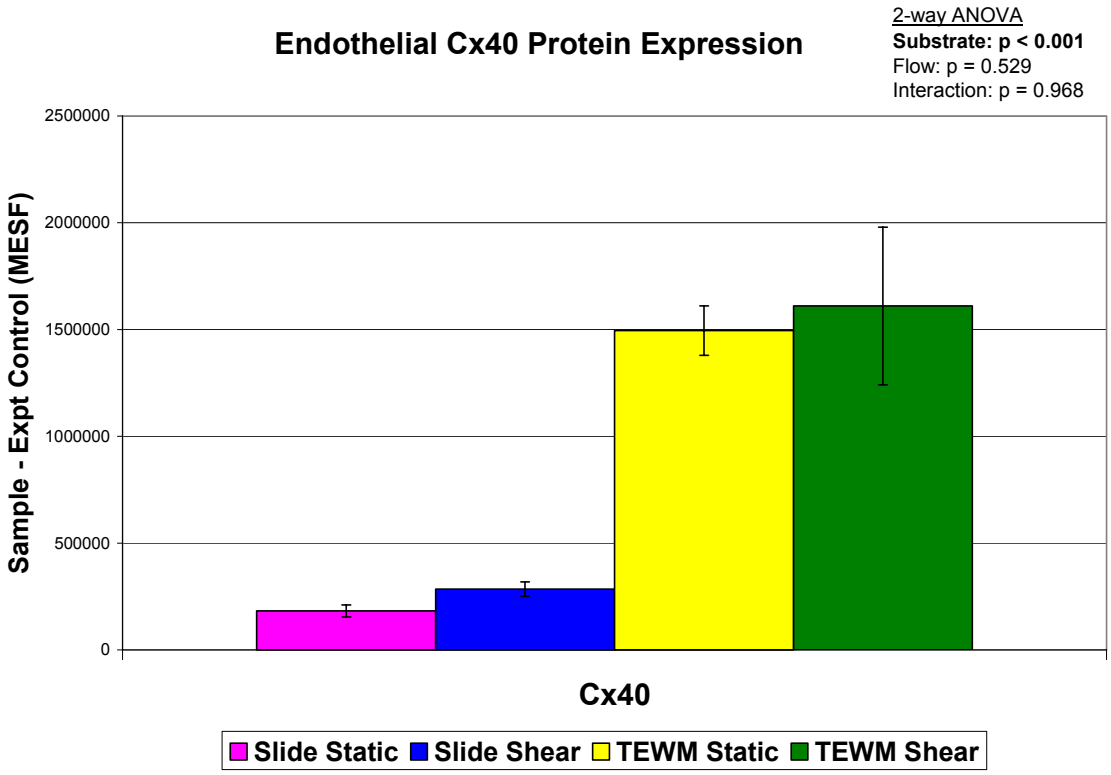

Figure 5.5 Endothelial Cx40 Protein Expression Assessed by Flow Cytometry
Error bars represent SEM and statistical analysis by 2-way ANOVA is detailed.

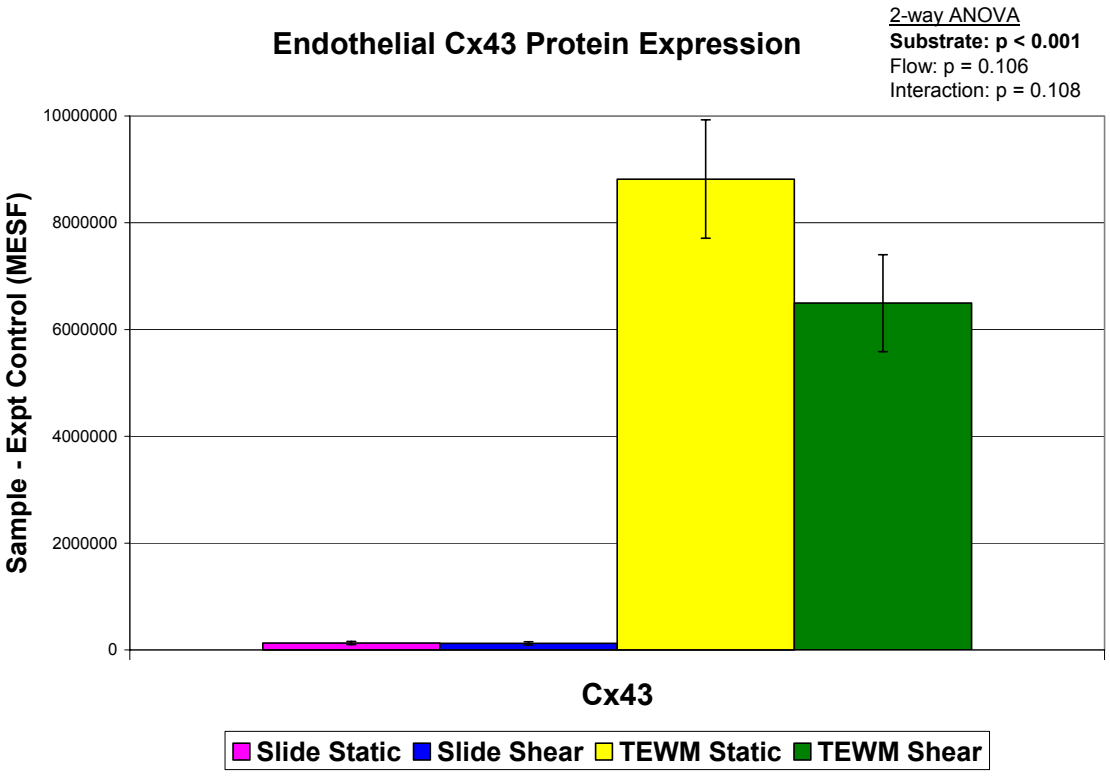

Figure 5.6 Endothelial Cx43 Protein Expression Assessed by Flow Cytometry
Error bars represent SEM and statistical analysis by 2-way ANOVA is detailed.

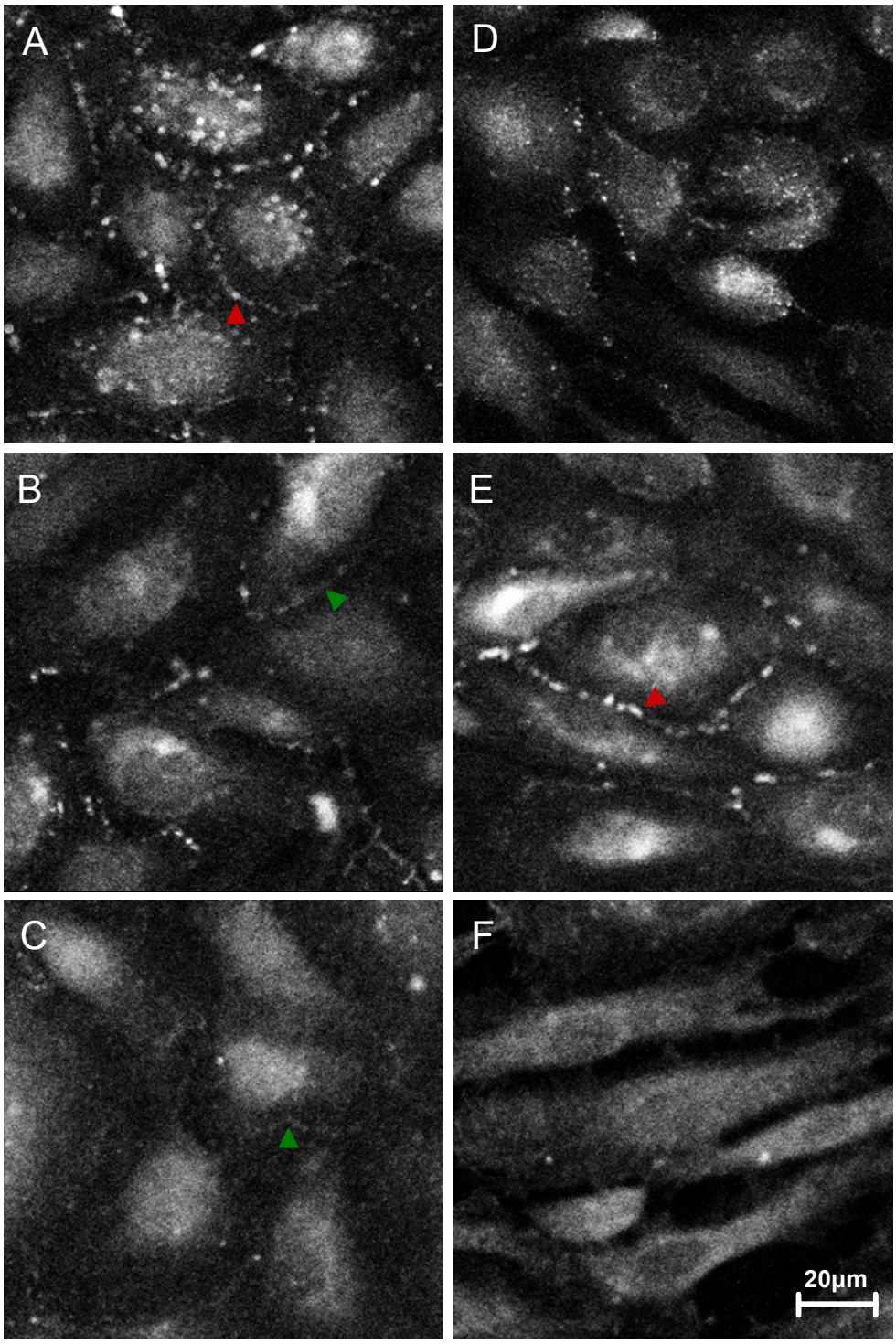

Figure 5.7 Endothelial Cell Connexin Protein Immunocytochemistry on a Slide
Endothelial cell monolayers exposed to static conditions (Panels A, B and C) or laminar shear conditions (Panels D, E and F). Staining shows expression of Cx37 (A and D), Cx40 (B and E) and Cx43 (C and F). Gap junction plaques visible by bright white punctate membrane staining (red arrowheads) and connexins in membrane visible by diffuse white staining (green arrowheads)

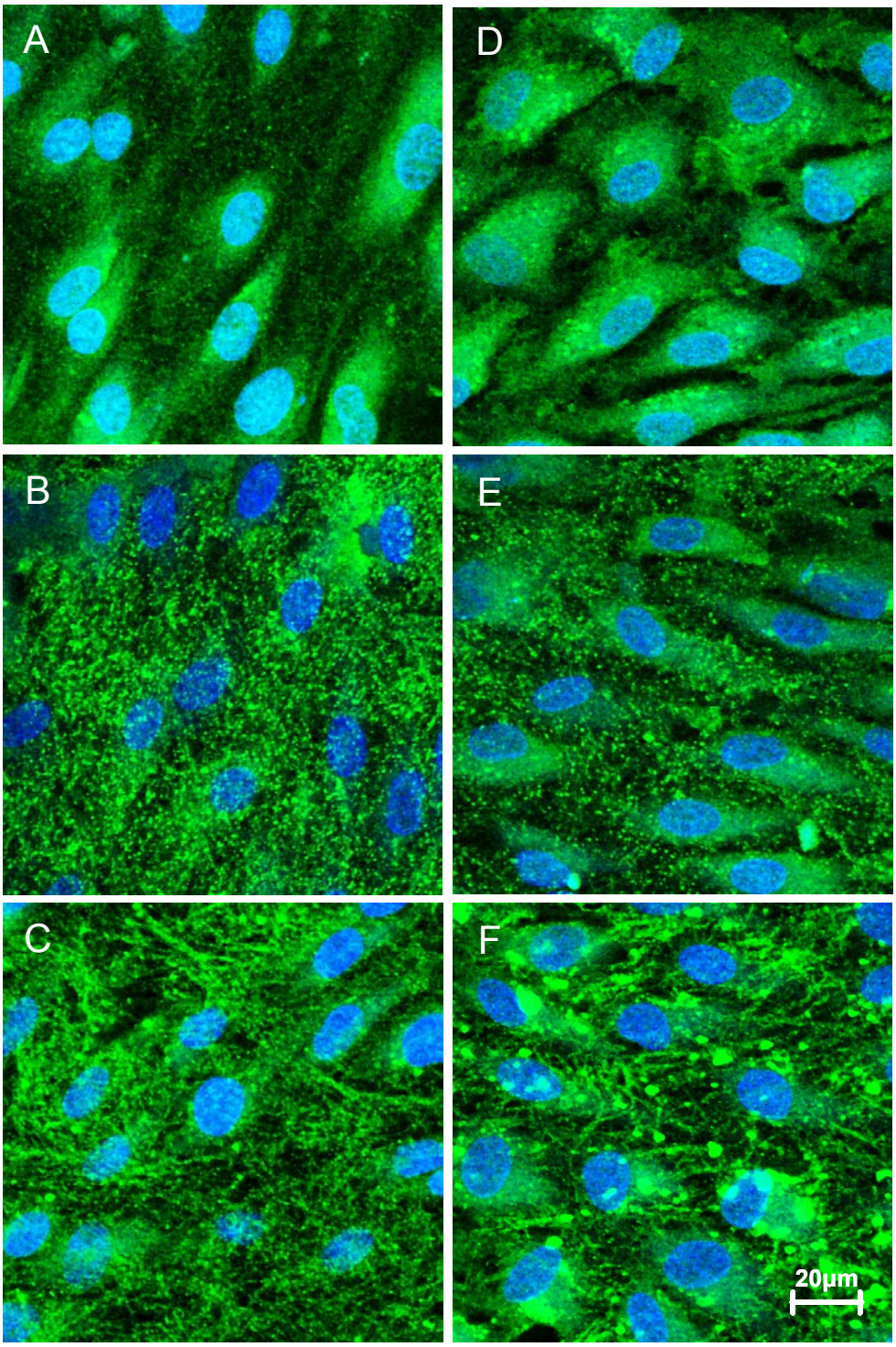

Figure 5.8 Endothelial Cell Connexin Protein Immunocytochemistry on the TEWM
Endothelial cell monolayers exposed to static conditions (Panels A, B and C) or laminar shear conditions (Panels D, E and F). Staining shows expression of Cx37 (A and D), Cx40 (B and E) and Cx43 (C and F) detected using FITC-conjugated secondary antibodies (green) and nuclei with Hoechst (blue).

Gap Junction Communication

Gap junctions serve to electrically and chemically couple neighboring cells to allow communication with a region of tissue. To evaluate function and level of gap junction communication, a dye transfer assay is used. Cells are loaded with two dyes: one of small molecular weight with favorable charge and steric properties which can pass through gap junctions and one of large molecular weight which cannot pass and is used to mark cells originally loaded with dye. By evaluating the extent of dye transferred from cells loaded with dye to their neighbors, one can assess the gap junction communication within the population.

Figure 5.9 shows dye transfer in endothelial cells on the slide substrate following exposure to static or laminar shear stress conditions for 24 hours. The left panels (A and B) show a region of endothelial cells on a Static Slide which have been scratched to load dye into cells adjacent to the scratch. The field is shown using a red filter in panel A to identify cells originally loaded with dye which contain the large Rhodamine-Dextran (MW 10,000) dye. The same field is shown using a green filter in panel B to identify cells containing the small dye Biocytin (MW 372) which include cells originally loaded with dye and those recipient cells that are linked to the donors by gap junctions. The right panels (C and D) show a region of endothelial cells on a Shear Slide which have been scratched and imaged in the same manner as the Static Slide. The images show a similar number of cells originally loaded with dye, however the endothelial cells exposed to static conditions pass the dye to more neighbors than cells exposed to laminar shear stress. Images were quantified by counting the number of donor and recipient cells and calculating a cell coupling index which the ratio of recipient to donor cells.

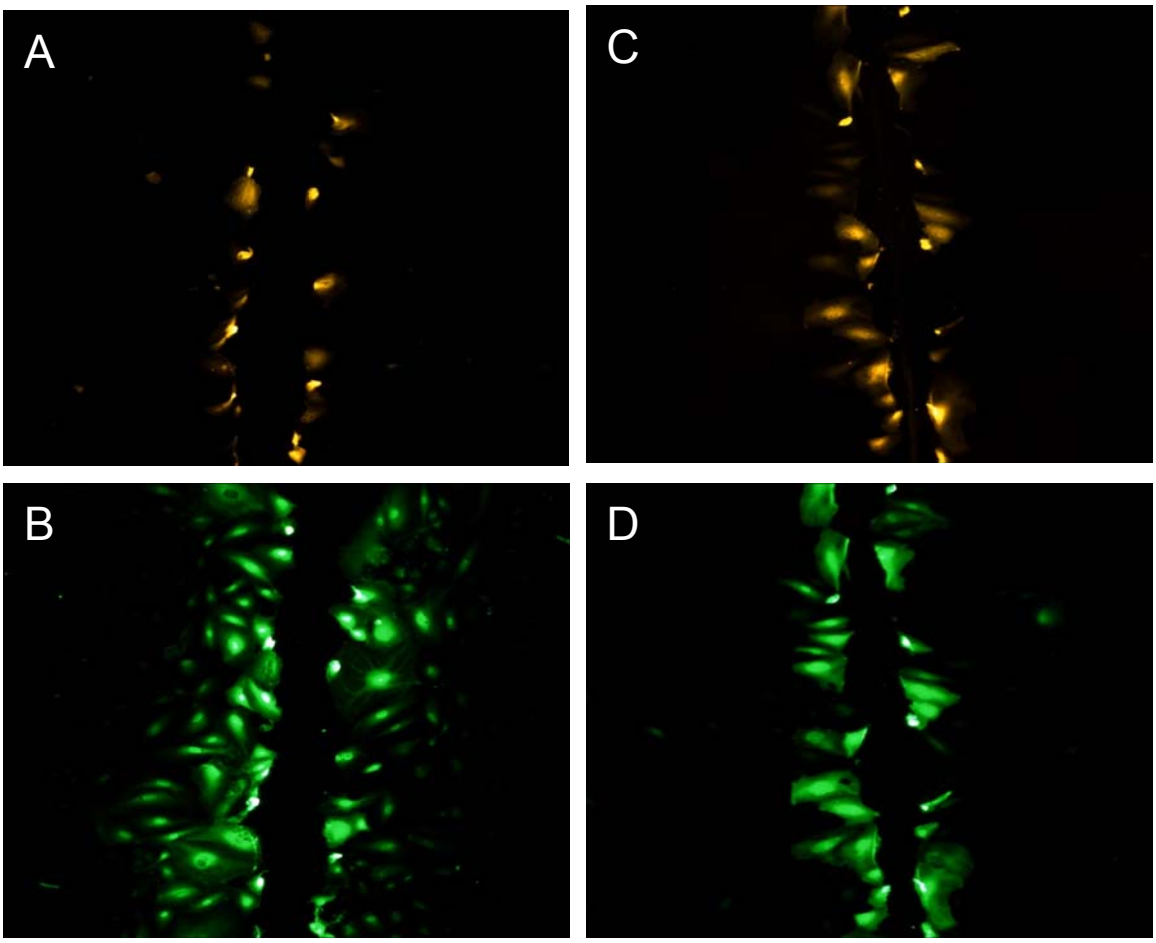

Figure 5.9 Dye Transfer in Endothelial Monolayers Exposed to Static or Shear
Endothelial cell monolayer exposed to static conditions for 24 hours (Panels A and B) and endothelial cell monolayer exposed to laminar shear stress (15 dynes/cm^2) for 24 hours (Panels C and D). Upper panels (A and C) identify cells loaded with dye by scraping which contain Rhodamine-Dextran (red, MW 10000). Lower panels (B and D) identify cells loaded with dye by scraping (donor) and adjacent cells in gap junction communication (recipient) containing Biocytin (MW 372) detected using Oregon Green 488 avidin secondary antibody (green).

Quantification of dye transfer for endothelial cells on slides is displayed in Figure 5.10 showing a significant reduction in cell coupling amongst endothelial cells exposed to laminar shear stress as assessed by biocytin dye transfer.

Due to the extensive restructuring endothelial cells undergo when initially exposed to shear stress in experimental conditions, additional studies were conducted where slide monolayers were exposed to static or shear conditions for 48 or 72 hours prior to dye transfer. Quantification of endothelial cell dye transfer after 24, 48 or 72 hours of static or laminar shear stress is displayed in Figure 5.11. There is a significant effect of flow environment on dye transfer but no significant effect of time as assessed by 2-way ANOVA. Post hoc Tukey's tests show a significant difference in each time matched static-shear pairing but no difference amongst static samples or shear samples of different time points.

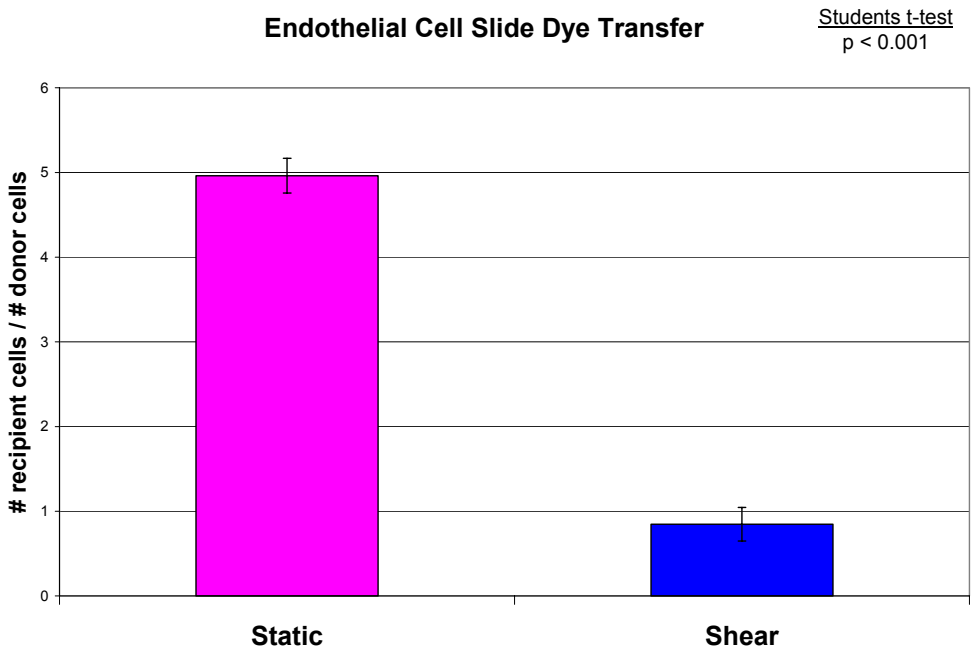

Figure 5.10 Dye Transfer of Endothelial Cells on a Slide
Error bars represent SEM and statistical analysis by Student's t-test is detailed.

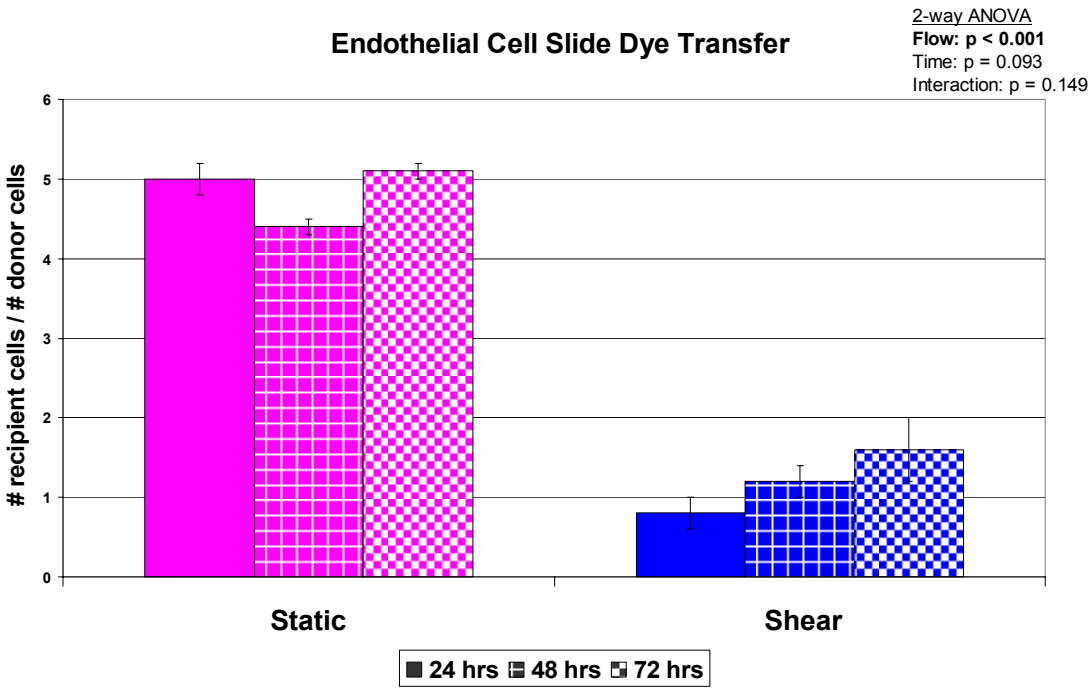

Figure 5.11 Time Course of Endothelial Cell Dye Transfer
Error bars represent SEM and statistical analysis by 2-way ANOVA is detailed.

Discussion

Previous reports of endothelial expression of connexins 37, 40 and 43 and endothelial communication through gap junctions have been confirmed in experiments here. Moreover, this study demonstrates that endothelial cell connexins and gap junction communication are influenced by substrate and shear stress.

Connexin Gene Expression

Significant differences in gene expression of Cx37 and Cx40 due to substrate or shear stress as indicated by microarray are confirmed by RT-PCR analysis. Additionally, significant regulation of Cx43 was identified by RT-PCR which was not previously identified by microarray. RT-PCR analysis shows significant influence of flow on Cx37 with an interaction effect of substrate, a significant effect of flow on Cx40 and a significant effect of substrate on Cx43. Therefore mRNA levels of all three connexin isotypes expressed by endothelial cells are significantly influenced by shear stress or substrate. Furthermore, the three connexins respond differently to stimuli leading to the hypothesis that they may be regulated independently and/or have unique functions which have not yet been elucidated.

Results of Cx43 gene expression in response to shear stress in this study confirm previous studies reporting Cx43 mRNA levels are comparable in endothelial cells exposed to laminar shear stress and static conditions. (188, 189) To date there have been no other investigations of endothelial mRNA expression of Cx37 and Cx40 in response to shear stress which were determined to be significantly regulated by fluid flow in this study. However several microarray studies have detected changes in Cx37 and Cx40

expression under various fluid flow profiles indicating there is additional support for the mechano-sensitive nature of these genes. (81, 83) Additionally, sensitivity of endothelial cell connexin gene expression to substrate is identified here for the first time.

Connexin Protein Expression

Analysis by flow cytometry showed no significant effect of flow environment on total protein expression of Cx37, Cx40 or Cx43. However, there is a significant effect of substrate on all three connexins with expression being upregulated in endothelial cells on the TEWM substrate compared to the Slide substrate. Immunocytochemistry shows presence of Cx37, Cx40 and Cx43 in endothelial cells on both substrates and under both mechanical environments. Connexins are visible in gap junction plaques in the cell membrane and clustered in the cytoplasm as well as diffusely spread in the membrane and cytoplasm. On the slide substrate, there is less abundant staining at the cell membrane under shear compared to static conditions but gap junction plaques are still visible. Subtle alterations in connexin location seen in this study were also reported recently in endothelial cells exposed to shear stress in a different type fluid flow chamber. (190) However due to the numerous mechanisms of connexin and gap junction regulation which have been identified or postulated, function cannot be determined based on location alone.

More intense staining of Cx40 and Cx43 in endothelial cells on the TEWM compared to the Slide confirms the increased levels of total expression detected by flow cytometry. It is interesting to note that these connexins appear to be clustered within the cytoplasm when examining the two-dimensional images. The significance of their

location is unknown: whether they may be internal storage of connexin proteins or gap junctions with underlying smooth muscle cells and thus are not cytoplasmic but in the endothelial basal membrane. A confocal z-stack of endothelial cells on the TEWM surface was not able to pinpoint endothelial-smooth muscle connections but the TEWM structure does not lend itself to such an analysis due to the variations in smooth muscle cell distribution.

Two previous studies have evaluated vascular connexins in co-culture systems and their results may provide some insight into data reported here. Cell-cell contact is necessary for differentiation during blood vessel assembly and it was determined that Cx43 is involved in endothelial-mesenchymal gap junction communication which is required for endothelial-induced differentiation of mural cells. (206) In a simplified co-culture system of endothelial and smooth muscle cells, results reported indicate that Cx40 and Cx43 in endothelial cells are the isotypes which form myoendothelial gap junctions with Cx43 in smooth muscle cells. (157) With the demonstrated importance of Cx40 and Cx43 in endothelial heterocellular communication, we can hypothesize that increased Cx40 and Cx43 protein expression seen in endothelial cells on the TEWM may be involved in myoendothelial gap junctions and their upregulation may be due to the presence of smooth muscle cells.

While there are no published reports of extracellular matrix influencing endothelial cell connexin expression, an effect has been demonstrated in other vascular cells. Cardiac myocytes were recently reported to alter Cx43 expression in response to substrate and mechanical forces through signaling pathways involving integrin β_1. (207) Thus results indicating altered connexin expression in endothelial cells on the TEWM

substrate may be due to either presence of smooth muscle cells, structure of extracellular matrix or a synergistic effect achieved only when including both stimuli.

Gene and Protein Levels

In evaluating results of gene and protein expression for Cx37, Cx40 and Cx43 in endothelial cells, we note that changes detected in gene expression do not necessarily correlate to changes detected in protein expression. Connexin 37 mRNA is significantly affected by flow with a substrate interaction effect while protein is significantly affected only by substrate. Connexin 40 mRNA is significantly affected by flow with an upregulation by shear stress while protein is significantly affected by substrate with an upregulation by the TEWM. Connexin 43 expression is significantly affected by substrate at the mRNA and protein levels; however mRNA levels are lower on the TEWM than the Slide while protein levels are higher on the TEWM than the Slide.

A widespread trend of mismatched levels of mRNA and protein for connexins in the literature is noted in multiple recent reviews. (128-130) Explanations for this phenomenon may lie in the complex processes used by cells to control connexin expression, gap junction formation and cell communication; however the mechanisms underlying these processes are largely unknown. Initial investigations of gene structure and mRNA translation provide some insight into potential mechanisms however studies in these areas are ongoing.

At the transcriptional level, mouse genes for Cx37, Cx40 and Cx43 have been analyzed to evaluate structure and potential regulatory mechanisms. All three genes contain a TATA box and numerous putative transcription factor sites. Cx37 is known to

also contain a GC box and a CCAAT box which may be involved in its regulation. (130) Cx40 and Cx43 both contain transcription factor binding sites for SP-1, AP-1 and AP-2 as well as several other sites unique to each gene. (131, 132) Human connexin sequences are similar to the mouse although some differences have been noted and future studies based on the sequencing of the human genome are sure to provide additional information. (133-135)

At the post-transcriptional level, multiple mechanisms are thought to be involved in connexin regulation including mRNA stability, mRNA localization, rate of translation, efficiency of translation, and translation in the absence of normal machinery. Specific mechanisms of control for connexins which are currently being investigated include sequences in the 5'UTR (untranslated region) and uORF (upstream open reading frame) as well as the presence of an IRES (internal ribosome entry sequence).

Cx37 is the least investigated of the vascular connexins due to its relatively recent identification and restricted expression in the body. Post-transcriptional control has not been specifically investigated for Cx37 although differing levels of mRNA and protein have been commonly seen. (130) Additionally, all connexin genes have a 5'UTR longer than the normal length for cellular mRNAs (>50 nucleotides) which has been suggested to include a mechanism of regulation which requires a longer sequence. (136) Mouse Cx40 was shown to contain a number of alternative promoters which result in multiple mRNA transcripts which contain identical coding regions but varied 5'UTR. (128) It is currently unknown if this influences the translatability of the Cx40 message but similar structures in Cx32 and Cx43 have just such an effect. Additionally, some Cx40 mRNA transcripts contain an extra noncoding exon whose function is currently unknown but has

been hypothesized to be involved in translataional control, mRNA localization or mRNA stability.

Due to the early identification and widespread importance of Cx43, it is the most heavily investigated of the vascular connexins. Analysis of Cx43 structure has identified mechanisms of post-transcriptional control involving an IRES and additional exons for alternative 5'UTRs. (129, 137) An internal ribosome entry sequence (IRES) as detected in Cx43 is relatively uncommon in cellular mRNA because it allows the ribosome to translate the mRNA into protein from a point inside the sequence rather than at the 5' cap which is normally required to start translation machinery. The advantage of this system is that translation can occur under cellular conditions where the 5' cap may be unavailable thus allowing the cell to maintain production of critical proteins. (136) Furthermore, it has been shown that IRES activity in cellular mRNAs can be modulated by mitotic stimuli, hypoxia and other stresses which adds an additional level of control. (138) Finally, analysis of mouse Cx43 structure has shown the presence of four additional exons encoding for different 5'untranslated regions (UTR). (129) Using different promoters and alternative splicing there are nine different mouse Cx43 mRNA transcripts which vary only in non-coding regions and have been demonstrated to exhibit a range of translational efficiencies. It is unknown at this time if the human Cx43 sequence also contains multiple additional 5'UTRs and if so, whether they play a role in mRNA stability and translation.

Results presented here do not determine where the influence of substrate or shear stress occurs for Cx37, Cx40 and Cx43. However based on the mounting evidence of mechanisms for transcriptional and post-transcriptional control of connexin expression,

explanations could include transcription factor upregulation, mRNA stability, rate of mRNA translation and protein stability. While the mechanisms of control are still being elucidated and factors influencing expression, such as substrate and shear stress, are still being identified, connexins appear intricately regulated indicating expression must be critical to cell function.

Gap Junction Communication

Levels of connexin mRNA and protein are only the beginning of the story in gap junction function. Following translation, connexins are organized into hemichannels which are inserted in the plasma membrane where they move laterally until joining the edge of a gap junction plaque. (113, 125) When docked in the cell membrane, the pore inside a gap junction can open allowing movement of chemical and electrical information from one cell to its neighbor. One technique for measuring this communication is the dye transfer assay whereby cells are loaded with dye and the movement of the dye is indicative of cell coupling by gap junctions.

Following exposure to static or shear stress, confluent endothelial monolayers were scrape-loaded to introduce Rhodamine-Dextran (MW 10,000) and Biocytin (MW 372, charge neutral) into cells adjacent to the scratch. Quantification of dye transfer images showed a reduced level of gap junction communication in shear monolayers compared to static monolayers. Reduction in dye transfer was maintained when endothelial cells were sheared for longer time points (48 or 72 hours) indicating it is not a transient phenomenon of cell adjustment to the onset of shear stress. Dye transfer experiments were also conducted in endothelial cells on the TEWM substrate but the

assay is difficult to control due to the softness of the collagen gel. When loading dye, it is possible to introduce dye into smooth muscle cells in addition to endothelial cells which could confound the results of endothelial-endothelial communication.

Altered endothelial dye transfer in response to shear stress has also been reported in two *in vitro* studies using microinjection of Lucifer Yellow dye. In a study evaluating dye transfer immediately following endothelial exposure to static, disturbed or laminar shear stress, cell coupling was found in cells under static and laminar shear while little coupling was present in cells under disturbed shear. (189) In a second study, samples were incubated up to 120 minutes following exposure to laminar shear or static conditions prior to dye transfer. Results indicated an increase in movement of Lucifer Yellow in cells that had been exposed to shear stress compared to static cells. (126) However, duration of the post-flow incubation period could have altered the endothelial gap junction profile as the half life of connexins is very short (1.5 hours for Cx43).

While emphasizing the link between shear stress and gap junction communication in endothelial cells, comparison of results in the literature is complicated by the use of different loading methods and different dyes. Lucifer yellow and biocytin dyes differ in molecular weight, charge characteristics and molecular structure. (153) Due to the specificity of gap junction gating properties, most likely resulting from connexin make-up, extent of transfer has been shown to depend on the dye used. In endothelial cells, biocytin has been shown to pass more easily through gap junctions and demonstrates cell coupling where Lucifer Yellow can fail to transfer. (153, 176, 180)

Additionally it is important to note that while this study has investigated the classical function of gap junctions, creation of a pore for communication between two

cells, there is mounting evidence for additional functions. Individual connexins and hemichannels are now also thought to play specific roles in cell growth, differentiation, tumorigenicity, injury and apoptosis. (113, 116, 117) These newly identified functions may give additional weight to observed presence of connexins and hemichannels not clustered in gap junction plaques but diffusely spread in the cell membrane or located in the nucleus or cytoplasm. Furthermore, functions in addition to pore formation for cell-cell communication may explain the need for multiple connexin isotypes, restricted distribution in cell types and potential specific roles in development and disease.

Conclusions

Results presented here indicate that while endothelial cell connexin expression and gap junction communication is influenced by substrate and shear stress, the response to these stimuli is complex. Connexin mRNA is influenced by substrate and shear stress but in an isotype dependent manner. Endothelial cells express Cx37, Cx40 and Cx43 protein in both the cell membrane and cytoplasm and quantification of total protein shows a significant regulation by substrate for all three connexins. Gap junction communication measured by transfer of biocytin dye shows reduced cell coupling in endothelial cells following exposure to laminar shear stress compared to static controls. While we have demonstrated novel sensitivities of endothelial cell gap junctions, mechanisms of influence for substrate and shear stress as well as explanations for differential response of connexin isotypes remain unknown.

Endothelial connexin and gap junction responses to shear stress include mRNA regulation for specific isotypes and an overall reduction in cell coupling. While these

results demonstrate mechanosensitivity, questions remain regarding the reasons for isotype-specific responses and mechanisms of influence. An additional limitation of the shear stress experiments conducted here is the type of fluid flow imposed on the cells. Unidirectional laminar shear stress, while more physiologic than static conditions, is a much simplified stimulus compared to forces experienced *in vivo*. To better understand connexin and gap junction mechanosensitivity and the potential link with atherosclerosis will require investigation using multiple waveforms representing forces felt in developmental, physiologic and pathologic conditions. With an improved system mimicking shear forces, questions can then be posed regarding the mechanisms of influence on endothelial cell connexins and gap junctions. Areas of investigation for future work should include control of transcription, translation, mRNA stability and degradation, protein stability and degradation as well as channel gating.

Connexin and gap junction response to substrate was demonstrated by comparing a traditional *in vitro* model of endothelial cells on monomer collagen adsorbed to glass to a more physiologic model using a tissue engineered blood vessel. While bridging the gap between traditional *in vitro* and *in vivo* experimental settings as well as demonstrating a substrate influence, numerous questions remain. By comparing two relatively different substrates, a limitation of this study is the identification of specific components of the substrate and their individual mechanisms of influence. The substrate influence detected in this study could be due to the two-dimensional vs. three-dimensional nature of the extracellular matrix or the monomer vs. fibrillar structure of collagen or the absence vs. presence of smooth muscle cells. While each substrate component most likely has an individual influence, studies into the complexity of cellular microenvironment lead us to

believe there is most likely a synergistic effect of multiple components which is important to grasp when considering multifaceted processes such as development or disease progression. Although the tissue engineered blood vessel wall model used in this study is a more physiologic *in vitro* model, a major limitation of this study is the simplicity of this system in comparison to a human blood vessel. Furthermore, its properties make assays such as immunocytochemistry and dye transfer more difficult to control and compare to other systems.

In evaluating results presented here, it also important to consider the advantages and limitations of techniques used to assess connexin expression and gap junction communication. RT-PCR, flow cytometry, immunocytochemistry and dye transfer provide fundamental information regarding the major steps in connexin synthesis through gap junction function in response to a stimulus. However, more advanced techniques are needed to evaluate the increasing complexity of connexin function and the increasing complexity of their regulation.

In conclusion, this study demonstrates novel influence of shear stress and substrate on endothelial cell connexins (37, 40, 43) and gap junction communication. Pursuit of mechanisms of influence for stimuli identified in this study has the potential to provide novel insight into characteristics of connexins and gap junctions. Furthermore, an understanding of microenvironment influences on endothelial cell connexins and gap junctions could aid in elucidating their roles in vascular development and disease.

CHAPTER SIX: Knockdown of Connexins 37, 40 and 43 Identifies Distinct Roles in Endothelial Cell Function

Introduction

Connexins and the gap junctions they form have long been identified as critical to cell communication and tissue function. Over 20 human connexin isotypes currently exist and they can be found in almost every tissue of the body. Within a cell, a single connexin protein assembles with five other connexins to form a hexameric array called a connexon or hemichannel. Each hemichannel is trafficked to the cell membrane where it docks and covalently seals with a hemichannel from a neighboring cell to form a gap junction. Gap junctions then cluster in the membrane at regions of cell-cell contact to form a gap junction plaque and regulate flow of chemical and electrical information through their pores. While classically connexins and hemichannels were thought to only function when assembled into gap junctions, new evidence demonstrates otherwise.

Hemichannels are routinely identified in the cell membrane but it has been assumed that their pores were closed and they were simply moving towards a gap junction plaque. (113) Data now shows that hemichannels do open with functions including release of ATP and propagation of calcium waves. Furthermore, their open/closed state is highly regulated by membrane voltage and pH. (114-116) There is also new evidence supporting functions for connexins which are independent of hemichannels or gap junctions. Connexins are often seen in the nucleus or cytoplasm and studies have shown they play roles in controlling cell growth and tumorigenicity as well as cell differentiation. (117) While knowledge regarding connexin and hemichannel

functions is building, understanding of specific functions and regulatory mechanisms remain unknown.

While connexins in the cardiovascular system were first studied in the heart, recent interest in the role of connexins in the vascular wall has begun to build with evidence that they play critical and poorly understood roles in vascular development and disease. Endothelial cells are known to express Connexin 37, Connexin 40 and Connexin 43 while smooth muscle cells express Connexin 40, Connexin 43 and Connexin 45. (13, 119) Distribution of these connexins varies amongst vascular beds and in different species as well as between *in vivo* and *in vitro* experimental settings. (120, 121) It is thought that the heterogeneity in cellular and vascular bed distribution is linked to specialized functions of the connexin isotypes and needs for cellular communication which are not yet understood. (122) Gap junctions coordinate cellular responses within the endothelium, within smooth muscle cells, and between endothelial and smooth muscle cells through myoendothelial gap junctions which all contribute to controlling vascular tone. (120, 123)

Contributing to the evidence supporting roles for connexins in vascular tone are studies implicating gap junctions in hypertension. Data from spontaneously hypertensive rats shows reduced connexin expression compared to normal controls. (164) Rats induced for hypertension also show reduced Cx37 and Cx43 expression but no change in Cx40 expression in endothelial cells compared to normotensive animals. (165)

Connexins in the vascular wall have also been linked to the prevalence of atherosclerosis and have been shown to vary in expression with the progression of plaques. Heterozygous Cx43+/- mice exhibit a 50% decrease in atherosclerotic plaques

in vivo and *in vitro* experiments have shown that statins reduce the Cx43 expression in endothelial and smooth muscle cell cultures. (166) Cx37 and Cx40 expression is reduced in endothelial cells of hyperlipidemic mice and only Cx37 levels recover with lipid-lowering drug treatment. (167) An altered pattern of connexin expression in endothelial and smooth muscle cells is seen in non-diseased arteries, early atheromas and advanced atheromas. (168) Finally, naturally occurring Cx37 variants have also been implicated in the prevalence of atherosclerosis in human populations. (169)

With links between gap junctions and atherosclerosis developing, there have been several studies investigating the response of vascular connexins to mechanical stimuli. In evaluating endothelial connexin expression, it was noted that while Cx37 and Cx40 appeared in similar widespread patterns, Cx43 expression was found mainly in regions near aortic branches where blood flow is disturbed. (187) Introduction of a flow disturbance into this model resulted in a strong upregulation of Cx43 in areas not previously showing high levels of expression. An *in vitro* study of vascular cells and mechanical forces found a transient upregulation in Cx43 mRNA in endothelial cells exposed to laminar shear stress. (188) Further investigation of endothelial cell Cx43 regulation by shear stress was conducted by exposing cells to four types of fluid shear from recirculating to fully developed laminar flow. (189) While Cx43 mRNA was transiently upregulated by all flow patterns, an increase was only sustained after 30 hours in areas of disturbed, recirculating flow. Furthermore, Cx43 protein appeared disorganized in regions of disturbed flow and cells showed little coupling as assessed by dye transfer indicating limited gap junction communication. More recently, other endothelial cell connexins (Cx37 and Cx40) were examined in this *in vitro* flow system.

(190) Patterns of protein expression and roles of different connexin isotypes in endothelial gap junction communication were investigated using dye transfer techniques in conjuction with peptide channel blockers.

In addition to studies demonstrating mechano-sensitivity of vascular gap junctions, numerous studies have investigated the response of specific connexins to chemical stimuli and pathologic conditions. In endothelial cells, Cx43 is highly expressed in subconfluent cultures and levels decrease at confluence while Cx37 levels are minimal at subconfluence and rise when cells contact. Furthering this polarity in behavior of connexin isotypes is response to TGF-β1 where Cx43 levels increase and Cx37 levels decrease. (181) Nitric oxide has also been shown to differentially affect endothelial connexin isotypes by decreasing coupling of gap junctions which contain Cx37 and increasing new formation of gap junctions which contain Cx40. (182, 183) In response to injury *in vivo*, rat endothelial connexin expression drops initially and then over time Cx40 expression returns to normal while Cx37 and Cx43 are expressed at higher levels than uninjured artery. (162) In response to injury *in vitro*, wounding of an endothelial monolayer results in upregulation of Cx43 at the wounded edge, decrease in Cx37 at the injury site and no change in Cx40. (184) Exposure of human endothelial cells to TNF-α resulted in a downregulation of Cx37 and Cx40 mRNA while Cx43 mRNA was unaffected. (185) Finally, sepsis induced in a rat model increased Cx40 mRNA but did not alter expression of endothelial Cx37 or Cx43. (186)

With their primary function being to promote communication between cells, gap junctions are critical in development of many tissues. Knockout connexin models elucidate functions in development but attempts to study connexin influence on vascular

wall biology have been hampered by the widespread expression of these molecules in other tissues and the drastic influence of a genomic knockout. Cx37-/- mice are viable but females are infertile because of abnormal development of both oocytes and ovarian follicles. (171) Cx40-/- mice are viable but have prolonged atrioventricular conduction, right bundle branch block and a predisposition for arrhythmias. Furthermore, Cx40-/- mice have diminished conduction of arteriolar dilatation in response to acetylcholine and bradykinin and are hypertensive but have no other obvious blood vessel abnormalities. (172) Cx43-/- mice die perinatally due to abnormal development of the pulmonary outflow tract from atypical migration of cardiac neural crest cells. (173) Single knockout connexin mice have characterized phenotypes which are largely non-blood vessel related because of the widespread expression of these molecules and their presumed functional overlap within the vessel wall. When *in vivo* expression of connexins is reduced further using a multiple knockout strategy, there are severe blood vessel abnormalities indicating an important interplay between the functions of connexin isotypes. Cx37-/- Cx40-/- mice die perinatally with hemorrhages and severe blood vessel dilatation. (174) Cx40-/- Cx43-/- have also been reported to die at E12.5 with malformed hearts including abnormally rotated ventricles.(175) In a recent study, the Cx43 gene was knocked out only in vascular endothelial cells therefore providing a model in which the role of connexins in the vascular wall can be studied without the confounding influence of perinatal death or impaired fertility of mice. The VEC Cx43-/- mice exhibit hypotension and bradycardia compared to heterozygous littermates indicating a role for endothelial cell Cx43 in maintaining normal vascular function.(163)

While knockout models provide valuable information regarding the missing gene, several reports have identified effects on non-ablated connexins. Evaluation of Cx40-/- mice found expression of Cx37 protein upregulated three-fold and redistributed in a more homogeneous manner. (176) In a separate study of Cx37-/- and Cx40-/- mice, data showed a drop in endothelial Cx40 protein in Cx37-/- animals and a drop in endothelial Cx37 protein in Cx40-/- animals however no changes in mRNA levels were detected. (177, 178) An additional evaluation of Cx40-/- animals showed reduced staining of endothelial Cx43 at the cell membrane and reduced expression of smooth muscle cell Cx43. (179) Evidence of reduced Cx43 expression in smooth muscle cells of animals where Cx43 was knocked out only in endothelial cells (VEC Cx43-/-) supports the hypothesis that effects on non-ablated connexins are not restricted to one cell type. (163) Following a complementary approach, a study which transfected endothelial cells with an adenovirus for Cx37 demonstrated no change in Cx43 mRNA but a substantial drop in Cx43 protein. (180)

Gap junction channels composed of each connexin isotype appear to have unique properties of permeability, conductivity and gating. While it was originally believed that hemichannels and gap junctions could only be created using a single type of connexin, data has proven otherwise. Hemichannels of one connexin type are termed homomeric and those of multiple connexin types are termed heteromeric. Gap junctions of two hemichannels containing one type of connexin are termed homotypic and gap junctions of two hemichannels containing multiple connexins are termed heterotypic. While many types of connexins can mix and match, not all isotypes are compatible. Of the vascular endothelial connexins, extensive compatibility and resulting channel types have been

shown. Cx40 and Cx43 can form homotypic, heterotypic and heteromeric channels which result in unique gating and conductance properties. (149, 150) In addition, the permeability properties of these channels can be predicted based on the ratio of components but the electrical properties appear to derive from protein interactions and are not an average of components. (151) Connexins 37 and 43 can also form homotypic, heterotypic and heteromeric channels. Again the characteristics of these heteromeric channels are not predicted based on single connexin channel properties indicating an interaction effect amongst the connexins. (142, 148) The final combination possible in endothelial cells is with Cx37 and Cx40 which have been shown to form heterotypic gap junctions but have not been evaluated for potential heteromeric mixing capabilities. (147)

With the common and unique functions displayed by endothelial connexins and effects seen using animal knockout strategies, a new approach of RNA interference promises insight into isotype function. The technique of RNA interference allows for selective destruction of specific mRNA sequences in a transient manner. By taking advantage of the native cellular system which destroys double stranded RNA, a short interfering RNA (siRNA) which is complementary in sequence to the target mRNA is introduced into a cell and allowed to bind the target which results in its destruction. (208, 209) While avoiding the complexity and often embryonic lethality of genome manipulation, studies can be conducted which temporarily silence a particular gene of interest. RNA interference of connexins was recently used to knock down Cx43 in a breast cancer cell line resulting in a higher growth rate and more migratory behavior. (210) Connexin gene silencing was also used to show mutual dependence of N-cadherin and Cx43 on each other for expression at the cell surface. (211) To date the only use of

RNA interference in studies of vascular connexins was a knockdown in Cx43 which demonstrated its role in the formation of myoendothelial gap junctions. (157)

With the growing evidence linking vascular connexins to pathological conditions and their complex responses to multiple stimuli, the goal of this study is to investigate the individual roles of Cx37, Cx40 and Cx43 in endothelial cell behavior.

Experimental Design and Methods

Experimental Design

The approach taken to investigate endothelial cell connexin function is to selectively knockdown gene expression and examine resulting effects on non-ablated connexin expression and on cell behavior. Connexin expression is evaluated at the mRNA level by RT-PCR and at the protein level using western blotting and immunocytochemistry. As important characteristics of endothelial cell function, effects of connexin knockdown on gap junction communication, cell proliferation and cell morphology are examined. Furthermore, to gain the most valuable insight into human physiology, experiments are conducted using human aortic endothelial cells under static and laminar shear stress conditions. Endothelial monolayers are transfected with siRNA (short interfering RNA) targeting each connexin sequence individually thus knocking down expression of one isotype. Cells are then exposed to static or shear stress and assessed for mRNA expression, protein expression, gap junction communication, cell proliferation and cell morphology. Effects of ablated connexins on non-ablated connexins provides insight into potential co-regulation or interactions between isotypes

and effects on the selected cell behaviors provides insight into roles of different isotypes on endothelial function and response to shear stress.

Experimental Methods

Cell Culture

Human aortic endothelial cells (HAEC) (Cambrex) were cultured to passage 6 in MCDB 131 supplemented with 5% FBS, antibiotics and growth factors. Cells were seeded on glass slides with sterile silicone frames around the border which provided a boundary to contain fluid volume during transfection. Experiments exposing monolayers to static or shear conditions were conducted in a co-culture media of MCDB 131 supplemented with 5% FBS, antibiotics and low level of growth factors.

RNA Interference

RNA interference was conducted using short interfering RNA (siRNA) designed by and purchased commercially from Ambion. Multiple sequences were tested for ability to knockdown target connexin mRNA at least 70% without other adverse effects (eg. cell death). The following siRNA sequences designed for the human sequence were successfully used to knockdown connexin mRNA.

Cx37: Ambion siRNA ID#7185, annealed, standard purity

Cx37 Sense (5' to 3'): GGACUUGAUCACAAAAAAAtt

Cx37 Antisense (5' to 3'): UUUUUUUGUGAUCAAGUCCtg

Cx40: Ambion siRNA ID#145161, annealed, standard purity

Cx40 Sense (5' to 3'): GGUAAACGAUGCUUGGAAUtt

Cx40 Antisense (5’ to 3’): AUUCCAAGCAUCGUUUACCtt

Cx43: Ambion siRNA ID# 144485, annealed, standard purity

Cx43 Sense (5’ to 3’): GCCUUAUUCAUGAGGCUUAtt

Cx43 Antisense (5’ to 3’): UAAGCCUCAUGAAUAAGGCtg

In addition to sequences targeting connexins, a negative control siRNA labeled with Cy3 (Negative Control #1 – Ambion 4621) which does not target any known human sequence was used to develop transfection protocols and to evaluate the effect of the transfection procedure on endpoints.

Endothelial cells were transfected under serum-free conditions using OptiMEM medium (Invitrogen) with the chemical transfection reagent Oligofectamine (Invitrogen). A time course study using 10nM siRNA demonstrated knockdown of mRNA for 96 hours following transfection (entire duration of the study). A dosage study showed knockdown of each connexin mRNA by >80% with siRNA concentrations ranging from 10nM to 80nM. To avoid any potential side effects of abundant siRNA in the cells but ensure adequate knockdown, a concentration of 40nM was chosen for all studies. Thus the siRNA transfection and experimental timeline is as follows.

Endothelial cells were seeded onto collagen coated glass slides and cultured for 24 hours prior to transfection at which point they are 90% confluent. Stock siRNA in sterile, RNase-free water is diluted in OptiMEM medium and oligofectamine transfection reagent is also diluted in OptiMEM medium. The two mixtures are combined to create a transfection cocktail which sits at room temperature for 20 minutes to allow complexing of siRNA by oligofectamine. Endothelial monolayers are rinsed twice in OptiMEM to remove any remaining culture medium and thus all serum and antibiotics. OptiMEM is

added to endothelial slides and the transfection cocktail is added dropwise to each sample. Cells are transferred to the incubator at 37°C and transfection proceeds for 6 hours. During the transfection process, the final concentration of siRNA is 40nM and the final concentration of oligofectamine is 0.4% (10μL in 2.5mL). After six hours, a volume of experimental medium with 22% FBS is added to the OptiMEM/oligofectamine/siRNA mixture to restore the total FBS concentration to 5%. Slides are incubated for an additional 42 hours (total of 48 hours since transfection) prior to removal of the mixture of OptiMEM/oligofectamine/siRNA/FBS/experimental media and beginning of the 24 hour experimental period where cells are exposed to static or laminar shear stress. All manipulations of siRNA are conducted under sterile, RNase-free, DNase-free conditions to preserve integrity of sequences and samples.

Exposure to Shear Stress

The parallel plate flow chamber used to expose endothelial cells to laminar shear stress has been previously established in our laboratory. (42, 49) In this closed loop, a peristaltic pump moves medium from a container into a pulse dampener and then through parallel plates where endothelial cells are exposed to a steady laminar shear stress. Shear stress is controlled by fluid flow rate and dimensions of the chamber according to the equation: $\tau = 6Q\mu/bh^2$. Silicone gaskets were removed from transfected slides prior to shear stress exposure of 15 dynes/cm^2 for 24 hours.

RNA Isolation and Quantitative RT-PCR

Total RNA was extracted from endothelial cells using an RNeasy kit (Qiagen) with an added DNAse digestion step. To evaluate quality of RNA prior to RT-PCR analysis, samples were assessed using the RNA 6000 Nano LabChip (Agilent) on an Agilent Bioanalyzer 2100. Profiles of ribosomal peaks were evaluated for degradation as a measure of overall RNA degradation and preliminary measurements of RNA quantity were determined. Quantity of high quality RNA was assessed by absorbance at 260nm prior to reverse transcription to cDNA for RT-PCR.

One microgram of high quality endothelial RNA was reverse transcribed using the First Strand cDNA Synthesis Kit (Invitrogen) for each experimental sample. Primers were designed using Primer Express (Applied Biosystems) and oligos were created by Integrated DNA Systems. Primer sequences are listed below for the three connexins expressed in endothelial cells.

Cx37 Forward: CATGGAGCCCGTGTTTGTG

Cx37 Reverse: GAGACAAAGCAGTCCACGAGG

Cx40 Forward: GGGCACTCTGCTCAACACCT

Cx40 Reverse: TGAAGCCCACCTCCATGGT

Cx43 Forward: TTAAGGGAAAGAGCGACCCTT

Cx43 Reverse: GACCCACAGTCTTTGGCAGG

Standards of known concentration were generated using PCR amplification and agarose gel extraction for each gene of interest. Quantitative RT-PCR was conducted using cDNA from samples (in triplicate) and standards (in triplicate) with SYBR® Green PCR Master Mix (Applied Biosystems) on an ABI 7700 (Applied Biosystems) real time PCR machine. Data was quantified using the absolute standard method where serial

dilutions of the standard were plotted against C_T values to generate a correlation used to convert sample C_T values into concentrations.

Western Blotting

Endothelial cells were lysed in RIPA buffer (Sigma) with added protease inhibitor cocktail (Sigma) and centrifuged at 10,000rpm for 10 minutes to pellet DNA. Supernatant was collected and protein content was quantified using the BCA protein assay (Pierce) in comparison to albumin standards. Samples were mixed with Laemmeli buffer and heated at 95°C for 5 minutes prior to loading onto 12% Tris-Glycine gels (Invitrogen). Following electrophoresis using Tris/Glycine/SDS running buffer (BioRad) of samples alongside a See Blue Plus 2 (Invitrogen) lane marker and a Magic Mark XP (Invitrogen) western protein standard of known molecular weights, proteins were transferred using Tris/Glycine transfer buffer (BioRad) to a PVDF membrane (BioRad). Blots were incubated overnight at 4°C in 5% milk in T-TBS to block non-specific binding before incubation with the primary antibody for 1 hour at room temperature. Blots were labeled with one of the following antibodies: Rabbit Anti-Mouse Cx37 (Alpha Diagnostic) at 1:500, Rabbit Anti-Mouse Cx40 (Alpha Diagnostic) at 1:500, Rabbit Anti-Mouse Cx43 (Chemicon) at 1:1000 in 5% milk in T-TBS. Following three washes in T-TBS, blots were labeled with the following secondary antibody: Horseradish Peroxidase Donkey Anti-Rabbit (Jackson ImmunoResearch) at 1:5000. To measure signal, blots were covered with ECL Plus (Amersham Biosciences) for 5 minutes and then exposed to film. Following staining of blots for the connexin protein of interest, membranes were stripped and reprobed for actin to ensure equal loading. Antibodies used for this step

were Mouse Anti-Actin (Calbiochem) and Horseradish Peroxidase Goat Anti-Mouse (Calbiochem).

Immunocytochemistry

Immunocytochemistry was conducted to visualize endothelial cell connexins following exposure to static or shear conditions. Endothelial cells on slides were fixed in 4% formaldehyde for 5 minutes, permeabilized in 0.1% Triton X-100 for 5 minutes and then incubated for 1 hour in 4% donkey serum to block non-specific binding of antibodies. Cells were labeled with one of the following primary antibodies at 1:100 dilution: Rabbit Anti-Mouse Cx37 (Alpha Diagnostic), Goat Anti-Human Cx40 (Santa Cruz Biotechnology), Goat Anti-Human Cx43 (Santa Cruz Biotechnology) for 1 hour at 37°C. Following two washes in PBS, cells were incubated with one of the following secondary antibodies: FITC-conjugated Donkey Anti-Rabbit (Jackson ImmunoResearch) or FITC-conjugated Donkey Anti-Goat (Jackson ImmunoResearch). Samples were imaged using a laser-scanning confocal microscope with a 40x oil objective.

Dye Transfer Assay

Following exposure of endothelial monolayers to static or shear stress conditions, assessment of dye transfer between cells was conducted as a measure of gap junction communication. In this assay of gap junction function, cells are loaded with two membrane-impermeant dyes: i) a small dye which can pass through gap junctions and ii) a large dye which cannot pass through gap junctions and is used to mark cells originally loaded with dye. Following a defined period of time, cells are fixed and imaged to

evaluate the extent of dye transferred from cells originally loaded with dye to neighboring cells as a measure of cell coupling by gap junctions. In this study the dye used to pass through gap junctions is Biocytin (ε-biotinoyl-L-lysine) with a molecular weight of 372Da and neutral charge (Molecular Probes) and the dye used to mark cells originally loaded with dye is Tetramethylrhodamine Dextran (flouro-ruby) with a molecular weight of 10,000Da (Molecular Probes).

Immediately upon removal from the static dish or flow chamber, monolayers are rinsed in Dulbecco's PBS and excess fluid is blotted off. A mixture of 4mg/ml Biocytin and 5mg/ml Rhodamine-Dextran in PBS is dripped onto the monolayer surface which is then scratched with a diamond-tipped pen (tip diameter 0.25mm). Samples are immediately placed in the incubator at 37°C for 2 minutes to allow passage of dye. Excess dye is quickly removed, samples are rinsed in PBS and fixed in 4% formaldehyde for 20 minutes. While the dextran is fluorescent, biocytin requires a secondary antibody for detection. Monolayers are permeabilized with 0.1% Triton X-100 for 5 minutes and incubated with 4% donkey serum for 30 minutes to block non-specific binding prior to labeling with a secondary antibody Oregon Green 488 NeutrAvidin (molecular probes). Samples were imaged using a Nikon E600 fluorescent microscope using filters to separately detect red and green signals.

Cell Proliferation Assay

Endothelial cell proliferation was assessed using BrdU which is incorporated into DNA being synthesized during S-phase of the cell cycle. BrdU is then detected using primary and secondary antibodies thus proliferating nuclei can be compared to non-

proliferating nuclei. BrdU (5-bromo-2'-deoxyuridine) (MP Biomedicals) is added to experimental medium of slides being exposed to static or shear stress at a final concentration of 20μg/mL for the final 6 hours of the 24 hour experimental time period. At the end of the 6 hour exposure to BrdU, slides are fixed in 4% formaldehyde for 20 minutes. Cells are permeabilized by exposure to ice cold acetone for 10 minutes and then DNA is denatured by exposure to 2N HCL for 15 minutes at 37°C. Following neutralization and restoration of pH, slides are incubated with 5% donkey serum for 1 hour at room temperature to block non-specific binding. Slides are then incubated for 2 hours at 37°C with 1:50 dilution of Mouse anti-BrdU (Sigma), rinsed with PBS and incubated with 1:200 Cy3-conjugated Donkey Anti-Mouse (Jackson ImmunoResearch) and 20μg/mL Hoechst 33258 (Molecular Probes) to detect both proliferating and non-proliferating nuclei. Slides are imaged using a laser scanning confocal microscope and images are analyzed using ImagePro software.

Cell Morphology Analysis

To evaluate cell morphology, endothelial monolayers are stained for actin filaments and measured for elongation and angle of orientation. Endothelial cell slides are fixed in 4% formaldehyde for 5 minutes, permeabilized in 0.1% Triton X-100 for 5 minutes and incubated in 4% donkey serum for 30 minutes at room temperature. Monolayers are stained using Rhodamine-conjugated phalloidin (Invitrogen) which is a mushroom toxin that binds tightly to actin filaments. Staining is conducted using 1:200 dilution of phalloidin and Hoechst 33258 to identify nuclei. Samples are imaged using a Nikon E600 fluorescent microscope using a triple filter to detect both red and blue

signals. Images are analyzed using LSM 5 Image Browser (Zeiss) and an overlay writing tool is used to manually determine perimeter, area and angle of orientation. Angle of orientation is measured from horizontal which is the axis of fluid shear stress. Using perimeter and area data, a shape index of each cell is calculated according to the formula: $SI = (4*\Pi*Area)/(Perimeter^2)$. The shape index ranges from 0 (indicating a straight line) to 1 (indicating a circle) and quantifies elongation of endothelial cells.

Results

Target Connexin Knockdown

To investigate the individual roles of connexins 37, 40 and 43 in endothelial cell biology, each isotype was targeted by siRNA specific to its coding sequence to knockdown expression starting at the mRNA level. Knockdown of target mRNA was assessed during development of the RNA interference protocol and identification of siRNA sequence to be used. Since experimental conditions could change the effectiveness of the knockdown, target mRNA levels were again assessed in experimental samples.

Figure 6.1 shows data for knockdown of Cx37 mRNA by Cx37 siRNA in slides which have been transfected and then exposed to static or shear conditions. Comparison of samples treated with Cx37 siRNA 40nM to OptiMEM controls shows significant reduction in Cx37 mRNA by 88% in static slides and significant reduction in Cx37 mRNA by 97% in shear slides. Data confirms knockdown in experimental samples which was previously seen in RNAi protocol development.

Figure 6.2 shows data for knockdown of Cx40 mRNA by Cx40 siRNA in slides which have been transfected and then exposed to static or shear conditions. Comparison of samples treated with Cx40 siRNA 40nM to OptiMEM controls shows significant reduction in Cx40 mRNA by 83% in static slides and significant reduction in Cx40 mRNA by 87% in shear slides. Data confirms knockdown in experimental samples which was previously seen in RNAi protocol development.

Figure 6.3 shows data for knockdown of Cx43 mRNA by Cx43 siRNA in slides which have been transfected and then exposed to static or shear conditions. Comparison of samples treated with Cx43 siRNA 40nM to OptiMEM controls shows significant reduction in Cx43 mRNA by 86% in static slides and significant reduction in Cx43 mRNA by 87% in shear slides. Data confirms knockdown in experimental samples which was previously seen in RNAi protocol development.

Immunocytochemistry and western blotting were used to evaluate the knockdown of connexin protein expression. Immunocytochemistry of static and shear slides showed no expression of Cx37 protein in samples treated with Cx37 siRNA 40nM, no expression of Cx40 protein in samples treated with Cx40 siRNA 40nM and no expression of Cx43 protein in samples treated with Cx43 siRNA 40nM. While immunocytochemistry is valuable in gaining information about expression and localization of proteins, connexins are difficult to detect and thus quantitative analysis of protein knockdown was conducted using western blotting. Western blotting of Cx43 in endothelial cells shows presence of protein in OptiMEM control samples and absence of protein in Cx43 siRNA 40nM treated samples. Western blots to detect Cx37 and Cx40 protein were also repeatedly attempted, however the proteins were not detected.

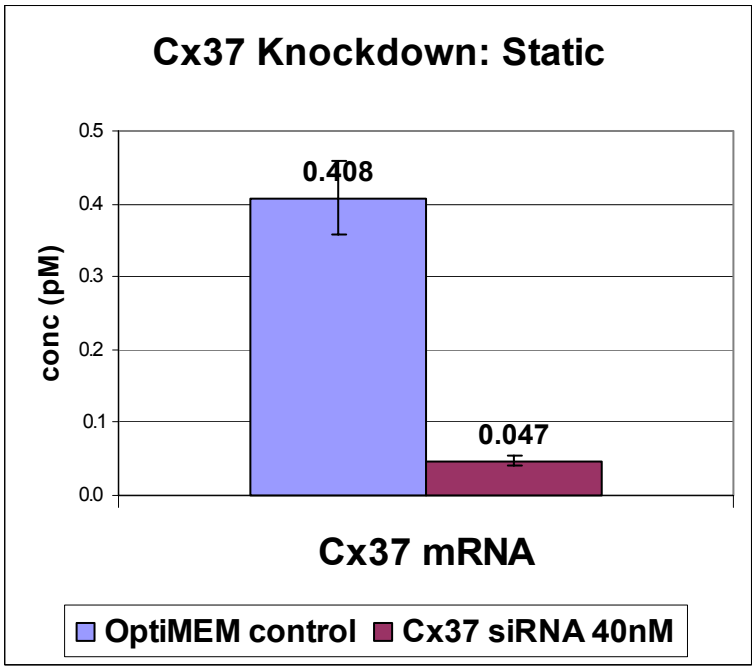

Cx37 Knockdown: Static	
% mRNA knockdown	88.4%
t-test p-value	0.0001

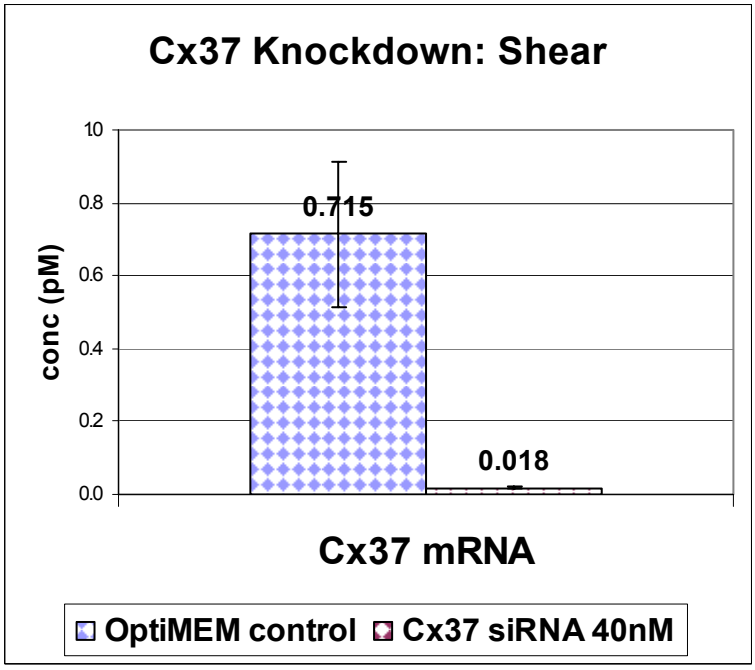

Cx37 Knockdown: Shear	
% mRNA knockdown	97.5%
t-test p-value	0.0128

Figure 6.1 Cx37 mRNA Knockdown by Cx37 siRNA
Cx37 mRNA is significantly reduced (>88%) in endothelial cells under static or shear conditions following treatment with Cx37 siRNA.

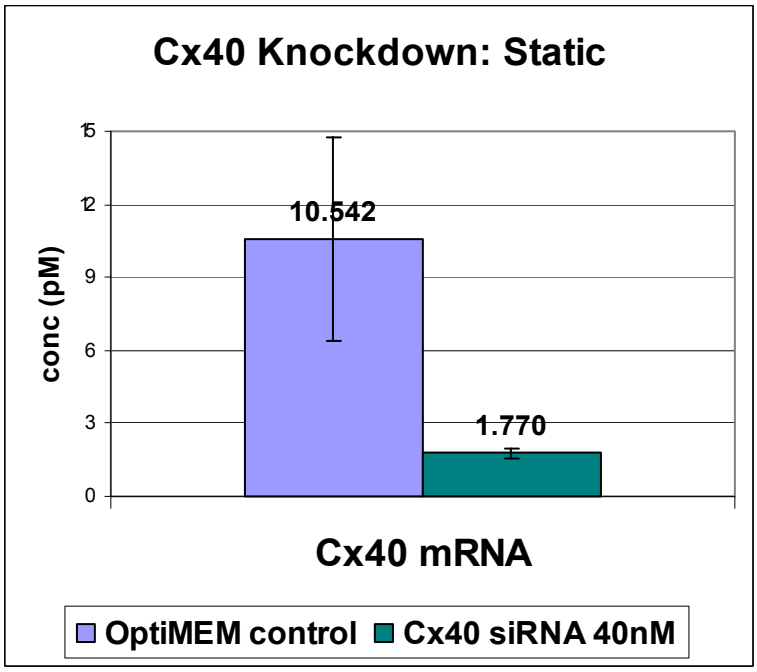

Cx40 Knockdown: Static	
% mRNA knockdown	83.2%
t-test p-value	0.0286

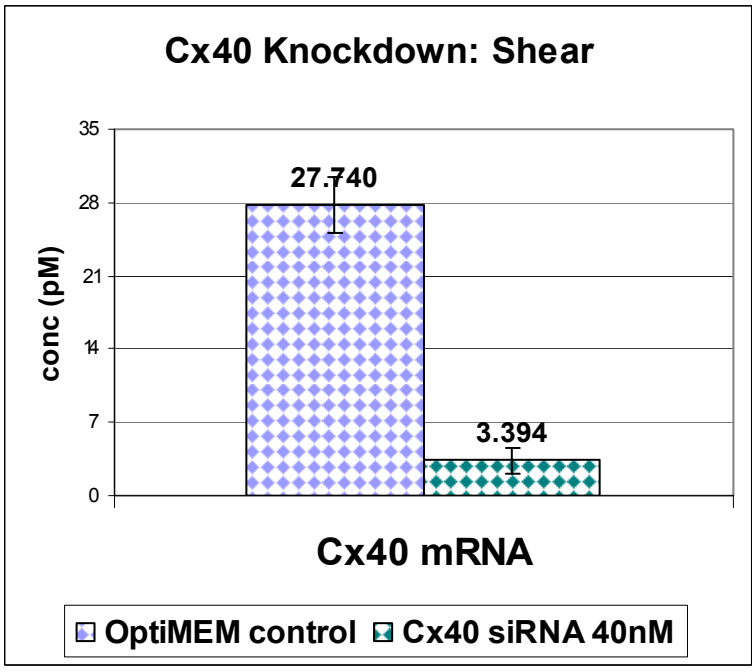

Cx40 Knockdown: Shear	
% mRNA knockdown	87.8%
t-test p-value	0.0002

Figure 6.2 Cx40 mRNA Knockdown by Cx40 siRNA
Cx40 mRNA is significantly reduced (>83%) in endothelial cells under static or shear conditions following treatment with Cx40 siRNA.

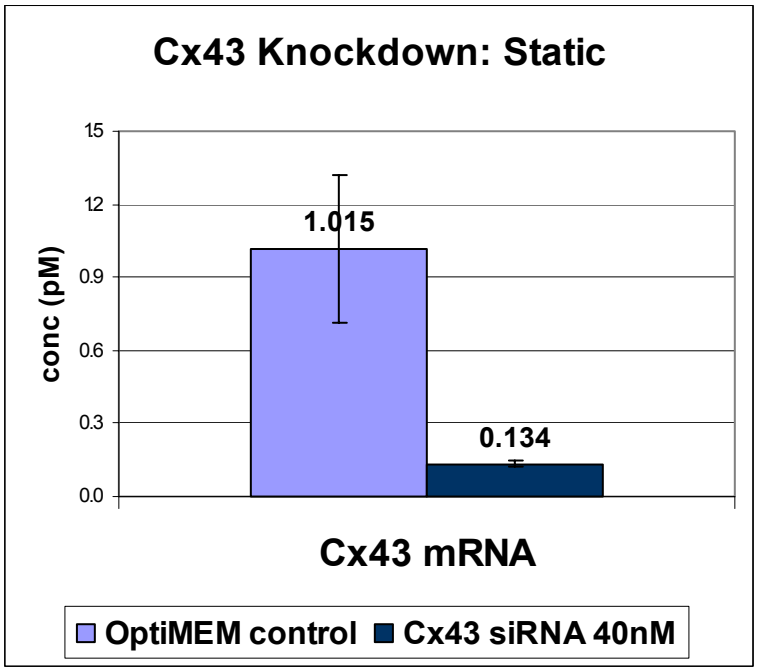

Cx43 Knockdown: Static	
% mRNA knockdown	86.8%
t-test p-value	0.0180

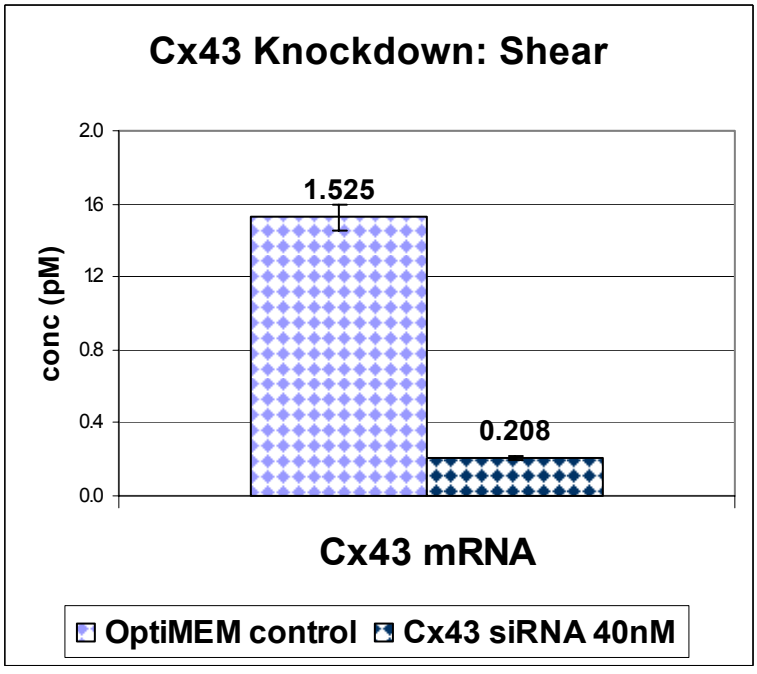

Cx43 Knockdown: Shear	
% mRNA knockdown	86.4%
t-test p-value	0.0000

Figure 6.3 Cx43 mRNA Knockdown by Cx43 siRNA
Cx43 mRNA is significantly reduced (>86%) in endothelial cells under static or shear conditions following treatment with Cx43 siRNA.

Changes in Non-Target Connexins

While knockdown of target connexins with siRNA was effective, studies in knockout animal models have demonstrated effects of connexin ablation on non-targeted connexins. Whether a compensatory response, a result of co-regulation or a result of mixed channels, changes in non-targeted connexins impact the conclusions drawn from data on overall cell function following siRNA treatment. For each siRNA treatment in this study, the effect on the target connexin and two other non-targeted connexins was evaluated in endothelial experimental samples under static and shear conditions.

Figure 6.4 shows the effects of Cx37 siRNA 40nM treatment on the mRNA expression of Cx37, Cx40 and Cx43 in comparison to OptiMEM controls. While Cx37 mRNA is significantly reduced as detailed in Figure 6.1, significant effects are also seen on Cx40 and Cx43. Evaluation of Cx40 mRNA shows a significant increase in cells treated with Cx37 siRNA under static and shear conditions with an increase in expression of approximately 3-fold. In addition, there is an increase in Cx40 mRNA expression by the presence of shear stress. Evaluation of Cx43 mRNA shows a significant increase in cells treated with Cx37 siRNA under static and shear conditions with a 20% and 40% increase, respectively.

Figure 6.5 shows the effects of Cx40 siRNA 40nM treatment on the mRNA expression of Cx37, Cx40 and Cx43 in comparison to OptiMEM controls. While Cx40 mRNA is significantly reduced as detailed in Figure 6.2, significant effects are also seen on Cx37 but not Cx43 expression.

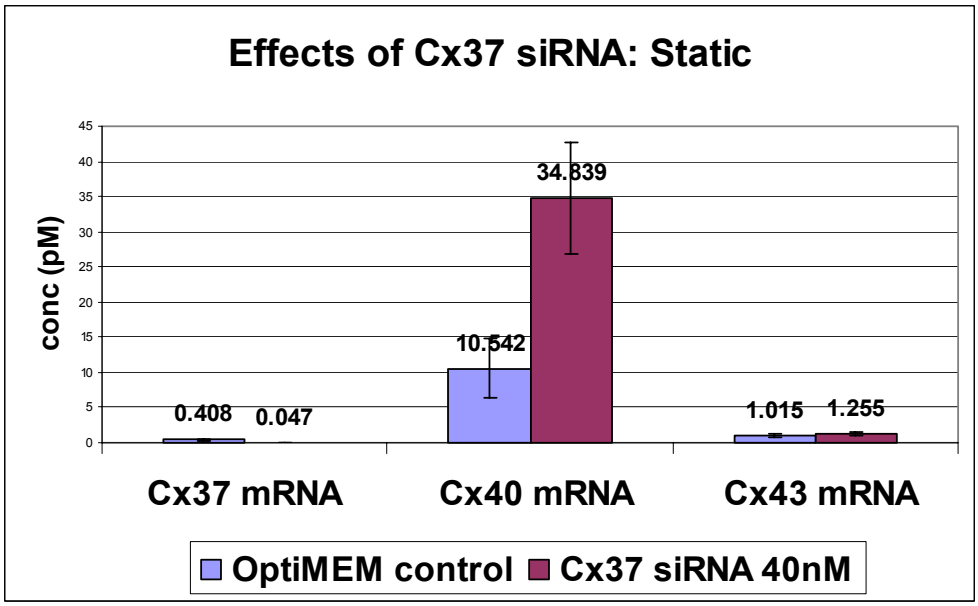

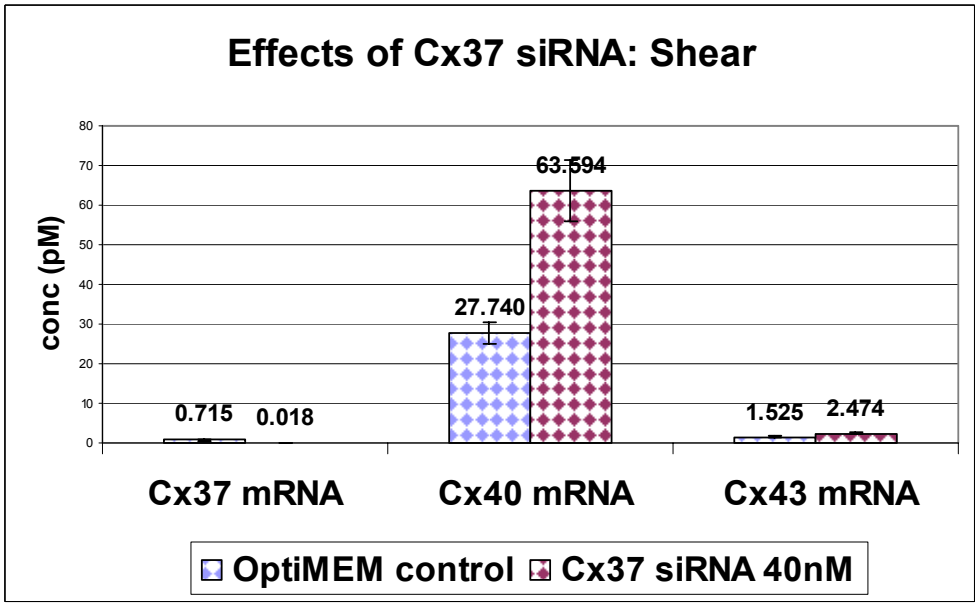

ANOVA of Cx37 siRNA on mRNA Expression			
	Cx37 mRNA	**Cx40 mRNA**	**Cx43 mRNA**
siRNA p-value	**0.001**	**0.001**	**0.017**
flow p-value	0.231	**0.004**	**0.002**
interaction p-value	0.155	0.374	0.123

Figure 6.4 Effects of Cx37 siRNA on Connexin mRNA Expression
Treatment with Cx37 siRNA significantly reduces Cx37 mRNA expression, but also significantly increases Cx40 mRNA and significantly increases Cx43 mRNA.

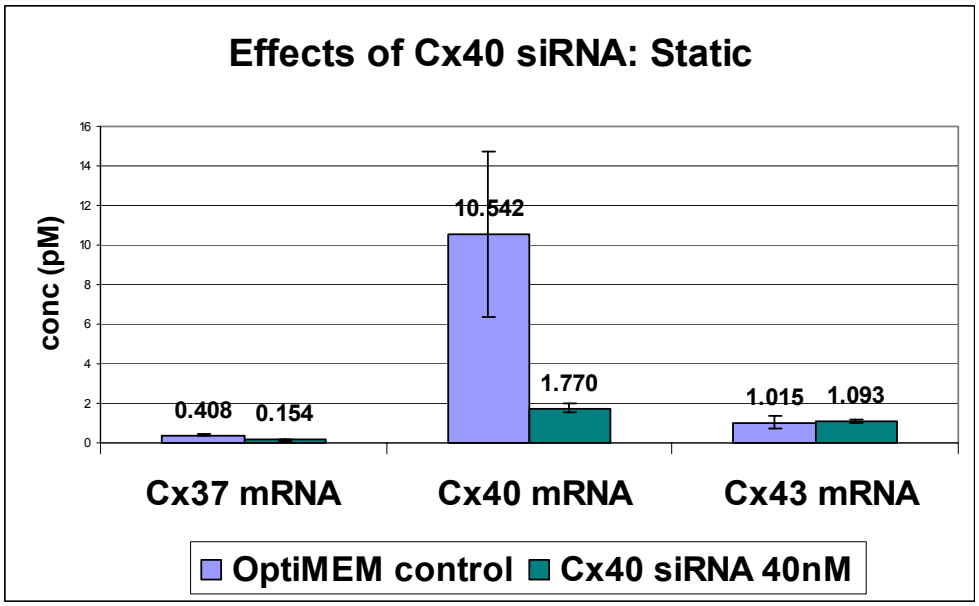

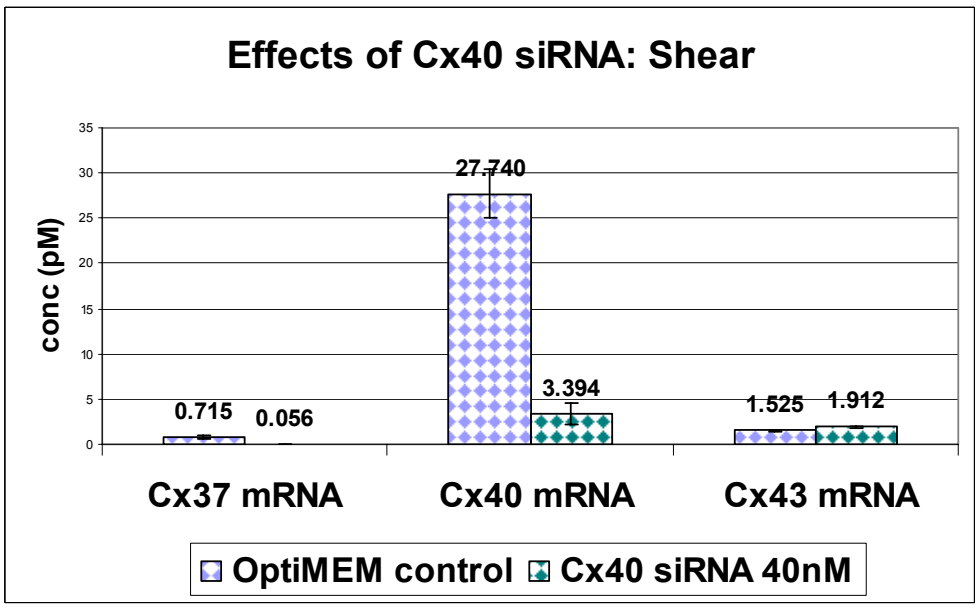

ANOVA of Cx40 siRNA on mRNA Expression			
	Cx37 mRNA	Cx40 mRNA	Cx43 mRNA
siRNA p-value	**0.002**	**0.000**	0.143
flow p-value	0.370	**0.002**	**0.001**
interaction p-value	0.097	**0.006**	0.316

Figure 6.5 Effects of Cx40 siRNA on Connexin mRNA Expression
Treatment with Cx40 siRNA significantly reduces Cx40 mRNA expression, but also significantly decreases Cx37 mRNA expression.

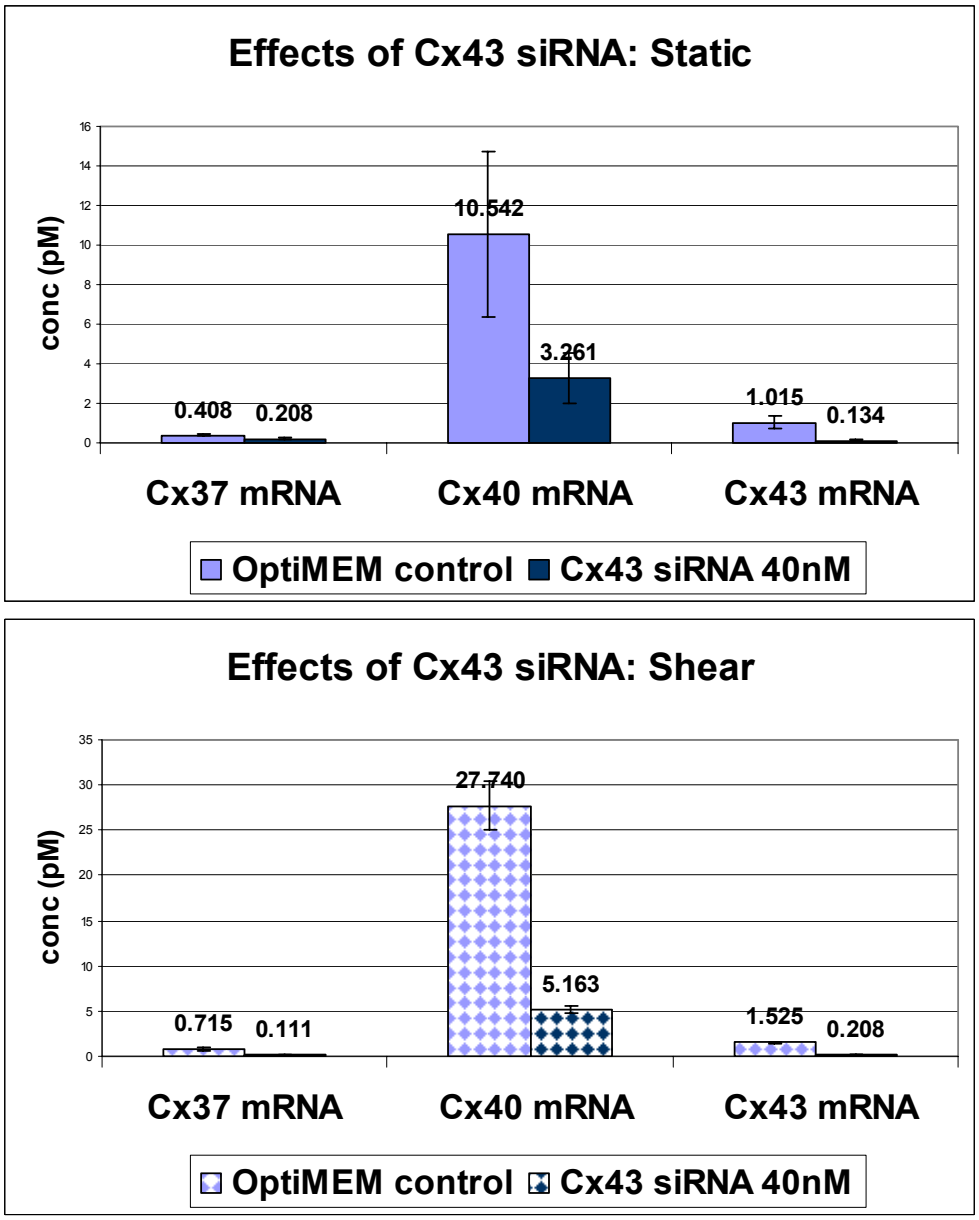

ANOVA of Cx43 siRNA on mRNA Expression			
	Cx37 mRNA	Cx40 mRNA	Cx43 mRNA
siRNA p-value	**0.015**	**0.000**	**0.000**
flow p-value	0.455	**0.006**	0.075
interaction p-value	0.165	**0.018**	0.170

Figure 6.6 Effects of Cx43 siRNA on Connexin mRNA Expression
Treatment with Cx43 siRNA significantly reduces Cx43 mRNA expression, but also significantly decreases Cx37 mRNA and significantly decreases Cx40 mRNA.

Evaluation of Cx37 mRNA shows a significant decrease in cells treated with Cx40 siRNA under static and shear conditions with a 2.6-fold and 12.7-fold reduction, respectively. Evaluation of Cx43 mRNA shows no significant effects of treatment with Cx40 siRNA. While there is no effect of shear stress on Cx37 mRNA expression, shear induces an upregulation in Cx40 mRNA and Cx43 mRNA.

Figure 6.6 shows the effects of Cx43 siRNA 40nM treatment on the mRNA expression of Cx37, Cx40 and Cx43 in comparison to OptiMEM controls. While Cx43 mRNA is significantly reduced as detailed in Figure 6.3, significant effects are also seen on Cx37 and Cx40. Evaluation of Cx37 mRNA shows a significant decrease in cells treated with Cx43 siRNA under static and shear conditions with a 2-fold and 6-fold reduction, respectively. Evaluation of Cx40 mRNA shows a significant decrease in cells treated with Cx43 siRNA under static and shear conditions with a 3.2-fold and 5.4-fold reduction, respectively. While there is no effect of shear stress on Cx37 or Cx43 mRNA expression, shear induces an upregulation in Cx40 mRNA.

Immunocytochemistry analysis shows no obvious changes in protein expression of non-target connexins, however due to the non-quantitative nature of this technique, it is difficult to draw measurable conclusions. Failure to detect Cx37 and Cx40 proteins in western blots has hampered the evaluation of non-target connexin protein expression following siRNA treatment.

Gap Junction Communication

The most established function of connexins is the assembly into hemichannels and formation of gap junction channels which allow passage of small molecules between

neighboring cells. To evaluate the role of specific connexin isotypes in endothelial gap junction communication, a dye transfer assay was conducted on experimental samples treated with siRNA and exposed to static or shear conditions. In the dye transfer assay, endothelial monolayers are scratched to load cells adjacent to the scratch with a dye mixture of Rhodamine-Dextran (MW 10,000) and Biocytin (MW 372, neutral charge). The large dye marks cells originally loaded with dye (donor cells) and the small dye passes to neighboring cells which are connected by gap junctions (recipient cells). Quantification of images following transfer of dye for 2 minutes allows calculation of a cell coupling index which is the ratio of recipient cells to donor cells. Figure 6.7 displays dye transfer data assessing gap junction communication in endothelial monolayers following RNA interference and static or shear stress conditions.

Statistical analysis identifies significant differences in gap junction communication due to siRNA treatment, shear stress and an interaction effect. Tukey post-hoc testing breaks down the statistical analysis with pairwise comparisons. Dye transfer is significantly reduced in endothelial cells exposed to shear stress compared to static for OptiMEM controls, NC (negative control) siRNA 40nM, Cx37 siRNA 40nM and Cx40 siRNA 40nM. However, no shear effect is seen in monolayers treated with Cx43 siRNA 40nM as the level of dye transfer is reduced regardless of mechanical environment. Static Cx43 siRNA monolayers have significantly less dye transfer than static OptiMEM and static NC siRNA monolayers and furthermore, shear Cx43 siRNA monolayers have significantly less dye transfer than shear OptiMEM monolayers.

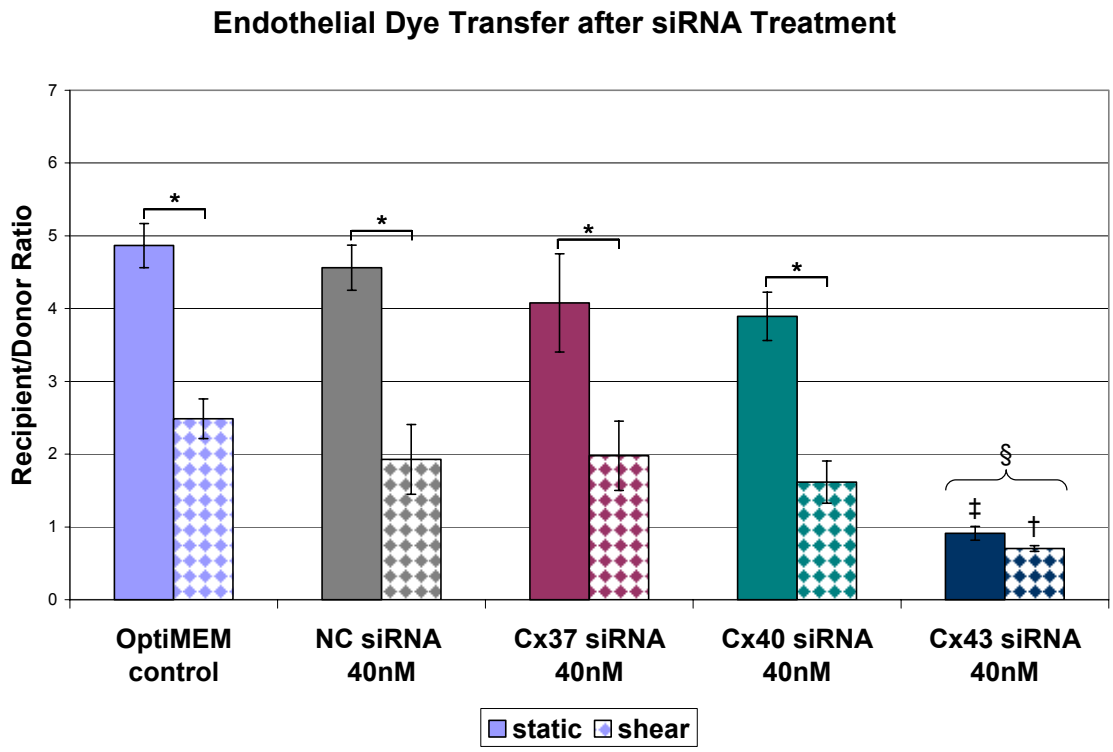

Figure 6.7 Effects of Connexin Knockdown on Gap Junction Communication

Treatment with Cx43 siRNA reduces endothelial cell gap junction communication and exposure to shear stress reduces endothelial cell gap junction communication. Treatment with Cx37 siRNA or Cx40 siRNA does not significantly alter gap junction communication.

ANOVA: siRNA $p = 0.000$, flow $p = 0.000$, interaction $p = 0.012$ Tukey post hoc tests denoted as follows:

* $p < 0.01$ for static vs. shear pairwise comparisons

‡ $p < 0.001$ Cx43 siRNA static vs. OptiMEM static, NC siRNA static

† $p < 0.05$ Cx43 siRNA shear vs. OptiMEM shear

§ $p < 0.0001$ Cx43 siRNA vs. OptiMEM, NC siRNA, Cx37 siRNA, Cx40 siRNA

With respect to siRNA treatment, Cx43 siRNA treated endothelial monolayers have significantly less gap junction communication compared to OptiMEM, NC siRNA, Cx37 siRNA and Cx40 siRNA treated monolayers.

Cell Proliferation

Gap junctions and possibly individual connexins are thought to play a role in cell proliferation therefore the effect of endothelial connexin knockdown on cell proliferation under static and shear conditions was evaluated. Proliferation was assessed by exposing cells to a thymidine analog, BrdU, for six hours and measuring its presence in cell nuclei indicating incorporation into DNA during S-phase of the cell cycle. Percentage of proliferating nuclei as a portion of total nuclei was calculated for cells following treatment with siRNA and exposure to static or shear conditions. Figure 6.8 shows data evaluating the effect of connexin knockdown on endothelial cell proliferation. Statistical analysis shows no significant effect of siRNA treatment on proliferation; however shear stress does significantly reduce endothelial cell proliferation.

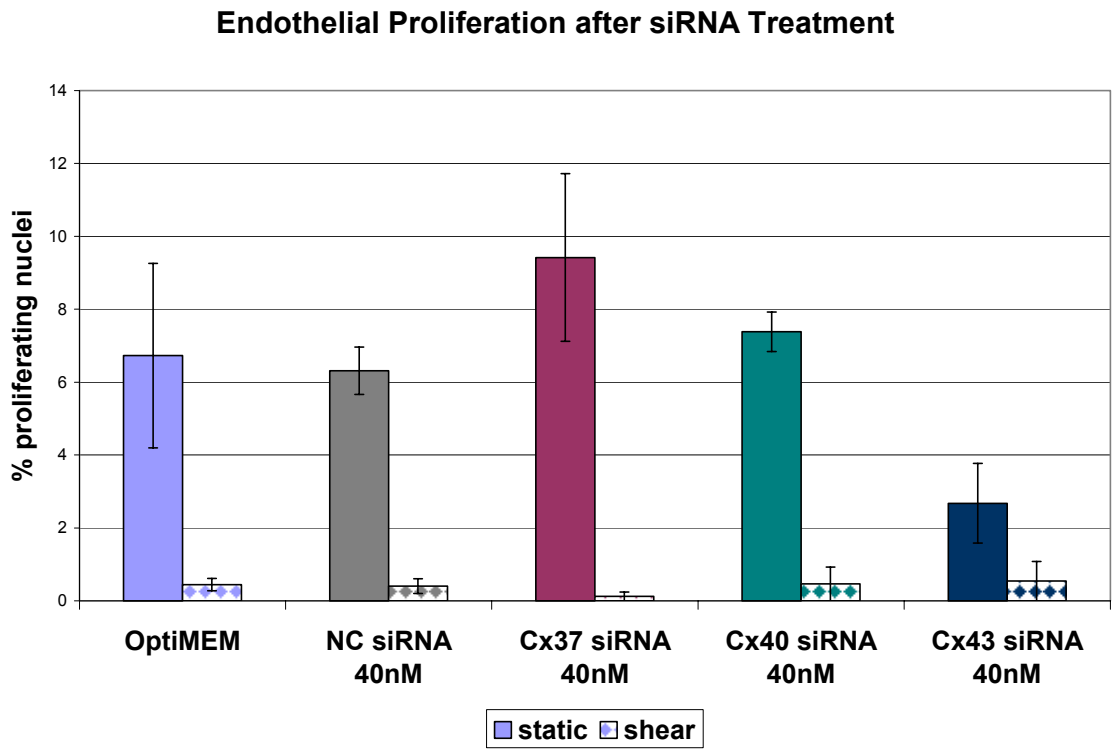

Figure 6.8 Effects of Connexin Knockdown on Cell Proliferation
Treatment with connexin siRNA has no significant effect on cell proliferation while exposure to shear stress significantly reduces cell proliferation.
ANOVA: siRNA p = 0.384, flow p = 0.000, interaction p = 0.280

Cell Morphology

Cell morphology and changes in response to fluid shear stress are a hallmark of endothelial cell biology. Two components of cell morphology are the angle of orientation and the elongation of the cell. Cell morphology following siRNA treatment and exposure to static or shear stress was assessed by imaging actin fibers of the cell. Angle of orientation with respect to the horizontal axis (also direction of fluid flow) was determined by evaluating the orientation of actin stress fibers within the cell. Elongation of the cell was evaluated by measuring the perimeter and area of a cell and calculating a shape index which assesses whether the shape more closely resembles a line or a circle.

Figure 6.9 shows the effect of siRNA treatment on endothelial angle of orientation following exposure to shear stress or static conditions. There is no significant difference on endothelial cell angle of orientation due to siRNA treatment; however cells do align in direction of flow following exposure to shear stress.

Figure 6.10 shows the effect of siRNA treatment on endothelial cell elongation following exposure to shear stress or static conditions. ANOVA statistical analysis indicates a significant effect of siRNA on cell elongation and a significant effect of flow with changes to a more elongated shape following exposure to shear stress. Tukey post hoc testing indicates a significant difference in elongation of cells treated with Cx40 siRNA compared to monolayers treated with OptiMEM, Cx37 siRNA and Cx43 siRNA. Endothelial cells are more elongated under static and shear stress conditions following RNA interference of Cx40.

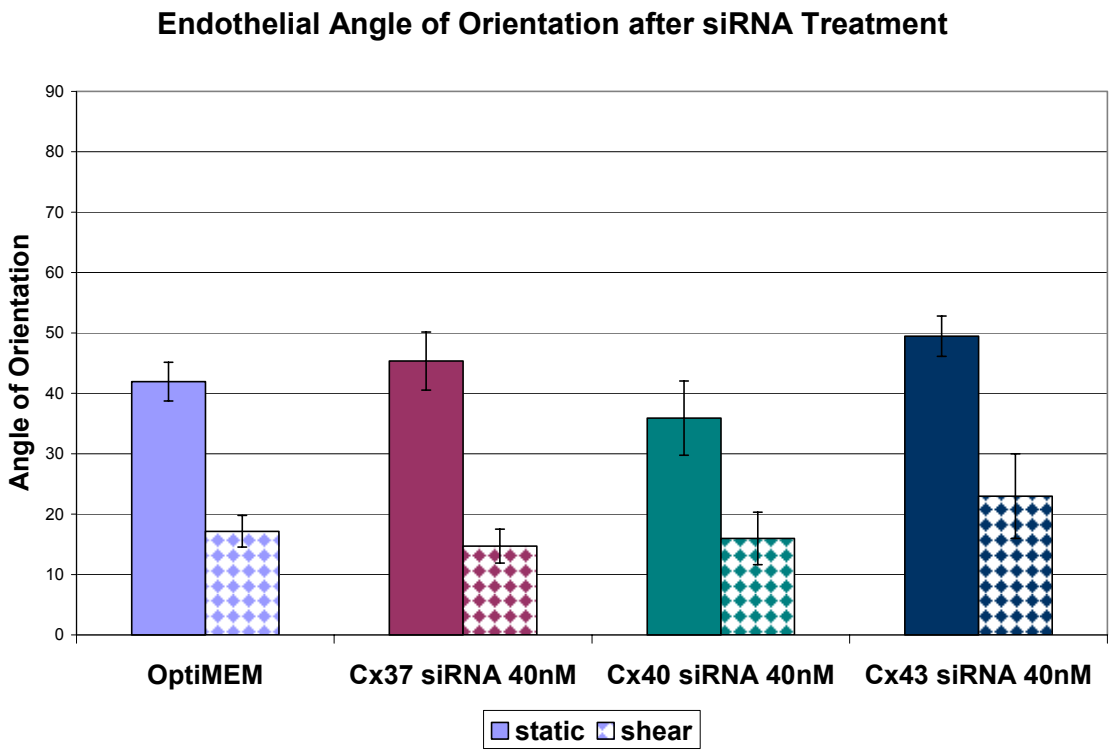

Figure 6.9 Effects of Connexin Knockdown on Cell Angle of Orientation
Treatment with connexin siRNA has no significant effect on cell angle of orientation while exposure to shear stress significantly alters angle of orientation by aligning cells in direction of fluid flow. ANOVA: siRNA p = 0.185, flow p = 0.000, interaction p = 0.711

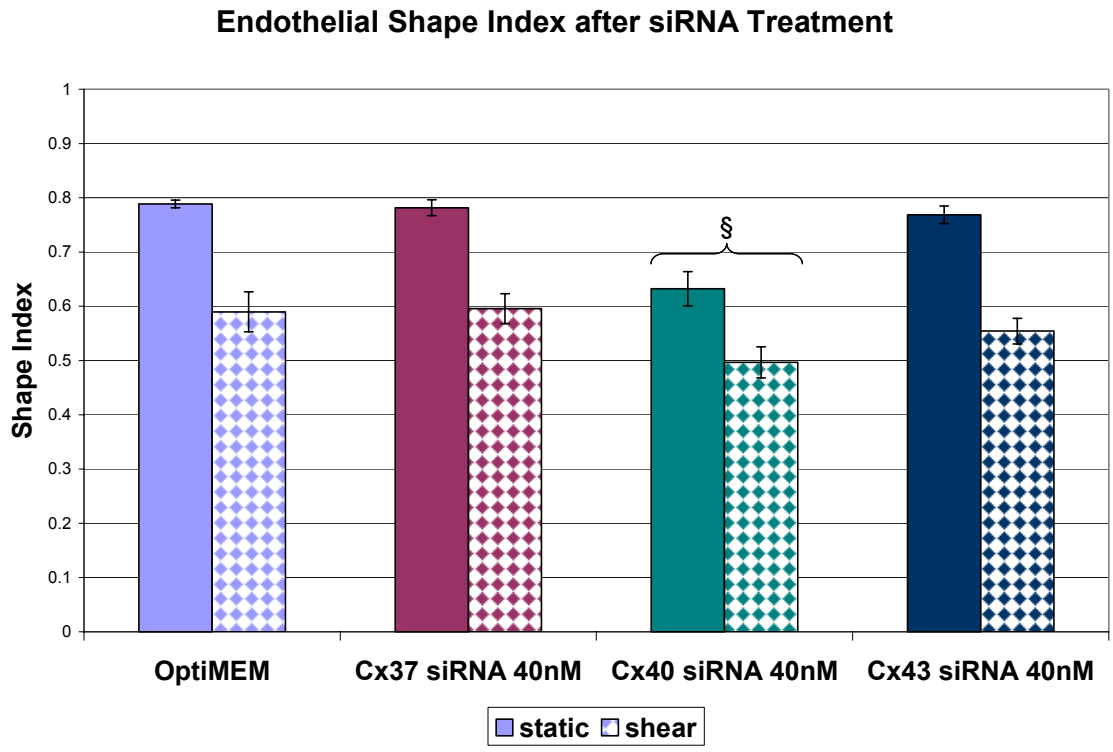

Figure 6.10 Effects of Connexin Knockdown on Cell Elongation

Treatment with Cx40 siRNA significantly alters endothelial shape index to a more elongated morphology. Exposure to shear stress also significantly alters endothelial shape index to a more elongated morphology. Treatment with Cx37 siRNA or Cx43 siRNA does not significantly alter cell elongation.
ANOVA: siRNA $p = 0.000$, flow $p = 0.000$, interaction $p = 0.418$ Tukey post hoc tests denoted as follows:
§ $p < 0.005$ Cx40 siRNA vs. OptiMEM, Cx37 siRNA, Cx43 siRNA

Discussion

Role of Connexin 37

Of the connexins expressed in vascular endothelium, Connexin 37 is the least investigated due to its recent identification and restricted tissue expression pattern. Within the vasculature, Cx37 is expressed only in endothelial cells and is not found in smooth muscle cells or myocytes. A naturally occurring variant of Cx37 has been implicated in the prevalence of atherosclerosis in the human population. (169) Altered endothelial cell Cx37 expression has been linked to hypertension along with its presumed role in atherosclerosis. (165, 167, 168) Cx37-/- mice are viable but females are infertile due to abnormal reproductive development. (171) No obvious vascular abnormalities are seen in Cx37-/- models, however this is presumed to be due to the presence of other vascular connexins since double knockouts exhibit severe vascular deformities. (174)

Knockdown of Cx37 expression using RNA interference was used in this study to evaluate its effects on endothelial cell function including gap junction communication, cell proliferation and cell morphology. Furthermore, knockdown using RNAi as opposed to animal model genomic knockouts provided a new opportunity to evaluate the effects of Cx37 loss on expression of other endothelial connexins, Cx40 and Cx43. A short interfering RNA (siRNA) sequence designed to target only Cx37 mRNA was successful in knocking down mRNA expression in endothelial cells exposed to static and shear stress conditions. When Cx37 was reduced, endothelial cells significantly upregulated Cx40 mRNA expression approximately three-fold under static and shear conditions. Additionally, there was a statistically significant upregulation in Cx43 mRNA although the change was less dramatic. While RNA interference of Cx37 resulted in changes of

Cx40 and Cx43 expression, targeting of other connexins also impacted Cx37 mRNA expression. Knockdown of Cx40 mRNA resulted in a decrease in Cx37 mRNA and knockdown of Cx43 mRNA also resulted in a decrease in Cx37 mRNA.

While treatment of endothelial cells with Cx37 siRNA significantly altered Cx40 and Cx43 mRNA expression, effects on cell function assessed in this study were less pronounced. Results from the dye transfer assay, which measures extent of gap junction communication within a cell population, showed no significant difference between Cx37 siRNA treated monolayers and control samples under static or shear stress. A significant difference was seen between Cx37 siRNA static slides and Cx37 siRNA shear slides with a reduced level of dye transfer in endothelial cells following exposure to shear stress. This response to shear stress is also seen in control samples and thus Cx37 siRNA treatment does not alter endothelial cell adaptation of gap junction communication following shear exposure. Dye transfer has been conducted in endothelial cells of mouse Cx37-/- aorta to investigate the role in Cx37 in communication during development. Evaluation found no significant differences compared to wild type in embryonic aortas, a reduction in dye transfer in young animals (3 weeks and 6-7 weeks) and no effect of Cx37-/- in dye transfer of adults. (177)

In evaluating endothelial cell proliferation by BrdU incorporation, Cx37 siRNA treatment has no significant effect on endothelial cell monolayers under static or shear stress conditions. While proliferation levels of Cx37 siRNA treated static endothelial cells are slightly higher than control samples, there is no statistical significance. A significant difference was seen between Cx37 siRNA static slides and Cx37 siRNA shear slides with a reduced level of proliferation following endothelial exposure to shear stress.

Thus the ability of endothelial cells to decrease proliferation in response to shear was not impacted by the treatment with Cx37 siRNA. While there are no previous reports investigating Cx37 knockdown on endothelial cell proliferation, a complementary approach of Cx37 adenovirus transfection into endothelial cells resulted in cell apoptosis. (180)

Endothelial cell morphology including angle of orientation and cell elongation was assessed using staining of actin filaments. Treatment with Cx37 siRNA did not significantly alter endothelial cell angle of orientation or elongation compared to controls under static or shear conditions. As with endothelial cell response to shear stress altering gap junction communication and cell proliferation, morphology is also modified. During exposure to steady laminar shear stress, endothelial cells align in direction of fluid flow and elongate in shape. Treatment with Cx37 siRNA did not impact this response as cells elongated and aligned in a manner similar to control monolayers.

Role of Connexin 40

Within the vascular system, Connexin 40 is expressed in endothelial cells, smooth muscle cells and myocardium. It is potentially thought to be the constitutive endothelial connexin with stable, widespread expression while Cx37 and Cx43 expression varies. (121, 123, 187) Connexin 40 has been implicated in vascular diseases including atherosclerosis and hypertension following both *in vivo* and *in vitro* studies. (167, 172) While Cx40-/- mice are viable, they exhibit multiple conduction abnormalities in the heart and blood vessels and are hypertensive. (172) Due to the potential overlap in

function or compensatory responses of other vascular connexins, Cx40 double knockout models show more extensive blood vessel abnormalities. (174, 175)

Knockdown of Cx40 expression using RNA interference was used in this study to evaluate its effects on endothelial cell function including gap junction communication, cell proliferation and cell morphology under static and shear stress conditions. Using RNAi to reduce Cx40 expression provided a novel opportunity to evaluate the effects of Cx40 loss on other endothelial cell connexins, Cx37 and Cx43, without the use of knockout animal models. A short interfering RNA (siRNA) sequence designed to target only Cx40 was successful in knocking down endothelial cell Cx40 mRNA in static and shear monolayers. Comparison of static and shear monolayers showed an upregulation of Cx40 mRNA in response to shear stress which was reported in previous studies from our laboratory using monolayers untreated with RNAi. Even though levels of Cx40 mRNA increase in response to shear stress, the knockdown using siRNA remained in effect. When Cx40 was reduced by siRNA, endothelial cells also decreased levels of Cx37 mRNA while there was no affect on levels of Cx43 mRNA. Furthermore, RNA interference targeting Cx37 resulted in increased levels of Cx40 mRNA while RNAi targeting Cx43 resulted in decreased levels of Cx40 mRNA.

Cx40 siRNA treatment of endothelial monolayers resulted in changes in endothelial cell behavior under static and shear stress. In evaluating gap junction communication by dye transfer, results from Cx40 siRNA treatment were not significantly different from controls under static or shear stress conditions. Control samples demonstrate that in response to shear stress, endothelial cells reduce gap junction communication as assessed by dye transfer. Treatment with Cx40 siRNA does not

impact this endothelial cell adjustment in communication due to fluid flow. Dye transfer has been conducted in endothelial cells of mouse Cx40-/- aorta to evaluate the role of Cx40 in communication during development. Investigation found significant reduction of dye transfer in knockout aortas during embryonic stages as well as during growth at 3 weeks, 6-7 weeks and 8 weeks indicating a prominent role in communication during mouse development. (177)

Assessment of endothelial cell proliferation under static or shear conditions by BrdU incorporation found no significant differences between control samples and Cx40 siRNA treated monolayers. Endothelial cells exhibit reduced proliferation under laminar shear stress compared to static conditions and treatment with Cx40 siRNA had no significant effect on this response to mechanical environment. Evaluation of endothelial cell morphology including angle of orientation and cell elongation was assessed by visualization of actin filaments. Cx40 siRNA treatment does not affect endothelial cell angle of orientation under static or shear conditions. Alignment of endothelial cells in direction of flow following exposure to shear stress is also not significantly affected by Cx40 siRNA treatment. Endothelial cell shape is significantly altered by treatment with Cx40 siRNA resulting in cells which are more elongated than control samples and monolayers treated with Cx37 or Cx43 siRNA. There are no previous reports of connexin knockdown affecting endothelial cell morphology and thus the mechanism behind this effect is unknown. We can hypothesize that knockdown of Cx40 alters contacts at endothelial cell-cell junctions, focal adhesions or interactions with cytoskeletal components. There is emerging evidence that connexins interact with other structural proteins including tight junction proteins, adherens junction proteins and

signaling molecules such as src. (212) However, most investigations on connexin-cytoskeletal interactions have focused on Cx43 due to its widespread expression and excellent model cell systems.

Role of Connexin 43

Connexin 43 is the most extensively studied connexin due to its widespread expression in the vascular system and other tissues. Furthermore, it contains several known phosphorylation sites and a complex pattern regulating expression is emerging. (113, 137) Focusing on the role of Cx43 in the vasculature, multiple studies have implicated it in both atherosclerosis and hypertension. (163, 165, 166, 168) While the genomic Cx43 knockout is embryonic lethal due to malformation of the heart, additional strategies have provided insight into its role in blood vessels. (173) A Cx43 knockout restricted to vascular endothelial cells (VEC Cx43-/-) was developed and this model exhibited both hypotension and bradycardia. (163)

Knockdown of Cx43 expression using RNA interference was used in this study to evaluate its effects on endothelial cell function including gap junction communication, cell proliferation and cell morphology. Use of RNAi to knockdown Cx43 expression provides a unique opportunity to study its function since mouse Cx43-/- are embryonic lethal. In addition, Cx43 siRNA treatment of endothelial cells allows for evaluation of effects on non-targeted connexins, namely Cx37 and Cx40. A short interfering RNA (siRNA) sequence designed to target only Cx43 was successful in knocking down endothelial cell Cx43 mRNA in static and shear monolayers. While a slight increase in Cx43 mRNA in shear samples compared to static samples can sometimes be observed,

this difference is not statistically significant which confirms data previously reported from our laboratory. When Cx43 mRNA is knocked down by siRNA, a decrease in Cx37 mRNA and a decrease in Cx40 mRNA are also seen. Moreover, Cx43 is also affected by siRNA targeting Cx37 but not in treatment targeting Cx40. When endothelial cells are treated with Cx37 siRNA, there is a statistically significant increase in Cx43 mRNA levels however the degree of change is small.

RNA interference of Cx43 in endothelial cells resulted in changes in cell behavior under static and shear stress conditions. Results from the dye transfer assay show significant impact of Cx43 siRNA on endothelial cell gap junction communication in monolayers exposed to static and shear stress conditions. Treatment with Cx43 siRNA results in significantly reduced dye transfer compared to OptiMEM control, NC siRNA, Cx37 siRNA and Cx40 siRNA. Under static conditions, Cx43 siRNA treated monolayers have reduced gap junction communication compared to medium and siRNA controls. Under shear conditions, dye transfer is further reduced and Cx43 siRNA treated monolayers are significantly lower than the medium control. With the low level of dye transfer under static conditions, Cx43 siRNA is the only treatment group which does not significantly reduce gap junction communication under shear compared to static conditions. Dye transfer of Cx43 genomic knockouts has not been conducted due to embryonic lethality and it was not reported in the study of Cx43 knockout restricted to endothelial cells. (163, 173)

Evaluation of endothelial cell proliferation by BrdU incorporation demonstrated no statistically significant effect of Cx43 siRNA treatment on levels of proliferation. However, there is a trend towards reduced proliferation in static monolayers of Cx43

siRNA treated cells compared to static controls. It is unknown if this trend is due to the loss of gap junction communication as seen by dye transfer or potentially effects due to loss of connexins or hemichannels. While only a trend, it is interesting that loss of gap junction communication corresponds to potentially lower proliferation rates since the trend often seen in cancer is a loss of gap junctions resulting in higher proliferation. (210) Endothelial cell angle of orientation and elongation were evaluated by actin filaments to provide measures of morphology. Under static conditions, there is no significant difference in angle of orientation or elongation in Cx43 siRNA treated monolayers compared to controls. Under shear conditions, endothelial cells elongate and align in direction of flow compared to static samples. Knockdown of Cx43 does not impact this morphological response to shear stress with similar elongation and orientation to controls. It is interesting to note that endothelial cell monolayers treated with Cx43 siRNA exhibited what appear to be fragmented actin filaments near cell-cell junctions. Figure 6.11 displays two fields of endothelial cells treated with Cx43 siRNA displaying this unusual staining pattern. While this was repeatedly observed, any mechanism remains unknown except for speculation regarding the potential interactions of connexins with cytoskeletal components.

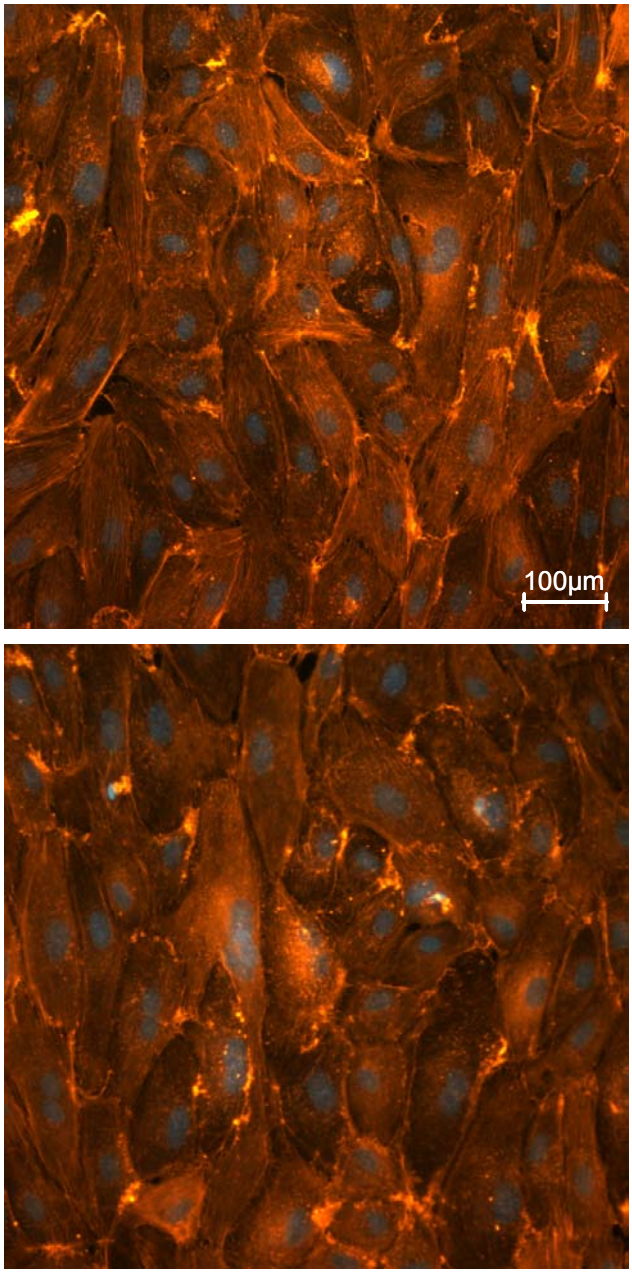

Figure 6.11 Endothelial Cell Actin Fragmentation in Cx43 siRNA Treated Samples
Endothelial monolayer stained for actin filaments (orange) and nuclei (blue) shows fragmentation of actin at cell-cell junctions.

Non-Target Connexin Expression

Knockdown of individually targeted connexins by RNA interference in this study resulted in numerous changes in expression of non-targeted connexins. Cx37 siRNA knocked down Cx37 expression, but also increased Cx40 expression and increased Cx43 expression. Cx40 siRNA knocked down Cx40 expression, but also decreased Cx37 expression with no changes in Cx43 expression. Cx43 siRNA knocked down Cx43 expression, but also decreased Cx37 expression and decreased Cx40 expression.

Multiple examples of effects on non-targeted connexins have been reported in studies of connexin knockouts in mouse models. Knockout of Cx37-/- has been reported to result in a decrease of Cx40 expression. (177) Multiple reports on Cx40-/- animals have arrived at conflicting conclusions with one group reporting an increase in Cx37 and another group reporting a decrease in Cx37. (176, 177) Furthermore, an additional study found no change in Cx43 expression levels in Cx40-/- but a change in the pattern of protein location. (179) While the Cx43-/- is embryonic lethal, the VEC Cx43-/- knockout study reported changes in Cx43 of smooth muscle cells but no other changes in endothelial connexin expression. (163) While it is unclear from these studies what the pattern of cross-regulation amongst connexin isotypes may be, it is clear that changes in non-targeted connexins occur. Further complicating the picture is the controversy over expression of Cx43 in mouse vasculature. While many groups report no detection, the VEC Cx43-/- mouse exhibits significant differences from wild-type suggesting its presence is required in this model for normal function. The only study altering the connexin balance in human cells used an adenovirus transfection approach to increase

connexin expression in HUVEC which showed that transfection with Cx37 resulted in decreased Cx43 expression. (180)

Thus questions remain regarding the ablation of one connexin affecting expression of other connexin isotypes. One hypothesis is that of compensation where cells are attempting to retain gap junction communication capability despite loss of one connexin. While this is certainly a possibility, one might expect that a knockdown of one connexin would always result in the upregulation of remaining isotypes which is not the effect seen in this study and previous investigations. However, if the connexin isotypes have very different properties including electrical conductivity, permeability and gating, maintenance of communication might require upregulation or downregulation depending on the connexins involved. A second rationale behind the effects on non-targeted connexins might be due to the profile of channels which are normally created in endothelial cells. Connexins 37, 40 and 43 are known to mix and match in forming heteromeric hemichannels and heterotypic gap junctions. (147, 148, 150) With characteristics of heteromeric and heterotypic combinations known to be distinct from homomeric and homotypic combinations, the loss of one connexin component could alter the levels of other connexins required to maintain cell function. In addition to unique properties resulting from mixed hemichannels and gap junctions, another hypothesis is that loss of one connexin isotype alters the stability of channels which remain. If the profile of stability in remaining channels is higher or lower than normal, an increase or decrease in levels of non-targeted connexin may be required to maintain cell function. While explanations for effects on non-targeted connexins remain unknown, this study confirms cross-regulation of connexins seen in mouse knockout systems. Furthermore,

individual knockdowns establish a pattern of dependence between the connexin isotypes which provides additional insight into their functions.

Connexins in Endothelial Function

Cx37, Cx40 and Cx43 are thought to have specific cellular functions, although their unique characteristics remain largely unknown. Differences in electrical conductivity of channels have been established but individual permeability and gating properties continue to be evaluated. (12) Previous studies have demonstrated individual responses of endothelial connexin isotypes to stimuli thus emphasizing their potential unique functions. Endothelial connexins are differentially regulated by cell density, presence of TGF-β and nitric oxide. (181, 183) *In vitro* and *in vivo* injury studies have shown differential regulation, location and expression patterns over time. (162, 184) Finally, danger signals such as TNF-α and sepsis have demonstrated changes in different endothelial cell connexin expression levels. (185, 186)

Individual knockdown of connexins in this study has added information regarding their unique functions in endothelial cells. Knockdown of Cx37 resulted in no significant differences in gap junction communication, proliferation, angle of orientation or elongation and did not alter the normal cellular responses to shear stress which are associated with these functions. Knockdown of Cx40 had no significant impact on gap junction communication, proliferation or angle of orientation, but unexpectedly altered cell morphology resulting in a more elongated shape. A link between Cx40 and cytoskeletal structures remains unknown but results from this study suggest it should be pursued. In addition, endothelial cell behavior in response to shear stress was not altered

by Cx40 siRNA treatment. Knockdown of Cx43 did not significantly alter endothelial cell morphology, however it did dramatically decrease gap junction communication and while not significant, appeared to reduce cell proliferation. The reduction in gap junction communication as assessed by dye transfer in Cx43 siRNA treated endothelial cells was so severe in static and shear samples that any effect due to shear was abolished. Whether shear reduction of endothelial gap junction communication is due to effects of mechanical forces on Cx43 remains to be conclusively determined, but it was the only knockdown treatment lacking a differential shear response.

Conclusions

While connexin knockouts in the mouse model have been generated, this study is the first to knockdown connexins in a transient manner in endothelial cells or human primary cells. Although this study takes a novel approach to understanding all three connexin isotypes expressed in endothelial cells, it has numerous limitations which must be considered in drawing conclusions. RNA interference, while an extremely powerful tool, does not result in a complete loss of mRNA transcript which could potentially complicate analysis. Treatment by RNAi may also have unanticipated side effects on cell function or on molecules of interest. A major shortfall of the data presented here is the lack of information on Cx37 and Cx40 protein expression due to the unsuccessful western blot analysis. Effects on non-targeted connexins, while providing insight on interactions between isotypes, complicate interpretation of cell function data due to multiple rather than isolated changes. As studies from this laboratory have previously demonstrated, while an *in vitro* two-dimensional substrate supporting a monolayer of

endothelial cells is not an accurate representation of the physiologic state, it is a controlled environment for the first step such as experiments presented here. Especially in light of myoendothelial gap junctions which exist between endothelial and smooth muscle cells, knockdown of endothelial connexins should also be conducted in a system which contains this neighboring cell type. In the spirit of recreating the physiologic environment in which endothelial cells reside, the mechanical forces used in this study are much simplified. While laminar shear stress is a better approximation of the fluid flow environment than static conditions, if the mechanosensitive nature of endothelial connexins is to be fully investigated, multiple flow regimes should be recreated.

Although this study provides novel insight into endothelial connexin function, it is merely a launching point for future studies incorporating the powerful technique of RNA interference. Future studies should include a multiple connexin knockdown strategy to more fully elucidate functions in a manner similar to double knockout animal models. Also of great interest is a more in depth analysis of known gap junction functions in endothelial cells under static and shear stress conditions. Primarily studies should incorporate additional permeability tracers to elucidate potential size or charge specificity and electrical conductance measurements since previous reports have established that movement of chemical and electrical signals are not always similarly modulated. Pursuit of mechanisms underlying results presented here provides numerous opportunities to add to understanding of connexin function. Notably, the interaction of connexins in response to knockdowns and how shifts in expression are regulated should be examined. Additionally, the role of Cx43 in endothelial gap junction communication and response to

shear stress as well as the role of Cx40 in endothelial cell morphology remain to be fully understood.

While major endothelial cell functions were investigated here: gap junction communication, cell proliferation and morphology, exploration of connexins in other critical endothelial functions such as barrier formation and coagulation balance could provide valuable insight. Expansion of the endothelial cell experimental setting to include components such as complex extracellular matrix, smooth muscle cells and fluid flow patterns would recreate a more physiologic microenvironment. In addition, the continued use of human cell systems is important in accurately capturing physiologic functions, especially in light of known differences in connexin expression patterns amongst species.

In conclusion, this study demonstrates specific roles of connexin isotypes in endothelial cell behavior under static and shear stress conditions and confirms adaptations in non-targeted connexins. The use of RNA interference to knockdown human endothelial connexins provides novel insight into individual isotypes and demonstrates the power of this technique for future studies. Taken together, results presented here contribute to the understanding of vascular connexins and may add insight to their functions in development and disease.

CHAPTER SEVEN: Discussion and Conclusions

Widespread prevalence of cardiovascular disease and the associated mortality and morbidity are the driving force behind numerous investigations including this dissertation. The staggering clinical statistics of atherosclerosis have motivated extensive study into endothelial cell biology in attempts to understand the clinical problem and have motivated the development of tissue engineered blood vessels in attempts to provide a new clinical therapy. While substantial progress has been made in both the understanding and treatment of atherosclerosis, cardiovascular disease remains the greatest threat to American health. Questions persist in endothelial cell biology and the disparity among results from *in vitro* experiments, *in vivo* animal studies and human patients perplexes the field. Development of tissue engineered blood vessels for use as vascular grafts continues to proceed rapidly but these tissue substitutes are not ready for clinical use. A new approach taken in this dissertation aims to combine the efforts to understand and treat the clinical problem by using a tissue engineered substitute a as more physiologic model for the study of human endothelial cell biology. Results from this novel strategy provide insights into human physiology and pathology as well as aid in the development of improved tissue engineered vascular grafts.

While studies presented here are among the first to combine these two areas into one strategy for novel discovery, discussion of limitations of this approach as well as work presented in this dissertation is important in developing conclusions and considering directions for future work. Use of engineered human tissues and inclusion of mechanical forces in the study of cell biology provides the opportunity to work with a

more physiologic, yet still controlled experimental setting. Although an improvement over traditional *in vitro* experimental settings, the environmental cues provided by the tissue engineered blood vessel wall model and laminar shear stress system used here are still simplistic approximations of the native environment.

The tissue engineered wall model (TEWM) is a basic reconstruction of the medial layer of the blood vessel wall by including the major cell type, smooth muscle cells, and the major extracellular matrix protein, collagen type I. While addition of these primary components adds significant complexity over traditional *in vitro* endothelial substrates, there is room for substantial improvement. The collagen fibers and smooth muscle cells of the TEWM do not achieve a configuration matching the native vessel with respect to fiber structure and cell density. Addition of other extracellular matrix components, such as elastin, proteoglycans and other types of collagen, would significantly improve the relevance of this model for use in investigating cell biology. Future modifications of the engineered substrate to recreate the native vascular environment should also include an adventitial layer and a vasa vasorum. Finally, while the TEWM used in these studies was an arterial model using aortic cells, an advantage of tissue engineering is the ability to customize the tissue for its downstream purpose. Therefore models of the venous system or capillary beds could also be developed.

Mechanical forces are increasingly recognized for their important roles in numerous vascular physiologic and pathologic processes. While shear stress effects on endothelial cells were first discovered many years ago, the complexity of forces which cells can interpret is only now being appreciated. The fluid flow system used in this dissertation provides a steady laminar shear stress across a flat surface of endothelial

cells. While inclusion of fluid flow is a significant component in recreating the native endothelial environment, the forces provided in this system are simplified approximations of blood flow *in vivo*. Fluid flow and therefore the shear stress exerted on the vessel wall differs both spatially and temporally in the human body. Profiles from athero-susceptible and athero-resistant areas of the vasculature vary in magnitude, reversal characteristics and frequency of oscillations which recent studies have shown can be detected by endothelial cells. A more physiologic fluid flow experimental setting would include waveforms representing multiple regions of the vasculature as well as characteristics over the time period of interest such as during bedrest or exercise. A more advanced fluid flow system could also be used to investigate differences in arterial versus venous flow environments and embryonic versus adult systems.

While each additional component increases the physiologic nature of the re-created endothelial cell microenvironment, it also increases the complexity in determining mechanisms behind the influence. For example, cellular differences detected between the TEWM and adsorbed collagen slide in this dissertation could be due to the presence versus absence of smooth muscle cells, the fibrillar versus monomer form of collagen, or the three-dimensional versus two-dimensional nature of the substrate. However with this trade-off in mind, the addition of other stimuli could provide new opportunities to understand endothelial function. Thus besides improving the current tissue engineered wall model and shear stress system, inclusion of other biological components such as plasma and blood cells or inclusion of other mechanical forces such as pressure and cyclic strain should be considered for future work.

A current drawback in using the tissue engineered wall model is the challenge it poses in applying traditional techniques for endpoint analysis. Many *in vitro* protocols commonly employed today are designed for use with a single cell type or in systems where a high level of sample recovery is possible. The challenge of the TEWM arises from its key advantage, which is the presence of multiple environmental components. To evaluate responses at the cellular and molecular level in this dissertation, new techniques had to be conceived. To analyze endothelial cells exposed to the TEWM substrate using non in situ techniques such as real time RT-PCR, flow cytometry and western blotting, an isolation procedure had to be developed. Furthermore, RNA amplification techniques incorporated into the microarray labeling procedure were required to work with small amounts of RNA achieved from the low yield of endothelial cells recovered from the TEWM lumen. Finally, due to the limited quantity of cells retrieved from this system, the number of experiments required to generate adequate sample for analysis is very high and thus less efficient than simplified systems.

While limitations are always present when branching into a new area, the use of a more physiologic *in vitro* environment also provides a fresh perspective to a heavily studied field. The goal of this dissertation was to contribute to vascular biology by investigating impact of smooth muscle cells, extracellular matrix and fluid flow on endothelial cell behavior. Using a tissue engineered human blood vessel as a model of the vascular wall and a mechanical environment of laminar shear stress, endothelial cell transcriptional profiles were compared to create a broad view of cellular function in response to these stimuli. As a case study of endothelial cell behavior, studies focused on cell-cell communication through gap junctions. Specifically, we investigated the

modulation of endothelial gap junctions by substrate and shear stress and examined the involvement individual connexin isotypes in endothelial cell function.

Chapter four details experiments conducted to address the first specific aim which was to compare transcriptional profiles of endothelial cells on a collagen coated slide to cells on a tissue engineered blood vessel under laminar shear stress and static conditions. Results from this study indicate that type of mechanical environment and nature of substrate have a broad impact on endothelial cell function which is exemplified in discussion of multiple areas of biological function. Within the cardiovascular and hematological systems, areas of cell function including adhesion through integrins, coagulation balance, matrix deposition and turnover, redox state, and vascular patterning illustrated some of the critical cell behaviors sensitive to substrate and shear stress. However, the regulation of gene expression by these stimuli depends on the function in question and the identity of each gene. Furthermore, for all areas of biological function examined, the profile of gene expression is different for each combination of stimuli which emphasizes the sensitivity of endothelial cells to cues from the microenvironment. Data presented here are a first step towards a better understanding of endothelial cell biology. The pursuit of mechanisms of influence for areas identified as differentially regulated could provide additional insight. How changes in transcriptional profile translate into changes in cell function was further investigated in chapters five and six with a focus on endothelial gap junctions and connexins 37, 40 and 43.

In addition to the limitations of the TEWM and flow environment previously discussed, this study of transcriptional profiling has additional drawbacks to be considered in formulating conclusions. Microarray analysis is an increasingly powerful

tool for gathering an enormous amount of information regarding cellular response to stimuli. While very useful for data mining and as a launching point for multiple in depth studies, interpretation of the data set as a whole can be difficult. Transcriptional information is extremely valuable; however it only provides a partial picture of the endothelial cell response. How changes in mRNA convert to changes in protein and how changes in protein mesh to alter cellular response are critical in understanding biological function. Advances in systems biology and modeling cellular behavior will be useful in assembling the large amounts of information generated by transcriptional profiling as well as from protein analysis and cell function assays.

Chapter five details experiments conducted to address the second specific aim which was to compare endothelial cell connexin expression and gap junction communication on a collagen coated slide and tissue engineered blood vessel under laminar shear stress and static conditions. Results indicate that while endothelial cell connexin expression and gap junction communication are influenced by substrate and shear stress, the response to these stimuli is complex. Connexin mRNA is altered by substrate and shear stress in an isotype dependent manner. Endothelial cells express Cx37, Cx40 and Cx43 proteins that are visible in the cell membrane and cytoplasm and quantification of expression shows significant increase in all three isotypes in cells on the TEWM substrate. Gap junction communication measured by dye transfer shows decreased cell coupling in endothelial monolayers exposed to laminar shear stress compared to static conditions. Data presented in this study are the first to demonstrate endothelial cell connexin sensitivity to substrate. The source of influence, whether induced primarily by the presence of smooth muscle cells or a three-dimensional fibrillar

extracellular matrix, remains to be determined. Mechanosensitivity of endothelial Cx43 has been previously investigated yet response to shear stress of the two other isotypes, Cx37 and Cx40 is demonstrated in this study. Furthermore, results presented here establish a reduction in endothelial cell gap junction communication following exposure to laminar shear stress compared to static culture.

While revealing novel sensitivity of endothelial connexins to substrate and shear stress, this study has limitations in both technique and approach. The techniques used in this study: RT-PCR, flow cytometry, immunocytochemistry and dye transfer, provide fundamental information about the expression levels and function of endothelial gap junctions which are important in establishing response to new stimuli. Nevertheless, an understanding of the underlying processes is lacking. Use of more advanced techniques to investigate the difference in expression patterns of connexin mRNA and connexin protein would greatly contribute to identifying the point of influence for substrate and shear stress. Use of additional dyes for permeability tracing and electrical conductivity measurements would provide further detail on the change in gap junction communication caused by exposure to laminar shear stress. Additionally, the multiple differences between the TEWM and adsorbed collagen slide demonstrate sensitivity of connexins to substrate and the importance of using more physiologic models in studying cell biology, but identification of specific components responsible for changing cell behavior is not possible using only these two models.

Chapter six details experiments conducted to address the third specific aim which was to knockdown expression of individual connexins to determine their specific roles in endothelial gap junction communication, cell proliferation and cell morphology. Results

demonstrate unique functions of connexin isotypes in endothelial cell behavior and also establish a pattern of adaptation in expression of non-ablated connexins. RNA interference of Cx37 results in successful knockdown of Cx37 mRNA but also increases Cx40 and Cx43 mRNA. RNA interference of Cx40 results in successful knockdown of Cx40 mRNA but also decreases Cx37 mRNA while not affecting Cx43 expression. RNA interference of Cx43 results in successful knockdown of Cx43 mRNA but also decreases Cx37 and Cx40 mRNA. While the mechanisms behind this pattern of off-target effects and the potential implication on cellular function remain unknown, one can speculate on potential explanations. Cx37 and Cx40 are both located on chromosome one while Cx43 is located on chromosome six and this spatial proximity could be involved in feedback mechanisms or sharing of regulatory molecules. Additionally, the three endothelial connexins are known to have several transcription factors in common which could be involved in modulating rates of mRNA synthesis.

Endothelial cells treated with Cx37 siRNA do not alter gap junction communication, cell proliferation or cell morphology under static or shear conditions and do not modify the normal response to shear stress seen in these functions. Treatment with Cx40 siRNA does not affect endothelial gap junction communication, cell proliferation or cell angle of orientation, however it does significantly elongate the cell morphology under both static and shear conditions. Cx40 RNAi also does not alter the normal response to shear stress for the examined cell functions. Endothelial cells treated with Cx43 siRNA do not alter cell morphology under static or shear stress conditions, however there are significant changes in gap junction communication and a trend towards an effect on cell proliferation. Cx43 RNAi significantly reduces gap junction

communication under static and laminar shear stress conditions and abolishes the change normally seen in response to shear stress. While not statistically significant, treatment with Cx43 siRNA also appears to reduce the level of endothelial cell proliferation under static conditions.

This study is the first to knockdown connexin expression using RNA interference in human primary cells or endothelial cells. Application of this powerful technique to research on endothelial cell communication can now be used to more fully understand connexin isotype expression, regulation and function. Data presented here establish a pattern of effects on non-ablated connexins which had previously only been seen in knockout animal models. Furthermore, it demonstrates connexin isotype-specific functions in endothelial cells and lays the groundwork for further investigation into differences and similarities of the three endothelial connexin isotypes.

Although novel in its approach and conclusions, this study is limited in its techniques and depth of understanding as more work in this area is clearly required. The technique of RNA interference, while extraordinarily powerful and revolutionizing studies of gene function, has several drawbacks. Potential pitfalls include the presence of remaining mRNA since it is a knockdown and not a knockout of expression as well as possible side effects of transfection reagents and siRNA on cell function and molecules of interest. A significant gap in data presented in this chapter is the lack of protein quantification of Cx37 and Cx40 by western blotting. Numerous adjustments in the protocol were made to find Cx37 and Cx40 expression, however a reliable series of steps was not determined. A drawback to the study of connexins is the lack of significant expression levels in native cells as well as the poor antibody availability for many

isotypes. Unfortunately, experiments in this study encountered these challenges resulting in incomplete information regarding protein expression with siRNA treatment. Results of this study did identify new areas of focus for research including determining mechanisms behind effects on non-ablated connexins, role of Cx43 in endothelial gap junction communication and role of Cx40 in endothelial cell morphology.

Collectively, results in this dissertation demonstrate that endothelial cell behavior is significantly altered by substrate and mechanical environment. Moreover, the response to these stimuli is dependent on the area of cell function and on the identity of genes in question. This specificity of response is demonstrated in both the transcriptional profiles of multiple areas of cell behavior and in the analysis of endothelial gap junctions. Families of genes involved in particular areas of cell function are regulated differently by these stimuli and individual components of any given family may also be regulated differently. Taken together, these results emphasize the complexity of cellular function and the sensitivity of endothelial cells to the whole of their microenvironment. Results also underline the need to use more physiologic *in vitro* models which recreate this microenvironment so we can gain a better understanding of the cellular complexity in physiologic and pathologic processes.

This case study of endothelial responsiveness to substrate and shear stress focused on gap junctions and their building blocks: connexins. Results from these experiments demonstrate that endothelial cell connexins are influenced by substrate and shear stress and gap junction communication is affected by the mechanical environment. Connexin isotypes are differentially regulated by substrate and shear stress and have unique contributions to fundamental endothelial cell behaviors. While endothelial connexins

have independent roles, their expression levels are linked together suggesting a need for co-expression in normal cell function.

As this dissertation is motivated by the clinical significance of atherosclerosis and the *in vitro* use of engineered human tissues leading to improved understanding of basic biology as well as development of superior tissue substitutes, the conclusions and impact of this work are focused in these areas.

While it is readily appreciated that endothelial cells alter their phenotype in response to shear stress, data presented here show an equally dramatic shift due to substrate. Just as many studies now focus on the influence of shear stress or include the presence of shear stress in investigating other endothelial cell functions, results presented here should motivate the field to investigate the influence of smooth muscle cells and extracellular matrix or include a more physiologic substrate in studying other areas of endothelial cell biology. Modulation of endothelial connexins and gap junctions in response to substrate and mechanical environment opens a new area of research in cell communication. Understanding the purpose behind response to these cues will bring insight into how this adaptation may occur in physiologic and pathologic conditions. Identification of differences in endothelial cell connexin isotypes also generates new questions. Ascertainment of their unique characteristics including permeability, electrical conductivity, gating and roles in other endothelial cell functions would greatly contribute to the current gaps in knowledge. Furthermore, an understanding of how the connexin isotypes may work together or work independently could clarify much of the confusion which currently surrounds their functions. Establishment of a co-expression pattern for individual isotypes is the first step in determining how connexins are linked together in

their regulation. Questions abound regarding whether this is a mechanism designed to protect cell communication, and if there are changes in expression, how the adjustments in multiple isotypes affect overall cell function. With clear differences in mRNA expression levels and protein expression levels established, determination of mechanisms underlying their regulation would also enhance understanding of their transcription, translation and stability.

Towards improving our understanding of atherosclerosis, results presented here can identify changes in response to substrate and mechanical environment which may lead to development of disease or may occur as a result of plaque progression. By understanding the combined influence of substrate and mechanical cues, therapies can be developed to control these interactions and prevent development or halt progression of disease. In the case of connexins and gap junctions, evidence exists linking changes in specific isotypes to atherosclerosis and hypertension. A better understanding of the individual roles of each isotype will aid in determining why mutations in some connexins lead to development of or protection from disease and also why different disease states alter endothelial connexin expression. Potential therapies targeting connexins or gap junctions could be used to control cell-cell communication to prevent disease development or slow its progression. Furthermore, a thorough understanding of endothelial cell gap junction regulation and function could lead to modulation of the cell communication system to increase spread of athero-resistant signals or prevent spread of athero-susceptible signals.

With the clinical goal of developing living tissue substitutes for therapeutic applications, a thorough understanding of cell interactions with extracellular matrix,

neighboring cell types and mechanical environments will provide the tools needed to modulate cell phenotype in developing these engineered tissues. For example, controlling cell proliferation, matrix deposition and matrix turnover during the steps of growing the tissue substitute, integrating the substitute with host tissue and maintaining mature tissue *in vivo* will be critical to therapeutic success. An understanding of cell-cell communication is fundamental to developing tissue substitutes because the links between cells are what transforms individual cellular responses into a unified tissue response. Connexins and gap junctions are also very involved in the differentiation and development of tissues in normal physiology thus modulation of these properties could be key in growing an engineered tissue. Gap junctions have special applicability in the development of cardiovascular tissue substitutes. Homocellular connections between endothelial cells and smooth muscle cells along with heterocellular connections between the two cell types are responsible for movement of signals critical to controlling vascular tone. Normal connexin expression and gap junction function will be required in a tissue engineered vascular graft if it is to be vasoactive and integrate with the host vessel. Gap junctions are also critical to electrical conduction in the heart and by controlling connections using extracellular matrix, multiple cell types, and mechanical or electrical stimuli, a myocardial patch can be developed which possesses the appropriate conduction pathways.

In conclusion, this dissertation demonstrates the sensitivity of endothelial cell phenotype to substrate and mechanical environment. Results presented here provide novel scientific insight into cell functions modulated by these stimuli and demonstrate a complex regulation of endothelial cell gap junctions. Furthermore, this work underlines

the importance of including more physiologic *in vitro* models into studies of basic cell biology. Finally, the use of engineered tissues to probe fundamental scientific questions results in novel conclusions which contribute to biological knowledge of endothelial cells, clinical understanding of disease, and development of advanced tissue engineered substitutes.

CHAPTER EIGHT: Recommendations for Future Work

Conclusions drawn and questions raised in this dissertation lay the foundation of recommendations for future work. These recommendations include next steps for the specific lines of experiments conducted here from the expansive microarray study to the knockdown of individual connexin isotypes. Suggestions are also made regarding the next steps in a broader sense for basic biology studies, atherosclerosis investigations, and tissue engineered substitute development.

With respect to the transcriptional profiling of endothelial cells using a more physiologic substrate and mechanical environment, analysis presented here barely scratches the surface. The microarray data sets are a significant source of potential insight and areas of new investigation. As new software analysis tools are developed and new literature evolves, substrate and shear stress will be shown to influence multiple areas of endothelial cell function. Of particular interest with respect to atherosclerosis and development of tissue engineered vascular grafts, experiments should be pursued in evaluating changes identified in the reduction-oxidation balance as well as the coagulation balance.

While demonstrating in detail the complexity of response to substrate and shear stress, the case study on endothelial gap junctions also provides numerous opportunities for future work in cell-cell communication. Connexins have traditionally been a major focus of cancer biology but less prominent in other fields. Even within the cardiovascular arena, the primary gap junction focus has been on myocardium and the important roles in electrical conduction. Only recently have cardiovascular gap junctions

been emphasized and momentum focused on communication in the vascular wall. While data presented here establish an endothelial sensitivity to substrate and mechanical environment, the next step is to pursue the specific components inducing these changes.

Formation of myoendothelial gap junctions and the communication of information in a third dimension of the vessel wall deserve primary focus. Determining the potential influence of smooth muscle cell presence on endothelial gap junctions could have significant impact on understanding clinical diseases such as atherosclerosis and restenosis where connections are lost between the two cell types. Furthermore, investigating of the flow of information between endothelial and smooth muscle cells and how this connection could alter endothelial-endothelial or smooth muscle-smooth muscle communication pathways could be critical to the understanding of vascular tone and hypertension. In addition to influence of smooth muscle cells, the question arises if gap junctions are sensitive to composition and structure of extracellular matrix. If so, do alterations in matrix structure and gap junctions play a role in atherosclerotic plaque development or angiogenesis? Is there a connection between integrin signaling and the connexin family which controls the cell-cell communication in different matrix environments?

Interaction amongst environmental components has been demonstrated at multiple points in this dissertation. Thus an investigation of smooth muscle cell or extracellular matrix influence on endothelial cells would not be complete without the concurrent presence of shear stress. In this context, experiments could be conducted to determine if mechanical environment alters communication from endothelial cells to smooth muscle cells and vice versa. With additional information regarding the components inducing

change in endothelial cell gap junctions, experiments should be conducted to determine the mechanisms of influence. Advanced techniques should be employed to investigate impact on levels of transcription, efficiency of translation, mRNA stability and protein stability, which have all been previously shown as points of regulation for gap junctions.

As this dissertation is the first study to systematically investigate all three endothelial connexin isotypes and in doing so, establish a pattern of interacting expression and individual roles in cell function, it is truly the beginning of an area of work rather than an ending. Experiments conducted using the knockdown approach in native cells are an excellent complement to other studies using transfected model cell lines and knockout animal models. Initial studies should focus on a multiple knockdown strategy to isolate roles of individual connexins and further detail the pattern of effects on non-ablated connexins. An in depth characterization of isotype properties using single and multiple knockdowns will provide fundamental information about endothelial connexins which is currently unknown. Evaluation of gap junction chemical permeability, electrical conductance and gating in channels composed of each connexin will determine a communication profile for each isotype. Furthermore, potential gap junction independent functions of hemichannels or connexin proteins can be evaluated. Use of advanced techniques can also be used to determine how the isotypes may interact and thus explain the effects on non-ablated connexins. Information on regulation would also provide additional data on conductivity and stability of heterotypic and heteromeric channels.

Specific to endothelial cell functions, additional experiments should be conducted to investigate the role of Cx40 in morphology and the role of Cx43 in gap junction

communication. A starting point for Cx40 morphology studies would be interactions with cytoskeletal proteins and how these interactions are different from relationships between the cytoskeleton and the Cx37 and Cx43 isotypes. While experiments indicate that Cx43 is the major player in endothelial gap junction communication, multiple questions remain. Where, how and when do Cx37 and Cx40 contribute to endothelial gap junction communication? Furthermore, is the mechanism behind shear-induced changes in gap junction communication due to modulation of Cx43 gating, channel number, or open/close probability?

Broader recommendations drawn from the overall dissertation conclusions can be applied to the scientific and clinical motivations behind this work. In the field of vascular biology, endothelial-smooth muscle and endothelial-extracellular matrix interactions are ripe for exploration. While work is ongoing in some of these areas, there is greater applicability of these interactions. Understanding of human vascular disease, vessel development and vessel stabilization would all benefit from experiments into these interactions. Moreover, a combined smooth muscle-extracellular matrix environment could provide key insight not possible when only one stimulus is present.

Towards understanding and treating atherosclerosis, creation of human tissue *in vitro* provides unique opportunities to study normal and diseased vessels. Comparison of healthy and diseased human engineered tissues provides a novel test bed for drug and device development. For example, how does a pharmacologic agent delivered via drug eluting stent behave when tested on a human vessel substitute rather than on a single cell type of in an animal model? In the development of next generation tissue engineered vascular grafts, data presented here provide insight into important characteristics needed

such as control of proliferation for endothelialization and control of blood coagulation. Understanding of gap junctions in the tissue engineered blood vessel environment aids in the progression towards vasoactive grafts. Finally, experimental iterations using tissue engineered blood vessels *in vitro* and evaluation of cellular response will demonstrate modifications needed to achieve successful clinical application.

Through large scale endothelial transcriptional profiling and a case study focused on cell-cell communication, this dissertation generates novel insight into vascular biology through the use of a tissue engineering model *in vitro*. By combining the efforts to understand and treat the clinical crisis of cardiovascular disease, we demonstrate that much remains to be learned regarding endothelial cell function and vascular tissue engineering. The challenges which remain can be addresses through novel strategies such as using tissue engineered substitutes for studies of basic human biology thus significant scientific and clinical advancements are within our reach.

APPENDIX A: Selected Protocols

Protocol Reference List

TLJ-P01: Culture Medium for Human Aortic Endothelial Cells (HAEC)

Reagents:

MCDB 131	Mediatech Cellgro, Cat No. 15-100-CV
L-Glutamine	Mediatech Cellgro, Cat No 25-005-C1
HyQ Penicillin-Streptomyocin	Mediatech Cellgro, Cat No SV30010
Hydrocortizone	Sigma, Cat No H-4001
hFGF-basic	PeproTech, Cat No 100-18B
hEGF	Gibco, Cat No 13247-051
IGF-1	Gibco, Cat No 13245-063
VEGF	Sigma, Cat No V-7259
Ascorbic Acid	Sigma, Cat No A-4034
Fetal Bovine Serum (FBS)	

Procedure:

1. Place the following reagents in the warm water bath until they have completely warmed:
    1) 2 x 500 mL MCDB-131
    2) 50 mL FBS
    3) 10 mL Pen-Strep
    4) 10 mL L-Glutamine
    5) 1 mg hydrocortizone aliquoted in 1 mL ethanol
    6) 2 µg FGF aliquoted in 1 mL tissue culture water
    7) 10 µg EGF aliquoted in 1 mL tissue culture water
    8) 2 µg IGF-1 aliquoted in 1 mL tissue culture water
    9) 1 µg VEGF aliquoted in 1 mL tissue culture water
    10) 50mg Ascorbic Acid aliquoted in 1 mL tissue culture water

2. Using a 1 Liter glass bottle and filter top, add all reagents and filter using vacuum suction
3. Label bottle with cell type, initials and date
4. Place bottle in cold room for storage or tissue culture fridge for immediate use

TLJ-P02: Culture Medium for Human Aortic Smooth Muscle Cells (HASMC)

Reagents:

MCDB 131	Mediatech Cellgro, Cat No. 15-100-CV
L-Glutamine	Mediatech Cellgro, Cat No 25-005-C1
HyQ Penicillin-Streptomyocin	Mediatech Cellgro, Cat No SV30010
Insulin	Gibco Cat No 12585-014
hFGF-basic	PeproTech, Cat No 100-18B
hEGF	Gibco, Cat No 13247-051
Fetal Bovine Serum (FBS)	

Procedure:

1. Place the following reagents in the warm water bath until they have completely warmed:
    1) 2 x 500 mL MCDB-131
    2) 50 mL FBS
    3) 10 mL Pen-Strep
    4) 10 mL L-Glutamine
    5) 5 mg insulin aliquoted in 1 mL tissue culture water
    6) 2 µg FGF aliquoted in 1 mL tissue culture water
    7) 0.5 µg EGF aliquoted in 1 mL tissue culture water

2. Using a 1 Liter glass bottle and filter top, add all reagents and filter using vacuum suction
3. Label bottle with cell type, initials and date
4. Place bottle in cold room for storage or tissue culture fridge for immediate use

TLJ-P03: Medium for HAEC/HASMC Co-Culture and Flow Experiments

Reagents:

MCDB 131	Mediatech Cellgro, Cat No. 15-100-CV
L-Glutamine	Mediatech Cellgro, Cat No 25-005-C1
HyQ Penicillin-Streptomyocin	Mediatech Cellgro, Cat No SV30010
hFGF-basic	PeproTech, Cat No 100-18B
hEGF	Gibco, Cat No 13247-051
Fetal Bovine Serum (FBS)	

Procedure:

1. Place the following reagents in the warm water bath until they have completely warmed:
    1) 2 x 500 mL MCDB-131
    2) 50 mL FBS
    3) 10 mL Pen-Strep
    4) 10 mL L-Glutamine
    5) 2 µg FGF aliquoted in 1 mL tissue culture water
    6) 0.5 µg EGF aliquoted in 1 mL tissue culture water

2. Using a 1 Liter glass bottle and filter top, add all reagents and filter using vacuum suction
3. Label bottle with cell type, initials and date
4. Place bottle in cold room for storage or tissue culture fridge for immediate use

TLJ-P04: Seeding HAEC on Adsorbed Collagen Slide

Reagents:

Trypsin
Sterile PBS (-Mg, -Ca)
Co-culture medium (TLJ-P03)

Solutions:

50 μg/mL Collagen type I Solution

Using Rat tail type I collagen (BD Biosciences), calculate for 50 μg/mL and dilute accordingly with sterile tissue culture water

Procedure:

Coating Slides with Collagen

1. Autoclave glass slide and tweezers.
2. Place slide into square dish with tweezers.
3. Add 1mL of collagen solution and spread evenly with cell scraper.
4. Incubate for 1 hour to allow passive adsorption of protein.

Adding Cells to Slide

1. Remove flasks with endothelial cells from incubator and place in cell culture hood. Aspirate spent medium, rinse culture surface with PBS and aspirate, add trypsin to detach cells, neutralize trypsin with media and collect cell suspension.
2. Centrifuge at 1000 rpm for 5 min and aspirate supernatant. Resuspend in fresh culture media and count using Coulter Counter.
3. Cells will be seeded at a density of 40,000/cm^2 with each slide having dimensions of 3.8 x 7.5 cm for a total area of 28.5 cm^2
4. Centrifuge appropriate number of cells for number of slides at 1000 rpm for 5 min and remove supernatant. Resuspend in media so that 1 mL of cell suspension will be added to each slide.
5. Add 1 mL of cell suspension to surface of slides and spread gently using cell scraper if necessary.
6. Add approximately 30 ml of co-culture medium, cover dish and place in incubator for 48 hours.

TLJ-P05: Embedding Tubular Constructs and Seeding HAEC on TEWM

Reagents:
3.5% Agar
3.5g Agar (Sigma A-9915) in 100ml DI water
Co-culture Medium (TLJ-P03)
Trypsin
PBS -Mg -Ca

Instruments:
Instrument tray:
Mandrel grabbers
Section lifter (spatula)
Smooth angled forceps
Serrated angled forceps
Flat tweezers
Angled scissors
Scalpel with No.20 blade

New glass slides
Used glass slides
Embedding molds

Procedure:
Preparation of Materials and Instruments

1. Make up 3.5% agar solution in a 100ml glass bottle.
2. Prepare tray of instruments on paper towel. Autoclave new glass slides, used glass slides, molds and tray of instruments in advance.
3. Right before embedding procedure, autoclave agar to melt and place immediately in hot water bath at 48°C to keep liquid.

Preparation of Constructs

Steps can be done to all constructs at once.

1. Place one autoclaved new glass slide in each square cell culture dish and set aside.
2. Remove dish of constructs from incubator and place in sterile cell culture hood. Remove rubber stopper from mandrel end and slide constructs on sleeves off the mandrel. Remove mandrels and rubber stoppers from dish.
3. Holding silicone sleeve with angled forceps, slowly cut sleeve and construct along the long axis with angled scissors. Then grab silicone sleeves at each end with forceps, stretch and free from construct.

Embedding Procedure

Steps should be done to only two constructs at a time to prevent drying and cell death.

1. Using smooth angled forceps, grab one corner of the construct and slide onto spatula with the lumen down. Transfer construct onto new glass slide in square dish keeping the lumen down.
2. Using scalpel, cut away ragged ends of construct and remove excess material. Center the construct on the glass slide with forceps.

3. Aspirate excess fluid off the slide being careful not to aspirate the construct but remove all fluid from around it to ensure a good agar seal.
4. Place mold over slide with hole over construct. Quickly remove agar from hot water bath and add 7 mL over construct. Quickly place used glass slide over agar and press hard with mandrel grabbers and flat tweezers until the agar solidifies to ensure a good seal.
5. After the agar has cooled, remove excess from the sides of the mold and discard. Add 30 mL of flow media to the dish. Using flat tweezers, flip the slide/mold/slide combination over and carefully slide off the top slide to expose the lumen.
6. Place the dishes of embedded construct into the incubator at 37°C and 5% CO_2.

Growing and Seeding HAEC

1. Remove flasks with endothelial cells from incubator and place in cell culture hood. Aspirate spent medium, rinse culture surface with PBS and aspirate, add trypsin to detach cells, neutralize trypsin with media and collect cell suspension.
2. Centrifuge at 1000 rpm for 5 min and aspirate supernatant. Resuspend in fresh culture media and count using Coulter Counter.
3. Cells will be seeded at a density of 40,000/cm^2 with each mold having dimensions of 3.8 x 7.5 cm for a total area of 28.5 cm^2
4. Centrifuge appropriate number of cells for number of slides at 1000 rpm for 5 min and remove supernatant. Resuspend in media so that 200ul of cell suspension will be added to each construct.
5. Allow cells to attach for 10 min in the hood, then transfer to the incubator for 20 min. Remove from incubator and add 30 mL of warm co-culture media

TLJ-P06: Separation of Endothelial Cells from Smooth Muscle Cells

Reagents:

PBS –Mg –Ca	Mediatech 21-031-CV
PECAM-1 antibody (PE or FITC conjugate) Microbeads	
Anti-FITC:	Miltenyi Biotech 120-000-293
Anti-PE:	Miltenyi Biotech 120-000-294
600 U/ml collagenase	
MCDB 131 base	Mediatech 15-100-CV
Collagenase	Worthington #4176
Co-culture medium (TLJ-P03)	
MACS Buffer (0.5% BSA, 1mM EDTA in PBS)	
PBS –Mg –Ca	Mediatech 21-031-CV
0.5 M EDTA	Gibco 15575-020
Bovine Albumin	Sigma A-1470

Procedure:

Removal of EC from SMC-seeded collagen gels

1) Cut away excess agar and place in 30mm dish then rinse construct in PBS
2) Add 3 mL of 600 U/ml collagenase to surface
3) Wait 4 min and scrape once
4) Add 2 mL media to neutralize and remove
5) Rinse with 4 mL PBS and remove
6) Centrifuge at 1000rpm for 5 min and remove supernatant

Removal of EC from EC/SMC Contact Monolayer Co-culture

1) Rinse slides in PBS then add 1ml of 600 U/ml collagenase to surface
2) Wait for cells to lift off and neutralize with 3ml media
3) Collect cell suspension in centrifuge tube, rinse slide with PBS and remove
4) Centrifuge at 1000rpm for 5 min and remove supernatant

Labeling with Antibody and Microbead

1) Resuspend in PBS and transfer to 15 mL centrifuge tube if necessary
2) Centrifuge at 1000rpm for 5 min and remove supernatant
3) Add 10µL CD31 antibody (PE or FITC conjugate) and vortex to mix solution
4) Place in fridge for 5 min
5) Add 10 mL PBS, centrifuge at 1000rpm for 5min and remove supernatant
6) Add 90 µL MACS buffer and resuspend cells
7) Add 20 µL Anti-FITC or Anti-PE microbeads, vortex and incubate for 15 min in fridge
8) Add 5 mL MACS buffer, centrifuge at 1000rpm for 5 min and remove supernatant
9) Resuspend cells in 500 µL MACS buffer

Magnetic Separation

1) Attach miniMACS separation unit to stand and place MS separation column in the unit
2) Place a collection tube under the column and apply 500µL of MACS buffer to the top of the column and let the buffer run through
3) Discard effluent and change collection tube
4) Pipet labeled cell suspension onto column and allow to run through
5) Collect effluent as negative fraction
6) Wash column 3 x 500 µL and collect total effluent as negative fraction
7) Remove column from separator and place column on a new collection tube
8) Apply 1 mL buffer to the reservoir of the column and firmly flush out cells using the plunger supplied

NOTES:
Use collagenase rather than trypsin to preserve EC surface markers for antibody labeling

TLJ-P07: RNA Interference of Endothelial Connexins on Slides

Reagents:

OptiMEM medium	Invitrogen 31985-070
Oligofectamine reagent	Invitrogen 12252-011
Cy3 labeled negative control #1 siRNA (5nmole)	Ambion 4621
Pre-designed siRNA, Cx37 siRNA, ID=7185 (5nmole)	Ambion 16708
Pre-designed siRNA, Cx40 siRNA, ID=145161 (5nmole)	Ambion 16708
Pre-designed siRNA, Cx43 siRNA, ID=144485 (5nmole)	Ambion 16708

Experimental medium (TLJ-P03)
FBS
Sterile, RNase-free microcentrifuge tubes
Sterile, RNase-free micropipette tips

Procedure:

Seeding Endothelial Cells on Slides

1. Adhere silicone gaskets to perimeter of glass slides to create well for culture and transfection (reduces slide area from 28 cm^2 to 25cm^2)
2. Autoclave slides then coat with 50 ug/ml collagen type I for 1 hour
3. Trypsinize and pellet endothelial cells from flask
4. Remove collagen solution from surface of slide and seed endothelial cells at 40,000/cm^2 in 2ml of HAEC culture media
5. Allow cells to adhere for 1 hour then add 1ml additional culture media to each slide and place in incubator.

Initial Preparation of siRNA stocks

1. siRNA is lyophilized upon arrival and therefore must be re-constituted (use ONLY sterile, nuclease-free water which is supplied with siRNA sequences)
2. Dilute 5nmole of siRNA in 250ul of water for stock concentration of 20uM (when this 20uM is later diluted in cocktail and samples are transfected, final concentration would be 100nM)

Preparation of Transfection Reagents

Note – transfection volumes are scaleable based on surface area being treated
For slide surface of 25cm^2: 2mL OptiMEM + 500ul cocktail + 750ul flow media with 22% FBS

Cocktail = tube #1 + tube #2

Tube #1 = 12.5ul siRNA + 450ul OptiMEM

Tube #2 = 10ul oligofectamine + 27.5ul OptiMEM

siRNA treatments: OptiMEM control, NC#1 siRNA 40nM, Cx37 40nM, Cx40 40nM, Cx43 40nM

For 20 slides total (10 static, 10 shear) → 4 slides per siRNA treatment

1. Prepare 13 sterile, RNase-free microcentrifuge tubes (4 for siRNA concentrate, 8 for tube #1 (2 each siRNA treatment due to volume) and 1 for tube #2)
2. Dilute siRNA from stock concentration so final concentration will be 40nM (4 tubes – NC, 37, 40, 43)
   22ul stock siRNA + 33ul water → 55ul siRNA (will only need 50ul)
3. Prepare one tube #2 for all samples – multiply tube#2 ratios listed above by number of slides plus adjustment for slight pipetting error (oligofectamine can be slightly viscous)
   20 slides total (4 are OptiMEM control) therefore 16 slides to be transfected

   tube #2 (x16.2) = 162ul oligofectamine + 445.5ul OptiMEM
   → Allow tube #2 to sit at room temperature for 5-10minutes
4. Prepare tube #1 for each siRNA transfection (2 tubes per condition due to volume)
   Each tube #1 = 25ul siRNA (from diluted samples) + 900ul OptiMEM
5. Add 75ul from tube #2 to each tube #1 and incubate at room temperature for 15-20min to allow siRNA to complex (no more than 30minutes)

<u>Transfection of Endothelial Cells on Slides</u>

1. Remove slides from incubator and aspirate to remove culture media
2. Add 2ml of OptiMEM per slide and remove as wash #1
3. Add 2ml of OptiMEM per slide and remove as wash #2
4. Add 2ml of OptiMEM to each slide
5. In a dropwise manner, add 500ul of cocktail (tube #1 + tube#2 mixture) to each slide; to OptiMEM control slides, add 500ul OptiMEM
6. Carefully return slides to incubator and allow transfection to proceed for 6 hours
7. After 6 hours, add 750ul of flow media with 22% FBS to restore total FBS concentration to normal culture levels (5%). Do not remove OptiMEM/oligofectamine/siRNA mixture – merely supplement – and return to incubator.

NOTES:

1. To adjust final siRNA concentration, create more dilute siRNA prior to creation of tube#1. Do not adjust ratios of siRNA/oligofectamine or siRNA/OptiMEM.
2. When transfecting other surface areas, adjust volumes of all reagents while maintaining ratios.
3. Always use sterile, RNase-free reagents – water, microcentrifuge tubes, micropipette tips to ensure quality of experiment

TLJ-P08: Cell Lysis & RNA Isolation

Reagents & Supplies:

RNeasy Mini Isolation kit	Qiagen 74104
Qiashredders	Qiagen 79654
RNase-free DNase kit	Qiagen 79254
RNase/DNase Free Water	Sigma W-4502
Ethanol – molecular biology	Sigma E702-3
RNase/DNase free B-mercaptoethanol	Sigma M3148
RNase/DNase free tubes	
Agilent UV-Vis Quartz Cuvette (50µL)	

Solutions:

DNase stock

Mix lyophilized DNase powder with water in kit to get DNase stock solution, then aliquot 100 µL and store at -20C

Lysis Buffer

Mix RLT buffer (10mL) with 100 µL B-ME; protect from light and store at room temp for up to a month (can scale down ie. 5ml RLT + 50µL B-ME)

70% Ethanol

Mix 200 proof ethanol for molecular biology with RNase/DNase Free Water and store solution at RT

DNase mix

Add 10 µL DNase stock to 70 µL RDD (in Qiagen kit) so there is 80 µL mix per sample. Prepare enough solution for 1 extra sample so there is plenty of DNase mix.

Procedure:

Prepare Cells

1. Aspirate media, rinse with PBS and add trypsin.
2. Quench trypsin with media and place cell/media/trypsin suspension into centrifuge tube; rinse flask with PBS and place in centrifuge tube.
3. Spin 5-10 min at 1000 rpm and 4C.
4. Completely aspirate supernatant and place tubes with cell pellet on ice.

Prepare Cell Lysate

1. Add 350 µL of lysis buffer to the tube and mix well; transfer mixture to qiashredder homogenizer column and spin in centrifuge at max for 2 minutes. (Alternative to qiashredder: Leave lysate mixture in tube and put 20-gauge needle on 3 mL syringe and place in tube. Pass the lysate 5-10 times through the needle)
2. FREEZE at -70C at this point if desired

Isolate RNA

If using frozen samples, allow to warm at 37C for 10 min before adding ethanol

1. Add 350 µL of 70% ethanol and mix well by pipetting
2. Transfer 700 µL of the sample to the RNeasy mini column placed in a 2mL collection tube. Centrifuge at 10,000 rpm for 30 sec.
3. Suck up supernatant with micropipette and add to top of column. Centrifuge at 10,000 rpm for 30 sec then discard effluent. (If solution remains above column, spin briefly to force through column)
4. Add 350 µL of RW1 solution to the RNeasy column. Centrifuge at 10,000 rpm for 30 sec and discard the effluent.
5. Add 80 µL DNase mix to the column and incubate at room temp for 15 minutes
6. Add 350 µL of RW1 solution to the RNeasy column. Centrifuge at 10,000 rpm for 30 sec and discard the effluent.
7. Discard the old collection tube and replace with a new collection tube. Add 500 µL of RPE Buffer; centrifuge at 10,000 rpm for 30 sec and discard the effluent
8. Add 500 µL RPE Buffer and centrifuge at MAX speed for 2 minutes. If any solution remains above the column, spin again for 30-60 seconds to force through column and then discard the effluent.
9. Label 1.5 mL collection tubes (in kit) and aliquot some RNase free water into a medium eppendorf tube
10. Transfer the RNeasy column to the new collection tube; Add 25 µL (or desired volume) of RNase free water and incubate for 1 minute. Centrifuge at MAX speed for 1 minute and discard the RNeasy column. Place collection tube with RNA on ice.

Spec Samples to Determine Concentration and Purity

1. Prepare small tubes (label for each sample)
2. Aliquot 58ul water into each tube
3. Put 2ul of sample (after mixing well) into corresponding tube
4. Read at 260nm and 280nm

Determine sample concentration:
(avg spec reading at 260nm)*(dilution factor)*(RNA quantification value) = sample conc (ug/ml)
sample conc (ug/ml)*(volume of sample remaining) = quantity of sample

Determine sample purity:
(Spec reading at 260nm/Spec reading at 280nm) should be 1.8-2.1 for pure RNA

Samples are also now ready for Bioanalyzer analysis.

TLJ-P09: RNA Concentration by Precipitation

Adapted from Ambion Technical Service

Reagents:

Ethanol – molecular biology grade	Sigma Aldrich E702-3
Sodium acetate – molecular biology grade	Sigma S-2889
Glycogen solution (20mg/ml) – molecular biology grade	Fermentas R0561
RNase/DNase Free Water	Sigma W-4502

Solutions:

100% Ethanol

70% Ethanol (ice cold)

Ethanol + RNase/DNase Free Water

3M sodium acetate solution, pH = 5.2

Sodium Acetate + RNase/DNase Free Water

5mg/ml glycogen solution

Glycogen (20mg/ml) + RNase/DNase Free Water

Procedure:

1. Add 1/10 volume of 3 M sodium acetate solution and 2.5 volumes 100% ethanol to RNA in solution
   (For 23.7 µl RNA solution; add 2.4 µl NaOAc and 59.25 µl ethanol)
   (For 21.7 µl RNA solution; add 2.2 µl NaOAc and 54.25 µl ethanol)
2. Add 0.5 – 1.0 µl of 5 mg/mL glycogen and mix well
3. Chill at -20°C for at least an hour (or overnight)
4. Centrifuge at 12,000 rpm for 10 minutes
5. Remove the supernatant and wash with ice cold 70% ethanol
6. Pulse vortex and spin again for 5 min
7. Remove all supernatant then resuspend in desired quantity of water

Notes:

Glycogen serves as a carrier for low quantities of RNA

Used when procedures require concentrated RNA from solutions of dilute RNA

TLJ-P10: cDNA Synthesis for RT-PCR

Reagents:

SuperScript III First-Strand Synthesis System for RT-PCR	Invitrogen 18080-051
RNase/DNase Free Water	Sigma W-4502
RNase/DNase free tubes	
RNA samples – concentrations known	

Procedure:

Carefully follow ALL steps as detailed in the SuperScript III procedure outline – details listed here are meant as a supplement only.

Controls: Several controls are used in RT-PCR reactions. At this step, be sure to create –RT controls. These are samples which contain sample RNA and all reagents for cDNA synthesis EXCEPT the reverse transcriptase enzyme (therefore no cDNA will be created and these samples will be a control to check for genomic DNA during the PCR amplification steps)

Preparing RNA Samples

1. Determine concentration and quality of RNA samples using spec and bioanalyzer prior to cDNA synthesis. You will need 1µg of RNA in NO MORE than 8µL of water for each tube (cDNA tube as well as –RT tube). If your RNA is more dilute than this, concentrate by precipitation (see protocol)
2. Based on spec readings and concentration calculations, determine volume of RNA for each sample which gives 1µg.
3. Using spreadsheet, calculate appropriate volumes of RNA and water for each sample for a total volume of 10µL. The components for the first step are in the following proportions:

Component	Amount
RNA (1µg)	*n* µL
Primer (50µM oligo dT)	1 µL
10mM dNTP mix	1 µL
RNase/DNase free water	10-(2+*n*) µL

cDNA Synthesis

Remember to use new tips when moving between reagents and between tubes!
Before preparing samples, turn on thermal cycler and load program to heat to 65°C.

Denaturation step:

1. Mix and briefly centrifuge RNA samples, oligodT, and dNTP mix
2. Label RNase/DNase free tubes for cDNA synthesis (remember –RT controls)

3. Add correct volume of RNA to each tube, then add correct volume of water to each tube (total at this point should be 8µL)
4. Add 1µL oligodT to each tube
5. Add 1µL dNTP mix to each tube
6. Vortex briefly and centrifuge to collect total volume
7. Place in thermal cycler for 5 minutes at 65°C then place on ice for at least 1 minute.

Annealing and cDNA synthesis step:

1. Mix and briefly centrifuge 10X RT buffer, 25mM $MgCl_2$, 0.1M DTT, RNase out and Superscript III RT.
2. Change program on thermal cycler to 50°C if using oligodT.
3. Prepare enough cDNA mix for all tubes + 0.15 extra for pipetting error
4. Create one tube for cDNA synthesis reactions and one tube for –RT reactions.
5. Always mix reagents together into one tube in the following order:

Component	**1 cDNA rxn**	**10 cDNA rxns**	**1 –RT rxn**	**10 –RT rxns**
10X RT buffer	2 µL	20.3 µL	2 µL	20.3 µL
25mM $MgCl_2$	4 µL	40.6 µL	4 µL	40.6 µL
0.1 M DTT	2 µL	20.3 µL	2 µL	20.3 µL
RNase Out	1 µL	10.15 µL	1 µL	10.15 µL
SuperScript III RT	1 µL	10.15 µL	0	0
Rnase free water	0	0	1 µL	10.15 µL

6. Vortex and centrifuge to collect total volume of mixture
7. Add 10ul of cDNA mix or –RT mix to each tube, then mix gently and centrifuge briefly to collect
8. If oligo dT was used, incubate at 50°C for 50 minutes.

Terminate Reaction and Remove RNA:

1. Terminate the reactions at 85°C for 5 minutes and then chill on ice.
2. Collect reactions by brief centrifugation and then add 1ul of RNase H to each tube.
3. Incubate at 37°C for 20 minutes.
4. Store cDNA samples at -20°C or use in PCR immediately

TLJ-P11: Preparation and Examination of an Agarose Gel

Reagents:

Hi-Lo DNA Marker	Minnesota Molecular – store at 4°C
Bromophenol Blue (for 300bp samples)	Sigma B-8026
Xylene Cyanol FF (for 4kb samples)	USB 23513
Ethidium Bromide	IBI/Shelton Scientific IB40075
Trizma Base	Sigma T-1503
Glacial Acetic Acid	JT Baker 9508-05
0.5 M EDTA	Gibco 15575-020
Agarose (molecular biology grade)	Fisher BP1356-100
EZNA Gel Extraction kit	Omega Biotek D2501-01

Erlenmyer flask (large – for bubbling solutions but small enough to fit in microwave)

Solutions:

50X TAE (Tris-Acetate-EDTA Buffer)

242g Tris (Trizma) Base
57.1 ml glacial acetic acid
100ml 0.5M EDTA (ph 8.0)
bring up to 1000ml with dH_2O

1X TAE

60ml of 50X TAE
2940 ml dH_2O

6X Loading Dye

0.25% bromophenol blue (for 300bp) – use 0.25% xylene cyanol FF for 4kb
30% glycerol in water

for 1ml: add 300ul glycerol
2.5 mg bromophenol blue
bring up to 1ml with water
store at 4°C

EtBr Staining Solution

25 ul 1% EtBr solution
250 ml TAE
→ enough for small gels, make more for larger gels
Use tip box for soaking small gels, tupperware for larger gels
CAUTION with EtBr – it is carcinogenic (can reuse solutions – protect from light)

Procedure:

Setup Gel Casting System

1. Choose appropriate comb for samples and tighten tray in gel casting system to avoid leaks
2. Balance feet of casting system and check for balance with balance bubble
3. Note comb is offset – put teeth inward

Make Agarose Solution

1. For small gel, need 50ml; for large gel, need 125ml agarose solution
2. Size of DNA fragment will dictate concentration of agarose gel
   Rule of thumb: 1% agarose gel = 125ml TAE + 1.25g agarose or 50ml TAE + 0.5g agarose
3. For amplicons 60-80bp in length, make 2% agarose gel (125ml TAE + 2.5g agarose). Shake TAE to mix, then add to flask and add agarose powder. Swirl to mix
4. Microwave flask – start with 2 minutes (HEAT but DON'T BOIL)
5. Watch in microwave – wearing orange autoclave gloves - remove every 15-20sec and swirl. Look for refractive crystals indicating that agarose is not totally dissolved. Total microwaving time ~ 3min.

Casting Agarose Gel

1. When agarose solution is completely dissolved, pour slowly into casting tray – avoid bubbles!
2. Let gel cool (takes 30-45 min) but do not let dry out. Once solidified, gel will have a bluish tint and you can add some 1X TAE to the top to prevent drying
3. When gel is completely solid, carefully remove the comb and mount the gel in the electrophoresis tank. Be sure that the wells are oriented so that the DNA (which is neg) can migrate from the cathode (black) to the anode (red).
4. Add just enough 1X TAE buffer to the tank to cover the gel by about 1mm.

Add Samples to Gel

When dispensing into wells, brace dispensing hand with other hand, have NO bubbles in micropipette tip, dispense slowly - moving hand back and forth in well

1. Add 10ul of Hi-Lo DNA ladder to first lane
2. Rip caps off PCR tubes and add 4ul of 6X loading buffer to each tube
3. Mix each sample thoroughly and slowly add to each well – volume of sample+buffer loaded will depend on the size of the well (number of teeth on comb)

Running Gel

1. Close the lid of the tank and attach the electrical leads.
2. Turn on the power supply and set to 75 volts for 90 minutes. Bubbles should be generated at the anode and cathode and the bromophenol blue should begin migrating towards the anode.
3. When the bromophenol blue has run through about 75% of gel (should take 80-90min), turn off the power supply and remove the lid.

Examining the Gel

When working with EtBr, ALWAYS double glove to avoid contact

1. Soak gel in 1ug/ml EtBr staining solution for 30-45 min.
2. Visualize the gel on a UV box. ALWAYS use protection with the UV box – face shield and goggles. Have razor blade, ruler and timer ready at UV box.

3. Use the ladder to focus your attention to the expected area, *quickly* turn on the UV box and make simple cuts with a razor blade. Note: DNA exposed to UV rays for more than 30seconds will be degraded.
4. Using simple cuts as a guide, cut out your band of interest and remove excess agarose.

Storing the Gel

1. The entire gel can be stored overnight – in saran wrap to prevent drying or a little TAE. Can also cut out area of interest and store at 4°C overnight.

Extracting Amplicons from Gel

1. Turn on hot water bath prior to preparing gel pieces in solutions.
2. Use gel extraction kit exactly according to directions
3. Carefully monitor complete melting of gel pieces
4. Following extraction, spec cDNA samples to determine concentration
5. Dilute to desired concentration for stock solution (30nM), aliquot and store standards.

TLJ-P12: Gel Electrophoresis and Western Blotting

Reagents:

Name	Supplier	Cat. No.
12% Novex Tris-Glycine Gels, 1.0mm, 10 well	Invitrogen	EC6005
10x Tris/Glycine/SDS Buffer	Bio-Rad	161-0732
10x Tris/Glycine Buffer	Bio-Rad	161-0734
SeeBlue Plus2 Pre-stained standard	Invitrogen	LC5925
Magic Mark XP Western Protein Standard	Invitrogen	LC5602
Tris Base (trizma base)	Sigma	T-1503
Tween-20	Sigma	P-5927
Sodium Chloride (NaCl)	Sigma	S-7653
Beta-mercaptoethanol	Sigma	M3148
SDS (sodium dodecyl sulfate)	USB	21651
Bromophenol Blue	Bio-Rad	M3978
Glycerol	Sigma	G8773
Tris HCl	Sigma	T3253
Nonfat dry milk powder	grocery store ☺	
BCA Protein Assay Kit	Pierce Biotechnology	23225
RIPA Buffer	Sigma	R-0278
Proteinase Inhibitor Cocktail	Sigma	P2714
ECL Plus Western Blotting Detection Reagents	Amersham	RPN 2132
Methanol	Sigma	494437
PVDF Membrane	Bio-Rad	162-0177
Filter Paper	Bio-Rad	1704085
Blotting Pads	Bio-Rad	1703914
Film	Phenix Research Products	F-BX57
Deionized water		

Solution Preparation:

Running Buffer

10x Tris/Glycine/SDS Buffer	100ml
Deionized water	900ml

Transfer Buffer

10x Tris/Glycine Buffer	100ml
Methanol	200ml
Deionized water	700ml

5x Sample Buffer

Deionized water	3.0ml
0.5M Tris-HCl, pH=6.8	1.0ml
Glycerol	1.6ml

10% SDS	1.6ml
0.5% Bromophenol blue	0.4ml

→ immediately prior to use: add 0.2ml B-ME per 1ml 5x sample buffer

10x TBS (pH = 7.6)

Tris base	2.42g
NaCl	8.0g
Deionized water	100ml

Use pH paper and adjust pH to 7.6

1x T-TBS

10x TBS	100ml
Tween-20	1ml
Deionized water	900ml

5% Milk

Nonfat dry milk powder	5g
1x T-TBS	100ml

Aliquot milk into 50ml conical tubes and centrifuge at 3000rpm for 10min. Collect supernatant with pipet and discard pellet.

Cell Lysis and Protein Isolation

Lysis Buffer: Add proteinase inhibitor to RIPA Buffer immediately before use
Adherent cells can be lysed in dish or in cell pellet following trypsinization and centrifugation. Lysis as a pellet may allow smaller volumes of lysis buffer to be used. Either way, be sure to wash with PBS to remove all media as serum proteins will reduce yield of cellular proteins.

1) Wash, trypsinize and collect cells in centrifuge tube.
2) Carefully remove ALL supernatant and add lysis buffer to pellet. Repeatedly pipet cell lysate to break apart cellular structures.
3) Collect cell lysate and place in microcentrifuge tube on ice for 5-10min.
4) Centrifuge cell lysate at 12,000g for 10min.
5) Carefully collect supernatant (containing protein) and place in new microfuge tube. Discard pellet containing DNA.
6) Store protein suspension at -20C.

Protein Quantification

Use BCA Protein Assay Kit to measure protein content of samples. Keep protein samples on ice at all times to prevent degradation.

1) Make serial dilutions of the BSA standard provided (2mg/ml) by diluting in PBS: 2 mg/ml, 1 mg/ml, 0.5 mg/ml, 0.25 mg/ml, 0 mg/ml
2) Aliquot 10ul of standards into a 96 well plate

3) Dilute protein samples in PBS (start with 1:2, or if concentrated sample use 1:5) in small microcentrifuge tubes then add 10ul of each (same volume as standards) to 96 well plate
4) Combine Reagent A and Reagent B in a 50:1 ratio (ie. 2ml A + 40ul B) then add 200ul of mixture to each well
5) Incubate plate at 37C for 30min to allow colorimetric reaction to proceed
6) Turn on absorbance spectrophotometer and allow to warm up for 30min
7) Scan plate at 562nm and export readings.
8) Create standard curve in excel and calculate protein concentration of samples.

Gel Electrophoresis

Prepare Samples:

1) Determine layout of samples in gel – including blotting standard, western standard and samples
2) 10-well gels have a maximum capacity of 25ul per well
3) Each lane will have 5x sample buffer, plus sample and water. Load an equal amount of protein in each lane based on protein assay calculations and bring total volume up with water.
4) Turn on hot plate to 95, add B-ME to 5x sample, and place the following items on ice: See Blue Plus 2 standard, Magic Mark Western standard, protein samples
5) Prepare fresh microcentrifuge tubes for each lane and add volume of water, protein and 5xSB
6) Heat tubes on hot plate at 95C for 5min

Prepare Gel:

1) Cut open package of Novex gel (other gel types can be used for other applications) and rinse off excess acrylamide with deionized water.
2) Remove white tape along bottom of gel and in one smooth motion, remove comb from wells.
3) Using micropipette, rinse wells with running buffer 2-3x – remove all bubbles with last rinse.

Assemble Gel and Load Samples:

1) Place the white buffer core in the mini-cell so that the gold electrode is in the notch on the left side.
2) Lower gel into front side of buffer core with the wells facing inside, then load plastic buffer dam (or second gel) into back side of buffer core.
3) Place gel tension wedge behind buffer core and lock into place.
4) Fill area between gel cassette and plastic buffer dam with running buffer to above level of wells and look for leaks into outer chamber. If there are leaks, remove pieces and buffer, readjust and test again until tight.
5) Using gel loading tips, carefully load lanes – be careful to avoid bubble and volcanoes!
6) Fill the outer buffer chamber with running buffer to help dissipate heat generated.
7) Attach lid to mini-cell and plug into power pack (red to red; black to black)

8) Turn on power pack, program to hold voltage constant at 125V and set timer for 90min.

Gel to Membrane – Protein Transfer

Preparing Transfer Pieces:

1) Fold piece of filter paper in half and cut along center line resulting in two identically sized pieces.
2) Pour some transfer buffer into Bio-Rad dishes and soak blotting pads.
3) Remove roll of PVDF membrane from tube – be sure to keep protective plastic on either side of membrane. Cut a piece just slightly smaller that the filter paper and carefully remove plastic pieces – only handle membrane by edges!
4) Pre-wet membrane in methanol for 30sec and dispose of methanol waste properly. Rinse membrane with deionized water and then soak in transfer buffer for a few minutes.

Removing Gel:

1) Turn off power pack, disconnect electrodes and remove lid from mini-cell.
2) Place gel cassette on edge of benchtop with notched (well) side up. Using gel knife, carefully crack open gel cassette on three edges and remove top plate.
3) Remove wells with gel knife and pour some transfer buffer over the gel to keep moist.
4) Wet one piece of filter paper and place over gel with edge just above "foot" of gel. Add more transfer buffer and make sure there are no bubbles (bubble will interfere with transfer).
5) Turn the plate over in your gloved hand and use the gel knife to push foot of gel through slot so you are left with filter paper and gel in your hand.
6) Lay on flat surface and cut off foot of gel with gel knife.
7) Wet surface of gel with transfer buffer, then carefully lay pre-soaked membrane on surface of gel ensuring there are no bubbles.
8) Add a second piece of wet filter paper to create a sandwich and add more transfer buffer.

Transfer Gel:

1) Place two soaked blotting pads in the base of the blot module (no bubbles in pads!).
2) Place sandwich of filter paper, gel, membrane, filter paper on top of blotting pads.
3) Add more blotting pads (2-3) so that they rise 0.5cm above the rim of the blot module base.
4) Place top of blot module over the pads and hold together securely. Slide blot module into mini-cell ensuring that gold electrode fits into slot on right.
5) Put gel tension wedge behind blot module and lock into place.
6) Fill blot module with transfer buffer until gel/membrane sandwich is covered but do not fill to top.
7) Fill the outer buffer chamber with deionized water until the level is 2cm below the blot module edge.
8) Attach lid to mini-cell and plug into power pack (red to red; black to black)

9) Turn on power pack, program to hold voltage constant at 25V and set timer for 2 hours.

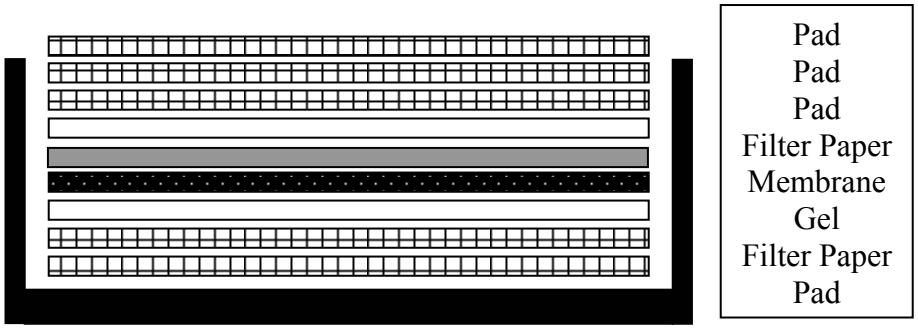

Staining Western Blot

1) Carefully place blot in staining dish and rinse blot briefly in TTBS.
2) Block overnight at 4C in 5% milk to reduce non-specific binding. Cover with saran wrap to prevent evaporation.
3) Dilute primary antibody in milk and add to staining dish. Place on orbital shaker at room temperature for 1 hour.
4) Rinse 3x in TTBS on orbital shaker for 5min each to remove excess primary antibody.
5) Dilute HRP secondary antibody in milk and add to staining dish. Magic Mark Western standard will react to any IgG secondary antibody. Note that actin control has an IgM secondary antibody.
6) Rinse 3x in TTBS on orbital shaker for 5min each to remove excess secondary antibody.

Apply Substrate and Develop Image

1) Sign up for developer on door to dark room – usually need 30min – and turn on machine to warm up.
2) Lay saran wrap on benchtop and carefully place blot onto saran wrap.
3) With lights off, prepare ECL solution: mix 2.5ml A with 62.5ul B and carefully pipet onto membrane. Allow reaction to proceed for 5min.
4) Prepare film cassette by laying down saran wrap in base of cassette.
5) When substrate reaction is complete, use forceps to lift blot and drip off excess substrate solution onto tissue.
6) Lay blot on saran wrap in cassette and cover with a second piece of saran wrap (no wrinkles!)
7) Take the following items to the developer: film cassette, film, scissors, timer

In the dark room…

1) Lift lid on developer and place items on benchtop so you know where they are.

2) Set timer for desired exposure time.
3) With red light on (NO WHITE LIGHT), carefully open the box of film and remove the bag.
4) Take one piece of film (handle with dry gloves) and cut one corner for orientation.
5) Open cassette and lay film with cut edge in upper left corner.
6) Close cassette and start timer.
7) Refold bag of film and place into box with folded side down then put lid on box. NEVER turn on lights with film out – will ruin all pieces.
8) When exposure is complete, open cassette and place film in tray of developer, then close developer lid.
9) Developer will develop, wash, fix and dry film. When film exits developer, turn on white lights.

TLJ-P13: Proliferation by BrdU Incorporation

Reagents:

BrdU (5-bromo-2'-deoxyuridine)	ICN Biomedicals 100171
Anti-BrdU antibody (mouse)	Sigma B2531
Cy3 Donkey Anti-mouse	Jackson ImmunoResearch

Solutions:

4% Formaldehyde in PBS

2N HCL

100ml 37.3% HCl
400ml water

Neutralizing Buffer

50mM NaCl
100mM Tris-HCl
in water and adjust pH to 7.4

BrdU stock solution

10mg/ml BrdU in DMSO

Procedure:

1. Add appropriate amount of BrdU stock solution to samples such that final concentration is 20μg/ml and incubate for 6 hours. For flow experiments with 110ml media, add 220μl of stock solution.
2. Remove slides from flow chamber or static dishes, rinse with PBS and fix in 4% formaldehyde for 10minutes.
3. Rinse with PBS and move to *glass dishes*
4. Permeabilize with ice cold acetone for 10 minutes, then remove and rinse twice in PBS
5. Incubate with 2N HCl for 15 minutes at 37C to denature the DNA
6. Remove and rinse in neutralizing buffer, then rinse twice in PBS to ensure restoration of neutral pH
7. Block in 4% Donkey serum in PBS for 30minutes at room temperature
8. Incubate with Anti-BrdU antibody for 2 hours at 37C
9. Rinse twice in PBS to remove primary antibody
10. Incubate with Cy3 Donkey Anti-Mouse and 20μg/ml Hoechst dye to label all non-proliferating nuclei for 30minutes at room temperature
11. Rinse twice and coverslip prior to imaging

APPENDIX B: Endothelial and Smooth Muscle Cell Co-Culture

Introduction

Work presented in this dissertation to address specific aims one and two compared the adsorbed collagen slide substrate to the tissue engineered blood vessel wall model substrate. The purpose of this comparison was to elucidate differences in endothelial cell behavior when presented with a traditional *in vitro* substrate (Slide) or a more physiologic *in vitro* model (TEWM). Data presented met this goal of demonstrating significant differences in cell function between the two substrates, however further questions also arose. Differences between the Slide and TEWM substrates are primarily in three areas: i) absence or presence of smooth muscle cells, ii) monomer or fibrillar collagen I, iii) two-dimensional or three-dimensional extracellular matrix. Thus the question which emerged from comparisons of the Slide and TEWM was: which difference was responsible for the changes seen in endothelial cell function? The answer is likely to be that each difference contributed uniquely to different areas of cell function and moreover, that the synergistic presence of these components is what shapes the endothelial phenotype. In the interest of pursuing mechanisms behind the differences seen in endothelial cells on the Slide versus TEWM, we decided to focus on the presence or absence of smooth muscle cells as a likely candidate for significant endothelial influence. Furthermore, the central hypothesis of this dissertation also includes investigation of shear stress effects on endothelial cells. Thus we hypothesized that the interactions of endothelial cells and smooth muscle cells would also be modulated by the mechanical environment. Pursuing this hypothesis, several strategies were taken and are outlined in the sections to follow.

Endothelial-Smooth Muscle Cell Direct Contact Co-Culture

The initial strategy taken was to directly co-culture endothelial cells on top of smooth muscle cells. In this way, contact and interactions between the two cell types could be maximized. Additionally, the model would be similar to the TEWM except for the presence of a bulk extracellular matrix and no artificial components would be added.

The direct contact co-culture model was based on combining the attributes of the Slide and TEWM substrates whereby a glass slide was coated with collagen I, then smooth muscle cells were seeded on the surface and cultured for 24 hours, followed by seeding of endothelial cells on top of the smooth muscle cells. A protocol was developed (see below) to achieve both a confluent smooth muscle cell layer and a confluent endothelial cell layer. This cellular bilayer on a glass slide was then inserted into the parallel plate flow chamber for exposure to shear stress. Thus endothelial cell and smooth muscle cell interactions were isolated from effects of extracellular matrix present in the TEWM, and endothelial cells could be concurrently exposed to shear stress and underlying smooth muscle cells. Figure B.1 shows depicts the endothelial-smooth muscle cell direct contact co-culture model both schematically and pictorially. Panel A demonstrates the confluent culture of smooth muscle cells on the glass slide and the confluent layer of endothelial cells on the surface. Panel B is a confocal microscope image taken of the direct contact co-culture model following exposure to shear stress (15 dynes/cm^2) for 24 hours. Prior to seeding onto the smooth muscle cells, endothelial cells were incubated with cell tracker orange to stain the cytoplasm and allow them to be distinguished from smooth muscle cells. The fixed cells were then stained for actin filaments (green) and nuclei (blue). Smooth muscle cell nuclei appear blue and

endothelial cell nuclei appear pink due to the overlay of orange cytoplasm and blue nucleus.

Work with this model continued with a focus on endothelial cell gap junctions and expression of Connexins 37, 40 and 43. Endothelial cells were separated from smooth muscle cells in the direct contact co-culture model using the same magnetic separation procedure which was used in analysis of endothelial cells on the TEWM. Pure endothelial cells were then lysed, RNA isolated, cDNA generated and analyzed using real time RT-PCR to determine connexin mRNA expression. Figure B.2 shows connexin mRNA expression in endothelial cells of the direct contact co-culture model under static and shear stress conditions. Figure B.3 compares the data from endothelial connexin expression in the direct contact co-culture model (from Figure B.2) to the data from chapter five of connexin mRNA expression in the Slide model under static and shear conditions. Statistics have not been conducted on this data because it is preliminary and following collection of the data, problems in the model were identified.

Achieving a confluent endothelial cell monolayer is critical to experimental analysis since endothelial cells exhibit very different behavior when subconfluent compared to confluent. Confluence was especially critical with our interest in gap junctions, which require cell-cell contact, and for comparison to previous data on the Slide and TEWM substrates which had confluent endothelial monolayers. Although the protocol for the direct contact co-culture model was carefully developed to ensure smooth muscle cell and endothelial cell confluence, subconfluent regions in the endothelium were detected as experiments progressed. While confluent initially, it appeared that due to movement or proliferation of underlying smooth muscle cells, gaps in the endothelial

monolayer would develop during the course of experiments. Additionally, another research group who was developing a similar model at the same time also began to encounter similar problems. (213)

Data presented in this section using the endothelial-smooth muscle cell direct contact co-culture model must then be examined with a critical eye since the authors felt a confluent endothelial monolayer was achieved prior to conducting these experiments, yet in retrospect cannot be assured that gaps on the endothelium did not develop. In continuing to pursue the effect of smooth muscle cells and shear stress on endothelial cells, an additional strategy for co-culture was investigated.

EC-SMC Direct Contact Co-Culture Protocol

Reagents:
Trypsin
Sterile PBS (-Mg, -Ca)
Complete HASMC medium
Co-culture medium
50 µg/mL Collagen type I Solution

Procedure:
Coating Slides with Collagen

1. Autoclave glass slide and tweezers.
2. Place slide into square dish with tweezers.
3. Add 1mL of collagen solution and spread evenly with cell scraper.
4. Allow to coat for 1hour at room temperature.

Adding SMC to Slide

1. Remove flasks with smooth muscle cells from incubator and place in cell culture hood. Aspirate spent medium, rinse culture surface with PBS and aspirate, add trypsin to detach cells, neutralize trypsin with media and collect cell suspension.
2. Centrifuge at 1000 rpm for 5 min and aspirate supernatant. Resuspend in fresh culture media and count using Coulter Counter.
3. Cells will be seeded at a density of 20,000/cm^2 with each slide having dimensions of 3.8 x 7.5 cm for a total area of 28.5 cm^2
4. Centrifuge appropriate number of cells for number of slides at 1000 rpm for 5 min and remove supernatant. Resuspend in media so that 1 mL of cell suspension will be added to each slide.
5. Add 1 mL of cell suspension to surface of slides and spread gently using cell scraper if necessary.
6. Cover dish and allow to adhere for 1 hour in hood at room temperature.
7. Add approximately 30 ml of complete HASMC medium, cover dish and place in incubator for 24 hours

Adding EC to SMC Slide

1. Remove flasks with endothelial cells from incubator and place in cell culture hood. Aspirate spent medium, rinse culture surface with PBS and aspirate, add trypsin to detach cells, neutralize trypsin with media and collect cell suspension.
2. Centrifuge at 1000 rpm for 5 min and aspirate supernatant. Resuspend in fresh culture media and count using Coulter Counter.
3. Seeding efficiency of EC on SMC is low thus a high seeding concentration is required to achieve a confluent EC monolayer. Seed EC corresponding to 90,000/cm^2 or a concentration of 3.4M cells/ml.
4. Centrifuge appropriate number of cells for number of slides at 1000 rpm for 5 min and remove supernatant.
5. Remove HASMC media from slide dishes and rinse with one wash of PBS.
6. Using sterile forceps, remove SMC slide from dish and place in fresh (dry) dish.
7. Resuspend EC in co-culture media (750 µl for 28cm^2 slide) and gently drip onto SMC slide.
8. Cover dish and allow to adhere for 1 hour in hood at room temperature.
9. Add approximately 30 ml of coculture medium, cover dish and place in incubator for 48 hours

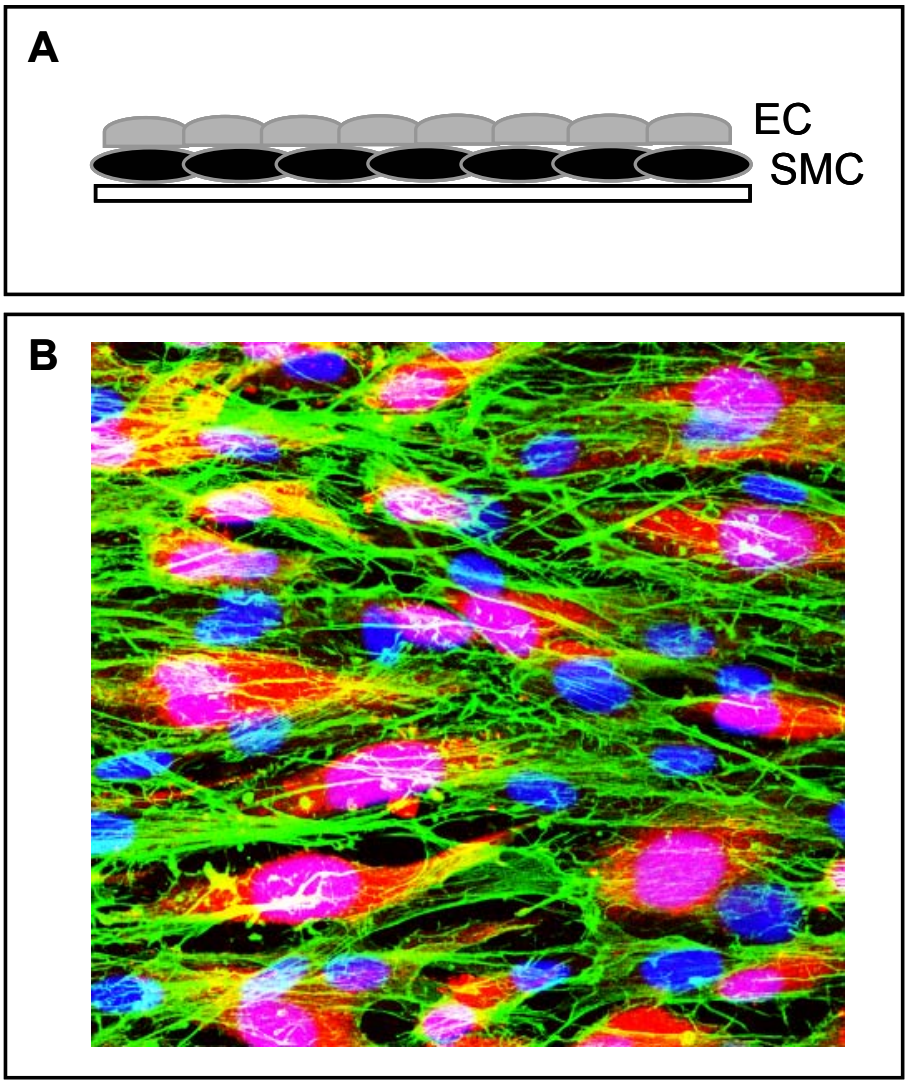

Figure B.1 Endothelial-Smooth Muscle Cell Direct Co-Culture Model
Panel A shows a schematic of the direct co-culture model where smooth muscle cells are seeded at confluence on a collagen type I coated glass slide and endothelial cells are seeded at confluence on their surface. Panel B shows a microscope image of the direct co-culture model following exposure to shear stress for 24 hours. Endothelial cells were prelabeled with cell tracker orange and the co-culture was then stained for actin filaments (green) and nuclei (blue or pink).

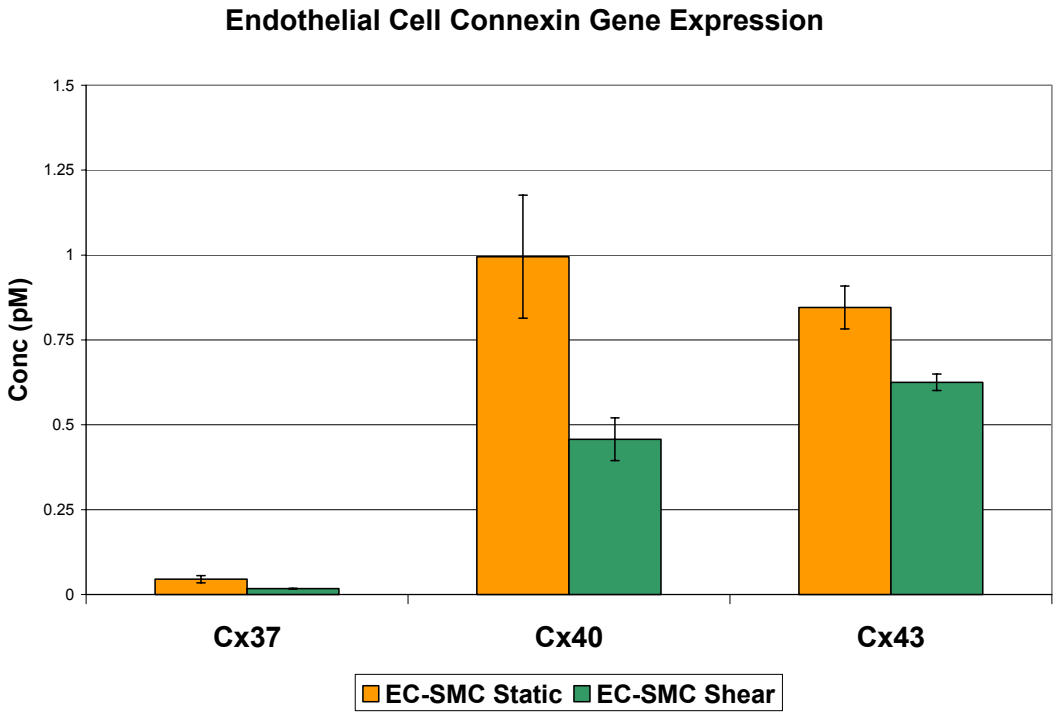

Figure B.2 Connexin mRNA Expression in the EC-SMC Direct Contact Model
Endothelial cells removed from the EC-SMC direct contact co-culture model following exposure to static or shear stress for 24 hours. Cells were analyzed by RT-PCR for connexin mRNA expression.

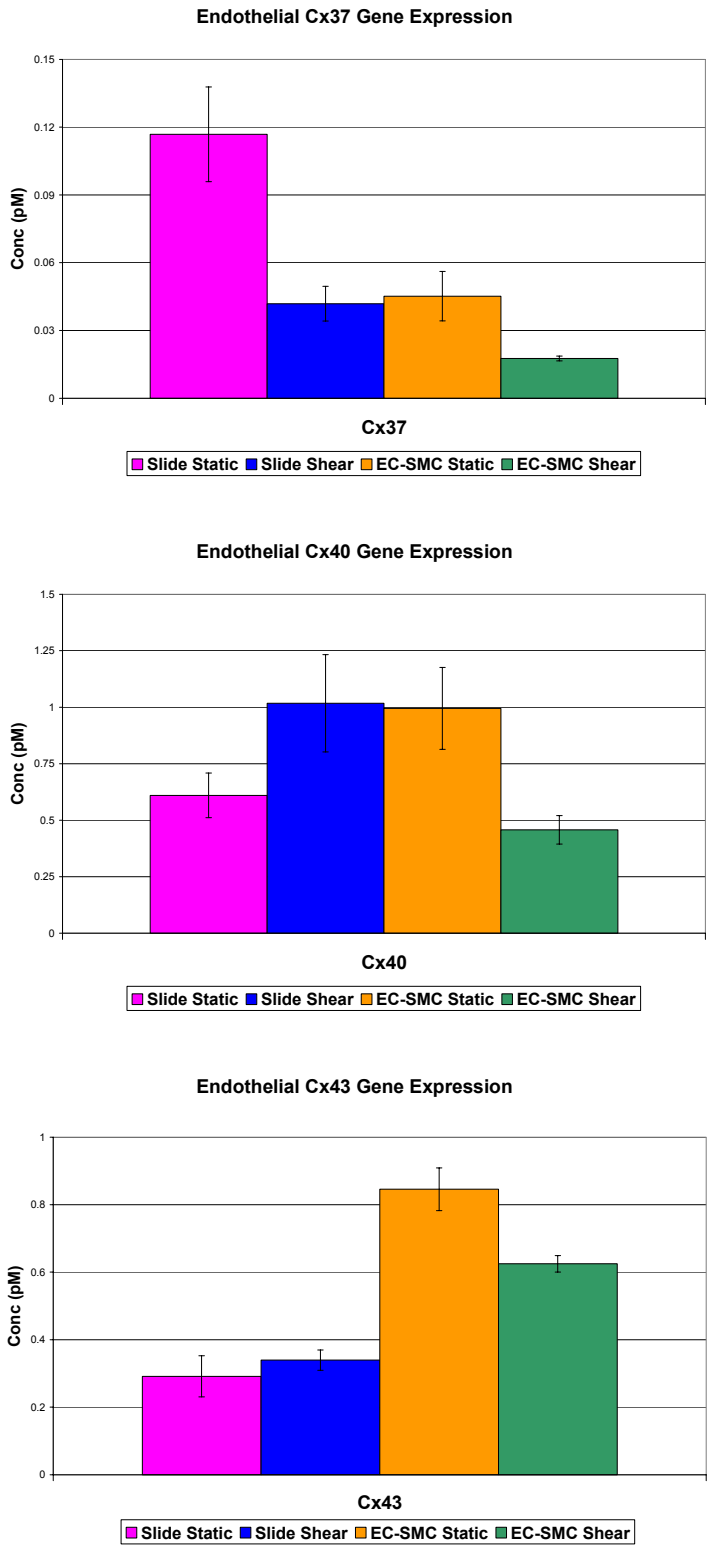

Figure B.3 Comparison of Cx mRNA Expression in Slide and Co-Culture Model
Endothelial cell connexin mRNA expression is compared amongst the slide and direct co-culture models following exposure to static and shear stress.

Endothelial-Smooth Muscle Cell Transwell Co-Culture

The second strategy taken was to develop a co-culture model which had the properties of the direct contact system in that endothelial cells and smooth muscle cells would be in physical contact with each other and additionally, endothelial cells could be exposed to shear stress. However, to address the problems encountered in the direct contact co-culture model, there would need to be an intermediary between the endothelial and smooth muscle cell layers to prevent gaps from developing in the confluent monolayer.

In numerous previous literature reports, a Transwell system is used to co-culture cells of different types and evaluate their effects on each other. This is achieved using a permeable membrane with defined pore size and pore density to separate the two cell types of interest. In a recent study, one group used this system to co-culture endothelial cells and smooth muscle cells and also modified a parallel plate flow chamber to expose only the endothelium to shear stress. (111) In our laboratory, we chose to use Transwell filters for co-culture with a pore size of 0.4μm which would be large enough to allow for heterocellular contact yet too small for cell migration. A protocol was developed (see below) to wet the membranes with culture medium, then seed one side of the membrane with endothelial cells and the other side of the membrane with smooth muscle cells. Figure B.4 depicts the endothelial-smooth muscle cell Transwell co-culture model. Panel A shows the control treatment of endothelial cells only on the membrane and Panel B should the co-culture of endothelial and smooth muscle cells on opposite sides of the membrane. With the endothelial cell monolayer on the outer surface of the cup, the flow

block in the parallel plate flow chamber could be modified to allow for insertion of the Transwell such that endothelial cells would be exposed to shear stress.

Prior to modification of the flow chamber, endothelial cell connexin mRNA expression was evaluated in static Transwells of endothelial cells in monoculture or in co-culture with smooth muscle cells. Due to the presence of the membrane between the endothelial and smooth muscle cells, endothelial cells could be removed for lysis and RNA isolation without the need for a separation process to purify them from the smooth muscle cells. Figure B.5 shows endothelial cell connexin expression in monoculture and co-culture on the Transwells under static condition. While there appears to be an effect of smooth muscle cell presence, the data suggests that it is isotype dependent.

Drawings were developed for modification of the polycarbonate flow block which would allow for insertion of the Transwell filter and exposure of the endothelium to shear stress. However, several questions arose in anticipation of these modifications. These included concerns regarding the ability to maintain a laminar flow profile, the possibility of fluid leak around the Transwell, and the loss of integrity of the flow block if a central hole was created. Due to these concerns and the interest in pursuing the differences between connexin isotypes and response to shear stress, the work on co-culture of endothelial cells and smooth muscle cells was not pursued further.

EC-SMC Transwell Co-Culture Protocol

Reagents & Supplies:
Transwell filters 0.4μm pore size PET membrane (BD 353090)
Transwell 6-well companion plates (BD 353502)
Sterile PBS (-Mg, -Ca)
Trypsin
Forceps
Co-culture medium

Procedure:
Pre-wet Transwell membrane

1. Place transwell filters into 6-well companion plate carefully using forceps
2. Add 3ml of coculture media to lower compartment and 1.5ml coculture media to inner compartment of transwell cup.
3. Soak overnight in incubator to fully prewet membrane (cells do not adhere well if seeded on dry membrane)

Seeding Outer Surface of Transwell

1. Remove flasks with endothelial cells from incubator and place in cell culture hood. Aspirate spent medium, rinse culture surface with PBS and aspirate, add trypsin to detach cells, neutralize trypsin with media and collect cell suspension.
2. Centrifuge at 1000 rpm for 5 min and aspirate supernatant. Resuspend in fresh culture media and count using Coulter Counter.
3. Cells will be seeded at a density of 250,000/cm^2 with each transwell having a surface area of 4.2 cm^2. Centrifuge appropriate number of cells for number of slides at 1000 rpm for 5 min and remove supernatant.
4. Aspirate media from upper and lower compartments of transwell plate. Using forceps, remove each transwell filter from the plate and place upside-down in Petri dish so lower filter surface is now accessible.
5. Resuspend in media so that 400μL of cell suspension will be added to each surface.
6. Carefully drip cell suspension on each filter, cover dish and allow to adhere for 2 hours in incubator. Set 6-well plates aside for later use.

Seeding Inner Surface of Transwell

1. Remove flasks with smooth muscle cells from incubator and place in cell culture hood. Aspirate spent medium, rinse culture surface with PBS and aspirate, add trypsin to detach cells, neutralize trypsin with media and collect cell suspension.
2. Centrifuge at 1000 rpm for 5 min and aspirate supernatant. Resuspend in fresh culture media and count using Coulter Counter.
3. Cells will be seeded at a density of 100,000/cm^2 with each transwell having a surface area of 4.2 cm^2. Centrifuge appropriate number of cells for number of slides at 1000 rpm for 5 min and remove supernatant.
4. Remove Petri dish of transwells from incubator and using forceps, carefully plate transwells back into 6-well plate being careful not to damage EC monolayer. Add 3ml media to lower compartment.
5. Resuspend SMC in final media volume of 1.5ml and add to inner compartment of transwell filters.

NOTES:

- Seeding densities and efficiencies should be evaluated for each cell type used in this system (HAEC @ 250,000/cm^2 and HASMC @ 100,000/cm^2 was shown to work well here)
- Multiple types of transwell filters are available (pore size, membrane type) and experimental goals should be evaluated before choosing a specific type

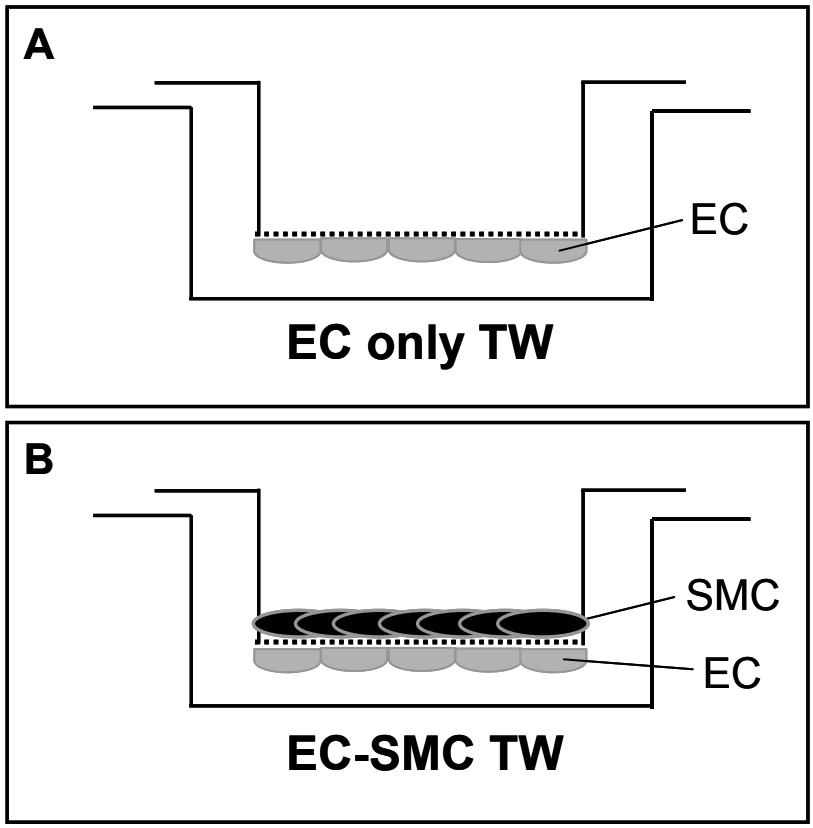

Figure B.4 Endothelial-Smooth Muscle Cell Transwell Co-Culture Model
Transwell filters with 0.4μm porous membrane are used for monoculture of endothelial cells (Panel A) or co-culture of endothelial cells and smooth muscle cells on opposite sides of the membrane (Panel B)

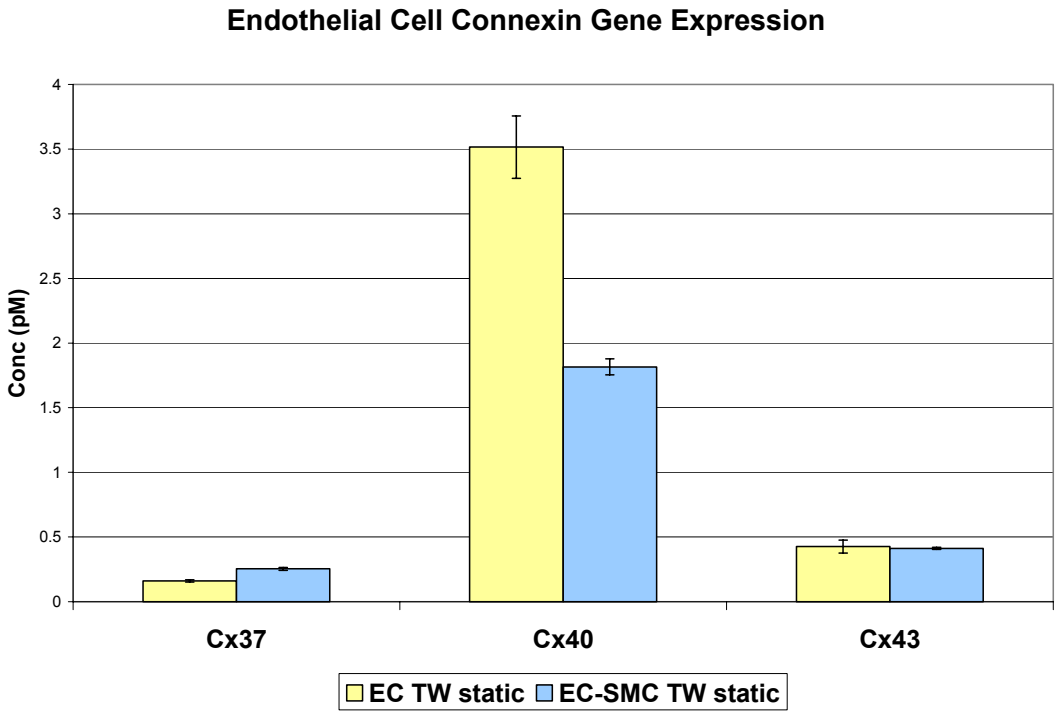

Figure B.5 Connexin mRNA Expression in the EC-SMC Transwell Model
Endothelial cells were removed from the monoculture and co-culture Transwell models and analyzed by RT-PCR for connexin mRNA expression.

REFERENCES

1. Thom, T., Haase, N., Rosamond, W., Howard, V. J., Rumsfeld, J., Manolio, T., Zheng, Z. J., Flegal, K., O'Donnell, C., Kittner, S., Lloyd-Jones, D., Goff, D. C., Jr., Hong, Y., Adams, R., Friday, G., Furie, K., Gorelick, P., Kissela, B., Marler, J., Meigs, J., Roger, V., Sidney, S., Sorlie, P., Steinberger, J., Wasserthiel-Smoller, S., Wilson, M., and Wolf, P. Heart disease and stroke statistics--2006 update: a report from the American Heart Association Statistics Committee and Stroke Statistics Subcommittee. Circulation, *113:* e85-151, 2006.

2. Gerritsen, M. Physiologic functions of normal endothelial cells. *In:* Vascular medicine, 2nd edition, pp. 1-38. Boston: Little, Brown & Co, 1996.

3. Cunningham, K. S. and Gotlieb, A. I. The role of shear stress in the pathogenesis of atherosclerosis. Lab Invest, *85:* 9-23, 2005.

4. Luscher, T. F. and Noll, G. The pathogenesis of cardiovascular disease: role of the endothelium as a target and mediator. Atherosclerosis, *118:* S81-90., 1995.

5. Lerman, A. and Zeiher, A. M. Endothelial function: cardiac events. Circulation, *111:* 363-368, 2005.

6. Nugent, H. M. and Edelman, E. R. Tissue engineering therapy for cardiovascular disease. Circ Res, *92:* 1068-1078, 2003.

7. Nerem, R. M. and Ensley, A. E. The tissue engineering of blood vessels and the heart. Am J Transplant, *4 Suppl 6:* 36-42, 2004.

8. Isenberg, B. C., Williams, C., and Tranquillo, R. T. Small-diameter artificial arteries engineered in vitro. Circ Res, *98:* 25-35, 2006.

9. Anand, R. J. and Hackam, D. J. The role of gap junctions in health and disease. Crit Care Med, *33:* S535-538, 2005.

10. Davies, P. F., Olesen, S. P., Clapham, D. E., Morrel, E. M., and Schoen, F. J. Endothelial communication. State of the art lecture. Hypertension, *11:* 563-572., 1988.

11. Rummery, N. M. and Hill, C. E. Vascular gap junctions and implications for hypertension. Clin Exp Pharmacol Physiol, *31:* 659-667, 2004.

12. Sohl, G. and Willecke, K. Gap junctions and the connexin protein family. Cardiovasc Res, *62:* 228-232, 2004.

13. Haefliger, J. A., Nicod, P., and Meda, P. Contribution of connexins to the function of the vascular wall. Cardiovasc Res, *62:* 345-356, 2004.

14. Figueroa, X. F., Isakson, B. E., and Duling, B. R. Connexins: gaps in our knowledge of vascular function. Physiology (Bethesda), *19:* 277-284, 2004.

15. Kher, N. and Marsh, J. D. Pathobiology of atherosclerosis--a brief review. Semin Thromb Hemost, *30:* 665-672, 2004.

16. VanderLaan, P. A., Reardon, C. A., and Getz, G. S. Site specificity of atherosclerosis: site-selective responses to atherosclerotic modulators. Arterioscler Thromb Vasc Biol, *24:* 12-22, 2004.

17. Widlansky, M. E., Gokce, N., Keaney, J. F., Jr., and Vita, J. A. The clinical implications of endothelial dysfunction. J Am Coll Cardiol, *42:* 1149-1160, 2003.

18. Mullenix, P. S., Andersen, C. A., and Starnes, B. W. Atherosclerosis as inflammation. Ann Vasc Surg, *19:* 130-138, 2005.

19. Robbie, L. and Libby, P. Inflammation and atherothrombosis. Ann N Y Acad Sci, *947:* 167-179; discussion 179-180, 2001.

20. Corti, R. and Badimon, J. J. Biologic aspects of vulnerable plaque. Curr Opin Cardiol, *17:* 616-625, 2002.

21. Almeda, F. Q. and Snell, R. J. Coronary revascularization in multivessel disease. Which is better, stents or surgery? Postgrad Med, *118:* 11-17, 2005.

22. Rumisek, J. D., Wade, C. E., Brooks, D. E., Okerberg, C. V., Barry, M. J., and Clarke, J. S. Heat-denatured albumin-coated Dacron vascular grafts: physical characteristics and in vivo performance. J Vasc Surg, *4:* 136-143, 1986.

23. Parsson, H., Jundzill, W., Johansson, K., Jonung, T., and Norgren, L. Healing characteristics of polymer-coated or collagen-treated Dacron grafts: an experimental porcine study. Cardiovasc Surg, *2:* 242-248, 1994.

24. Williams, S. K., Rose, D. G., and Jarrell, B. E. Microvascular endothelial cell sodding of ePTFE vascular grafts: improved patency and stability of the cellular lining. J Biomed Mater Res, *28:* 203-212, 1994.

25. Meinhart, J., Deutsch, M., and Zilla, P. Eight years of clinical endothelial cell transplantation. Closing the gap between prosthetic grafts and vein grafts. Asaio J, *43:* M515-521, 1997.

26. Foster, E. D. Reoperation for coronary artery disease. Circulation, *72:* V59-64, 1985.

27. Mann, M. J., Gibbons, G. H., Kernoff, R. S., Diet, F. P., Tsao, P. S., Cooke, J. P., Kaneda, Y., and Dzau, V. J. Genetic engineering of vein grafts resistant to atherosclerosis. Proc Natl Acad Sci U S A, *92:* 4502-4506, 1995.

28. Greenwald, S. E. and Berry, C. L. Improving vascular grafts: the importance of mechanical and haemodynamic properties. J Pathol, *190:* 292-299., 2000.

29. Nerem, R. M. Cellular engineering. Ann Biomed Eng, *19:* 529-545, 1991.

30. Langer, R. and Vacanti, J. P. Tissue engineering. Science, *260:* 920-926, 1993.

31. Lantz, G. C., Badylak, S. F., Hiles, M. C., Coffey, A. C., Geddes, L. A., Kokini, K., Sandusky, G. E., and Morff, R. J. Small intestinal submucosa as a vascular graft: a review. J Invest Surg, *6:* 297-310, 1993.

32. Schmidt, C. E. and Baier, J. M. Acellular vascular tissues: natural biomaterials for tissue repair and tissue engineering. Biomaterials, *21:* 2215-2231, 2000.

33. Teebken, O. E., Bader, A., Steinhoff, G., and Haverich, A. Tissue engineering of vascular grafts: human cell seeding of decellularised porcine matrix. Eur J Vasc Endovasc Surg, *19:* 381-386., 2000.

34. Minuth, W. W., Schumacher, K., Strehl, R., and Kloth, S. Physiological and cell biological aspects of perfusion culture technique employed to generate differentiated tissues for long term biomaterial testing and tissue engineering. J Biomater Sci Polym Ed, *11:* 495-522., 2000.

35. Hirschi, K. K., Skalak, T. C., Peirce, S. M., and Little, C. D. Vascular assembly in natural and engineered tissues. Ann N Y Acad Sci, *961:* 223-242., 2002.

36. Weinberg, C. B. and Bell, E. A blood vessel model constructed from collagen and cultured vascular cells. Science, *231:* 397-400., 1986.

37. L'Heureux, N., Paquet, S., Labbe, R., Germain, L., and Auger, F. A. A completely biological tissue-engineered human blood vessel. Faseb J, *12:* 47-56., 1998.

38. Niklason, L. E., Gao, J., Abbott, W. M., Hirschi, K. K., Houser, S., Marini, R., and Langer, R. Functional arteries grown in vitro. Science, *284:* 489-493., 1999.

39. Niklason, L. E., Abbott, W., Gao, J., Klagges, B., Hirschi, K. K., Ulubayram, K., Conroy, N., Jones, R., Vasanawala, A., Sanzgiri, S., and Langer, R. Morphologic and mechanical characteristics of engineered bovine arteries. J Vasc Surg, *33:* 628-638, 2001.

40. Campbell, J. H., Efendy, J. L., and Campbell, G. R. Novel vascular graft grown within recipient's own peritoneal cavity. Circ Res, *85:* 1173-1178, 1999.

41. Ziegler, T., Alexander, R. W., and Nerem, R. M. An endothelial cell-smooth muscle cell co-culture model for use in the investigation of flow effects on vascular biology. Ann Biomed Eng, *23:* 216-225., 1995.

42. Imberti, B., Seliktar, D., Nerem, R.M., Remuzzi, A. The response of endothelial cells to fluid shear stress using a co-culture model of the arterial wall. Endothelium, *9:* 11-23, 2002.

43. Kladakis, S. M. and Nerem, R. M. Endothelial cell monolayer formation: effect of substrate and fluid shear stress. Endothelium, *11:* 29-44, 2004.

44. Zarins, C. K., Giddens, D. P., Bharadvaj, B. K., Sottiurai, V. S., Mabon, R. F., and Glagov, S. Carotid bifurcation atherosclerosis. Quantitative correlation of plaque localization with flow velocity profiles and wall shear stress. Circ Res, *53:* 502-514., 1983.

45. Flaherty, J. T., Pierce, J. E., Ferrans, V. J., Patel, D. J., Tucker, W. K., and Fry, D. L. Endothelial nuclear patterns in the canine arterial tree with particular reference to hemodynamic events. Circ Res, *30:* 23-33., 1972.

46. Schwartz, S. M. and Benditt, E. P. Clustering of replicating cells in aortic endothelium. Proc Natl Acad Sci U S A, *73:* 651-653., 1976.

47. Levesque, M. J., Liepsch, D., Moravec, S., and Nerem, R. M. Correlation of endothelial cell shape and wall shear stress in a stenosed dog aorta. Arteriosclerosis, *6:* 220-229., 1986.

48. Passerini, A. G., Polacek, D. C., Shi, C., Francesco, N. M., Manduchi, E., Grant, G. R., Pritchard, W. F., Powell, S., Chang, G. Y., Stoeckert, C. J., Jr., and Davies, P. F. Coexisting proinflammatory and antioxidative endothelial transcription profiles in a disturbed flow region of the adult porcine aorta. Proc Natl Acad Sci U S A, *101:* 2482-2487, 2004.

49. Levesque, M. J. and Nerem, R. M. The elongation and orientation of cultured endothelial cells in response to shear stress. J Biomech Eng, *107:* 341-347., 1985.

50. Dewey, C. F., Jr., Bussolari, S. R., Gimbrone, M. A., Jr., and Davies, P. F. The dynamic response of vascular endothelial cells to fluid shear stress. J Biomech Eng, *103:* 177-185., 1981.

51. Helmlinger, G., Geiger, R. V., Schreck, S., and Nerem, R. M. Effects of pulsatile flow on cultured vascular endothelial cell morphology. J Biomech Eng, *113:* 123-131., 1991.

52. Nomura, H., Ishikawa, C., Komatsuda, T., Ando, J., and Kamiya, A. A disk-type apparatus for applying fluid shear stress on cultured endothelial cell. Biorheology, *25:* 461-470, 1988.

53. Blackman, B. R., Garcia-Cardena, G., and Gimbrone, M. A., Jr. A new in vitro model to evaluate differential responses of endothelial cells to simulated arterial shear stress waveforms. J Biomech Eng, *124:* 397-407, 2002.

54. Eskin, S. G., Ives, C. L., McIntire, L. V., and Navarro, L. T. Response of cultured endothelial cells to steady flow. Microvasc Res, *28:* 87-94, 1984.

55. Dewey, C. F., Jr. Effects of fluid flow on living vascular cells. J Biomech Eng, *106:* 31-35., 1984.

56. Ando, J., Nomura, H., and Kamiya, A. The effect of fluid shear stress on the migration and proliferation of cultured endothelial cells. Microvasc Res, *33:* 62-70., 1987.

57. Ando, J., Komatsuda, T., and Kamiya, A. Cytoplasmic calcium response to fluid shear stress in cultured vascular endothelial cells. In Vitro Cell Dev Biol, *24:* 871-877., 1988.

58. Helmlinger, G., Berk, B. C., and Nerem, R. M. Calcium responses of endothelial cell monolayers subjected to pulsatile and steady laminar flow differ. Am J Physiol, *269:* C367-375, 1995.

59. Olesen, S. P., Clapham, D. E., and Davies, P. F. Haemodynamic shear stress activates a K+ current in vascular endothelial cells. Nature, *331:* 168-170., 1988.

60. Sprague, E. A., Steinbach, B. L., Nerem, R. M., and Schwartz, C. J. Influence of a laminar steady-state fluid-imposed wall shear stress on the binding, internalization, and degradation of low-density lipoproteins by cultured arterial endothelium. Circulation, *76:* 648-656., 1987.

61. Shyy, Y. J., Hsieh, H. J., Usami, S., and Chien, S. Fluid shear stress induces a biphasic response of human monocyte chemotactic protein 1 gene expression in vascular endothelium. Proc Natl Acad Sci U S A, *91:* 4678-4682., 1994.

62. Bao, X., Lu, C., and Frangos, J. A. Temporal gradient in shear but not steady shear stress induces PDGF-A and MCP-1 expression in endothelial cells: role of NO, NF kappa B, and egr-1. Arterioscler Thromb Vasc Biol, *19:* 996-1003., 1999.

63. Chappell, D. C., Varner, S. E., Nerem, R. M., Medford, R. M., and Alexander, R. W. Oscillatory shear stress stimulates adhesion molecule expression in cultured human endothelium. Circ Res, *82:* 532-539., 1998.

64. Mohan, S., Mohan, N., Valente, A. J., and Sprague, E. A. Regulation of low shear flow-induced HAEC VCAM-1 expression and monocyte adhesion. Am J Physiol, *276:* C1100-1107., 1999.

65. Diamond, S. L., Eskin, S. G., and McIntire, L. V. Fluid flow stimulates tissue plasminogen activator secretion by cultured human endothelial cells. Science, *243:* 1483-1485, 1989.

66. Takada, Y., Shinkai, F., Kondo, S., Yamamoto, S., Tsuboi, H., Korenaga, R., and Ando, J. Fluid shear stress increases the expression of thrombomodulin by cultured human endothelial cells. Biochem Biophys Res Commun, *205:* 1345-1352, 1994.

67. Sokabe, T., Yamamoto, K., Ohura, N., Nakatsuka, H., Qin, K., Obi, S., Kamiya, A., and Ando, J. Differential regulation of urokinase-type plasminogen activator expression by fluid shear stress in human coronary artery endothelial cells. Am J Physiol Heart Circ Physiol, *287:* H2027-2034, 2004.

68. De Keulenaer, G. W., Chappell, D. C., Ishizaka, N., Nerem, R. M., Alexander, R. W., and Griendling, K. K. Oscillatory and steady laminar shear stress differentially affect human endothelial redox state: role of a superoxide-producing NADH oxidase. Circ Res, *82:* 1094-1101, 1998.

69. Inoue, H., Taba, Y., Miwa, Y., Yokota, C., Miyagi, M., and Sasaguri, T. Transcriptional and posttranscriptional regulation of cyclooxygenase-2 expression by fluid shear stress in vascular endothelial cells. Arterioscler Thromb Vasc Biol, *22:* 1415-1420, 2002.

70. Sorescu, G. P., Sykes, M., Weiss, D., Platt, M. O., Saha, A., Hwang, J., Boyd, N., Boo, Y. C., Vega, J. D., Taylor, W. R., and Jo, H. Bone morphogenic protein 4 produced in endothelial cells by oscillatory shear stress stimulates an inflammatory response. J Biol Chem, *278:* 31128-31135, 2003.

71. Tseng, H., Peterson, T. E., and Berk, B. C. Fluid shear stress stimulates mitogen-activated protein kinase in endothelial cells. Circ Res, *77:* 869-878., 1995.

72. Takahashi, M. and Berk, B. C. Mitogen-activated protein kinase (ERK1/2) activation by shear stress and adhesion in endothelial cells. Essential role for a herbimycin-sensitive kinase. J Clin Invest, *98:* 2623-2631, 1996.

73. Mohan, S., Mohan, N., and Sprague, E. A. Differential activation of NF-kappa B in human aortic endothelial cells conditioned to specific flow environments. Am J Physiol, *273:* C572-578., 1997.

74. Hu, Y. L. and Chien, S. Effects of shear stress on protein kinase C distribution in endothelial cells. J Histochem Cytochem, *45:* 237-249., 1997.

75. Resnick, N., Collins, T., Atkinson, W., Bonthron, D. T., Dewey, C. F., Jr., and Gimbrone, M. A., Jr. Platelet-derived growth factor B chain promoter contains a cis-acting fluid shear-stress-responsive element. Proc Natl Acad Sci U S A, *90:* 4591-4595., 1993.

76. Papadaki, M. and Eskin, S. G. Effects of fluid shear stress on gene regulation of vascular cells. Biotechnol Prog, *13:* 209-221., 1997.

77. Traub, O. and Berk, B. C. Laminar shear stress: mechanisms by which endothelial cells transduce an atheroprotective force. Arterioscler Thromb Vasc Biol, *18:* 677-685, 1998.

78. Ali, M. H. and Schumacker, P. T. Endothelial responses to mechanical stress: where is the mechanosensor? Crit Care Med, *30:* S198-206., 2002.

79. Nollert, M. U., Panaro, N. J., and McIntire, L. V. Regulation of genetic expression in shear stress-stimulated endothelial cells. Ann N Y Acad Sci, *665:* 94-104., 1992.

80. Chen, B. P., Li, Y. S., Zhao, Y., Chen, K. D., Li, S., Lao, J., Yuan, S., Shyy, J. Y., and Chien, S. DNA microarray analysis of gene expression in endothelial cells in response to 24-h shear stress. Physiol Genomics, *7:* 55-63., 2001.

81. McCormick, S. M., Eskin, S. G., McIntire, L. V., Teng, C. L., Lu, C. M., Russell, C. G., and Chittur, K. K. DNA microarray reveals changes in gene expression of shear stressed human umbilical vein endothelial cells. Proc Natl Acad Sci U S A, *98:* 8955-8960., 2001.

82. Dekker, R. J., van Soest, S., Fontijn, R. D., Salamanca, S., de Groot, P. G., VanBavel, E., Pannekoek, H., and Horrevoets, A. J. Prolonged fluid shear stress induces a distinct set of endothelial cell genes, most specifically lung Kruppel-like factor (KLF2). Blood, *100:* 1689-1698., 2002.

83. Dai, G., Kaazempur-Mofrad, M. R., Natarajan, S., Zhang, Y., Vaughn, S., Blackman, B. R., Kamm, R. D., Garcia-Cardena, G., and Gimbrone, M. A., Jr. Distinct endothelial phenotypes evoked by arterial waveforms derived from atherosclerosis-susceptible and -resistant regions of human vasculature. Proc Natl Acad Sci U S A, *101:* 14871-14876, 2004.

84. Gimbrone, M. A., Jr., Topper, J. N., Nagel, T., Anderson, K. R., and Garcia-Cardena, G. Endothelial dysfunction, hemodynamic forces, and atherogenesis. Ann N Y Acad Sci, *902:* 230-239; discussion 239-240, 2000.

85. Davies, P. F., Shi, C., Depaola, N., Helmke, B. P., and Polacek, D. C. Hemodynamics and the focal origin of atherosclerosis: a spatial approach to

endothelial structure, gene expression, and function. Ann N Y Acad Sci, *947:* 7-16; discussion 16-17., 2001.

86. Form, D. M., Pratt, B. M., and Madri, J. A. Endothelial cell proliferation during angiogenesis. In vitro modulation by basement membrane components. Lab Invest, *55:* 521-530, 1986.

87. Sund, M., Xie, L., and Kalluri, R. The contribution of vascular basement membranes and extracellular matrix to the mechanics of tumor angiogenesis. Apmis, *112:* 450-462, 2004.

88. Grant, D. S. and Kleinman, H. K. Regulation of capillary formation by laminin and other components of the extracellular matrix. Exs, *79:* 317-333, 1997.

89. Eichmann, A., Le Noble, F., Autiero, M., and Carmeliet, P. Guidance of vascular and neural network formation. Curr Opin Neurobiol, *15:* 108-115, 2005.

90. Gospodarowicz, D. and Ill, C. Extracellular matrix and control of proliferation of vascular endothelial cells. J Clin Invest, *65:* 1351-1364., 1980.

91. Schor, A. M., Schor, S. L., and Allen, T. D. The synthesis of subendothelial matrix by bovine aortic endothelial cells in culture. Tissue Cell, *16:* 677-691., 1984.

92. Iivanainen, E., Kahari, V. M., Heino, J., and Elenius, K. Endothelial cell-matrix interactions. Microsc Res Tech, *60:* 13-22., 2003.

93. Balcells, M. and Edelman, E. R. Effect of pre-adsorbed proteins on attachment, proliferation, and function of endothelial cells. J Cell Physiol, *191:* 155-161, 2002.

94. Carey, D. J. Control of growth and differentiation of vascular cells by extracellular matrix proteins. Annu Rev Physiol, *53:* 161-177, 1991.

95. Kleinman, H. K., McGarvey, M. L., Hassell, J. R., Star, V. L., Cannon, F. B., Laurie, G. W., and Martin, G. R. Basement membrane complexes with biological activity. Biochemistry, *25:* 312-318, 1986.

96. Ingber, D. E. Mechanical signaling and the cellular response to extracellular matrix in angiogenesis and cardiovascular physiology. Circ Res, *91:* 877-887., 2002.

97. Tzima, E., del Pozo, M. A., Shattil, S. J., Chien, S., and Schwartz, M. A. Activation of integrins in endothelial cells by fluid shear stress mediates Rho-dependent cytoskeletal alignment. Embo J, *20:* 4639-4647, 2001.

98. Jalali, S., del Pozo, M. A., Chen, K., Miao, H., Li, Y., Schwartz, M. A., Shyy, J. Y., and Chien, S. Integrin-mediated mechanotransduction requires its dynamic interaction with specific extracellular matrix (ECM) ligands. Proc Natl Acad Sci U S A, *98:* 1042-1046., 2001.

99. Hirschi, K. K. and D'Amore, P. A. Pericytes in the microvasculature. Cardiovasc Res, *32:* 687-698., 1996.

100. Hirschi, K. K., Rohovsky, S. A., and D'Amore, P. A. PDGF, TGF-beta, and heterotypic cell-cell interactions mediate endothelial cell-induced recruitment of 10T1/2 cells and their differentiation to a smooth muscle fate. J Cell Biol, *141:* 805-814., 1998.

101. Ono, O., Ando, J., Kamiya, A., Kuboki, Y., and Yasuda, H. Flow effects on cultured vascular endothelial and smooth muscle cell functions. Cell Struct Funct, *16:* 365-374., 1991.

102. Waybill, P. N., Chinchilli, V. M., and Ballermann, B. J. Smooth muscle cell proliferation in response to co-culture with venous and arterial endothelial cells. J Vasc Interv Radiol, *8:* 375-381., 1997.

103. Peiro, C., Redondo, J., Rodriguez-Martinez, M. A., Angulo, J., Marin, J., and Sanchez-Ferrer, C. F. Influence of endothelium on cultured vascular smooth muscle cell proliferation. Hypertension, *25:* 748-751., 1995.

104. Fillinger, M. F., Sampson, L. N., Cronenwett, J. L., Powell, R. J., and Wagner, R. J. Coculture of endothelial cells and smooth muscle cells in bilayer and conditioned media models. J Surg Res, *67:* 169-178., 1997.

105. Jones, P. A. Construction of an artificial blood vessel wall from cultured endothelial and smooth muscle cells. Proc Natl Acad Sci U S A, *76:* 1882-1886., 1979.

106. Korff, T., Kimmina, S., Martiny-Baron, G., and Augustin, H. G. Blood vessel maturation in a 3-dimensional spheroidal coculture model: direct contact with smooth muscle cells regulates endothelial cell quiescence and abrogates VEGF responsiveness. Faseb J, *15:* 447-457., 2001.

107. Xu, C. B., Falke, P., and Stavenow, L. Interactions between cultured bovine arterial smooth muscle cells and endothelial cells; studies on the release of growth inhibiting and growth stimulating factors. Artery, *17:* 297-310., 1990.

108. Asakawa, H. and Kobayashi, T. The effect of coculture with human smooth muscle cells on the proliferation, the IL-1 beta secretion, the PDGF production and tube formation of human aortic endothelial cells. Cell Biochem Funct, *17:* 123-130., 1999.

109. Redmond, E. M., Cahill, P. A., and Sitzmann, J. V. Perfused transcapillary smooth muscle and endothelial cell co-culture--a novel in vitro model. In Vitro Cell Dev Biol Anim, *31:* 601-609., 1995.

110. Hendrickson, R. J., Cappadona, C., Yankah, E. N., Sitzmann, J. V., Cahill, P. A., and Redmond, E. M. Sustained pulsatile flow regulates endothelial nitric oxide synthase and cyclooxygenase expression in co-cultured vascular endothelial and smooth muscle cells. J Mol Cell Cardiol, *31:* 619-629, 1999.

111. Chiu, J. J., Chen, L. J., Lee, P. L., Lee, C. I., Lo, L. W., Usami, S., and Chien, S. Shear stress inhibits adhesion molecule expression in vascular endothelial cells induced by coculture with smooth muscle cells. Blood, *101:* 2667-2674., 2003.

112. Evans, W. H. and Martin, P. E. Gap junctions: structure and function (Review). Mol Membr Biol, *19:* 121-136, 2002.

113. Saez, J. C., Berthoud, V. M., Branes, M. C., Martinez, A. D., and Beyer, E. C. Plasma membrane channels formed by connexins: their regulation and functions. Physiol Rev, *83:* 1359-1400, 2003.

114. Saez, J. C., Retamal, M. A., Basilio, D., Bukauskas, F. F., and Bennett, M. V. Connexin-based gap junction hemichannels: gating mechanisms. Biochim Biophys Acta, *1711:* 215-224, 2005.

115. Stout, C., Goodenough, D. A., and Paul, D. L. Connexins: functions without junctions. Curr Opin Cell Biol, *16:* 507-512, 2004.

116. Goodenough, D. A. and Paul, D. L. Beyond the gap: functions of unpaired connexon channels. Nat Rev Mol Cell Biol, *4:* 285-294, 2003.

117. Jiang, J. X. and Gu, S. Gap junction- and hemichannel-independent actions of connexins. Biochim Biophys Acta, *1711:* 208-214, 2005.

118. Severs, N. J., Coppen, S. R., Dupont, E., Yeh, H. I., Ko, Y. S., and Matsushita, T. Gap junction alterations in human cardiac disease. Cardiovasc Res, *62:* 368-377, 2004.

119. Yeh, H. I., Rothery, S., Dupont, E., Coppen, S. R., and Severs, N. J. Individual gap junction plaques contain multiple connexins in arterial endothelium. Circ Res, *83:* 1248-1263., 1998.

120. Hill, C. E., Phillips, J. K., and Sandow, S. L. Heterogeneous control of blood flow amongst different vascular beds. Med Res Rev, *21:* 1-60., 2001.

121. van Kempen, M. J. and Jongsma, H. J. Distribution of connexin37, connexin40 and connexin43 in the aorta and coronary artery of several mammals. Histochem Cell Biol, *112:* 479-486., 1999.

122. Dora, K. A. Cell-cell communication in the vessel wall. Vasc Med, *6:* 43-50., 2001.

123. Hill, C. E., Rummery, N., Hickey, H., and Sandow, S. L. Heterogeneity in the distribution of vascular gap junctions and connexins: implications for function. Clin Exp Pharmacol Physiol, *29:* 620-625., 2002.

124. Griffith, T. M., Chaytor, A. T., and Edwards, D. H. The obligatory link: role of gap junctional communication in endothelium-dependent smooth muscle hyperpolarization. Pharmacol Res, *49:* 551-564, 2004.

125. Laird, D. W. The life cycle of a connexin: gap junction formation, removal, and degradation. J Bioenerg Biomembr, *28:* 311-318, 1996.

126. Berthoud, V. M., Minogue, P. J., Laing, J. G., and Beyer, E. C. Pathways for degradation of connexins and gap junctions. Cardiovasc Res, *62:* 256-267, 2004.

127. Laing, J. G. and Beyer, E. C. The gap junction protein connexin43 is degraded via the ubiquitin proteasome pathway. J Biol Chem, *270:* 26399-26403, 1995.

128. Anderson, C. L., Zundel, M. A., and Werner, R. Variable promoter usage and alternative splicing in five mouse connexin genes. Genomics, *85:* 238-244, 2005.

129. Pfeifer, I., Anderson, C., Werner, R., and Oltra, E. Redefining the structure of the mouse connexin43 gene: selective promoter usage and alternative splicing mechanisms yield transcripts with different translational efficiencies. Nucleic Acids Res, *32:* 4550-4562, 2004.

130. Seul, K. H. and Beyer, E. C. Mouse connexin37: gene structure and promoter analysis. Biochim Biophys Acta, *1492:* 499-504, 2000.

131. Sullivan, R., Ruangvoravat, C., Joo, D., Morgan, J., Wang, B. L., Wang, X. K., and Lo, C. W. Structure, sequence and expression of the mouse Cx43 gene encoding connexin 43. Gene, *130:* 191-199, 1993.

132. Seul, K. H., Tadros, P. N., and Beyer, E. C. Mouse connexin40: gene structure and promoter analysis. Genomics, *46:* 120-126, 1997.

133. Dupays, L., Mazurais, D., Rucker-Martin, C., Calmels, T., Bernot, D., Cronier, L., Malassine, A., Gros, D., and Theveniau-Ruissy, M. Genomic organization and alternative transcripts of the human Connexin40 gene. Gene, *305:* 79-90, 2003.

134. Fishman, G. I., Spray, D. C., and Leinwand, L. A. Molecular characterization and functional expression of the human cardiac gap junction channel. J Cell Biol, *111:* 589-598, 1990.

135. Reed, K. E., Westphale, E. M., Larson, D. M., Wang, H. Z., Veenstra, R. D., and Beyer, E. C. Molecular cloning and functional expression of human connexin37, an endothelial cell gap junction protein. J Clin Invest, *91:* 997-1004., 1993.

136. Werner, R. IRES elements in connexin genes: a hypothesis explaining the need for connexins to be regulated at the translational level. IUBMB Life, *50:* 173-176, 2000.

137. Schiavi, A., Hudder, A., and Werner, R. Connexin43 mRNA contains a functional internal ribosome entry site. FEBS Lett, *464:* 118-122, 1999.

138. Bonnal, S., Boutonnet, C., Prado-Lourenco, L., and Vagner, S. IRESdb: the Internal Ribosome Entry Site database. Nucleic Acids Res, *31:* 427-428, 2003.

139. Dhein, S. Gap junction channels in the cardiovascular system: pharmacological and physiological modulation. Trends Pharmacol Sci, *19:* 229-241, 1998.

140. Suarez, S. and Ballmer-Hofer, K. VEGF transiently disrupts gap junctional communication in endothelial cells. J Cell Sci, *114:* 1229-1235., 2001.

141. Traub, O., Hertlein, B., Kasper, M., Eckert, R., Krisciukaitis, A., Hulser, D., and Willecke, K. Characterization of the gap junction protein connexin37 in murine endothelium, respiratory epithelium, and after transfection in human HeLa cells. Eur J Cell Biol, *77:* 313-322, 1998.

142. Larson, D. M., Seul, K. H., Berthoud, V. M., Lau, A. F., Sagar, G. D., and Beyer, E. C. Functional expression and biochemical characterization of an epitope-tagged connexin37. Mol Cell Biol Res Commun, *3:* 115-121, 2000.

143. Sosinsky, G. E. and Nicholson, B. J. Structural organization of gap junction channels. Biochim Biophys Acta, *1711:* 99-125, 2005.

144. Cottrell, G. T. and Burt, J. M. Functional consequences of heterogeneous gap junction channel formation and its influence in health and disease. Biochim Biophys Acta, *1711:* 126-141, 2005.

145. Beyer, E. C., Gemel, J., Seul, K. H., Larson, D. M., Banach, K., and Brink, P. R. Modulation of intercellular communication by differential regulation and heteromeric mixing of co-expressed connexins. Braz J Med Biol Res, *33:* 391-397., 2000.

146. Beyer, E. C., Gemel, J., Martinez, A., Berthoud, V. M., Valiunas, V., Moreno, A. P., and Brink, P. R. Heteromeric mixing of connexins: compatibility of partners and functional consequences. Cell Commun Adhes, *8:* 199-204., 2001.

147. Bruzzone, R., Haefliger, J. A., Gimlich, R. L., and Paul, D. L. Connexin40, a component of gap junctions in vascular endothelium, is restricted in its ability to interact with other connexins. Mol Biol Cell, *4:* 7-20, 1993.

148. Brink, P. R., Cronin, K., Banach, K., Peterson, E., Westphale, E. M., Seul, K. H., Ramanan, S. V., and Beyer, E. C. Evidence for heteromeric gap junction channels formed from rat connexin43 and human connexin37. Am J Physiol, *273:* C1386-1396, 1997.

149. Valiunas, V., Gemel, J., Brink, P. R., and Beyer, E. C. Gap junction channels formed by coexpressed connexin40 and connexin43. Am J Physiol Heart Circ Physiol, *281:* H1675-1689., 2001.

150. Cottrell, G. T. and Burt, J. M. Heterotypic gap junction channel formation between heteromeric and homomeric Cx40 and Cx43 connexons. Am J Physiol Cell Physiol, *281:* C1559-1567, 2001.

151. Cottrell, G. T., Wu, Y., and Burt, J. M. Cx40 and Cx43 expression ratio influences heteromeric/ heterotypic gap junction channel properties. Am J Physiol Cell Physiol, *282:* C1469-1482, 2002.

152. Xia, J., Little, T. L., and Duling, B. R. Cellular pathways of the conducted electrical response in arterioles of hamster cheek pouch in vitro. Am J Physiol, *269:* H2031-2038, 1995.

153. Little, T. L., Xia, J., and Duling, B. R. Dye tracers define differential endothelial and smooth muscle coupling patterns within the arteriolar wall. Circ Res, *76:* 498-504, 1995.

154. Sandow, S. L. and Hill, C. E. Incidence of myoendothelial gap junctions in the proximal and distal mesenteric arteries of the rat is suggestive of a role in endothelium-derived hyperpolarizing factor-mediated responses. Circ Res, *86:* 341-346., 2000.

155. Sandow, S. L., Tare, M., Coleman, H. A., Hill, C. E., and Parkington, H. C. Involvement of myoendothelial gap junctions in the actions of endothelium-derived hyperpolarizing factor. Circ Res, *90:* 1108-1113., 2002.

156. Yashiro, Y. and Duling, B. R. Integrated Ca(2+) signaling between smooth muscle and endothelium of resistance vessels. Circ Res, *87:* 1048-1054, 2000.

157. Isakson, B. E. and Duling, B. R. Heterocellular contact at the myoendothelial junction influences gap junction organization. Circ Res, *97:* 44-51, 2005.

158. Fujimoto, K. Pericyte-endothelial gap junctions in developing rat cerebral capillaries: a fine structural study. Anat Rec, *242:* 562-565, 1995.

159. Larson, D. M., Carson, M. P., and Haudenschild, C. C. Junctional transfer of small molecules in cultured bovine brain microvascular endothelial cells and pericytes. Microvasc Res, *34:* 184-199, 1987.

160. Zahler, S., Hoffmann, A., Gloe, T., and Pohl, U. Gap-junctional coupling between neutrophils and endothelial cells: a novel modulator of transendothelial migration. J Leukoc Biol, *73:* 118-126, 2003.

161. Pepper, M. S. and Meda, P. Basic fibroblast growth factor increases junctional communication and connexin 43 expression in microvascular endothelial cells. J Cell Physiol, *153:* 196-205, 1992.

162. Yeh, H. I., Lai, Y. J., Chang, H. M., Ko, Y. S., Severs, N. J., and Tsai, C. H. Multiple connexin expression in regenerating arterial endothelial gap junctions. Arterioscler Thromb Vasc Biol, *20:* 1753-1762, 2000.

163. Liao, Y., Day, K. H., Damon, D. N., and Duling, B. R. Endothelial cell-specific knockout of connexin 43 causes hypotension and bradycardia in mice. Proc Natl Acad Sci U S A, *98:* 9989-9994, 2001.

164. Rummery, N. M., McKenzie, K. U., Whitworth, J. A., and Hill, C. E. Decreased endothelial size and connexin expression in rat caudal arteries during hypertension. J Hypertens, *20:* 247-253, 2002.

165. Yeh, H. I., Lee, P. Y., Su, C. H., Tian, T. Y., Ko, Y. S., and Tsai, C. H. Reduced expression of endothelial connexins 43 and 37 in hypertensive rats is rectified after 7-day carvedilol treatment. Am J Hypertens, *19:* 129-135, 2006.

166. Kwak, B. R., Veillard, N., Pelli, G., Mulhaupt, F., James, R. W., Chanson, M., and Mach, F. Reduced connexin43 expression inhibits atherosclerotic lesion formation in low-density lipoprotein receptor-deficient mice. Circulation, *107:* 1033-1039., 2003.

167. Yeh, H. I., Lu, C. S., Wu, Y. J., Chen, C. C., Hong, R. C., Ko, Y. S., Shiao, M. S., Severs, N. J., and Tsai, C. H. Reduced expression of endothelial connexin37 and connexin40 in hyperlipidemic mice: recovery of connexin37 after 7-day simvastatin treatment. Arterioscler Thromb Vasc Biol, *23:* 1391-1397, 2003.

168. Kwak, B. R., Mulhaupt, F., Veillard, N., Gros, D. B., and Mach, F. Altered pattern of vascular connexin expression in atherosclerotic plaques. Arterioscler Thromb Vasc Biol, *22:* 225-230., 2002.

169. Kumari, S. S., Varadaraj, K., Valiunas, V., Ramanan, S. V., Christensen, E. A., Beyer, E. C., and Brink, P. R. Functional expression and biophysical properties of polymorphic variants of the human gap junction protein connexin37. Biochem Biophys Res Commun, *274:* 216-224., 2000.

170. Delorme, B., Dahl, E., Jarry-Guichard, T., Briand, J. P., Willecke, K., Gros, D., and Theveniau-Ruissy, M. Expression pattern of connexin gene products at the early developmental stages of the mouse cardiovascular system. Circ Res, *81:* 423-437, 1997.

171. Simon, A. M., Goodenough, D. A., Li, E., and Paul, D. L. Female infertility in mice lacking connexin 37. Nature, *385:* 525-529, 1997.

172. Simon, A. M., Goodenough, D. A., and Paul, D. L. Mice lacking connexin40 have cardiac conduction abnormalities characteristic of atrioventricular block and bundle branch block. Curr Biol, *8:* 295-298, 1998.

173. Lo, C. W., Waldo, K. L., and Kirby, M. L. Gap junction communication and the modulation of cardiac neural crest cells. Trends Cardiovasc Med, *9:* 63-69, 1999.

174. Simon, A. M. and McWhorter, A. R. Vascular abnormalities in mice lacking the endothelial gap junction proteins connexin37 and connexin40. Dev Biol, *251:* 206-220., 2002.

175. Simon, A. M., McWhorter, A. R., Dones, J. A., Jackson, C. L., and Chen, H. Heart and head defects in mice lacking pairs of connexins. Dev Biol, *265:* 369-383, 2004.

176. Kruger, O., Beny, J. L., Chabaud, F., Traub, O., Theis, M., Brix, K., Kirchhoff, S., and Willecke, K. Altered dye diffusion and upregulation of connexin37 in mouse aortic endothelium deficient in connexin40. J Vasc Res, *39:* 160-172., 2002.

177. Simon, A. M. and McWhorter, A. R. Decreased intercellular dye-transfer and downregulation of non-ablated connexins in aortic endothelium deficient in connexin37 or connexin40. J Cell Sci, *116:* 2223-2236, 2003.

178. Simon, A. M. and McWhorter, A. R. Role of connexin37 and connexin40 in vascular development. Cell Commun Adhes, *10:* 379-385, 2003.

179. Isakson, B. E., Damon, D. N., Day, K. H., Liao, Y., and Duling, B. R. Connexin40 and connexin43 in mouse aortic endothelium: evidence for coordinated regulation. Am J Physiol Heart Circ Physiol, 2005.

180. Seul, K. H., Kang, K. Y., Lee, K. S., Kim, S. H., and Beyer, E. C. Adenoviral delivery of human connexin37 induces endothelial cell death through apoptosis. Biochem Biophys Res Commun, *319:* 1144-1151, 2004.

181. Larson, D. M., Wrobleski, M. J., Sagar, G. D., Westphale, E. M., and Beyer, E. C. Differential regulation of connexin43 and connexin37 in endothelial cells by cell density, growth, and TGF-beta1. Am J Physiol, *272:* C405-415., 1997.

182. Hoffmann, A., Gloe, T., Pohl, U., and Zahler, S. Nitric oxide enhances de novo formation of endothelial gap junctions. Cardiovasc Res, *60:* 421-430, 2003.

183. Kameritsch, P., Hoffmann, A., and Pohl, U. Opposing effects of nitric oxide on different connexins expressed in the vascular system. Cell Commun Adhes, *10:* 305-309, 2003.

184. Kwak, B. R., Pepper, M. S., Gros, D. B., and Meda, P. Inhibition of endothelial wound repair by dominant negative connexin inhibitors. Mol Biol Cell, *12:* 831-845., 2001.

185. van Rijen, H. V., van Kempen, M. J., Postma, S., and Jongsma, H. J. Tumour necrosis factor alpha alters the expression of connexin43, connexin40, and connexin37 in human umbilical vein endothelial cells. Cytokine, *10:* 258-264, 1998.

186. Rignault, S., Haefliger, J. A., Gasser, D., Markert, M., Nicod, P., Liaudet, L., Waeber, B., and Feihl, F. Sepsis up-regulates the expression of connexin 40 in rat aortic endothelium. Crit Care Med, *33:* 1302-1310, 2005.

187. Gabriels, J. E. and Paul, D. L. Connexin43 is highly localized to sites of disturbed flow in rat aortic endothelium but connexin37 and connexin40 are more uniformly distributed. Circ Res, *83:* 636-643., 1998.

188. Cowan, D. B., Lye, S. J., and Langille, B. L. Regulation of vascular connexin43 gene expression by mechanical loads. Circ Res, *82:* 786-793., 1998.

189. DePaola, N., Davies, P. F., Pritchard, W. F., Jr., Florez, L., Harbeck, N., and Polacek, D. C. Spatial and temporal regulation of gap junction connexin43 in vascular endothelial cells exposed to controlled disturbed flows in vitro. Proc Natl Acad Sci U S A, *96:* 3154-3159, 1999.

190. Ebong, E. E., Kim, S., and Depaola, N. Flow Regulates Intercellular Communication in HAEC by Assembling Functional Cx40 and Cx37 Gap Junctional Channels. Am J Physiol Heart Circ Physiol, 2005.

191. Simmons, C. A., Grant, G. R., Manduchi, E., and Davies, P. F. Spatial heterogeneity of endothelial phenotypes correlates with side-specific vulnerability to calcification in normal porcine aortic valves. Circ Res, *96:* 792-799, 2005.

192. Inai, T., Mancuso, M. R., McDonald, D. M., Kobayashi, J., Nakamura, K., and Shibata, Y. Shear stress-induced upregulation of connexin 43 expression in endothelial cells on upstream surfaces of rat cardiac valves. Histochem Cell Biol, *122:* 477-483, 2004.

193. Rajavashisth, T. B., Liao, J. K., Galis, Z. S., Tripathi, S., Laufs, U., Tripathi, J., Chai, N. N., Xu, X. P., Jovinge, S., Shah, P. K., and Libby, P. Inflammatory cytokines and oxidized low density lipoproteins increase endothelial cell expression of membrane type 1-matrix metalloproteinase. J Biol Chem, *274:* 11924-11929, 1999.

194. Ruegg, C. and Mariotti, A. Vascular integrins: pleiotropic adhesion and signaling molecules in vascular homeostasis and angiogenesis. Cell Mol Life Sci, *60:* 1135-1157, 2003.

195. Jalali, S., del Pozo, M. A., Chen, K., Miao, H., Li, Y., Schwartz, M. A., Shyy, J. Y., and Chien, S. Integrin-mediated mechanotransduction requires its dynamic interaction with specific extracellular matrix (ECM) ligands. Proc Natl Acad Sci U S A, *98:* 1042-1046, 2001.

196. Galis, Z. S. and Khatri, J. J. Matrix metalloproteinases in vascular remodeling and atherogenesis: the good, the bad, and the ugly. Circ Res, *90:* 251-262, 2002.

197. Rundhaug, J. E. Matrix metalloproteinases and angiogenesis. J Cell Mol Med, *9:* 267-285, 2005.

198. Stocker, R. and Keaney, J. F., Jr. Role of oxidative modifications in atherosclerosis. Physiol Rev, *84:* 1381-1478, 2004.

199. Eskin, S. G., Turner, N. A., and McIntire, L. V. Endothelial cell cytochrome P450 1A1 and 1B1: up-regulation by shear stress. Endothelium, *11:* 1-10, 2004.

200. Williams, J. L., Weichert, A., Zakrzewicz, A., Da Silva-Azevedo, L., Pries, A. R., Baum, O., and Egginton, S. Differential gene and protein expression in abluminal sprouting and intraluminal splitting forms of angiogenesis. Clin Sci (Lond), 2006.

201. Klagsbrun, M. and Eichmann, A. A role for axon guidance receptors and ligands in blood vessel development and tumor angiogenesis. Cytokine Growth Factor Rev, *16:* 535-548, 2005.

202. Kishimoto, K., Liu, S., Tsuji, T., Olson, K. A., and Hu, G. F. Endogenous angiogenin in endothelial cells is a general requirement for cell proliferation and angiogenesis. Oncogene, *24:* 445-456, 2005.

203. Illi, B., Scopece, A., Nanni, S., Farsetti, A., Morgante, L., Biglioli, P., Capogrossi, M. C., and Gaetano, C. Epigenetic histone modification and cardiovascular lineage programming in mouse embryonic stem cells exposed to laminar shear stress. Circ Res, *96:* 501-508, 2005.

204. Wang, B., Xiao, Y., Ding, B. B., Zhang, N., Yuan, X., Gui, L., Qian, K. X., Duan, S., Chen, Z., Rao, Y., and Geng, J. G. Induction of tumor angiogenesis by Slit-Robo signaling and inhibition of cancer growth by blocking Robo activity. Cancer Cell, *4:* 19-29, 2003.

205. Dhein, S. and Jongsma, H. J. Forming the network-gap junctions in the cardiovascular system. Cardiovasc Res, *62:* 225-227, 2004.

206. Hirschi, K. K., Burt, J. M., Hirschi, K. D., and Dai, C. Gap junction communication mediates transforming growth factor-beta activation and endothelial-induced mural cell differentiation. Circ Res, *93:* 429-437, 2003.

207. Shanker, A. J., Yamada, K., Green, K. G., Yamada, K. A., and Saffitz, J. E. Matrix-protein-specific regulation of Cx43 expression in cardiac myocytes subjected to mechanical load. Circ Res, *96:* 558-566, 2005.

208. Elbashir, S. M., Harborth, J., Lendeckel, W., Yalcin, A., Weber, K., and Tuschl, T. Duplexes of 21-nucleotide RNAs mediate RNA interference in cultured mammalian cells. Nature, *411:* 494-498, 2001.

209. Elbashir, S. M., Lendeckel, W., and Tuschl, T. RNA interference is mediated by 21- and 22-nucleotide RNAs. Genes Dev, *15:* 188-200, 2001.

210. Shao, Q., Wang, H., McLachlan, E., Veitch, G. I., and Laird, D. W. Down-regulation of Cx43 by retroviral delivery of small interfering RNA promotes an aggressive breast cancer cell phenotype. Cancer Res, *65:* 2705-2711, 2005.

211. Wei, C. J., Francis, R., Xu, X., and Lo, C. W. Connexin43 associated with an N-cadherin-containing multiprotein complex is required for gap junction formation in NIH3T3 cells. J Biol Chem, *280:* 19925-19936, 2005.

212. Duffy, H. S., Delmar, M., and Spray, D. C. Formation of the gap junction nexus: binding partners for connexins. J Physiol Paris, *96:* 243-249, 2002.

213. Lavender, M. D., Pang, Z., Wallace, C. S., Niklason, L. E., and Truskey, G. A. A system for the direct co-culture of endothelium on smooth muscle cells. Biomaterials, *26:* 4642-4653, 2005.